Master thesis : The Hull Optimisation for an Open 60 IMOCA Single Handed Race yacht

Auteur : Gournay, Lazare
Promoteur(s) : 18523
Faculté : Faculté des Sciences appliquées
Diplôme : Master : ingénieur civil mécanicien, à finalité spécialisée en "Advanced Ship Design"
Année académique : 2021-2022
URI/URL : http://hdl.handle.net/2268.2/16414

With the support of the Erasmus+ Programme of the European Union

FACULTY OF CREATIVE INDUSTRIES, ARCHITECTURE AND ENGINEERING

UNIVERSITY OF SOLENT

Master Thesis Report

Investigation of the benefits of modern foils on an IMOCA 60 sailing boat

Presented in partial fulfillment of the requirements for the double degree:

Erasmus Mundus Master Program EMSHIP+

Master of Sciences in Applied Mechanics, Naval Architecture and Advanced Ship Design, conferred by the University of Liege, with a second year specialisation in *Hydrodynamics for Ocean Engineering* (Master HOE) conferred by the Ecole Centrale de Nantes.

Performed by:	GOURNAY Lazare (lazare.gournay@gmail.com)
Supervisor:	BARKLEY Giles
Reviewers:	GENTAZ Lionel, LE TOUZE David, BOOTE Dario
Thesis duration:	From the 1st of March to the 31st of July 2022
Thesis location:	Solent University, East Park Terrace, SO14 0YN

This page is intentionally left blank.

ACKNOWLEDGEMENTS

This master thesis could not have seen the light without the precious and continuous help of my supervisor, Professor Giles Barkley, to whom I am sincerely grateful for his genuine involvement and dedication in my project.

I would particularly like to thank Professor Steve Crook for helping me to learn the software Maxsurf and Rhinoceros during the beginning of my thesis. He also provided me with the reversed engineered Maxsurf hull form of the IMOCA Hugo Boss, which was of great use for the hull design process.

Special thanks to Jack Cunningham-Burley who helped me throughout the process of manufacturing my model scale hull form and its appendages. His overall knowledge in ship building, and his manufacturing skills, helped me to go through the challenges of the manufacturing one after the other. I have learnt many things by sharing this part of my thesis with him, and in great company, and I can only be grateful.

I would also like to warmly thank Professor Jonathan Ridley for 3D printing the appendages of my model scale Open 60.

I would finally like to sincerely thank the professors and students of Solent university's yacht design degree who helped me throughout my thesis. My learning process was clearly enhanced by the numerous discussions and interactions that I had with them.

To my lovely parents and my beloved twin brother,
who always support me in what I am getting into.

DECLARATION OF AUTHORSHIP

I declare that this thesis and the work presented in it are my own and have been generated by me as the result of my own original research.

Where I have consulted the published work of others, this is always clearly attributed.

Where I have quoted from the work of others, the source is always given. With the exception of such quotations, this thesis is entirely my own work.

I have acknowledged all main sources of help.

Where the thesis is based on work done by myself jointly with others, I have made clear exactly what was done by others and what I have contributed myself.

This thesis contains no material that has been submitted previously, in whole or in part, for the award of any other academic degree or diploma.

I cede copyright of the thesis in favour of the University of Solent.

Done on the 16th of July 2022 in Southampton.

Abstract

This paper investigates the benefits of using modern foils on an IMOCA 60 sailing boat. This was achieved for a designed IMOCA hull form, and designed foils, using different approaches.

A parametric study and researches on existing IMOCA 60 was first realised. Different hull forms were then modelled in the nurbs-based hull form modelling software Maxsurf. They were investigated through VPP analyses to determine the fastest design. Two of them are the reversed engineered hull forms of Hugo Boss and L'Occitane. They were used as reference to validate the design, by comparing the boat speeds found using the designed hull and these reference ones, in various sailing configurations (headings and wind speeds) chosen in the VPP.

The selected hull form design was manufactured at model scale (1:10) using composite materials, to be tank tested with its keel and foil. Tank tests were realised with and without the foil, at different boat speeds, heel angles, and leeway angles. The data recorded during the tests comprises the total drag, the side force, the roll (or righting) moment, the heave, and the pitch of the boat. The data measured without foil was subtracted from the one measured with foil, which allowed to determine the effect of the foil on the boat.

Meanwhile, a theoretical model was developed under the assumptions of the lifting-line theory, to try to predict the hydrodynamic forces generated by the designed foil, and their influence on the overall righting moment of the boat. The results were compared to the experimental foil results, which allowed to validate the model.

Finally, "direct experimental" VPP analyses were performed based on the experimental data found with and without foil. It enabled to find the gains in boat speed due to the foil, in various sailing configurations. The influence of the righting lever (GZ) was also investigated.

After two iterations including a re-design process, the designed hull form proved to be relatively fast compared to the reversed engineered hull forms. Moreover, it was found that the developed theoretical model provides realistic trends when compared to the experimental foil results. The theoretical foil results generally overestimated the experimental ones, which means that the foil was slightly less efficient than predicted in theory. The direct experimental VPP analyses showed that the designed foils globally increased the boat speeds, when the increase in GZ was accounted for. However, a few boat speeds were smaller with foil than without it, regardless of the GZ values used. It was found to correspond to configurations (boat speeds, heel, and leeway angles) in which the foil ventilated in the tank. The downwind speeds were unchanged since the foil was not immersed at the corresponding small heel angles. Hence, a design modification was proposed to solve that issue, and also benefit from the lift of the foils when sailing downwind.

Keywords: IMOCA, sailing yacht design, hull optimisation, performance prediction, velocity prediction program (VPP), foil lifting-line theory, experimental hydrodynamics, tank testing.

Contents

List of Figures

List of Tables

List of Symbols

Chapter 2 - Hull design procedure

T	Water draft $[m]$
B_h	Hull beam $[m]$
L_h	Hull length $[m]$
B_{max}	Transverse section of maximum beam $[m]$
Δ	Displacement $[t]$
SA_{max}^{UPW}	Maximum Sail Area Upwind $[m^2]$
SA_{max}^{DW}	Maximum Sail Area Downwind $[m^2]$
LWL	Waterline Length $[m]$
BWL	Waterline Beam $[m]$
WSA	Wetted Surface Area $[m^2]$
LCB	Longitudinal Center of Buoyancy $[m]$
VCB	Vertical Center of Buoyancy $[m]$
LCF	Longitudinal Center of Flotation $[m]$
t	Thickness $[m]$
c	Chord $[m]$
s	Span $[m]$
t/c	Thickness to chord ratio [-]
P	Height of the mainsail luff $[m]$
E	Foot length of the mainsail $[m]$
BAD	Height of the boom above deck $[m]$
IG	Height of the foresail from deck to its top $[m]$
J	Horizontal distance from tack of genoa to mast foot $[m]$
LP	Perpendicular distance from clew of genoa to forestay $[m]$
HBI	Freeboard height at the tack of genoa $[m]$
ISP	Height from bottom to top of the genoa $[m]$
SPL	Spinnaker pole length $[m]$
SMW	Spinnaker girth at mid length $[m]$
SLU	Spinnaker luff length $[m]$
SLE	Spinnaker leach length $[m]$
$MDT1$	Mast small diameter at the root $[m]$
$MDL1$	Mast large diameter at the root $[m]$
$MDT2$	Mast small diameter at the top $[m]$
$MDL2$	Mast large diameter at the top $[m]$
TL	Mast tapper length $[m]$

Chapter 4 - Theoretical model for foil performance prediction

i	Index of the foil sections, s.t: $i \in \{A, B, C, D\}$ [-]
s_i	Span of foil section i $[m]$
ρ	Sea water density $[kg/m^3]$
A	Planform area $[m^2]$
C_l^{2D}	2D lift coefficient [-]
C_d^{2D}	2D drag coefficient [-]
C_l^{3D}	3D lift coefficient [-]
C_d^{3D}	3D drag coefficient [-]
C_{di}	Induced drag coefficient [-]
AR	Aspect Ratio [-]
AR_{eff}	Effective Aspect Ratio [-]
V_{app}	Apparent inflow speed on the section $[m/s]$
V_b	Boat speed $[m/s]$
γ	Leeway angle [°]
θ	Heel angle [°]
α_i	Angle of foil section i to horizontal waterline when the boat is upright [°]
$(\alpha_i \pm \theta)$	Angle of foil section i to horizontal waterline when the boat is heeled [°]
ξ	Apparent angle of attack in the plane perpendicular to the foil [°]
η	Apparent leeway angle of the foil [°]
$L_{section}$	Lift generated relative to the foil section $[N]$
$D_{section}$	Drag generated relative to the foil section $[N]$
L_i	Lift generated by foil section i relative to the waterplane $[N]$
D_i	Drag generated by foil section i relative to the waterplane $[N]$
SF_i	Side force generated by foil section i relative to the waterplane $[N]$
L	Lift generated by the entire foil relative to the waterplane $[N]$
D	Drag generated by the entire foil relative to the waterplane $[N]$
SF	Side force generated by the entire foil relative to the waterplane $[N]$
k_1	Factor to account for the sign of the lift [-]
k_3	Factor to account for the sign of the side force [-]
GZ	Righting lever arm of the boat $[m]$
GZ'	Revised righting lever arm of the boat with foils $[m]$
g	Acceleration of gravity $[N/kg]$
RM_{foil}	Righting moment generated by the foil $[N.m]$
RM_{boat}	Static righting moment of the boat (without foils) $[N.m]$
d_1	Horizontal center of lift (or horizontal righting arm) of the foil $[m]$
d_2	Vertical center of side force (or vertical righting arm) of the foil $[m]$

M_1	Righting moment generated by the foil's lift [$N.m$]
M_2	Righting moment generated by the foil's side force [$N.m$]
x_i	Horizontal center of lift of foil section i [m]
z_i	Vertical center of side force of foil section i [m]
B	Beam of the boat at foil height [m]
Δ'	Boat's displacement reduced by foil's vertical lift [t]
T'	Boat's water draft reduced by foil's vertical lift [t]

Chapter 6 - Experimental testing in the towing tank facility

T_e	Effective draft [m]
R_{di}	Induced drag [N]
R_T	Total resistance [N]

List of Abbreviations

Chapter 2 - Hull design procedure

AP	Aft Perpendicular
FP	Forward Perpendicular
SA	Sail Area
Max	Maximum
UPW	Upwind
DW	Downwind
CE	Center of Effort
CLR	Center of Lateral Resistance
VPP	Velocity Prediction Program
LPP	Lines Processing Program
GUI	Graphical User Interface
VMG	Velocity Made Good
VS	Versus
WSA	Wetted Surface Area

Chapter 4 - Theoretical model for foil performance prediction

Im	Immersion
SF	Side Force
DWL	Design Waterline
CL	Centreline
LCG	Longitudinal Center of Gravity
TCG	Transversal Center of Gravity

Chapter 5 - Manufacturing of the model scale hull form and appendages

CNC	Computer Numerical Control
GSM	Gram per Square Meter
CAD	Computer Aided Design

Chapter 7 - Comparison of foil predictions and experimental results

AOA	Angle Of Attack
RM	Righting Moment
CFD	Computational Fluid Dynamics

1 Introduction

The concept of the foil was invented long ago. As surprising as it can be, Leonardo da Vinci already thought about it during the 15th century. However, this technology could not be developed at the time, due to a lack of availability of suitable engineering materials and advanced manufacturing techniques. For that reason, the foils are still a relatively new technology that is in constant development [1]. They are used for a broad range of vessels, which implies that various foil geometries exist depending on the requirements that they have to fulfill.

In the past few years, the International Monohull Open Class Association (IMOCA) saw numerous new Open 60 sailing boats entering its fleet, all of which were equipped with modern "moustache" foils. These boats, which are made for offshore racing, now fully rely on these foils to stay in the lead during races. Their performance is directly related to the efficiency of their foils, which have become the major element around which they are designed. Therefore, designers and engineers constantly work hand in hand to improve the existing IMOCA foils, and optimise their efficiency to build the fastest Open 60.

One of the major benefits of the foils is to lift the boat out of the water and reduce its hull drag significantly. The drag due to the immersed foil is added, but the loss in hull drag is largely greater, given that the wind is strong enough for the boat to sail fast enough, so that the foil generates enough upward force to lift the boat up. Nowadays, this is typically possible over 3 knots of wind [1], and this reduction in hull drag decreases the overall drag of the boat, which makes it much faster. Moreover, these foils also generate extra righting moment which helps to keep the boat upright. This allows the skippers to carry more sail area without reaching an excessive heel angle, and therefore increase the driving force of the boat.

These IMOCA 60 sailing boats are also equipped with a keel that can be canted up to 38 degrees to place the weight of the bulb windward, and use it as a counterweight to increase the righting moment of the boat. This is generally done when the boat sails close to the wind, since the aerodynamic side force is larger, which pushes the boat to heel further. However, when the keel is canted, the hydrodynamic side force that it generates is reduced, which makes the boat likely to drift leeward. In this situation, the leeward foil is also used to mitigate this effect [1].

In every IMOCA design office, there is a need to assess the benefits brought by given foil designs, prior from building them, which costs a lot of money. Nowadays, this is also generally needed before designing the rest of the hull, which highly depends on the chosen foils. Hence, different methodologies used to assess the benefits coming from a proposed foil design are investigated in this project. Moreover, the project aims at describing how much, and by which means, such foils improve the speed of IMOCA 60 sailing boats. This was achieved for a designed hull form and designed foils, through tank testing, and the use of a Velocity Prediction

Program (VPP) to perform analyses relying on the tank tests data.

The first section of the project presents the procedure followed to design the IMOCA hull form.

A theoretical model was developed under the assumptions of the lifting-line theory, to try to predict the hydrodynamic forces generated by a given foil design, and the resulting righting moment. This was achieved for various boat speeds, heel angles, and leeway angles. All the procedures and assumptions considered in the development of the model are explained in the second section of the paper. Demonstrations and proofs of the equations used in the model are proposed in Appendix.

The choices considered in the design of the appendages of the boat are briefly discussed in the third section. The corresponding drawings are found in Appendix, at the end of the paper.

The next section explains in details the manufacturing procedures followed to build the model scale hull form with its appendages. The difficulties experienced during the building process are discussed.

The model scale Open 60 was tank tested with and without its foil. It allowed to record, in each case, the overall drag, the side force, the roll (or righting) moment, the heave, and the pitch of the boat. The tests were performed for chosen boat speeds, heel angles, and leeway angles. The data gathered without foil was subtracted from the one found with foil, which allowed to deduce the effect of the foil on the boat. The tank testing procedures undertaken and the results obtained are presented in the fifth section. The potential sources of error are discussed.

The next section presents a comparison between the experimental foil results obtained from the tank tests, and the theoretical ones obtained using the theoretical model. The discussion allowed to validate the model.

The last section of the project presents in details the methodology followed to find the speed of the boat, with and without its foil, in chosen sailing configurations (headings and wind speeds). This was achieved through “direct experimental“ VPP analyses that were performed based on the tank data found with and without foil. It allowed to appreciate the effect of adding the foil to the boat, by comparing the boat speeds and the corresponding heel and leeway angles found with and without foil. The effect of the righting lever (GZ) values used in the VPP on the boat speeds was also investigated.

2 Hull design procedure

The first stage of the project was to design a suitable hull form that would allow the boat to maintain a reasonable average speed compared to existing IMOCAs. The hull was developed using the nurbs-based hull design software Maxsurf Modeler. The design had to satisfy the requirements of the IMOCA class rules [2] (c.f. section 2.1). A parametric study of existing IMOCAs was completed (c.f section 2.2). Based on the above, different hull forms were generated and their theoretical speeds were assessed using a VPP, the results of which allowed the selection of the fastest design (c.f. section 2.6).

2.1 IMOCA class rules consideration

Regarding the hull dimensions, section D.2 of the IMOCA class rules imposes the following maximum values for the water draft T (measured from the waterline to the bottom of the bulb), the air draft (mast length measured from the waterline), the hull beam B_h, and hull length L_h.

Table 1: Maximum dimensions imposed by the IMOCA class rules

Lh (m)	**Bh (m)**	**T (m)**	**Mast length (m)**
18.28	5.85	4.5	29

Other important rules considered in the design are the following:

i) The hull beam measured 1000 mm behind its foreward extent does not exceed 1120 mm.

ii) No negative curvature is allowed on the hull from its foreward extent to the transverse section of maximum beam (B_{max}).

iii) The minimum freeboard is 1550 mm at foreward perpendicular (FP), and 1050 mm at aft perpendicular (AP).

2.2 Parametric study

Some key parameters of 40 IMOCAs, such as hull length (L_h) and beam (B_h), displacement (Δ), and maximum sail area upwind (Max UPW SA) and downwind (Max DW SA) were found [3, 4], and are presented in Table 17 of Appendix A. Further information such as skipper, sail number, launch date, foils usage, and mast type are also given (c.f. Table 18). More parameters typically used in parametric studies, such as waterline length (LWL) or breadth (BWL) were not found, since they are kept secret by the teams. The study was therefore limited.

In order to reduce the number of boats used as a design reference and select only the top performing ones, a study of the IMOCAs' rankings for the latest most important international races was realised. The races include the last two editions of the Vendée Globe, the Transat Jacques Vabre, the Rolex Fastnet Race, and the Défi Azimut [5]. The results of the study are presented in Appendix A.1. All the Open 60s appearing in the top 5 of any of these races were selected for the study, leading to 14 reference boats. Their main parameters are presented in Table 2, and were considered for the design of the Open 60.

Table 2: Main parameters of the 14 selected IMOCAs

Boat	**Lh (m)**	**Bh (m)**	**Δ (t)**	**Max UPW SA (m2)**	**Max DW SA (m2)**
Maitre Coq IV	18.28	5.8	8	310	550
Apivia	18.28	5.85	8	350	560
Bureau Vallée 2	18.28	5.5	7.8	270	535
Yes We Cam!	18.28	5.85	8	300	620
Sea Explorer	18.28	5.7	7.6	290	490
Linkedout	18.28	5.85	8	320	430
Banque Pop. X	18.28	5.7	7.7	340	570
Charal	18.28	5.85	8	320	600
MACSF	18.28	5.7	8	300	650
Initiative-Cœur	18.28	5.7	8.5	280	600
Arkéa Paprec	18.28	5.7	8	260	600
Hugo Boss	18.28	5.4	7.6	330	630
PRB	18.28	5.5	-	300	600
11th Hour Alaka'i	18.28	5.5	7.5	340	570
Average	18.28	5.7	7.9	307.86	571.79

Based on the values gathered in Table 2 for the 14 reference IMOCAs, Figures 1 and 2 respectively present their displacement Δ plotted against their hull beam B_h, and their maximum downwind sail area (SA_{max}^{DW}) plotted against their maximum upwind sail area (SA_{max}^{UPW}). Each dot corresponds to a reference IMOCA. The average beam to displacement ratio $\overline{B_h}/\overline{\Delta} = 5.7/7.9 = 0.72$, and the average ratio $\overline{SA_{max}^{UPW}}/\overline{SA_{max}^{DW}} = 307.86/571.79 = 0.54$, are represented by the red lines. These ratios are a good indication of the values to have for the design.

It can be seen on Figure 1 that the boats which have a larger beam tend to have a larger displacement. Note that some boats are sisterships and have the same set of beam and displacement values, which explains why only nine data points are seen on the graph. Globally, the range of beam and displacement is quite narrow ($B_h \in [5.4, 5.85]$ meters, and $\Delta \in [7.5, 8.5]$ tonnes). This is the result of the class regulations combined with a high level of development of these Open 60s, therefore giving an accurate idea of the values to use for these quantities.

Figure 2 shows that the range of sail areas used by the boats is quite large ($SA_{max}^{UPW} \in [260, 350]\, m^2$, and $SA_{max}^{DW} \in [430, 650]\, m^2$). Also, it is seen that some boats have a large upwind, but low

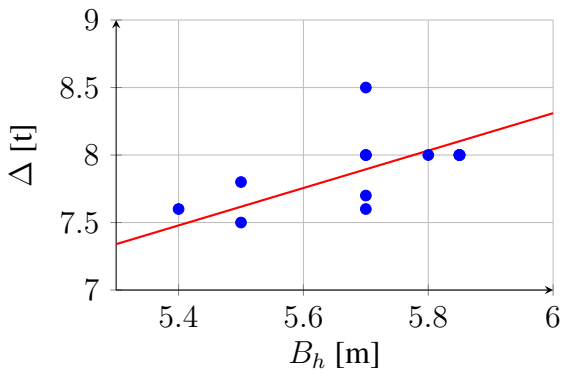

Figure 1: Regression analysis - displacement Δ VS hull beam B_h

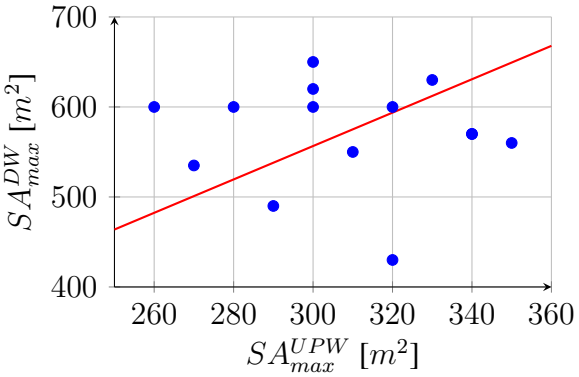

Figure 2: Regression analysis - SA^{DW}_{max} VS SA^{UPW}_{max}

downwind sail area (which is the case of Linkedout, c.f. Table 2), and vice-versa. The standard deviation from the mean ratio is therefore larger than for beam and displacement. This comes from the fact that the choice of the sail area is based on many parameters of the boat such as weight and shape of the appendages, and it is also subjected to the skipper's preference. This leads to more variation between the boats.

Table 3 presents additional information regarding the selected boats.

Table 3: Additional information for the 14 selected IMOCAs

Boat	Skipper	Sail Nb	Launch date	Foils?	Mast type
Maitre Coq IV	Yannick Bestaven	FRA 17	02/03/2015	Yes	Wing
Apivia	Charlie Dalin	FRA 79	05/08/2019	Yes	Wing
Bureau Vallée 2	Louis Burton	FRA 18	31/01/2020	Yes	Wing
Yes We Cam!	Jean Le Cam	FRA 01	29/05/2007	No	Wing
Sea Explorer	Boris Herrmann	MON 10	07/08/2015	Yes	Wing
Linkedout	Thomas Ruyant	FRA 59	07/09/2019	Yes	Wing
Banque Pop. X	Clarisse Cremer	FRA 30	16/08/2011	No	Wing
Charal	Jérémie Beyou	FRA 08	20/08/2018	Yes	Wing
MACSF	Isabelle Joschke	FRA 27	06/08/2007	Yes	Wing
Initiative-Cœur	Samantha Davies	FRA 109	18/09/2010	Yes	Wing
Arkéa Paprec	Sébastien Simon	FRA 04	19/07/2019	Yes	Wing
Hugo Boss	Alex Thomson	GBR 99	01/10/2015	Yes	-
PRB	Kevin Escoffier	FRA 85	11/03/2021	Yes	-
11th Hour Alaka'i	Pascal Bidegorry	USA 11	01/09/2015	Yes	Wing

As it could be expected, most of these top performing boats are recent and use foils. Foils are used to decrease the total drag of the boat by lifting it out of the water, and also to increase its righting moment. The extra righting moment allows the skipper to choose to either carry more sail area, or sail the boat more upright. Both of these points lead to an increase in speed over non foiling boats. In fact, as the boat heels, its center of buoyancy usually shifts aft, which induces

a tendency of the bow to point downwards, increasing slamming and overall resistance. Moreover, when sailing upwind, an excessive heel angle leads to weather helm, which corresponds to the natural tendency of the boat to head up into the wind due to a misalignment between the aerodynamic center of effort (CE) (which moves aft) and the hydrodynamic center of lateral resistance (CLR) [6]. Weather helm is counteracted by turning the rudder in a position where it will create a moment of the same magnitude, which opposes the imbalance between the sail and hull side forces acting through the CE and CLR. However, an excessive rudder angle creates extra drag. Therefore, in some sailing configurations and sea states, the skipper can choose to sail the boat more upright to reduce the effect of slamming and minimise the extra rudder drag. Based on the above, one understands the importance of mitigating heeling of a boat in certain conditions, which justifies the use of foils.

2.3 Design loop

The final hull form was achieved through successive iterations within a design loop, which gathers the following steps:

i) Create different hull forms which comply with the rules using Maxsurf Modeler.

ii) Implement these hull forms in a Velocity Prediction Program (VPP).

iii) Use the output data given by the VPP to compare the performance of the designs.

iv) Select the fastest hull and re-design it to enhance its performance if necessary.

v) Go back to ii.

2.4 Hull modelling in Maxsurf

Numerous intermediate versions of the hull were created until obtaining a satisfactory one. The hull form considered as the best attempt (later referred to as “first design version“) was implemented in the VPP to assess its theoretical performance. The hull forms of the IMOCAs L’Occitane (now Bureau Vallee) and Hugo Boss were reversed engineered using their lines plan drawings [7], and implemented in the VPP to compare their performances to the one of the design. These boats were chosen as reference since they present two very distinct shapes (c.f. Figures 36 and 37), and proved to perform very well in races (c.f. Appendix A.1). Considering the VPP results, a new design version (later called “final design version“) was modelled and studied in the VPP, and a second iteration of the design loop was performed. The Maxsurf models of these four Open 60s are presented in Appendix B.1.

2.5 Preparation of the VPP analyses

The VPP used is WinDesign 4, provided by the Wolfson Unit. Before launching the computations in the VPP, different steps had to be performed in order to define the appendages, the rigs, and the sails of the boats to be studied. These steps were undertaken for the two reference IMOCA hull forms (Hugo Boss and L'Occitane), as well as the two successive hull design versions, as part of two iterations of the design loop.

2.5.1 Preparation of the hull using a Lines Processing Program (LPP)

The Maxsurf model of the bare hull was first exported to the LPP, in which the different appendages were added to the hull. The same appendages were added to the four boats, to allow a fair comparison of the hull forms. Their characteristics are presented in Tables 4 and 5.

Table 4: Characteristics of the appendages created in the LPP - 1

Name	**Vol.** (m^3)	**WSA** (m^2)	**LCB (m)**	**VCB (m)**	**NACA section**
Keel	0.1403	5.4485	-0.418	-1.739	64A
Bulb	0.1811	2.023	-0.691	-4.30	0000
Rudder	0.0225	2.6197	-8.693	-0.638	0000
Foil	0.0583	2.1715	0.6974	-0.482	64A

Table 5: Characteristics of the appendages created in the LPP - 2

Keel		**Bulb**		**Rudders**		**Foil**	
Span s (m)	4.112	Span s (m)	2.0	Span s (m)	1.5	Span s (m)	1.5
Weight (kg)	200	Weight (kg)	2500	Root c (m)	0.5	Chord c (m)	0.7
Root c (m)	0.8	VCG (m)	-4.30	Tip c (m)	0.35	Cant angle (°)	50
Tip c (m)	0.5	-	-	t/c (-)	0.12	t/c (-)	0.12
t/c (-)	0.12	-	-	-	-	-	-

Note that before exporting the bare hull to the LPP, few steps were carried out in Maxsurf to allow the LPP to correctly read the data contained in the file. These included the creation of 41 stations evenly distributed along the length of the hull (many stations were needed since the LPP reads the hull's geometrical data at each station), and setting the zero point at the foreward extend of the boat. The file was then exported to a IMS LPP format, which generated a set of data points along each station, allowing the LPP to read the file (see Figures 3 and 4).

As shown in Figures 3 and 4, different cant angles of the keel were implemented: 0°, and 38° which is the maximum angle allowed by the class rules. It is worth mentioning that, since the LPP did not allow to implement curvature on the appendages, the foil is a simple dagger board for which the largest part involved in lift creation was kept.

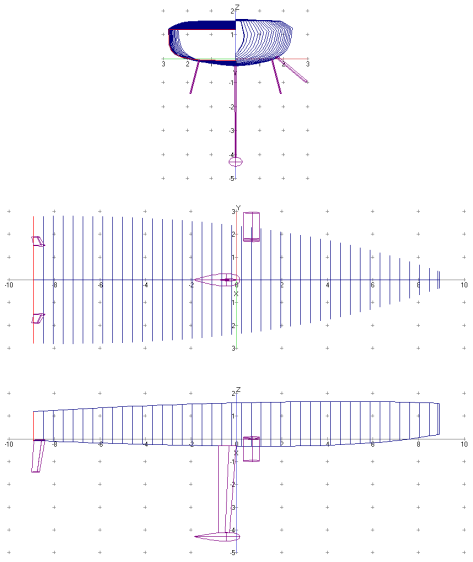

Figure 3: Hull and appendages as displayed in the LPP's GUI - 0° of keel cant

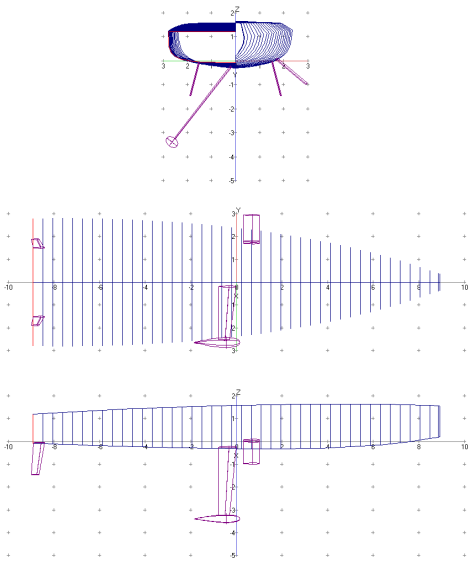

Figure 4: Hull and appendages as displayed in the LPP's GUI - 38° of keel cant

2.5.2 Definition of the rigs, sails, sailsets, and opsets, in the VPP

The LPP file containing the hull and appendages geometry, including the two keel cant angles, was imported in the VPP. The rigs were first defined, and their dimensions, chosen under the guidance of Barkley (personal communication), are presented in Table 6.

Table 6: Rigs created in the VPP

Main		**Fore**		**Spin**		**Main Mast**	
P (m)	26.5	IG (m)	27.5	ISP (m)	27.5	MDT1 (m)	0.28
E (m)	8	J (m)	10	SPL (m)	12	MDL1 (m)	0.4
BAD (m)	1	LP (m)	11	SMW (m)	25	MDT2 (m)	0.18
-	-	HBI (m)	1.5	SLU (m)	24	MDL2 (m)	0.25
-	-	-	-	SLE (m)	22	TL (m)	3

The signification of the rig dimensions is found in the List of Symbols, at the beginning of the paper. The sails were then defined based on personal researches [8, 9, 10] (see Table 7).

Table 7: Sails created in the VPP

Name	**Area** (m^2)	**Span (m)**
Main	180	26.5
Spin	400	27.5
A3	300	27.5
A5	200	19.5
J1	140	24.5
J2	100	20
J3	50	13.5

Note that the IMOCA class rules impose the boats to carry at most eight sails, one of which is a storm jib (also called tormentin) of 20 m^2 minimum. It is not defined in the VPP since it is almost never used in practice [8].

The VPP also allowed to define sail sets, corresponding to different sets of sails likely to be used together in different sailing configurations (headings and wind speeds). Note that only sets of two sails were considered, although the skippers sometimes use three. Table 8 presents the sail sets chosen to sail the boats in three different wind speed ranges (light, medium, and strong), both downwind (DW) and upwind (UPW).

Table 8: Sails sets created in the VPP

Name	**Short name**	**Sail 1**	**Sail 2**	**Total SA (m^2)**
DW light wind	DWl	Main	Spin	580
DW medium wind	DWm	Main	A3	480
DW strong wind	DWs	Main	A5	380
UPW light wind	UPl	Main	J1	320
UPW medium wind	UPm	Main	J2	280
UPW strong wind	UPs	Main	J3	230

One can see from Table 8 that the chosen sail sets allow the maximum upwind and downwind sail areas, respectively of 320 and 580 m^2, to fall within the range found for the IMOCAs of the parametric study, and very close to the mean values (c.f. Figure 2).

Different opsets were finally created. Each opset corresponds to a given cant angle of the keel and sail set, as shown in Table 9.

Table 9: Opsets created in the VPP

Name	**Short Name**	**Sail Set**	**Keel cant angle (°)**
DW light wind 0	DWl0	DWl	0
DW medium wind 0	DWm0	DWm	0
DW strong wind 0	DWs0	DWs	0
UPW light wind 0	UPl0	UPl	0
UPW medium wind 0	UPm0	UPm	0
UPW strong wind 0	UPs0	UPs	0
DW light wind 38	DWl38	DWl	38
DW medium wind 38	DWm38	DWm	38
DW strong wind 38	DWs38	DWs	38
UPW light wind 38	UPl38	UPl	38
UPW medium wind 38	UPm38	UPm	38
UPW strong wind 38	UPs38	UPs	38

When the VPP calculations are launched, the boat speed is assessed for each created opset, in each chosen wind speed and heading. This allowed to find the best keel cant angle and sail set,

in each case (c.f. Appendix B.4 and B.5). The rigs, sails, sail sets, and opsets, were kept the same for all the boats studied, to allow the comparison of the hull forms exclusively (like for the appendages). Once all these parameters were defined, the VPP calculations were performed for the four boats. The results are presented in the following, and the hulls are compared.

2.6 Analysis of the VPP results and selection of the final hull design

A comparison of the reference hulls is first proposed, to better grasp their differences in term of theoretical performance. Then, a comparison is realised between these hulls and, successively, the first and second hull design versions, to assess the likely success of the designs. Note that more output data given by the VPP can be found in Appendix B. It includes tables of the best boat speeds (Appendix B.2), polar plots (Appendix B.3), best keel cant angles (Appendix B.4), and best sail sets (Appendix B.5) for the four boats. The best boat speeds are reached using the best keel cant angle and sail set, for each wind speed and heading. The polar plots represent the data contained in the best boat speeds tables.

2.6.1 Comparison of the two reference hull forms

The best boat speeds of the IMOCAs Hugo boss and L'Occitane are presented in Appendix B.2, for each wind speed and heading. In order to ease the comparison of these speeds, it was decided to compute the ratio between the best boat speeds of L'Occitane and Hugo Boss. This was achieved using Excel, and the result is depicted in Figure 5.

	4	6	8	10	14	16	20	25	30	35
32	1,00	1,02	1,04	1,03	1,02	1,02	1,03	1,05	1,07	1,15
36	1,00	1,03	1,02	1,01	1,01	1,01	1,02	1,02	1,04	1,07
40	1,00	1,03	1,01	1,01	1,01	1,01	1,01	1,02	1,03	1,04
45	1,01	1,01	1,00	1,01	1,01	1,01	1,02	1,03	1,03	1,04
52	1,01	1,00	1,00	1,01	1,02	1,02	1,03	1,03	1,04	1,04
60	1,01	0,99	1,00	1,02	1,02	1,03	1,04	1,05	1,06	1,06
70	1,01	1,00	1,01	1,02	1,03	1,04	1,05	1,07	1,08	1,09
80	1,00	1,00	1,02	1,02	1,04	1,05	1,07	1,08	1,10	1,11
90	0,99	1,00	1,02	1,03	1,05	1,06	1,07	1,09	1,09	1,09
100	0,99	1,01	1,02	1,03	1,06	1,06	1,08	1,07	1,06	1,06
110	0,99	1,00	1,02	1,03	1,06	1,07	1,07	1,05	1,04	1,04
120	0,99	0,98	1,02	1,03	1,06	1,08	1,06	1,04	1,03	1,02
135	1,00	0,97	0,98	1,00	1,05	1,06	1,05	1,02	1,02	1,01
150	1,00	1,00	0,99	0,98	1,00	1,01	1,02	1,03	1,01	1,00
160	0,99	1,00	1,00	0,99	0,99	1,00	1,01	1,01	0,99	0,98
170	1,00	1,00	1,00	1,00	0,99	1,00	1,00	1,01	1,00	0,99
180	1,00	1,00	1,00	1,00	0,99	0,99	1,00	1,01	1,01	0,99
Up.Vmg	1,01	1,02	1,01	1,01	1,01	1,01	1,01	1,02	1,03	1,04
Dn.Vmg	1,00	0,97	0,97	0,99	1,03	1,04	1,03	1,01	0,99	0,99

Figure 5: Comparison of the best boat speeds - L'Occitane VS Hugo Boss

The speed ratios are given for a range of wind speeds and headings chosen in the VPP, respectively from 4 to 35 knots, and 32 to 180 degrees. The last two rows present the ratios of the upwind and downwind VMG (Velocity Made Good), which represent the speed projected on the wind axis, i.e. the speed at which the boat goes upwind or downwind. A conditional formatting was used with a color scale in Excel to better visualise the speed pattern. The ratios are close to 1 since the boats have similar speeds for a given wind speed and heading. When

the ratios are over 1, L'Occitane is faster than Hugo Boss, and the corresponding cells tend to green. Conversely, when they are less than 1, L'Occitane is slower than Hugo Boss, and the cells tend to red.

It is clear from Figure 5 that L'Occitane's hull form makes the boat theoretically faster than Hugo Boss overall, since most of the cells are larger than 1. This is especially the case when the wind blows over 8 knots, and sailing from 32° to 150° to the wind, which is the most important range, since the boat sails under these conditions most of the time. However, Hugo Boss seems to be slightly faster downwind which is reflected in the VMG ratios, while the upwind VMG of L'Occitane is larger than Hugo Boss' regardless of the wind speed.

2.6.2 First design iteration

As previously, Figures 6 and 7 respectively present the ratios between the best boat speeds of the first design version and the ones of Hugo Boss and L'Occitane. Therefore, where the ratios are over 1 (green cells), the designed Open 60 is faster than the reference boat.

	4	6	8	10	14	16	20	25	30	35
32	0,97	1,00	1,02	1,01	1,02	1,03	1,03	1,05	1,07	1,09
36	0,97	1,01	1,01	1,01	1,02	1,02	1,02	1,02	1,05	1,04
40	0,97	1,01	1,01	1,01	1,01	1,01	1,01	1,02	1,03	1,05
45	0,98	1,00	1,01	1,01	1,01	1,01	1,01	1,02	1,03	1,04
52	0,98	1,00	1,01	1,01	1,01	1,01	1,01	1,01	1,01	1,03
60	0,99	1,00	1,00	1,00	1,00	1,00	1,00	1,01	1,02	1,00
70	0,98	1,00	1,00	1,00	1,00	1,00	1,01	1,01	1,02	1,04
80	0,97	1,00	1,00	1,00	1,00	1,01	1,01	1,02	1,03	1,04
90	0,99	1,00	1,00	1,00	1,00	1,01	1,02	1,03	1,04	1,05
100	0,99	1,00	0,99	1,00	1,01	1,01	1,02	1,03	1,04	1,05
110	0,98	1,00	1,00	0,99	1,01	1,01	1,02	1,03	1,04	1,05
120	0,96	0,97	0,99	1,01	1,00	1,01	1,02	1,03	1,04	1,04
135	0,96	0,95	0,97	0,96	0,97	1,02	1,02	1,02	1,03	1,03
150	0,98	0,97	0,97	0,97	0,97	0,96	0,95	1,03	1,02	1,02
160	0,98	0,98	0,98	0,98	0,98	0,97	0,96	0,97	0,98	0,99
170	0,99	0,99	0,99	0,98	0,98	0,98	0,97	0,97	0,97	0,98
180	0,99	0,99	0,99	0,99	0,98	0,98	0,98	0,97	0,97	0,98
Up.Vmg	0,98	1,00	1,00	1,01	1,02	1,01	1,02	1,02	1,03	1,04
Dn.Vmg	0,95	0,95	0,97	0,97	0,96	0,97	0,99	1,04	0,96	1,01

Figure 6: Comparison of the best boat speeds - 1^{st} design version VS Hugo Boss

	4	6	8	10	14	16	20	25	30	35
32	0,97	0,98	0,98	0,99	1,00	1,00	1,01	0,99	1,00	0,95
36	0,97	0,98	0,98	1,00	1,01	1,01	1,01	1,00	1,01	0,97
40	0,97	0,98	0,99	1,01	1,01	1,00	1,00	1,00	1,00	1,01
45	0,97	0,99	1,00	1,01	1,00	1,00	0,99	0,99	0,99	1,00
52	0,97	1,00	1,00	1,00	0,99	0,98	0,98	0,97	0,97	0,98
60	0,98	1,00	1,00	0,99	0,98	0,98	0,96	0,97	0,97	0,94
70	0,98	1,00	0,99	0,98	0,97	0,97	0,96	0,94	0,94	0,95
80	0,98	1,00	0,99	0,98	0,96	0,96	0,95	0,95	0,94	0,94
90	1,00	0,99	0,98	0,97	0,95	0,95	0,95	0,94	0,96	0,97
100	1,00	0,99	0,98	0,97	0,95	0,95	0,94	0,96	0,98	0,99
110	0,99	0,99	0,98	0,96	0,95	0,95	0,95	0,98	0,99	1,01
120	0,96	0,99	0,98	0,98	0,95	0,93	0,97	0,99	1,01	1,02
135	0,95	0,98	0,99	0,96	0,93	0,96	0,97	1,00	1,01	1,03
150	0,98	0,97	0,98	0,99	0,96	0,95	0,93	1,00	1,01	1,02
160	0,99	0,98	0,98	0,99	0,98	0,97	0,95	0,96	0,99	1,01
170	1,00	0,99	0,99	0,99	1,00	0,99	0,97	0,96	0,98	0,99
180	0,99	0,99	0,99	0,99	0,99	0,99	0,98	0,96	0,97	0,99
Up.Vmg	0,97	0,99	1,00	1,01	1,01	1,01	1,00	1,00	1,00	1,00
Dn.Vmg	0,95	0,98	0,99	0,98	0,93	0,93	0,96	1,03	0,96	1,02

Figure 7: Comparison of the best boat speeds - 1^{st} design version VS L'Occitane

It is clear from Figures 6 and 7 that this first hull design attempt is not very successful, especially downwind. It seems slightly faster than Hugo Boss' upwind, particularly in strong winds, but slower in 4 knots of wind for any heading, and for any wind speed past 150°.

When compared to L'Occitane, the designed hull is reasonable under 60°, although not quite improving the upwind performance. Additionally, it is clearly slower at larger angles, especially from 60 to 150 degrees, and 8 to 25 knots, in which conditions the boats usually reach their top speeds (c.f. Appendix B.2).

Although the designed hull slightly improves the upwind performance when compared to Hugo Boss, its overall speed is too low to ensure keeping a reasonable average speed during a race against the reference IMOCAs. These observations led to modify this first version of the design in order to obtain a faster boat, and a second iteration of the design loop was performed. Since L'Occitane was shown to be theoretically faster than Hugo Boss overall, the design changes were inspired from its hull form rather than Hugo Boss'.

2.6.3 Second design iteration

The first hull design was modified in Maxsurf (see Figures 38 and 39 for comparison), and the major design changes include:

- Increase of the volume at the bow, mainly by increasing the hull depth.
- Decrease of the volume at the aft, mainly by decreasing the hull depth.
- Increase of the fairness and smoothness of the hull.
- Optimisation of the bow shape to lower water spray resistance and ease wave piercing.

Figures 8 and 9 present the comparison between the best boat speeds of this second design version and, respectively, Hugo Boss and L'Occitane. Once again, when the speed ratios are over 1, the cells tend to green, and the designed hull is faster than the reference one.

	4	6	8	10	14	16	20	25	30	35
32	1,00	1,02	1,04	1,03	1,02	1,01	1,02	1,05	1,07	1,12
36	1,01	1,03	1,03	1,01	1,01	1,01	1,01	1,01	1,03	1,07
40	1,01	1,03	1,01	1,01	1,01	1,01	1,01	1,01	1,02	1,03
45	1,01	1,03	1,00	1,01	1,01	1,01	1,02	1,02	1,02	1,03
52	1,02	1,01	1,00	1,01	1,02	1,02	1,02	1,03	1,03	1,03
60	1,02	1,00	1,01	1,01	1,02	1,02	1,03	1,04	1,04	1,05
70	1,01	1,00	1,01	1,02	1,03	1,03	1,04	1,05	1,06	1,07
80	1,01	1,00	1,02	1,02	1,03	1,04	1,05	1,06	1,07	1,08
90	1,00	1,01	1,02	1,03	1,04	1,05	1,06	1,07	1,07	1,07
100	1,00	1,01	1,02	1,03	1,05	1,05	1,06	1,06	1,06	1,06
110	1,00	1,01	1,02	1,03	1,05	1,05	1,06	1,05	1,05	1,04
120	1,01	1,00	1,02	1,05	1,04	1,06	1,05	1,04	1,04	1,03
135	1,01	0,98	1,00	1,01	1,04	1,04	1,04	1,03	1,03	1,02
150	1,00	1,00	0,99	0,99	1,01	1,02	1,03	1,03	1,02	1,01
160	1,00	1,00	1,00	1,00	1,00	1,00	1,01	1,02	1,01	1,00
170	1,00	1,00	1,00	1,00	0,99	1,00	1,01	1,01	1,01	1,00
180	1,00	1,00	1,00	1,00	0,99	0,99	1,00	1,01	1,01	1,00
Up.Vmg	1,02	1,03	1,01	1,00	1,01	1,01	1,01	1,01	1,02	1,02
Dn.Vmg	1,01	0,98	0,99	1,00	1,03	1,04	1,04	1,04	1,01	1,01

Figure 8: Comparison of the best boat speeds - final design version VS Hugo Boss

	4	6	8	10	14	16	20	25	30	35
32	1,00	1,00	1,01	1,00	0,99	0,99	0,99	1,00	1,00	0,98
36	1,00	1,00	1,01	1,00	0,99	1,00	0,99	0,99	0,99	1,00
40	1,01	1,01	1,00	1,00	1,00	1,00	1,00	1,00	0,99	0,99
45	1,01	1,01	1,00	1,00	1,00	1,00	1,00	0,99	0,99	0,99
52	1,01	1,01	1,00	1,00	1,00	1,00	1,00	0,99	0,99	0,99
60	1,01	1,01	1,00	1,00	1,00	1,00	0,99	0,99	0,99	0,99
70	1,01	1,01	1,00	1,00	1,00	0,99	0,99	0,99	0,98	0,98
80	1,01	1,01	1,00	1,00	0,99	0,99	0,99	0,99	0,97	0,97
90	1,01	1,00	1,00	1,00	0,99	0,99	0,99	0,98	0,99	0,99
100	1,02	1,00	1,00	1,00	0,99	0,99	0,98	0,99	1,00	1,00
110	1,01	1,00	1,00	1,00	0,99	0,98	0,99	1,00	1,00	1,00
120	1,01	1,02	1,00	1,02	0,98	0,98	0,99	1,00	1,01	1,01
135	1,01	1,02	1,02	1,01	0,99	0,98	1,00	1,01	1,01	1,01
150	1,00	1,00	1,00	1,01	1,01	1,01	1,01	1,00	1,01	1,01
160	1,00	1,00	1,00	1,00	1,00	1,00	1,00	1,01	1,02	1,03
170	1,00	1,00	1,00	1,00	1,01	1,00	1,00	1,00	1,01	1,01
180	1,00	1,00	1,00	1,00	1,00	1,00	1,00	1,00	1,00	1,01
Up.Vmg	1,01	1,01	1,00	1,00	1,00	1,00	1,00	0,99	0,99	0,99
Dn.Vmg	1,01	1,02	1,02	1,01	1,00	1,00	1,01	1,03	1,02	1,02

Figure 9: Comparison of the best boat speeds - final design version VS L'Occitane

When comparing Figures 8 and 9 obtained for this second hull design to Figures 6 and 7 obtained for the first one, it is clear that the re-design process enhanced the boat speeds. Indeed, when compared to Hugo Boss', the new hull is faster overall, and particularly in the range of interest (from 60° to 150°, and 8 to 35 knots). The upwind and downwind VMG show that the design globally dominates, although in 6 and 8 knots of wind, its downwind VMG is slightly smaller than Hugo Boss' (by a maximum of 2%).

Regarding the comparison with L'Occitane, the new design is slightly faster under 10 knots of wind regardless of the heading (probably due to its smaller WSA), and when sailing over 135° for any wind speed. However, it is still slightly slower in the range of interest, by a maximum amount of 3%, which is still acceptable considering that it is the case for only two values ([30 kts; 80°] and [35 kts; 80°]). Both upwind and downwind VMG are satisfying, and the new hull form design would possibly be an interesting opponent for the reference IMOCAs. Considering these promising results, and the unavailability of an optimisation software coupled with the VPP, which would have allowed to easily realise more iterations, this second design version was chosen as final hull form. The drawings presented in Appendix I show its main particulars.

3 Design of the appendages

Designs were also proposed for the keel, foils, and rudders, since they had to be manufactured and attached to the model scale hull to perform the tank tests (see later). The design choices were based on existing designs, as explained below. Drawings 04, 05, and 06, depicted in Appendix I, show their main characteristics.

3.1 Keel

The shape of the keel and bulb were inspired from existing ones, and they were modelled in Maxsurf Modeler. The keel span was maximised up to the water draft limitation of 4.5 meters imposed by the class rules, to increase its efficiency, and lower the bulb as much as possible, to improve the righting moment of the boat. The angle between the vertical and the keel (longitudinal angle) was fixed to 6 degrees, to respect the range (4 to 9 degrees) imposed by the rules. The keel profile was chosen as a NACA0010 (c.f. drawing 04 of Appendix I).

3.2 Foils

Based on a comparative study of the assets of different foil sections [11], the Eppler 817 foil section was chosen for its very good overall performance, and because it is supposed to be less likely to ventilate close to the free surface, compared to other classic foil sections. After a revue of existing IMOCA foil designs, the geometry of the foils was inspired from the one of the IMOCA team 11th Hour Racing Team, which is considered among the most proven nowadays. 'They are the best foils ever made up to date', explained the famous french naval architect Guillaume Verdier [12]. Their very flat shape supposedly generates more vertical lift than foils with more curvature, which is interesting to better lift the boat out of the water and reduce its drag. The foils were modelled in Rhinoceros® (c.f. drawing 05 of Appendix I).

3.3 Rudders

The rudders were also modelled in Rhinoceros®, and their geometry was inspired from typical IMOCA twin rudders with a high aspect ratio. Their profile was chosen to be a NACA0063 (c.f. drawing 06 of Appendix I).

4 Theoretical model for foil performance prediction

A theoretical model was developed in Excel to predict the hydrodynamics around the designed foil, and assess its influence on the boat. It will be used as a benchmark for the validation of the experimental results, and to consider the designed foils in the VPP predictions, by computing the revised righting lever arm of the boat with its foils (see later). The methodology around the model is described in the following, and its major elements are presented in Appendix C.

4.1 First model version

4.1.1 Major assumptions, equations and development procedure

The model first allows to find the lift, drag, and side force created by a chosen foil design, at a chosen angle of attack, chosen boat speeds, and angles of heel and leeway. It was developed under the assumptions of the lifting-line theory, whose major assumption is to consider that the foil can be represented by linear sections on which the lift, drag, and side force components are computed. Four sections were used, and their spans s_i and angles to the horizontal α_i were chosen to represent the geometry of the designed foil, as accurately as possible (c.f. Figure 10).

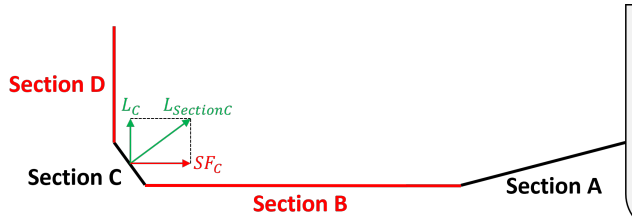

	Section A	Section B	Section C	Section D	Entire foil
Span s (m)	1	1.8	0.3	0.75	3.85
Angle to horizontal α (m)	10	0	45	90	-
Horizontal span (m)	0.98	1.8	0.21	0	3.00

Figure 10: Foil decomposition in sections and geometrical properties

The lift $L_{section}$ and drag $D_{section}$ are first computed on each foil section, in directions relative to the section (respectively perpendicular and parallel to it). They are then projected in common directions relative to the waterplane, to allow summing the contribution of the different foil sections considered. Note that this is illustrated in Figure 10 for the lift on section C. This summation leads to the overall hydrodynamic forces created by the entire foil, i.e. the lift L in a direction z perpendicular to the waterplane, the drag D in a direction x parallel to the waterplane, and the side force SF in a direction y also parallel to the waterplane.

The equations used to compute the forces and project them in the directions relative to the waterplane were inspired from a previous project written by Timothée Villain-Amirat [13]. They were derived again using trigonometry to better grasp their origin, and their demonstrations are proposed in Appendix C.4. Some of them were modified to better represent the physics of the problem. These equations are presented and explained below.

The lift and drag are initially computed on each foil section using equations 1 and 2, in the directions relative to each of them (lift perpendicular to the section, drag parallel to it).

$$L_{section} = \frac{1}{2}\rho A V_{app}^2 C_l^{3D} \tag{1}$$

$$D_{section} = \frac{1}{2}\rho A V_{app}^2 C_d^{3D} \tag{2}$$

Where $\rho = 1025\,kg/m^3$ is the sea water density, and A is the planform area of the section, given by the product of its span s and chord c, s.t: $A = s \times c$.
C_l^{3D} and C_d^{3D} are respectively the 3D lift and drag coefficients of the chosen Eppler 817 section, computed from the 2D coefficients C_l^{2D} and C_d^{2D} (found using the software Xfoil for a range of angles of attack, c.f. Table 35), s.t: $C_l^{3D} = \frac{C_l^{2D}}{1+3/AR}$ and $C_d^{3D} = C_d^{2D} + C_{di}$.
C_{di} is the induced drag coefficient, given by: $C_{di} = \frac{C_l^{3D}}{\pi \times AR}$, and AR is the aspect ratio of the section, s.t: $AR = \frac{s}{c} \times AR_{eff}$. The effective aspect ratio multiplier AR_{eff} is used to account for tip losses. V_{app} is the apparent speed of the flow seen by the considered foil section. It was found from trigonometry (see proof in Appendix C.4), and writes:

$$V_{app} = \sqrt{(V_b \times sin\gamma \times sin(\alpha \pm \theta))^2 + (V_b \times cos\gamma)^2} \tag{3}$$

V_b is the boat speed in m/s, α is the angle that the foil section makes with the horizontal waterline when the boat is upright, and γ and θ are respectively the leeway and heel angles of the boat. The angle $(\alpha_i \pm \theta)$ is the angle that a given foil section i ($i = \{A, B, C, D\}$) makes with the horizontal waterline when the boat heels to an angle θ. Under the assumptions that the foil is located starboard, and that the boat heels towards starboard, this angle is found for each foil section as shown in Figure 11.

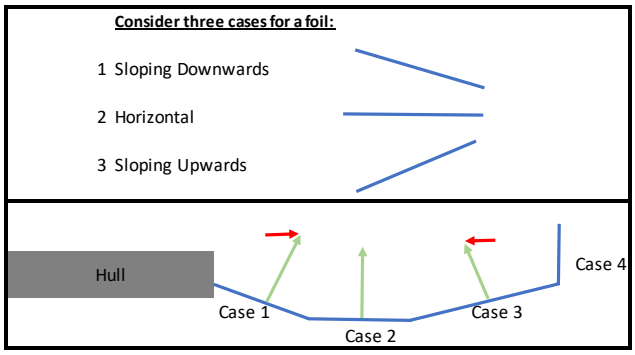

Angle α of foil to horizontal waterline		
Case 1: Downwards	10	deg
Case 2: Horizontal	0	deg
Case 3: Upwards	45	deg
Case 4: Upwards	90	deg
Angle ($\alpha \pm \theta$) of foil to heeled waterline		
Case 1: Downwards		($\alpha + \theta$)
Case 2: Horizontal		($\alpha + \theta$)
Case 3: Upwards		($\alpha - \theta$)
Case 4: Upwards		($\alpha - \theta$)

Figure 11: Convention chosen to determine the angles of the foil sections to the waterline

When the boat heels towards starboard, the angles α_A and α_B (resp. cases 1 and 2 in Figure 11) increase s.t. $(\alpha_A + \theta)$ and $(\alpha_B + \theta)$, whereas α_C and α_D (resp. cases 3 and 4) decrease s.t.

$(\alpha_C - \theta)$ and $(\alpha_D - \theta)$. It is worth noticing that α_C decreases with heel as long as $\theta \leq \alpha_C$, which is the case since the largest heel angle considered is 25 degrees.

Once $L_{section}$ and $D_{section}$ are known, equations 4 to 6 are used to project these forces in the directions relative to the waterplane (respectively perpendicular and parallel to it), and deduce the resulting side force. This is achieved for each foil section i, at any angle of heel and leeway of the boat.

$$L_i = (L_{section} \cos\xi - D_{section} \sin\xi) \times \cos(\alpha \pm \theta) \times k_1 \tag{4}$$

$$D_i = (L_{section} \sin\xi + D_{section} \cos\xi) \times \cos(\gamma - \eta) \tag{5}$$

$$SF_i = (L_{section} \cos\xi - D_{section} \sin\xi) \times \sin(\alpha \pm \theta) \times k_3 \tag{6}$$

k_1 and k_3 are factors implemented to account for the sign of the lift and side force, s.t:

$$k_1 = \begin{cases} 1, & \text{if lift upwards} \\ -1, & \text{if lift downwards} \end{cases} \qquad k_3 = \begin{cases} 1, & \text{if SF towards hull} \\ -1, & \text{if SF outwards hull} \end{cases} \tag{7}$$

ξ and η are respectively the apparent angle of attack in the plane perpendicular to the foil section, and the apparent leeway angle in the plane of the foil. They are found for each foil section using the following trigonometric expressions (proofs in Appendix C.4).

$$\xi = \tan^{-1}\left(\frac{\sin\gamma \times \sin(\alpha \pm \theta)}{\cos\gamma}\right) \tag{8}$$

$$\eta = \tan^{-1}\left(\tan\gamma \sin^2(\alpha \pm \theta)\right) \tag{9}$$

Finally, the hydrodynamic forces generated by the entire foil in the directions relative to the waterplane are found by summing L_i, D_i, and SF_i over each section i, s.t:

$$L = \sum_i L_i \tag{10}$$

$$D = \sum_i D_i \tag{11}$$

$$SF = \sum_i SF_i \tag{12}$$

This procedure was achieved for four chosen boat speeds, heel, and leeway angles. The angle of attack of the foil is fixed but can be changed, which changes the value of the lift and drag coefficients used in equations 1 and 2 (c.f Table 35 of Appendix C). Based on the most frequent boat speeds found from the VPP analysis performed using the final hull form design (c.f Table 26 of Appendix B), it was decided to carry out the theoretical predictions at $V_b = 10,\ 15,\ 20,\ 25$ knots, since the boat is theoretically more likely to sail at these speeds. The heel angles were chosen as $\theta = 0,\ 5,\ 15,\ 25$ degrees, and the angle of attack of the foil was fixed to 2°. Table 10 presents the foil sections' parameters used as input data for the calculations.

Table 10: Foil sections' parameters used as input

Foil section	**A**	**B**	**C**	**D**
Span c (m)	1.0	1.8	0.3	0.75
Chord c (m)	0.5	0.5	0.5	0.5
α (°)	10	0	45	90
A (m^2)	0.5	0.9	0.15	0.375
AR_{eff} (-)	1.6	1.0	1.4	1.2
AR (-)	3.2	3.6	0.84	1.8
k_1 (-)	1	1	1	1
k_3 (-)	-1	-1	1	1

4.1.2 Foil immersion assessment

In order to obtain realistic hydrodynamic forces, one must account for the immersion of the different foil sections, since the forces are proportional to the immersed area of each section (c.f. equations 1 and 2). Therefore, a routine was developed to accurately determine the immersions, depending on the heel angle of the boat. Using Maxsurf Stability, a large angle stability analysis was performed to find the heeled equilibrium of the boat. For each considered heel angle, the body plan view was exported to Autocad® on which the foil was drawn, as shown in Figure 12.

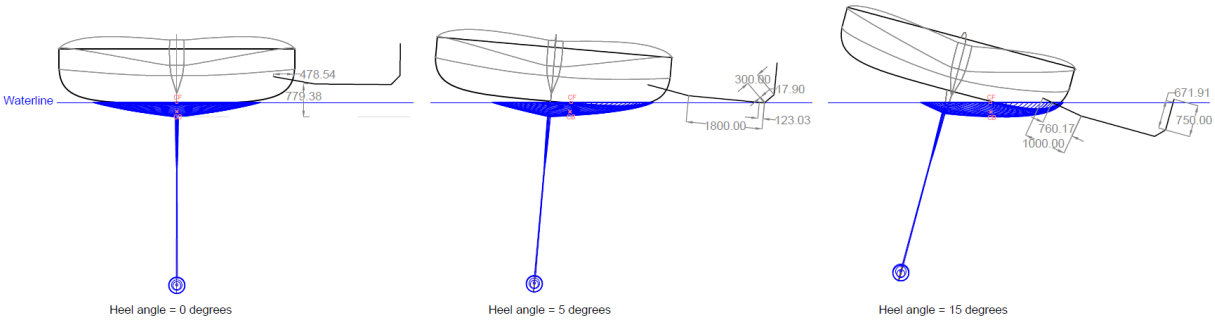

Figure 12: Drawings to find the foil sections immersions

Note that the boat's aft section is highlighted in black to indicate that it is at the foreground of the drawings, meaning that the boat heels towards starboard with its foil attached on the same

side, as assumed previously. The case $\theta = 25°$ is not drawn since the foil is fully immersed.

The position of the foil was taken as on the model scale hull form, to later be able to accurately compare the predictions with the results of the experimental tank tests. The dimensions indicated in the zero heeled case of Figure 12 (given in mm) were used to place the foil at this position in each drawing. Similar dimensions are indicated to measure the immersed span of the sections. This allowed to compute the immersion of each section, in each heeled case, s.t:

$$\text{Immersion} = \frac{\text{Immersed span}}{\text{Total span}} \times 100 \tag{13}$$

Equations 1 and 2 were then modified to account for the immersion of the foil sections, and the hydrodynamic forces were reduced proportionally (equations 14 and 15).

$$L_{section} = \frac{1}{2}\rho A V_{app}^2 C_l^{3D} \times \text{Immersion} \tag{14}$$

$$D_{section} = \frac{1}{2}\rho A V_{app}^2 C_d^{3D} \times \text{Immersion} \tag{15}$$

Note that the results of the calculations performed following the aforementioned procedure, for each considered boat speed, heel, and leeway angle, can be found in Appendix C, in which Tables 36 to 39 also give the contribution of each foil section to the overall lift, drag and side force generated by the foil. Table 40 presents the results found for the entire foil. These results are discussed in section 4.1.4.

4.1.3 Determination of the righting moment added by the foils

Once the foil's hydrodynamic forces are known for each boat speed, heel, and leeway, the horizontal and vertical lever arms of the foil can be calculated to deduce the righting moment that it generates in each case. The righting moment of the boat with its foils can then be found, and its corresponding revised righting lever GZ is deduced. This is detailed below.

The righting moment created by the immersed foil is determined using equation 16.

$$RM_{foil} = L \times d_1 - SF \times d_2 = M_1 - M_2 \tag{16}$$

Where d_1 and d_2 are respectively the horizontal and vertical righting lever arms of the foil, corresponding to its horizontal center of lift and vertical center of side force. d_1 is measured horizontally from the boat's centreline ($x = 0$), and d_2 vertically from the DWL ($z = 0$), as shown in Figure 13.

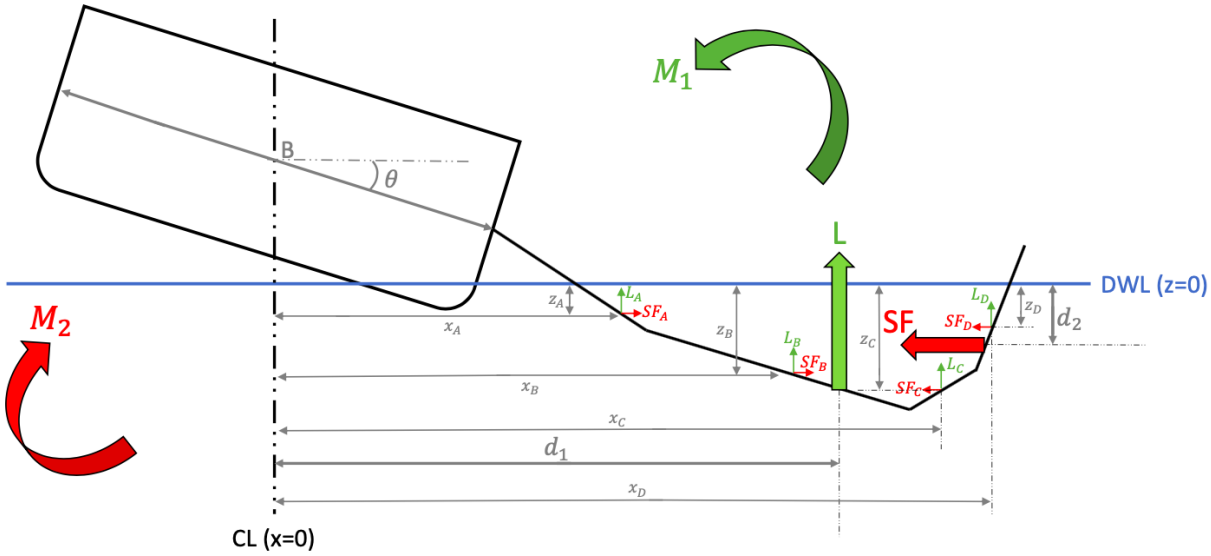

Figure 13: Sketch to determine the lever arms of each immersed section

As equation 16 and Figure 13 show, the foil's lift creates a counterclockwise moment $M_1 = L \times d_1$ acting about the boat's centreline. It is reduced by a clockwise moment $M_2 = SF \times d_2$ coming from a positive SF (towards the hull), and acting about the DWL. Due to the foil's geometry, the lift generated is greater than the SF in all cases (c.f. Table 40), and since the heel angle is limited to 25 degrees, $d_1 > d_2$ (c.f. Table 44), implying that $M_1 > M_2$. This means that the foil increases the moment of the boat, even if it would generate positive SF. It actually generates negative SF (see Table 40), meaning that M_2 is added to M_1, as per equation 16.

The lever arms d_1 and d_2 are determined using the following weighted average equations:

$$d_1 = \frac{\sum_i (L_i \times x_i)}{\sum_i L_i} \tag{17}$$

$$d_2 = \frac{\sum_i (SF_i \times z_i)}{\sum_i SF_i} \tag{18}$$

Where x_i and z_i are respectively the horizontal center of lift and vertical center of SF of section i (also taken from the CL and the DWL, as shown in Figure 13). These distances vary with heel, since the immersion of the foil sections, and thus the location of the forces, depend on it. They are calculated for each section using the equations shown in Appendix C.2.2. The values found for x_i, z_i, d_1, d_2, and RM_{foil} in each heeled case, are presented in Tables 43 and 44.

Once RM_{foil} is known in the different heeled cases considered, the static righting moment of the boat without its foils RM_{boat} is computed for the different heel angles using equation 19.

$$RM_{boat} = GZ \times \Delta \times g \tag{19}$$

GZ is the righting lever of the boat without its foils, found using Maxsurf Stability, $\Delta = 7864\,kg$ is the boat's displacement, and $g = 9.81\,N/kg$ is the acceleration of gravity used to convert Δ in newtons. Table 11 presents the GZ values given by Maxsurf for the different heel angles considered, and the corresponding RM_{boat} values calculated using equation 19.

Table 11: GZ and righting moment of the boat without foils

Heel (deg)	GZ **(m)**	RM_{boat} **(N.m)**
0	0	0
5	0.627	48370.44
15	1.5	115718.76
25	2.014	155371.72

The overall righting moment of the boat with its foils is found by adding the foil's righting moment RM_{foil} to the boat's static righting moment RM_{boat}, and the equivalent revised righting lever arm of the boat with its foils GZ' can be found using equation 20.

$$GZ' = \frac{(RM_{boat} + RM_{foil})}{\Delta \times g} \tag{20}$$

GZ' is computed for each boat speed, heel, and leeway angle considered. It is later used to replace the original GZ value in the VPP, to consider the foils in the analysis (section 8).

Figure 14 presents a comparison between the initial GZ of the boat without foils, and the revised values with foils, for different boat speeds. Note that the GZ' values are shown for a leeway angle $\gamma = 0°$.

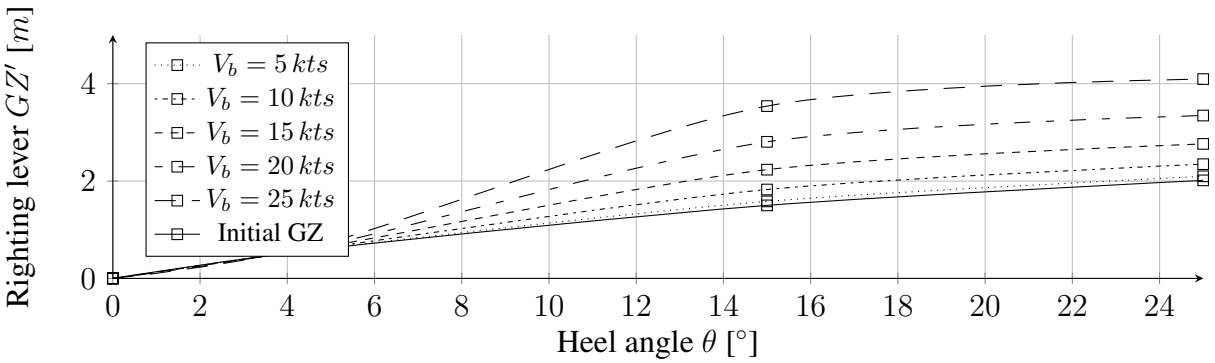

Figure 14: Influence of the foils on the righting lever GZ, leeway=0°

As mentioned earlier, the immersed foil creates a positive (counterclockwise) righting moment RM_{foil} which increases the overall righting moment of the boat. Since the boat's displacement is constant, this yields larger equivalent righting lever values (as per equation 20). This additional moment increases with boat speed and heel, since the lift (hence side force) generated by the foil increases with V_b, and the foil's immersion increases with heel. This leads to increasing revised GZ values, as seen in Figure 14.

The same GZ' calculation was then performed accounting for the cant angle of the keel, which is often canted on an Open 60 to increase even more its righting moment. Since the IMOCA class restricts the cant angle to a maximum of 38 degrees, this angle was chosen to better visualise the effect of the canted keel on the righting moment and corresponding GZ. The LCG and TCG of the canted keel and bulb were computed and updated in Maxsurf Stability's loadcases to consider their new positions. A large angle stability analysis was performed again, and the new GZ values given by Maxsurf were used in equation 19 to compute the corresponding static righting moment RM_{boat} (c.f. Table 12).

Table 12: GZ and righting moment of the boat without foils - keel canted

Heel (deg)	GZ **(m)**	RM_{boat} **(N.m)**
0	1.058	81620.30
5	1.623	125207.70
15	2.337	180289.83
25	2.716	209528.10

It is clear when comparing Tables 11 and 12 that the canted keel increases the initial GZ of the boat. As realised previously, GZ' is computed using the same RM_{foil}, and the new RM_{boat} values, and the increase of righting lever due to the foil is shown in Figure 15.

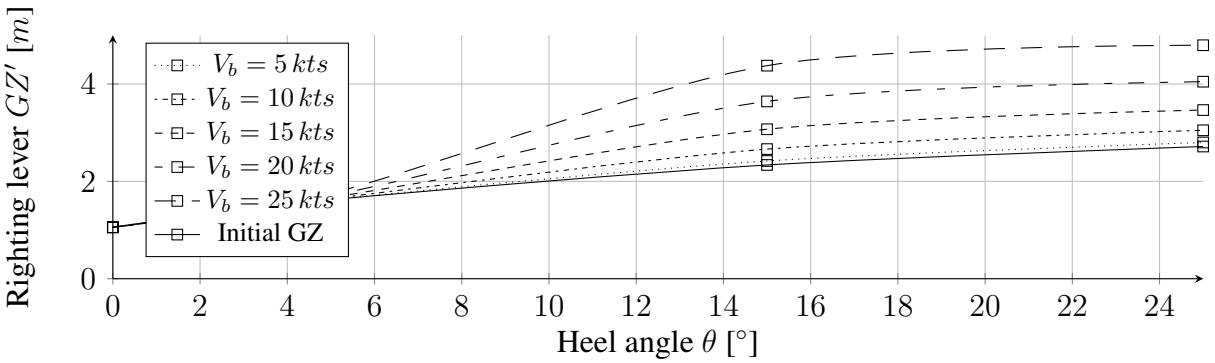

Figure 15: Influence of the foils on the righting lever GZ, leeway=0° - keel canted

Similar GZ curves as in Figure 14 are seen, which comes from the fact that RM_{foil} was unchanged. Only RM_{boat} was increased due to the cant angle of the keel, leading to a global increase of the equivalent revised righting lever GZ'. Note that the values of RM_{foil}, RM_{boat}, GZ, and GZ', found for each boat speed, heel, and leeway, and for both keel cant angles, are presented in Tables 44 and 45 of Appendix C.

4.1.4 Major results and analysis

The hydrodynamic data found for the entire foil (given in Table 40) is presented in the following. Figure 45 shows 3D plots of the overall lift, drag, and side force generated by the foil. The

plots show all the foil's hydrodynamic forces data gathered by the model, as the forces are plotted against the different boat speeds, heel, and leeway angles considered. In order to better visualise the evolution of these forces with boat speed, heel, and leeway, 2D plots are preferred, and presented in Figures 16 and 17. They respectively highlight the influence of the heel and leeway angles on the forces, by respectively showing values for a fixed leeway angle of 1° and varying heel angles, and for a fixed heel angle of 15° and varying leeway angles. The absolute value of the SF is plotted since it is always negative, meaning that it is directed outwards the hull. This is the case since the foil sections A and B create more SF than sections C and D.

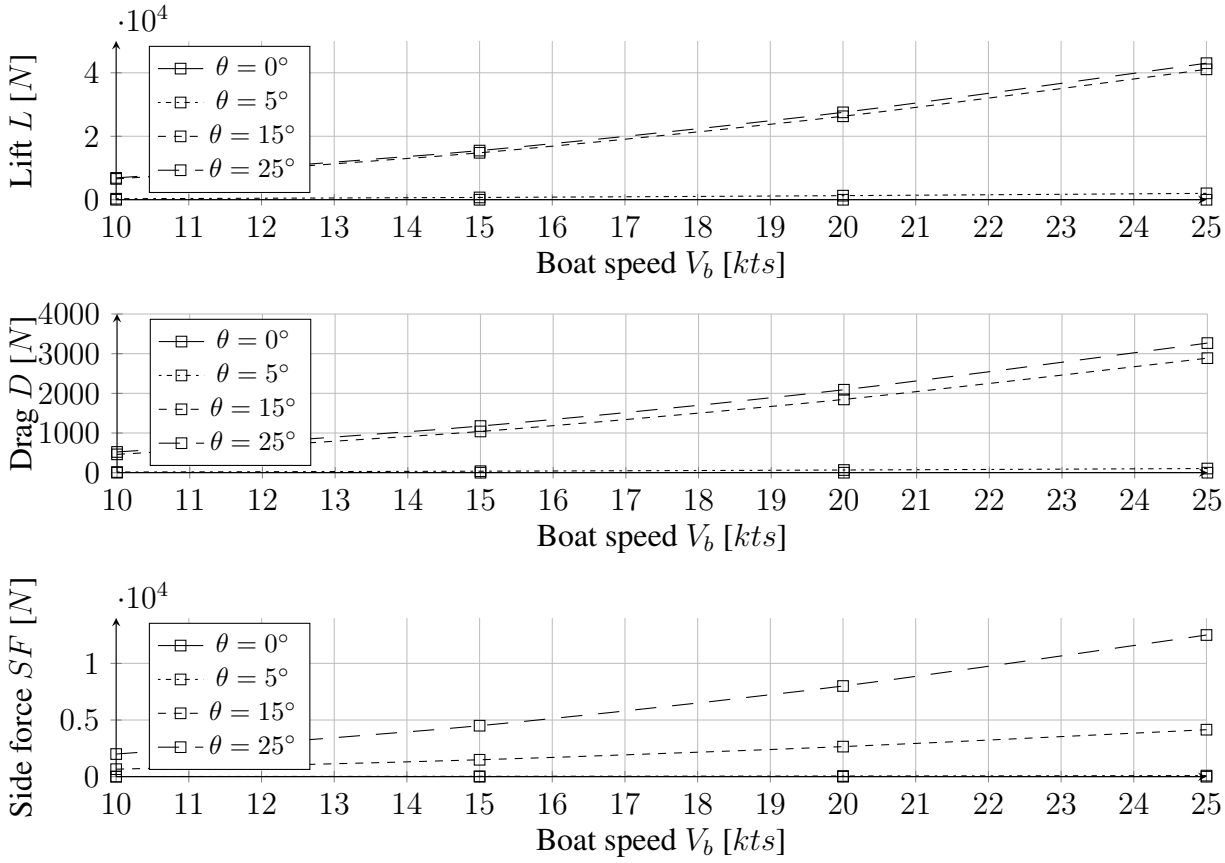

Figure 16: Influence of heel angle on foil's hydrodynamic forces, leeway=1°

It can be seen in Figure 16 that the three forces follow a similar quadratic increase with boat speed, which is expected from equations 1 and 2. The lift generated by the foil is about thirteen (at $\theta = 25°$) to twenty (at $\theta = 5°$) times larger than its drag (see L/D ratios in Table 40), and about three (at $\theta = 25°$) to twenty (at $\theta = 5°$) times larger than its side force. All the forces are zero at $\theta = 0°$, since the foil is out of the water when the boat is upright, and almost zero at $\theta = 5°$, since it barely touches the water (c.f. immersions in Table 40). At $\theta = 15°$, the foil is immersed at 91,4 %, and it is fully immersed at $\theta = 25°$, which plays a role in increasing the forces equally between 15° and 25° of heel. However, it is seen that the increase is not the same for all the forces, as the lift does not seem very affected by this change of heel, while the drag slightly more, and the side force much more. The small increase in lift observed from 15°

to 25° of heel, can be understood from the fact that, the reduction of lift from 15° to 25° due to the angle of the foil to the horizontal waterline, is slightly smaller than the increase due to the considered immersions. Also, the increase in drag from 15° to 25° seems logical since the overall lift and side force are larger at $\theta = 25°$, which implies more induced drag. The increase of side force comes from the fact that a larger part of the foil is inclined at 25° of heel.

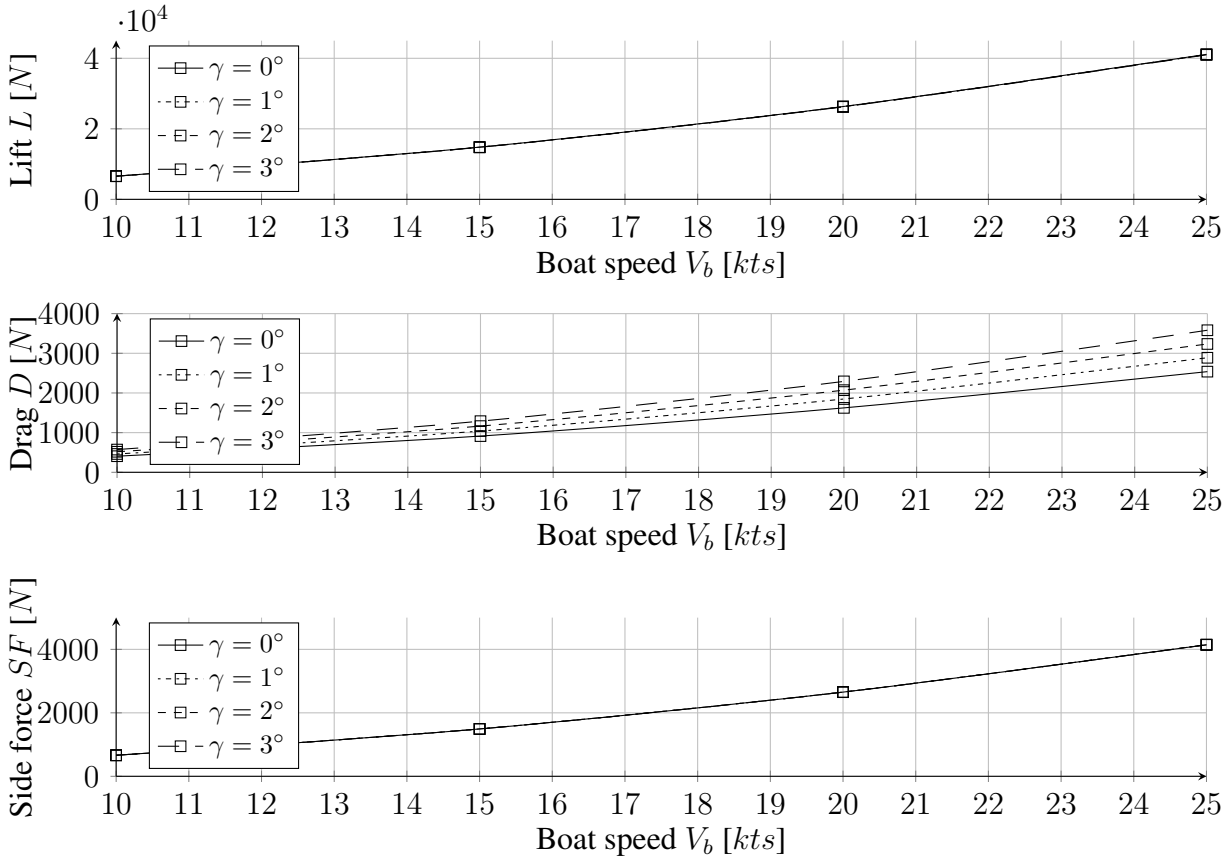

Figure 17: Influence of leeway angle on foil's hydrodynamic forces, heel=15°

Regarding the leeway angle influence highlighted in Figure 17, it is seen that the lift and side force are almost not affected by leeway, only slightly reduced (see numerical values in Table 40), while the drag increases with it. This is also seen in the 3D plots (c.f. Figure 45).

4.2 Second model version

4.2.1 Major improvements

Since the boat is supposed to be vertically lifted out of the water by the upward lift generated by the foil, it was decided to try to improve the first model version presented above, in order to consider the reduction of the boat's displacement due to the foil's lift. The corresponding draft of the boat was found, which allowed to retrieve more realistic immersions of the foil sections. The magnitudes of the hydrodynamic forces were then updated using equations 14 and 15.

Since the foil's lift varies between each boat speed, heel, and leeway angle, the displacement should be reduced in each case. Yet, it was decided to do it for a constant leeway angle $\gamma = 0°$ to reduce the number of cases, since the lift does almost not vary with leeway (c.f. Figure 17).

The new displacement of the boat Δ' is its original displacement $\Delta = 7.864\,t$ reduced by the amount of upward lift produced by the foil, at a given boat speed V_b and heel angle θ, s.t:

$$\Delta'(V_b, \theta) = \Delta - \frac{L(V_b, \theta)}{9.81} \times 0.001 \tag{21}$$

Where the upward lift L generated by the foil is converted from newtons to tons. This new displacement value was computed for each considered boat speed and heel angle. In each case, the corresponding draft T' was found using Maxsurf Modeler. The values found are presented in Table 13. The lift values are taken from the first model's results, and will be updated after finding the new immersions of the foil sections.

Table 13: Calculation of the updated displacement, and corresponding draft

V_b **(m/s)**	θ (°)	**Foil's lift** L **(N)**	**New displacement** Δ' **(t)**	**New draft** T' **(m)**
10	0	0	7.864	4.500
	5	322.31	7.831	4.500
	15	6579.79	7.193	4.487
	25	6889.64	7.162	4.486
15	0	0	7.864	4.500
	5	725.19	7.790	4.498
	15	14804.54	6.355	4.469
	25	15501.68	6.284	4.468
20	0	0	7.864	4.500
	5	1289.23	7.733	4.498
	15	26319.18	5.181	4.444
	25	27558.55	5.055	4.440
25	0	0	7.864	4.500
	5	2014.42	7.659	4.496
	15	41123.71	3.672	4.406
	25	43060.23	3.475	4.400
35	0	0	7.864	4.500
	5	3948.26	7.462	4.492
	15	80602.47	-0.352	4.080
	25	84398.04	-0.739	4.071

Table 13 shows that the displacement and draft are more reduced at higher boat speeds since the foil's lift is greater. The case $V_b = 35\,kts$ was considered to understand what happens at a top speed, where the foil's lift is much larger. It is doubled from $V_b = 25\,kts$ to $V_b = 35\,kts$, which implies that the new displacement Δ' becomes negative. In this scenario, the boat is fully lifted out of the water by the immersed foil, which is often seen on Open 60s at such speeds.

4.2.2 Foil immersion assessment

For each [boat speed, heel angle] configuration, the new displacement Δ' was implemented in Maxsurf Stability, and a large angle stability analysis was performed to find the position of the boat on the waterline. The body plan view was exported to Autocad® to draw the new immersions of the foil sections, as previously realised. This is depicted in drawing 00 of Appendix C.3.2. As before, the dimensions indicated on the drawings allowed to compute the new immersions of the foil sections (according to equation 13). Their values are presented in Tables 46 to 49, together with the updated hydrodynamic forces. The results found for the entire foil are given in Table 50. The major difference from the first model version is that the foil's immersions now depend on boat speed, and are reduced at $\theta = 5,\ 15°$, as highlighted by Table 14.

Table 14: Comparison of the foil immersion for first and second model versions

Boat speed (kts)	**Heel (°)**	**Im. 1^{st} model (%)**	**Im. 2^{nd} model (%)**
10	0	0	0
	5	3.20	3.12
	15	91.40	89.10
	25	100	100
15	0	0	0
	5	3.20	2.66
	15	91.40	87.34
	25	100	100
20	0	0	0
	5	3.20	2.48
	15	91.40	84.19
	25	100	100
25	0	0	0
	5	3.20	1.83
	15	91.40	78.96
	25	100	100

4.2.3 Determination of the righting moment added by the foils

The procedure followed in the first model version is used again to compute the righting moment added by the immersed foil, and deduce the equivalent revised GZ', for different boat speeds. x_i and z_i were computed using the same equations (see Tables 41 and 42), but since the immersions of the foil sections now vary with boat speed, these distances were assessed for each boat speed and heel angle configuration. The values found are given in Table 51 of Appendix C.

As previously, Figures 18 and 19 present the increase of righting lever arm GZ due to the presence of foils on the boat, both with an upright and canted keel. In comparison with the first model version, the boat's static moment RM_{boat} is unchanged, but the foil's righting moment

RM_{foil} is modified, since the magnitudes of L and SF are reduced by the new immersions of the foil sections. This also leads to slightly different lever arms x_i and z_i, and therefore updated d_1 and d_2 values. All the righting moment data gathered by the model is given in Tables 52 and 53 of Appendix C.

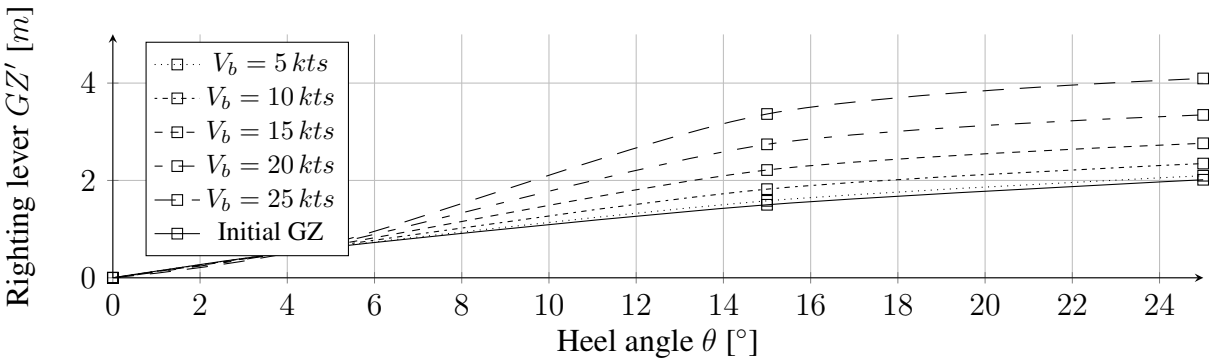

Figure 18: Influence of the foils on the righting lever GZ

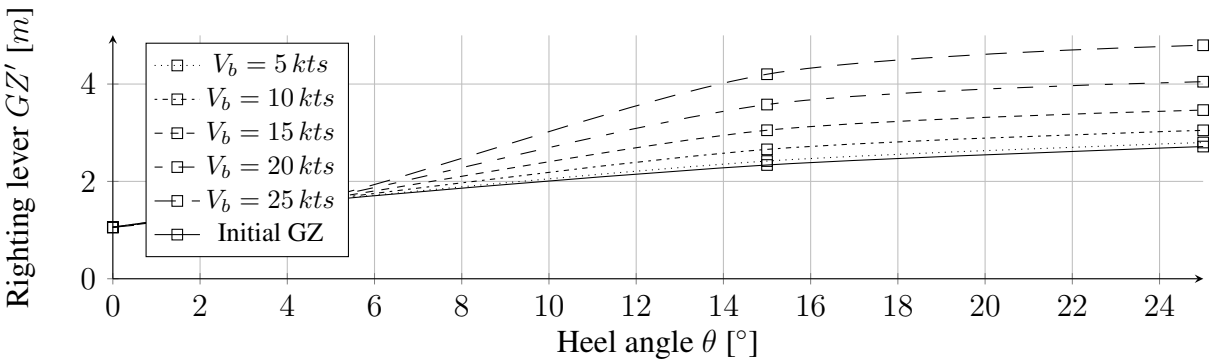

Figure 19: Influence of the foils on the righting lever GZ - keel canted

When compared to Figures 14 and 15 obtained with the first model version, it can be seen that the revised GZ' values are slightly smaller for $\theta = 5°$ and $\theta = 15°$. This is resulting from the fact that L and SF became smaller with the new immersions. This reduction is larger at higher boat speeds, since the immersions were more reduced due to a greater foil's lift.

4.2.4 Major results and comparison with the first model version

The same data as for the first model version is presented below for comparison. The 3D plots are depicted in Figure 46 of Appendix C. Figures 20 and 21 present the variation of the new hydrodynamic forces with heel and leeway. Note that the data plotted is taken from Table 50.

Similar comments previously made for Figure 16 can be deduced from Figure 20. However, when the foil is partially immersed (at $\theta = 5°$ and $\theta = 15°$), the new immersions reduce slightly the forces, and even more at higher boat speeds (c.f. Table 14). This is also the case when comparing Figures 17 and 21, and the curves have slightly less curvature than before.

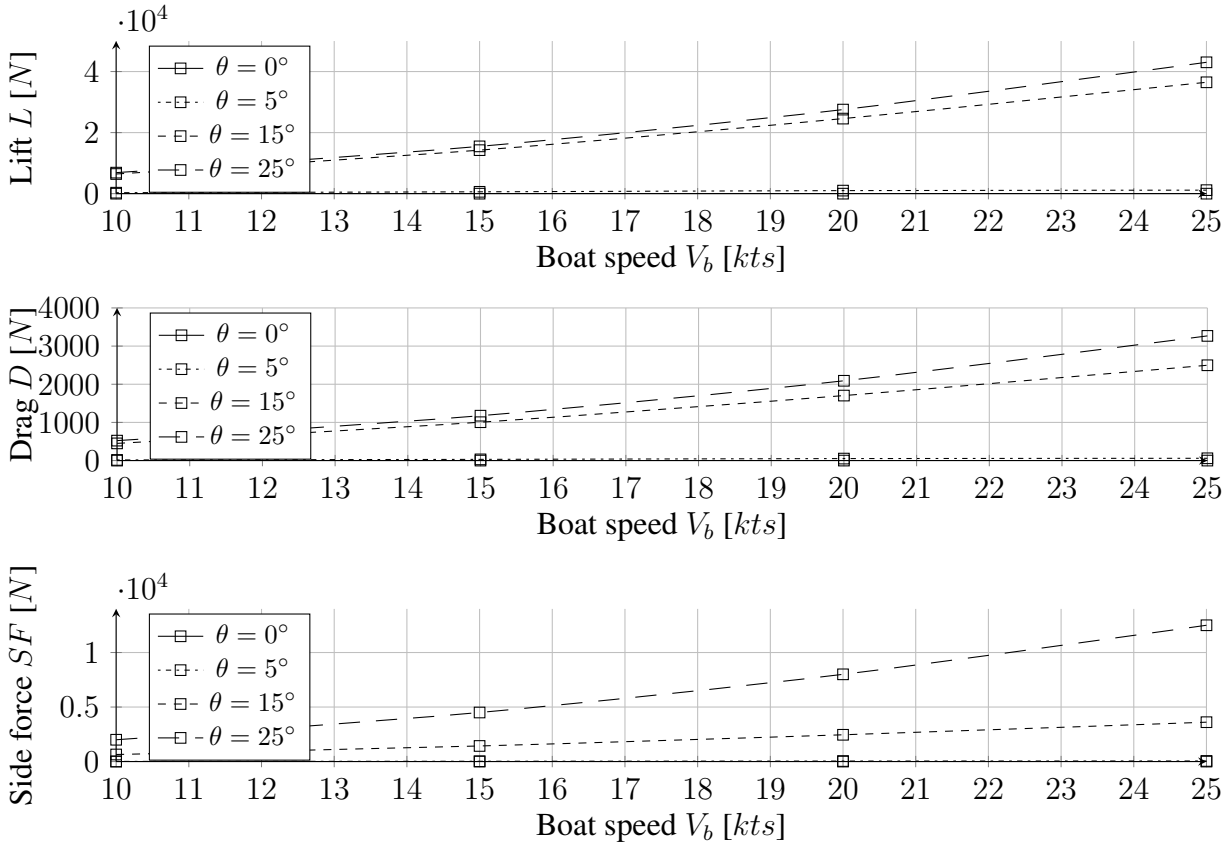

Figure 20: Influence of heel angle on foil's hydrodynamic forces, leeway=1°

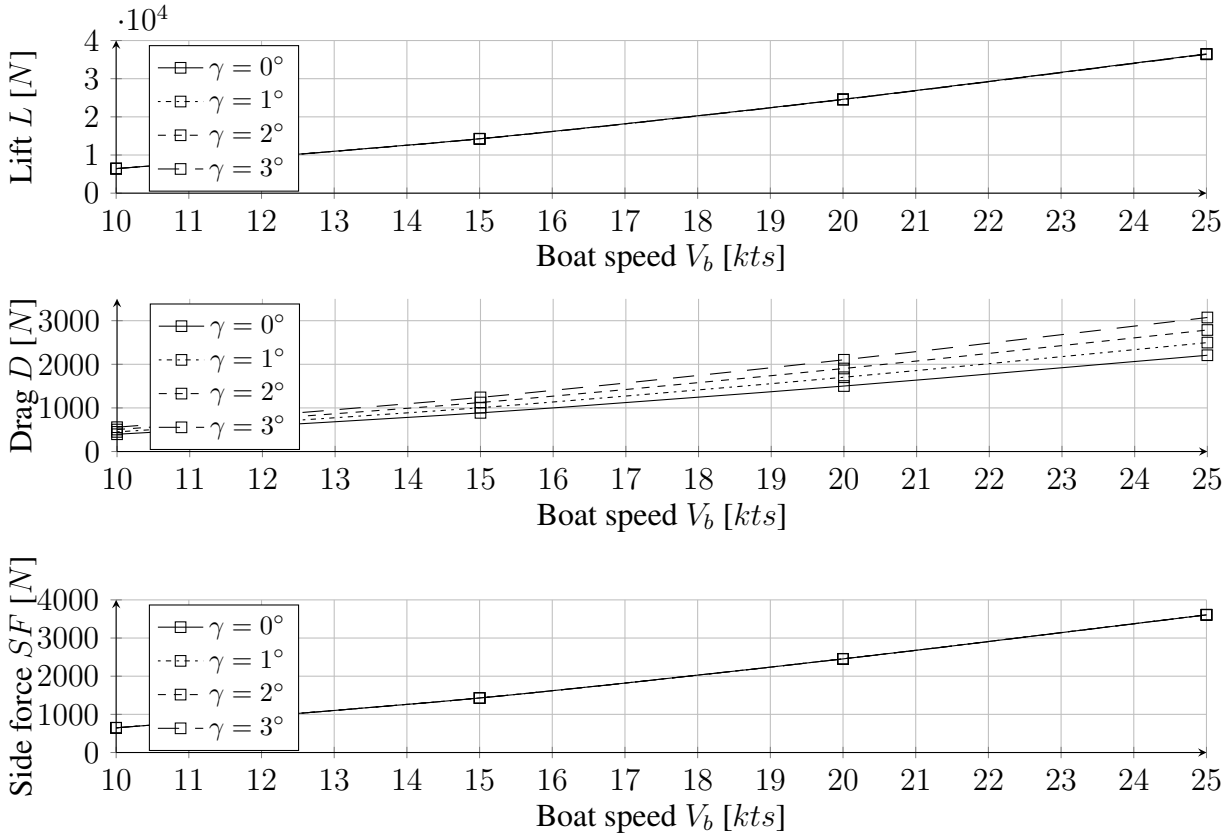

Figure 21: Influence of leeway angle on foil's hydrodynamic forces, heel=15°

5 Manufacturing of the model scale hull form and appendages

The steps followed to manufacture the model scale hull and appendages to be tank tested, are explained in the following. All the work was performed in the workshop of the university, dedicated to ship design. Some pictures are presented in Appendix D to illustrate the work.

5.1 Manufacturing of the hull

Drawing 07 presented in Appendix I shows the 3D model made in Rhinoceros® and sent to the manufacturing department of the university ("Monstercam"), to be CNC milled in a block of polystyrene. Considering the dimensions of the boat, the ones of the towing tank, and its maximum driving speed, it was decided to scale the model by 10, which gives it the largest size that allows to test the fast speeds of the boat. The 3D Rhino model of the hull was scaled accordingly, and the deck was leveled horizontally to allow the CNC milling process. Three large openings were made on the deck in order to attach the model to the carriage, and put the weights needed to recover the displacement and desired trim of the boat (c.f. section 6). Three smaller openings were defined to attach the appendages to the hull. Note that only openings for one rudder and one foil were made, since the boat almost never has both its foils and rudders simultaneously immersed.

The surface of the CNC milled polystyrene hull being quite rough (see Figure 54), it was sanded before starting to laminate it with composite materials. The fiber used is a twill weave glass fiber of 100 GSM. One layer was applied on the majority of the hull using resin, and the appendages openings and transom were done afterwards (see Figure 55). A second layer of resin ("hot coat") was applied to reach enough thickness to cover the fiber and get a smooth surface through wet and dry sanding. The hull was then painted with yellow paint to get a good contrast with the water color. A primer was first applied to fill the remaining low spots, on which a light sand was done. Two layers of broom yellow spray paint were applied. The hull was finally waxed with few layers to obtain a very smooth and glossy finish (c.f. figure 56).

5.2 Manufacturing of the appendages

While working on the hull, the appendages were 3D printed with resin. Their CAD files, generated by the 3D printing software from 3D Rhino models, are depicted in drawings 08 to 11 of Appendix I. Note that the keel chord was chosen constant since the original design would lead to a too thin tip chord at model scale. As the model scale appendages were too large to be 3D printed entirely, they were printed in separate pieces. They were sanded and assembled using carbon rods to provide a basic stiffness, and glued together with resin (c.f. Figure 57).

At the exception of the bulb, the appendages had to be stiffened since the 3D printed resin is quite soft, and the resin joints brittle, making the appendages weak at this stage. Note that the rudder broke while drilling in it, so it was decided to go along without it, since it would not affect the hydrodynamics too much. The keel was wrapped with one layer of bidirectional carbon fiber, and two layers of resin were applied before sanding (c.f. Figure 58). Unfortunately, the keel broke after few hours of tank testing (under about 8 newtons of load), and another one had to be built. This time plywood was chosen as core material, and three layers of 3 mm thick plywood were glued together. The NACA profile of the keel was reproduced through sanding, and expanded along its span using the different plies of the wood as reference (c.f. Figure 59). A layer of unidirectional carbon and kevlar fibers was then applied on the keel before wrapping it with two layers of bidirectional carbon fiber, to ensure that it would not break again.

More attention was devoted to the foil since its geometry made laminating more challenging. Unidirectional carbon fibers were first added with resin along its span (on both sides), to increase its resistance to tension. After sanding back the surface, the junction (considered as the weak spot) between the base of the foil (rectangular box that goes in the hull) and its blade, was tabbed with carbon fibers (application of a decreasing number of layers). This allowed to reinforce it more than the rest of the structure, while distributing as uniformly as possible the stiffness. The foil was then entirely wrapped in carbon, after what a hot coat of resin (last layer) was applied before sanding. It was finally polished to reach a glossy finish (see Figure 60).

The next challenge was to fit the appendages to the openings made on the hull. Quite a lot of adjustments were necessary to reach a proper and solid fit. The base of the rudder was permanently sealed to the hull with resin, but it was decided to create systems that allow to temporarily join the keel and foil to the hull, to enable testing with and without foil, and possibly test a canted keel or different designs in the future. This was achieved by sealing wooden panels in the bottom of the openings, to screw the appendages in (c.f. Figure 61).

5.3 Preparing the model for testing

Before being able to use the model for testing, the bulb was fixed to the keel using superglue. Sand strips were placed on the bow of the hull, from station 1.5 at the bottom to 2.5 at the deck (from FP), to simulate flow detachment as it would occur at full scale. Two testing configurations were prepared, as the model was intended to be tested with and without its foil. When testing without foil, the foil opening was filled with a 3D printed box and modelling clay. When testing with foil, the foil was screwed on the hull (at starboard), and the gap was filled with modeling clay, as done for the keel (c.f. Figure 62). The heel fitting (connection between the model and the carriage) was attached at the intersection between the boat's centreline and LCB, where a wooden plate was glued on the model to reinforce the joint (see Figure 80).

6 Experimental testing in the towing tank facility

The procedures followed during the tank testing of the model are explained. The results are presented in Appendix E. Some pictures taken during the tests are presented in Appendix F.

6.1 Presentation of the towing tank

The tank tests were realised in the towing tank of Solent University, which is depicted in Figure 22. Its main characteristics are given in Table 15.

Figure 22: Solent University's towing tank

Table 15: Main characteristics of the towing tank

Length (m)	Width (m)	Depth (m)	Max. carriage speed (m/s)
60	3.70	1.85	4.60

6.2 Experimental procedure

Before performing the tests, the dynamometer used to measure the forces exerted on the model was calibrated. The model was weighted to determine the weight to add in it to recover its displacement. Two sets of weights were placed in the model, and moved during the tests depending on the boat speed, to get a satisfying trim angle. The weights were moved foreward at higher speeds to account for the effect of the sails, which push the bow further down when the aerodynamic driving force increases. The dynamometer was used to measure the mean values (over 10 seconds) of drag, side forces (on starboard and port side), roll moment, heave, and pitch of the model. The software Lasso was used to start the acquisitions and visualise the data.

The model was tested with fixed roll (heel) and yaw (leeway) angles, but free to heave and pitch. It was heeled to starboard and yawed to port side to reproduce realistic sailing configurations. Tests were performed with and without the foil, to be able to extract its effect on the boat (sections 7, 8). The corresponding chosen test matrices are shown in Table 16.

Table 16: Tank test matrices

	Without foil	**With foil**
Vb (kts)	5, 10, 15, 20	10, 15, 20
Heel (deg)	0, 5, 15, 25	10, 15, 25
Leeway (deg)	1, 1.5, 2, 2.5	1, 1.5, 2, 2.5
Total number of runs (-)	64	36

Each configuration was set up by changing the heel angle on the heel fitting (see Figure 80), the leeway angle on the carriage, and by moving the weights depending on the tested model's speed. Before each testing day, the instruments were zeroed with the boat upright. Note that the lowest speed of 5 knots was not tested again for the tests with foil. This choice was made to save time, since, at this speed, the carriage's vibrations were affecting the results substantively.

6.3 Discussion of the results

The results obtained from the tank tests are presented. All the data gathered during the tests is given in Appendix E. The methodology followed to extract the input data needed to perform VPP analyses based on the experimental data is detailed. This will later be used to get a bigger picture of the benefits of adding the foil to the boat (section 8).

6.3.1 Upright resistance

18 runs were first performed to assess the upright resistance of the boat. The results were extrapolated to full scale using the ITTC 1978 procedure, including the ITTC 57 formula for friction drag calculation, and a Prohaska plot to determine the form factor [14]. This was carried out for the hull, keel, and bulb, and the sum gave the overall full size data (c.f. Appendix E).

6.3.2 Heeled and yawed resistance

The heeled and yawed resistance results were scaled using the same method as for the upright resistance, since any induced drag scales alongside wave resistance with Froude number. The total upright, and heeled and yawed resistances found at full scale are shown in Figure 23. Different heel angles are plotted to visualise its effect on drag, with a leeway fixed to 2 degrees.

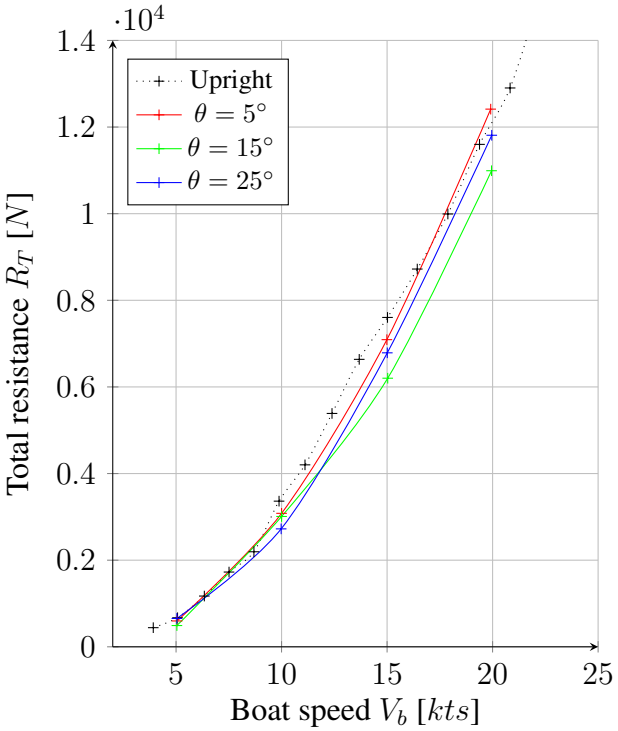

Figure 23: Full scale upright, and heeled and yawed resistances, leeway=2°

Although its trend is realistic, few bumps can be seen in the upright resistance data, since more data points were acquired than for heeled and yawed resistance. (Barkley, personal communication) suggested that, 'as the boat heels, its wetted surface area is reduced (see the heeled waterlines in drawing 02 of Appendix I), which reduces its frictional drag. As the boat goes faster, its wave drag becomes more significant, and it is larger when the boat heels further, since the immersed hull is more asymmetric. However, the wetted surface area loss generally affects more the total resistance than the increase in wave drag due to the asymmetry of the hull'. This analysis is reflected in the shape of the curves found, since the heeled resistances are smaller than the upright one due to the loss in frictional resistance, and increase faster at higher boat speeds, mostly due to the increase of wave drag, which is more significant at higher heel angles.

6.3.3 Effective draft calculation

A usual procedure used to find the effective draft T_e (which quantifies the efficiency of the boat's underwater body at producing hydrodynamic side force) is presented below. This is useful since T_e is required as input data in the VPP to perform analyses based on the experimental data.

It can be shown using lifting-line theory that the effective draft can be expressed as follows.

$$T_e = \sqrt{\frac{1}{\rho V_b^2 \pi (R_{di}/SF^2)}} \tag{22}$$

Where R_{di} is the induced drag. It is seen from equation 22 that R_{di}/SF^2 must be determined to find T_e. In practise, this is achieved by plotting the total resistance R_T against the SF squared SF^2. This was realised for each speed and heel angle considered (c.f. Figure 63), for the tests with and without foil. An example is given in Figure 24 for a heel angle of 15° (without foil).

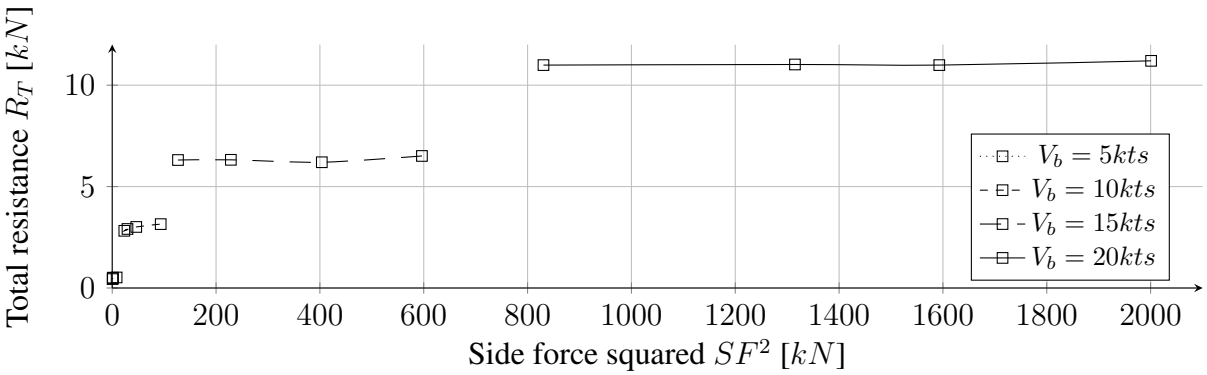

Figure 24: Total resistance against side force squared, heel=15 degrees - no foil

Four data points are plotted for each speed, corresponding to leeway angles of 1, 1.5, 2, and 2.5 degrees. It is seen that the side force squared increases a lot with leeway at high boat speeds, while the total resistance much less, and both increase with boat speed, which was expected. The intercept of one of these lines with the y axis ($SF = 0$) gives the sum of the heeled and upright resistance at the corresponding boat speed. The slope of the line gives R_{di}/SF^2, which allows to find T_e at the corresponding boat speed. The slopes are calculated in each case, and the resulting effective draft is found using equation 22. It is depicted in Figure 25 for the different boat speeds and heel angles considered (for the tests without foil).

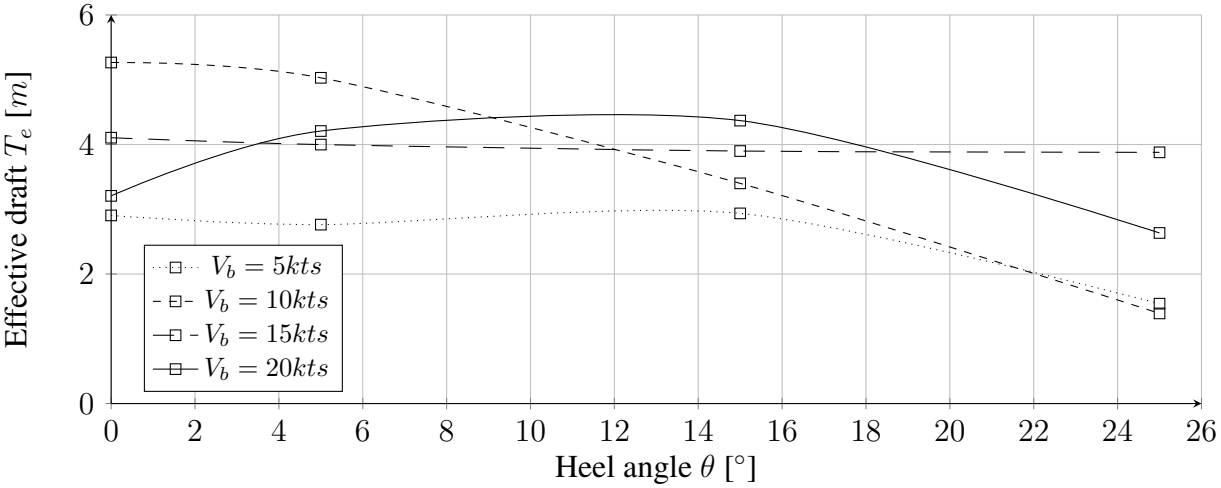

Figure 25: Effective draft against heel at different boat speeds - no foil

It is logically seen from Figure 25 that the keel becomes less efficient at producing hydrodynamic side force as the heel angle increases, hence the effective draft reduces. This is clearly shown at 10 knots, and it is also the trend at the other speeds.

7 Comparison of foil predictions and experimental results

The effect of the foil on the boat was found by subtracting the experimental results obtained when tank testing without foil (shown in Table 59) to the ones obtained with foil (Table 60). The resulting forces and motions due to the foil are analysed, and compared with the ones obtained using the theoretical model developed in section 4.

7.1 Sources of error

Before discussing the obtained experimental foil results, it is worth mentioning the potential sources of error that they are affected by. They must be considered in the analysis.

A first source of error is due to the inaccuracies in manufacturing the model scale foil. The reinforcement with unidirectional carbon fibers created a thicker region in the center part of the section, which could only partially be levelled through sanding (see Figure 60). Also, since the foil was wrapped in carbon, its overall thickness was increased. Moreover, the foil's trailing edge was sanded to obtain a minimum thickness and make it stronger. Hence, the chord of the foil was slightly reduced. Even if good care was devoted to the building process, few bumps were visible on the final foil. This could cause extra foil drag generation when tank testing. For these reasons, the resulting foil profile was not exactly the Eppler 817 accounted in theory.

The angle of attack (AOA) of the model foil was fixed to 2° relative to the horizontal waterplane (when the boat is in static equilibrium). This angle was chosen to match the theoretical data, for which an AOA of 2° was considered. However, it was observed that the AOA of the model foil changed between each run, due to the trim variation of the boat (see Appendix E.3.6). This change of AOA was not accounted for in the theoretical model. Also note that the theoretical AOA was considered to be 2° for the four foil sections, even though this is not realistic since the AOA of the tip of the foil is different from the one of its horizontal part (almost zero if no leeway).

The Reynolds numbers involved in the model scale experiments are smaller than for the full scale theoretical calculations, due to the use of Froude similitude to scale the results. This is the case even if sand strips were placed on the model to simulate a more turbulent flow and mitigate the difference. This implies that the flows are not completely equivalent at both scales.

Probably the major error is the result of the vibrations of the carriage due to friction of the wheels on the rails. They were found to strongly disturb the results at low speeds, since the magnitude of the measurements is smaller, and their effect was reduced at higher speeds.

Another source of error can be attributed to the experimental procedure followed, since the weights moved between each speeds were visually placed on marks drawn on the model (see

Figure 80). This implies that their positions were not exactly the same between the runs of similar speeds, which could have slightly changed the pitch of the boat, hence the AOA of the foil. Moreover, each run was followed by a waiting period of few minutes to let the water calm down, but perfect calm water was not reached since it was too time consuming.

7.2 Comparison of the experimental and theoretical foil results

Figures 26 to 30 present a comparison between the experimental data extracted for the foil and the theoretical data coming from the foil predictions. Each quantity is given at full scale for heel angles of 15 and 25 degrees, and for a fixed leeway angle of 1 degree. Note that the comparison of the data found for the other leeway angles of 1.5, 2, and 2.5 degrees, is given in Appendix E.3. The experimental foil drag was scaled using ITTC 1978 procedure, as already done for the upright resistance, the side force by multiplying by the cube of the scale factor (10), the roll (or righting) moment by multiplying by its power 4, and the heave by multiplying by the scale factor. The pitch is the same at model and full scales since it is an angle.

It was found that the theoretical data generally overestimated the experimental results. Thus, it was decided to reduce the effective aspect ratios AR_{eff} of the foil sections, in order to get closer results. All the hydrodynamic forces calculated in the theoretical model were reduced accordingly (c.f. section 4). Different aspect ratios were investigated within a sensitivity analysis to study their influence on the data, and the values that yielded theoretical data closest to the experimental one were chosen. The best configuration was found by dividing by two the effective aspect ratios of all the foil sections (presented in Table 10). This allowed to obtain closer data, while keeping similar trends between experiment and theory. The theoretical data presented in Figures 26 to 30 is given for this optimal choice of effective aspect ratios.

7.2.1 Righting moment and revised righting lever

Figure 26 shows that the roll (or righting) moment trends predicted at both heel angles using equation 16, are quite similar to the measured ones. However, the theory seems to overestimate the experimental values quite a lot, especially at 25 degrees of heel. Note that the later case is supposed to be less representative of a true sailing condition of the boat, since the foils usually avoid it to heel to such an angle at the considered speeds. For that reason, the results found at 15 degrees of heel are of higher relevance (which is also true for the other physical quantities).

It is worth reminding that the experimental foil results come from the difference between the results found when testing with and without foil, s.t: $X_{foil} = X_{test\,with\,foil} - X_{test\,without\,foil}$, if one considers X as the measured quantity. This implies that, when the data is negative, the value recorded with foil is smaller than the one measured without foil. This is the case at 15°

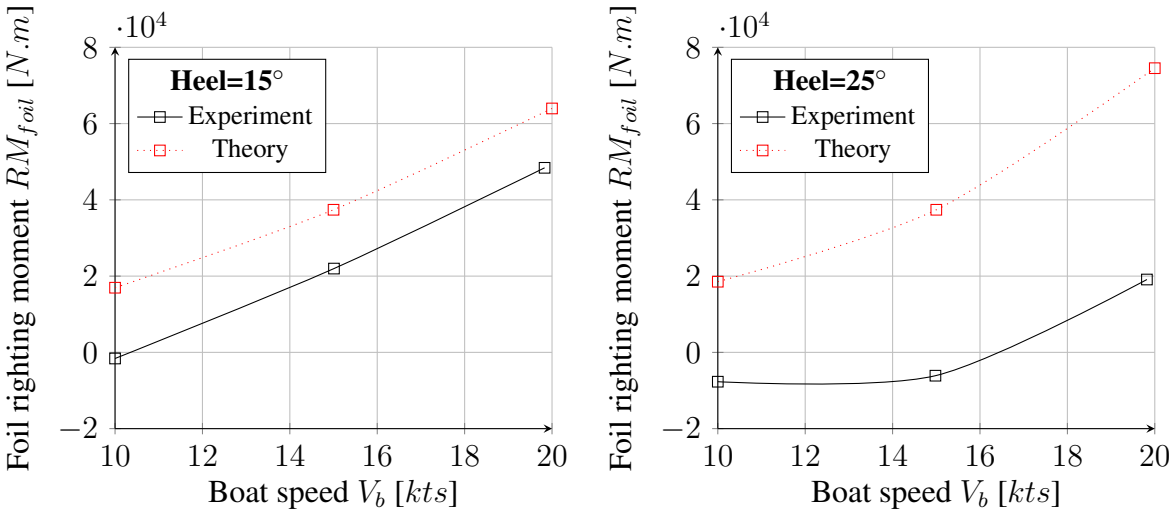

Figure 26: Comparison of experimental and theoretical foil RM, leeway=1°

of heel and at a boat speed of 10 knots, since the difference yielded a value slightly below zero. It is also the case at 10 and 15 knots for a heel of 25°. As a result, it seems that the foil is not efficient at creating extra righting moment in these cases. An explanation could be that the profile was creating more drag and turbulence, reducing the forces generated by the hull and keel, rather than generating positive lift and negative side force (outwards the hull) useful to increase the righting moment. This is seen in Figures 28, 29, and 30, since the heave due to the foil is negative, meaning that it does not lift the boat up, its drag is positive, and its side force positive or small. On the other hand, the theoretical predictions do not include the effect of the foil on the flow around the hull and keel, which explains why they yield positive results.

The experimental revised GZ (righting lever of the boat with foils) was found using the same equation as in theory (equation 20), but replacing the predicted righting moment of the foil RM_{foil} by its experimental value (c.f. Figure 26). The results are shown in Figure 27.

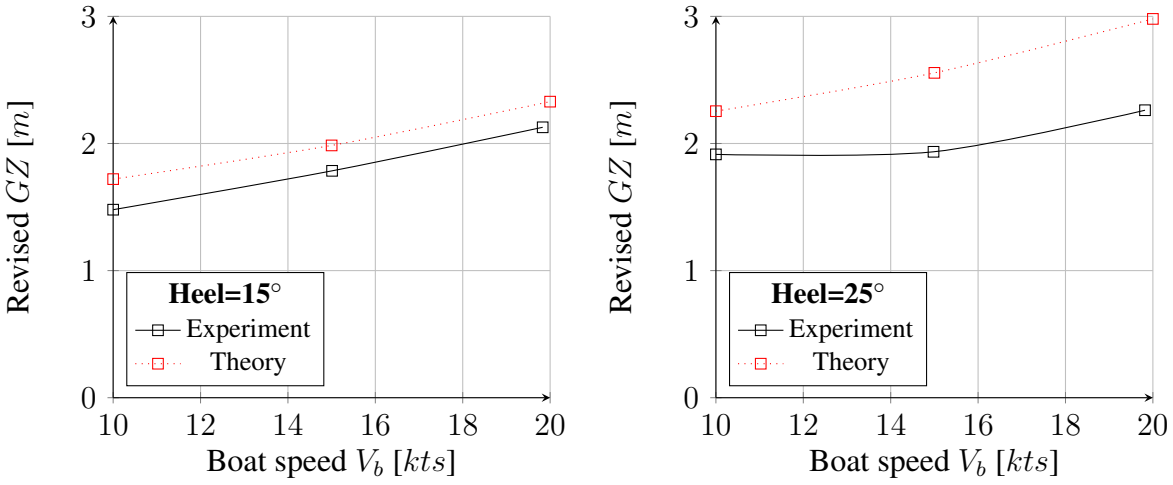

Figure 27: Comparison of experimental and theoretical revised GZ, leeway=1°

Similar comments as for the righting moment can be made regarding the GZ values, and the results are satisfying, especially at 15 degrees of heel.

7.2.2 Heave

The experimental heave due to the foil was also found by subtracting the data measured with and without foil. A theoretical estimation of this quantity could be found from the reduction of the boat's displacement due to the foil's lift, which was considered in the second model version (c.f. section 4.2). Indeed, since the draft values corresponding to the reduced displacements were found in Maxsurf for each boat speed, and heel angle, the differences of draft due to the upward lift of the foil could be determined in each case. The results are compared in Figure 28.

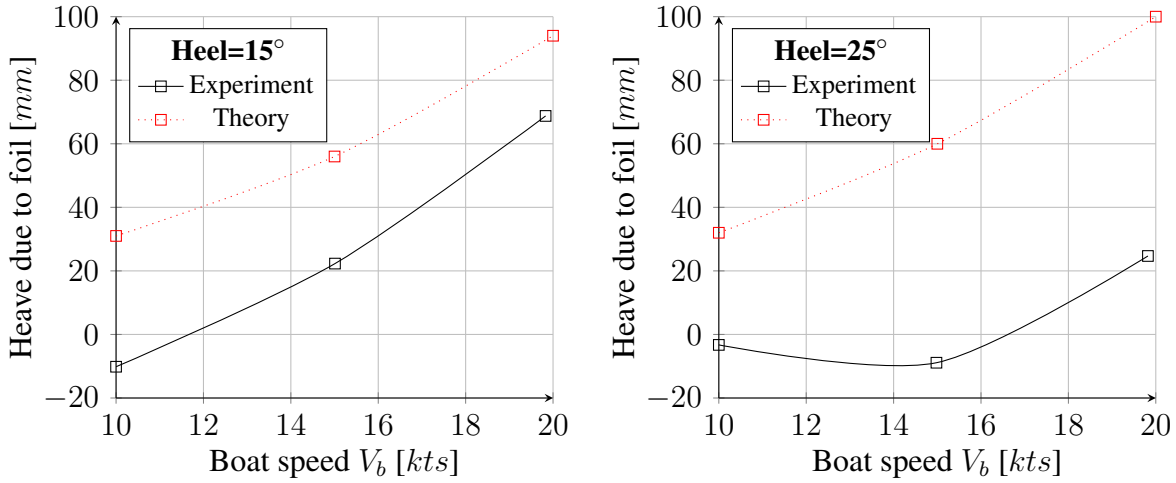

Figure 28: Comparison of experimental and theoretical heave due to foil, leeway=1°

Once again, the results are closer at 15° of heel, in which case the heave trends are quite similar. Yet, the results are relatively far, even in that case. This seems logical since the theoretical estimations of heave are very approximate. They only include the influence of the upward lift L generated by the foil, which explains why they are strictly positive. Moreover, they were found using the static immersions of the foil to compute its lift, while it was found during the testing that the foil was getting more immersed when the boat was moving (dynamic immersions). For these reasons, plus the numerous assumptions considered in the theoretical model, the predictions are limited and can not accurately describe the experimental heave values.

Regarding the experimental values, it is seen at 15° of heel and 10 knots, that the model was measured about 10 mm lower with foil than without it. Similar results were found at 25° of heel and 10 and 15 knots. This is not straightforward to understand, since the foil is expected to generate upward lift and heave the boat up. The values are small, meaning that they might be due to experimental errors. However, they highlight that the foil is not efficient at producing upward lift in these configurations (as seen for the righting moment).

7.2.3 Drag

Figure 29 presents the comparison of the experimental and theoretical drag at both heel angles.

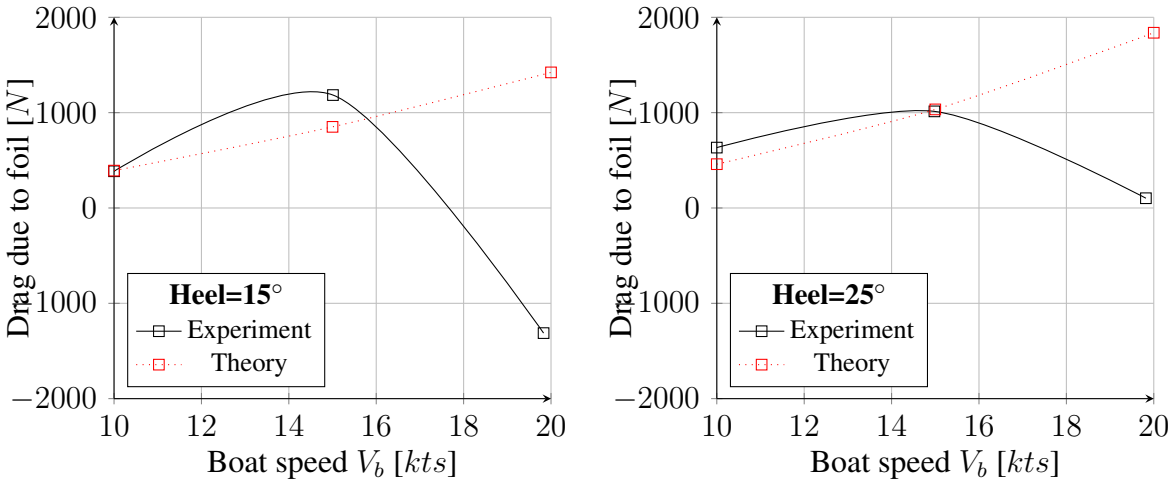

Figure 29: Comparison of experimental and theoretical drag due to foil, leeway=1°

It is seen that the predicted drag values are close to the experimental ones at 10 and 15 knots for both heel angles. These experimental values are positive since the addition of the foil increased the measured drag. At 20 knots, the experimental values drop a lot, and the one at 15° of heel becomes negative. This is because, at this speed and heel angle, the lift created by the foil lifts the boat up further than at the lower speeds, and the hull drag is reduced substantively. This implies that the drag measured with foil is smaller than without foil, since the reduction in hull drag is larger than the increase due to the foil. Also note that, at 20 knots, the fact that the drag is more reduced at 15° of heel than at 25°, is an indication that the foil better lifts the boat up at this lower heel angle (see Figure 28). This is not the case in theory (see Figure 28), since the predicted lift is larger at 25° than at 15°, due to the considered immersions (c.f. Table 50).

On the other hand, the theoretical data corresponds to the drag of the foil without any correlation to the hull's. This explains why it simply increases with speed, and why it is always positive. The values compared in Figure 29 are therefore not exactly the same physical quantities, since the theory purely gives the drag of the foil, while the experiments give the difference between the drag of the boat measured with and without its foil. The data measured during the tests with foil includes the drag due to the foil, and the reduction in hull drag due to the influence of the foil on the heave of the boat. Hence, the foil's experimental drag values (found by doing the difference between the drag measured with foil, and the one measured without foil) also include the reduction in hull drag due to the foil's lift. Therefore, one would expect the experimental results to be smaller than the theoretical ones by the amount of hull drag lost, also at 10 and 15 knots. Although it is seen that this is not the case, which is understood since the foil proved not to be really efficient at these speeds (except at 15 knots and 15° of heel).

7.2.4 Side force

The experimental and theoretical side forces due to the foil are presented in Figure 30.

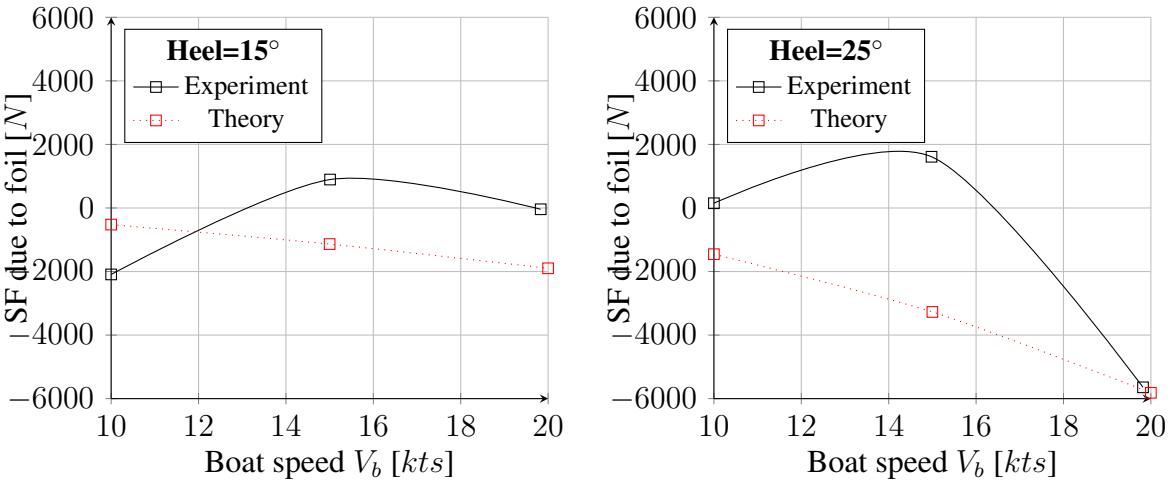

Figure 30: Comparison of experimental and theoretical SF due to foil, leeway=1°

It is seen on Figure 30 that the theory predicts a negative side force (outwards the hull) that increases with boat speed and heel. It seems reasonable since the largest part of the foil (horizontal bit defined in the theoretical model by the foil sections A and B) is inclined in a position that makes it likely to produce negative side force. The side force increases with heel due to the increased angle of the foil to the waterline.

On the other hand, it is seen that the experimental data changes sign with boat speed. This behavior does not follow the expected trend, and most likely comes from the fact that the effect of the foil on the position (heave) of the hull and keel is implicitly included in the results. The side force drop at 20 knots (also seen at higher leeway angles, c.f. Appendix E.3.5) could be explained by the fact that the foil becomes more efficient at that speed. Hence, it generates more negative side force due the orientation of its largest part, which reduces the positive side force (towards port side) produced by the hull and keel. This is amplified at 25° of heel, since the angle of the foil to the waterline increases. Note that, at higher leeway angles, the positive SF created by the foil globally increases, most likely due to the angle of its tip (more inward) (c.f. Appendix E.3.5).

The results analysed above are quite satisfying, since sensible trends were predicted from the developed theoretical model. However, it was found that the benefits of the foil only appear over 10 knots at 15° of heel, and over 15 knots at 25° of heel. The foil was therefore less efficient than what was predicted in theory, which can be attributed to the numerous experimental and theoretical sources of error discussed.

8 Direct experimental VPP analyses

In order to get a better appreciation of the benefits of adding the foil to the boat, "direct experimental" VPP analyses were performed based on the tank test results obtained with and without foil. It allowed to find the boat speeds for chosen sailing configurations (wind speeds and headings), in each case. This could be achieved by creating a DEX file in the VPP, in which the calculated effective draft, together with the upright and heeled resistances (determined as explained in section 6.3.3), were implemented as input. The GZ value of the boat also had to be changed in the VPP to consider its increase due to the foil. It was carried out using the experimental and theoretical values found (see Figure 27), to see how it affects the boat speeds.

Figure 31 presents the GZ values used in the VPP. The line named *"No foil"* corresponds to the original GZ values of the boat without foil, as calculated by the VPP. The line *"Foil, experiment"* is based on the experimental GZ values found at 15° and 25° of heel, to which the values at the other heel angles (required as input in the VPP) were chosen to keep a smooth curve. Similarly, the line *"Foil, theory"* is based on the theoretical GZ values found (see Figure 27). The line *"Foil, median"* is the average between the experimental and theoretical GZ values. It is supposed to be a more realistic guess of the revised righting lever of the foiling boat.

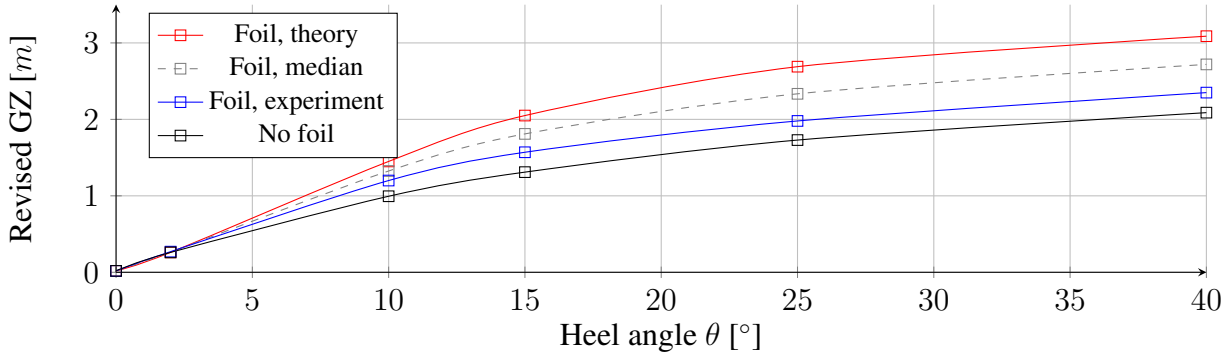

Figure 31: Revised GZ values used in the VPP

The VPP analyses were performed for the following cases:

1. **No foil**, i.e. DEX file based on the tank test data without foil, and use of the GZ values without foil.
2. **Foil, experiment**, i.e. DEX file based on the tank test data with foil, and use of the GZ values without foil.
3. **Foil, experiment+RM**, i.e. DEX file based on the tank test data with foil, and use of the experimental GZ values with foil.
4. **Foil, theory+RM**, i.e. DEX file based on the tank test data with foil, and use of the theoretical GZ values with foil.

5. **Foil, median+RM**, i.e. DEX file based on the tank test data with foil, and use of the average between the experimental and theoretical GZ values with foil.

These cases allowed to study the effect of adding the foil without changing the initial GZ values, and more realistically, of adding it while using the different revised GZ values shown in Figure 31. The output boat speeds, and the corresponding polar plots, heel, and leeway angles, can be found in Appendix G, for each case considered. Figures 32 to 35 present the speed ratios of the four cases with foil over the one without foil. This procedure is the same as the one achieved in section 2.6. Each row corresponds to a fixed heading, and each column to a fixed wind speed. The color scales were all chosen the same (with yellow corresponding to a ratio of 1) in order to allow an easy comparison between the cases. The cells tend to green when ratios are over 1, meaning that the boat is faster with foil than without it. Note that, unlike in section 2.6, no cant angle of the keel was considered for these VPP analyses, but the same sail sets were used.

	4	6	8	10	12	14	16	20	25	30	35
40	1,04	1,06	1,06	1,06	1,03	1,02	1,02	1,03	1,05	1,05	1,00
45	1,02	1,05	1,05	1,01	1,00	1,00	1,00	1,01	1,02	1,08	1,14
52	1,01	1,03	1,00	0,99	0,99	0,98	0,94	0,94	0,94	0,94	0,94
60	1,01	1,01	0,99	0,98	0,94	0,92	0,94	0,94	0,94	0,94	0,93
70	1,00	0,99	0,98	0,92	0,94	0,94	0,94	0,94	0,93	0,92	0,92
75	1,00	0,98	0,96	0,94	0,94	0,94	0,94	0,93	0,92	0,93	0,93
80	1,00	0,98	0,94	0,94	0,94	0,94	0,94	0,92	0,93	0,94	0,95
90	1,01	1,03	0,94	0,94	0,94	0,93	0,93	0,94	0,95	0,97	0,99
100	1,00	0,98	0,94	0,94	0,94	0,93	0,93	0,95	0,98	1,02	1,03
110	1,00	0,98	0,94	0,94	0,94	0,93	0,94	0,96	1,00	1,02	1,02
120	1,00	0,99	0,93	0,94	0,94	0,94	0,95	0,98	1,01	1,01	1,02
130	1,00	0,99	0,99	0,95	0,92	0,95	0,95	0,98	1,00	1,01	1,02
135	1,00	1,00	1,01	0,97	0,94	0,92	0,95	0,98	1,00	1,00	1,02
140	1,00	1,00	1,00	1,01	0,98	0,95	0,93	0,97	1,01	1,01	1,02
150	1,00	1,00	1,00	1,00	1,00	1,00	0,99	0,97	0,96	0,97	0,99
160	1,00	1,00	1,00	1,00	1,00	1,00	1,00	1,00	1,00	0,98	0,98
165	1,00	1,00	1,00	1,00	1,00	1,00	1,00	1,00	1,00	1,00	0,99
170	1,00	1,00	1,00	1,00	1,00	1,00	1,00	1,00	1,00	1,00	1,00
180	1,00	1,00	1,00	1,00	1,00	1,00	1,00	1,00	1,00	1,00	1,00

Figure 32: Best boat speeds comparison - Foil, experiment VS No foil

	4	6	8	10	12	14	16	20	25	30	35
40	1,04	1,07	1,10	1,13	1,07	1,05	1,05	1,06	1,09	1,10	1,05
45	1,03	1,06	1,11	1,04	1,03	1,03	1,04	1,05	1,08	1,15	1,22
52	1,02	1,05	1,03	1,02	1,02	1,02	0,99	0,98	0,99	1,00	1,00
60	1,01	1,04	1,02	1,01	0,98	0,97	0,98	0,99	0,99	0,99	0,99
70	1,01	1,00	1,01	0,97	0,98	0,98	0,98	0,98	0,98	0,99	0,99
75	1,00	0,99	0,99	0,98	0,98	0,98	0,98	0,98	0,99	1,00	1,00
80	1,00	0,99	0,98	0,98	0,98	0,98	0,98	0,98	0,99	1,00	1,02
90	1,02	0,99	0,98	0,98	0,98	0,98	0,98	0,99	1,01	1,03	1,07
100	1,00	1,00	0,98	0,98	0,98	0,98	0,99	1,00	1,03	1,07	1,07
110	1,00	0,99	0,98	0,98	0,98	0,99	0,99	1,01	1,06	1,05	1,05
120	1,00	0,99	0,95	0,98	0,98	0,99	1,00	1,02	1,04	1,04	1,05
130	1,00	1,02	0,99	0,95	0,95	0,99	1,00	1,02	1,02	1,04	1,06
135	1,00	1,00	1,01	0,97	0,95	0,94	0,99	1,03	1,03	1,03	1,05
140	1,00	1,00	1,00	1,01	0,98	0,96	0,93	0,99	1,03	1,04	1,06
150	1,00	1,00	1,00	1,00	1,00	1,00	0,99	0,97	0,96	0,97	1,01
160	1,00	1,00	1,00	1,00	1,00	1,00	1,00	1,00	1,00	0,98	0,98
165	1,00	1,00	1,00	1,00	1,00	1,00	1,00	1,00	1,00	1,00	0,99
170	1,00	1,00	1,00	1,00	1,00	1,00	1,00	1,00	1,00	1,00	1,00
180	1,00	1,00	1,00	1,00	1,00	1,00	1,00	1,00	1,00	1,00	1,00

Figure 33: Best boat speeds comparison - Foil, experiment+RM VS No foil

	4	6	8	10	12	14	16	20	25	30	35
40	1,06	1,08	1,16	1,19	1,13	1,13	1,14	1,18	1,24	1,27	1,23
45	1,04	1,07	1,17	1,09	1,10	1,13	1,15	1,19	1,22	1,31	1,44
52	1,02	1,07	1,07	1,08	1,12	1,13	1,10	1,09	1,10	1,12	1,13
60	1,01	1,06	1,06	1,10	1,08	1,07	1,07	1,08	1,11	1,14	1,16
70	1,01	1,01	1,06	1,06	1,06	1,07	1,08	1,11	1,13	1,15	1,17
75	1,02	1,00	1,05	1,06	1,06	1,07	1,09	1,11	1,13	1,15	1,18
80	1,02	1,00	1,02	1,05	1,06	1,08	1,09	1,11	1,13	1,17	1,21
90	1,02	1,08	1,04	1,06	1,07	1,09	1,09	1,11	1,16	1,18	1,19
100	1,01	1,01	1,03	1,05	1,08	1,08	1,09	1,12	1,16	1,16	1,16
110	1,02	0,99	1,01	1,05	1,08	1,08	1,09	1,13	1,14	1,13	1,15
120	1,00	0,99	0,96	1,01	1,07	1,07	1,09	1,13	1,12	1,12	1,16
130	1,00	1,02	0,99	0,96	0,96	1,04	1,07	1,12	1,09	1,11	1,16
135	1,00	1,00	1,01	0,98	0,95	0,95	1,01	1,10	1,10	1,11	1,14
140	1,00	1,00	1,00	1,01	0,99	0,96	0,94	1,00	1,07	1,12	1,15
150	1,00	1,00	1,00	1,00	1,00	1,00	0,99	0,97	0,96	0,97	1,01
160	1,00	1,00	1,00	1,00	1,00	1,00	1,00	1,00	1,00	0,98	0,98
165	1,00	1,00	1,00	1,00	1,00	1,00	1,00	1,00	1,00	1,00	0,99
170	1,00	1,00	1,00	1,00	1,00	1,00	1,00	1,00	1,00	1,00	1,00
180	1,00	1,00	1,00	1,00	1,00	1,00	1,00	1,00	1,00	1,00	1,00

Figure 34: Best boat speeds comparison - Foil, theory+RM VS No foil

	4	6	8	10	12	14	16	20	25	30	35
40	1,06	1,08	1,13	1,17	1,10	1,09	1,10	1,12	1,16	1,19	1,14
45	1,03	1,07	1,15	1,07	1,07	1,08	1,09	1,13	1,16	1,24	1,35
52	1,02	1,06	1,05	1,05	1,07	1,08	1,05	1,04	1,05	1,06	1,07
60	1,01	1,06	1,04	1,06	1,04	1,03	1,03	1,04	1,05	1,06	1,07
70	1,01	1,00	1,04	1,02	1,02	1,02	1,03	1,04	1,06	1,07	1,08
75	1,00	1,00	1,03	1,02	1,02	1,03	1,03	1,05	1,06	1,08	1,10
80	1,02	0,99	1,00	1,02	1,02	1,03	1,04	1,05	1,07	1,09	1,11
90	1,02	1,08	1,02	1,02	1,02	1,04	1,04	1,05	1,08	1,12	1,14
100	1,01	1,01	1,01	1,02	1,03	1,04	1,04	1,06	1,11	1,12	1,11
110	1,00	0,99	1,00	1,02	1,03	1,04	1,05	1,07	1,11	1,09	1,10
120	1,00	0,99	0,96	1,00	1,03	1,04	1,05	1,08	1,08	1,08	1,10
130	1,00	1,02	0,99	0,95	0,95	1,02	1,04	1,08	1,06	1,07	1,11
135	1,00	1,00	1,01	0,98	0,95	0,95	1,00	1,07	1,07	1,07	1,09
140	1,00	1,00	1,00	1,01	0,98	0,96	0,94	1,00	1,05	1,08	1,10
150	1,00	1,00	1,00	1,00	1,00	1,00	0,99	0,97	0,96	0,97	1,01
160	1,00	1,00	1,00	1,00	1,00	1,00	1,00	1,00	1,00	0,98	0,98
165	1,00	1,00	1,00	1,00	1,00	1,00	1,00	1,00	1,00	1,00	0,99
170	1,00	1,00	1,00	1,00	1,00	1,00	1,00	1,00	1,00	1,00	1,00
180	1,00	1,00	1,00	1,00	1,00	1,00	1,00	1,00	1,00	1,00	1,00

Figure 35: Best boat speeds comparison - Foil, median+RM VS No foil

It is seen from Figure 32 that adding the foil to the boat without updating its GZ value is not beneficial, since most of the ratios are below 1. This comes as no surprise, since not increasing the GZ is equivalent to considering that the foil does not increase the righting moment of the boat. Note that the speed ratios are below 1 especially for a particular range of wind speeds and

headings, for which the corresponding heel angles are amongst the largest (c.f. Appendix G.1), which makes the foil well immersed. This range is thus where the foil has the largest impact on the boat speeds in terms of drag, and the reduction in speed comes from the added drag due to the foil. Nevertheless, the very upwind speeds are slightly increased. Note that for every case considered, a range of speed ratios equal to 1 is seen at large headings (downwind). This is the case since the boat does not heel enough (less than 5 degrees) for the foil to be immersed in these downwind conditions (c.f. Appendix G.1).

It is clear when comparing Figure 33 to Figure 32, that the boat speeds are considerably increased when the righting lever gain due to the foil is considered. However, the region where the speeds were decreased due to the added drag of the foil is still slightly below 1. This means that the boat is still slower with foil for the corresponding range of wind speeds and headings. This comes from the fact that the increase in GZ found from the experimental data is quite small (see Figure 31), implying that the boat still heels quite a lot (see Table 71), which slows it down.

When using the theoretical revised GZ values which are larger than the experimental ones, it is seen by comparing Figure 34 to Figure 33, that most of the speeds are increased, which was expected. However, few low values remain, corresponding to heel angles at which only a small part of the foil is immersed (see Table 73). Hence, at these heel angles, the foil creates drag without being efficient, i.e. it has a low lift to drag ratio. Moreover, since the foil is close to the free surface at low heel angles, ventilation was observed when tank testing at a boat speed of 20 knots and heel angle of 10°, for most leeway angles (see Figure 82). It is interesting to notice that ventilation could also affect these speeds, since, for instance, for a wind speed of 16 knots and a heading of 140°, the boat speed is 15.42 knots (see Table 68) which is close to 20 knots, and the heel angle is 7.58° (see Table 73), also close to 10°. The other cases are also fairly close to the ventilation conditions, in which case the lift generated by the foil is almost zero, but its drag is increased. This explains why these speed ratios do not increase much when increasing the GZ values, since the righting moment does almost not increase due to the very small lift. These speed ratios stay below 1 due to the extra drag coming from ventilation.

Finally, in order to predict most accurately the revised GZ of the foiling boat, and come up with boat speeds as realistic as possible, intermediate GZ values were chosen as the average between the experimental and theoretical values. The resulting boat speed ratios obtained using these GZ values are depicted in Figure 35. They logically seat in between the ones found using the experimental and theoretical GZ values (Figures 33 and 34), and the features described previously are still present. This last estimation of the boat speeds of the foiling Open 60 can be considered as the most realistic one that can be achieved through this process.

Overall, the addition of the foil on the boat clearly enhanced its speeds (by up to 35% when using the average GZ values), particularly when sailing upwind and in strong winds. The fact

that the boat speeds stayed unchanged in downwind sailing configurations (because the foil only starts touching the water from about 5° of heel), shows that the choice of the foil design and its orientation on the hull were not optimal. In order to benefit from the foil in downwind sailing configurations, it could have been set more downwards, or ideally, more curvature could have been implemented in its design. This would ensure that the foil enters the water at a lower heel angle, while keeping an horizontal wing span to maximise the upward lift generation. An optimised foil design proposal is depicted in Appendix G.3 to face that issue.

9 Conclusion

Reflecting onto the work conducted during the project, it can be concluded that its goals were achieved quite successfully. The different parts of the project led to an accurate description of the effects of adding the designed foils to the proposed Open 60.

After two design iterations, the designed IMOCA 60 hull form proved to be quite fast when compared (in the VPP) to the reversed engineered hull forms of the IMOCAs Hugo Boss and L'Occitane. For the sailing configurations (wind speeds and headings) chosen in the VPP, an overall increase in speed was observed from the first design attempt. The re-design process of the hull (achieved in Maxsurf Modeler) was therefore beneficial.

The model scale hull form and its appendages were manufactured successfully, even if the keel broke during the tank tests, and another one had to be built. The tests were performed again with the new keel to obtain consistent results. The model could be tank tested both with and without its foil, thanks to the temporary foil fixation system manufactured. This was done for various boat speeds, heel angles, and leeway angles. The tank results (drag, side force, roll moment, heave, and pitch) obtained in both cases showed sensible trends, although a few values were corrupted due to experimental errors. The data found without foil was subtracted from the one found with it, which allowed to extract the effect of the foil on the boat. The results were extrapolated to full scale, and ITTC 1978 procedures were used for the drag.

The theoretical model developed (based on lifting-line theory) to predict the benefits of the foil, seemed to give reasonable results. The comparison between the experimental and theoretical foil results (at full scale) allowed to validate the model. It was concluded that the foil was less efficient than predicted in theory, since the theoretical foil results overestimated the experimental ones. This was attributed to the numerous assumptions and approximations considered in theory. Even if the experimental foil results were also exposed to various sources of error that were discussed (such as inaccuracies in the manufacturing of the foil), they were considered as more reliable. However, satisfying trends of the righting (or roll) moment generated by the foil, revised righting lever of the boat with its foil, and heave due to the foil, were found using the theoretical model. Yet, the predicted foil drag and side force trends were quite different from the experimental ones. This was attributed to the fact that only the foil was considered in theory, while the influence of the foil on the hydrodynamics of the hull and keel was present in the experimental data (since the experimental foil data comes from the difference between the results measured with foil and without it). Hence, it was concluded from the analysis that, not only the foil, but, the foil, the hull, and the keel, would have had to be considered in theory to obtain closer results. This seems too complicated to be realised using a method similar to the one used to develop the theoretical model. However, it could be achieved through 3D CFD simulations, although it represents a much higher computational cost.

It is worth mentioning that the overall side force generated by the foil was predicted from the theoretical model to be negative, i.e. leeward (e.g. towards starboard if the boat heels towards that side). Although this increases the righting moment created by the foil (as per equation 16), it would mean that the foil does not help to prevent the boat from drifting leeward (which is a consequence of the aerodynamic side force generated on the sails). This role is generally assumed by the keel, but in the case where it is canted windward to increase the righting moment of the boat (done when sailing close to the wind to counterbalance the large aerodynamic side force), its hydrodynamic side force is reduced due to the angle. In this scenario, the foil would need to generate positive side force (windward) to compensate the loss of side force created by the keel, and prevent the boat from drifting leeward [1]. Hence, if one trusts the theoretical results, it is deduced that the foil geometry proposed could have been designed with a larger vertical tip, to generate positive side force in the sailing configurations where the keel is usually canted (from beam reach to close-hauled, i.e. heading from 90° to about 30°). This would allow to cant the keel up to the limit of 38 degrees to increase the righting moment of the boat, without that it drifts too much leeward.

"Direct experimental" VPP analyses were performed based on the data measured during the tank tests realised with and without foil. This allowed to find the boat speeds in each case, and for different sailing configurations (chosen in the VPP). The effect of the foil on the boat speeds could therefore be quantified accurately, by comparing the speeds of the boat obtained with and without its foil. The corresponding heel and leeway angles of the boat were also considered, to understand in which positions the foil is the most efficient.

The VPP analyses were performed for five different cases (one without foil, and four with foil). This enabled to highlight the effect of adding the foil without increasing the original righting lever values (GZ) of the boat, and the effect of adding it while accounting for the GZ increase due to the foil. The effect of different GZ increases (which were estimated from the experiments and theory) on the boat speeds, were investigated.

It was found that the addition of the foil without increase of GZ slowed the boat down in certain sailing configurations. It was understood as the result of the extra drag due to the foil, since the boat heeled significantly in these sailing configurations, implying that the foil was mostly immersed. When the GZ values were revised using the experimental increases, the speeds globally increased from the previous case. This seemed logical, since, increasing the GZ values is equivalent to accounting for the extra righting moment created by the foil. Yet, for the sailing configurations where the foil drag decreased the speeds, the boat was still slightly slower with foil than without it. This was due to the fact that the GZ increases estimated experimentally are quite small. When using the theoretical GZ increases that are larger, all the boat speeds increased further. Hence, the boat became faster with foil, also in the sailing configurations

where the foil drag initially reduced the speeds. This means that the speed increase due to the extra righting moment provided by the foil, became greater than the speed losses due to the extra foil drag.

A last case was investigated by using the average between the experimental and theoretical revised GZ values of the boat with foil. These revised GZ values were considered more realistic. This case yielded boat speeds seating in between the ones found using the experimental and theoretical revised GZ values, which was expected. An overall increase in speed was observed due to the foil (up to 35 %, for a wind speed of 35 knots, and heading of 45 degrees). The boat speeds corresponding to the sailing configurations in which the foil drag initially reduced the speeds, were once again larger with foil than without it. However, for each of the cases with foil considered, it was found that a few boat speeds were lower with foil than without it (regardless of the revised GZ values used). This was considered to be the result of the ventilation of the foil, since the corresponding boat speeds and heel angles were close to the ones used when the foil ventilated in the tank (boat speed of 20 knots, and heel angle of 10 degrees).

Finally, it was observed that the foil did not improve the downwind speeds of the boat. This is due to the fact that it starts to enter the water at about 5 degrees of heel, which was not reached in downwind sailing configurations. Hence, it was deduced that the foil should have been set further downwards, or with more curvature, to be immersed at smaller heel angles, and increase the boat speeds also in these cases. Optimised foils were proposed to solve that issue.

The work proposed in this thesis could represent a solid basis for future research projects. It would be interesting to investigate other foil sections and geometries, and test them using the same model hull to characterise their benefits. This could create the foundation of an empirical database which would help naval architects to select Open 60 foils depending on their needs. Alternatively, a foil design that maximises the boat speeds over chosen sailing configurations, could be achieved using a dedicated optimisation software, coupled with VPP analyses. Moreover, the developed theoretical model could be improved by implementing new elements in it, to make it more realistic. A Matlab or Python script could also be written to ease handling of the data, and enhance the flexibility of the program. Another improvement would be to perform 2D and 3D CFD simulations on the foil, and compare the results to both the experimental and theoretical ones. If one felt more ambitious, such 3D CFD simulations could be performed on the entire Open 60 with and without foil, and the results (boat speeds, resistance, etc) could be compared to the ones found using the direct experimental VPP analyses based on the tank data. This would most likely require the help of a professional CFD company, such as Cape Horn Engineering.

References

[1] Sailboats with foils: the evolution seen by Sirena, Soldini and Pedote [accessed online: 25/07/2022]. https://globalsolochallenge.com/fr/voiliers-foils/

[2] IMOCA.org, class rules official documents [accessed online: 02/03/2022]. https://www.imoca.org/en/imoca/official-documents

[3] www.imoca.org, Boats [accessed online: 08/03/2022]. https://www.imoca.org/en/boats

[4] www.vendeeglobe.org, Boats [accessed online: 08/03/2022]. https://www.vendeeglobe.org/en/glossary

[5] www.imoca.org, Standings [accessed online: 08/03/2022]. https://www.imoca.org/en/standings/races/225#

[6] Aero-hydrodynamics and the performance of sailing yachts, the science behind sailing yachts and their design. Fabio Fossati. Bloomsburry editions, Politecnico di Milano.

[7] François Chevalier website, Vendée Globe Challenge 2020-2021 - Yacht Design [accessed online: 08/03/2022]. http://chevaliertaglang.blogspot.com/2020/11/vendee-globe-challenge-2020-2021-yacht.html

[8] North Sails news, IMOCA's sails, from the drawing board to the post [accessed online: 28/03/2022]. https://www.northsails.com/sailing/fr/2020/08/voiles-imoca-de-la-planche-de-dessin-a-la-mise-a-poste

[9] www.bateaux.com, Understand IMOCA's sails [accessed online: 28/03/2022]. https://www.bateaux.com/article/24168/apprentissage-voiles-d-un-imoca-vendee-globe

[10] www.vendeeglobe.org, IMOCA's sails explained by Yann Eliès [accessed online: 28/03/2022]. https://www.vendeeglobe.org/fr/actualites/15264/dossier-les-voiles-d-un-imoca-expliquees-par-yann-elies

[11] Design of a Low-Emissions Trimaran Fast Ferry with an Investigation into the Applicability of Hydrofoils, Anson Baker-Berry, submitted in part fulfilment of the Degree of Bachelor of Engineering with Honours in Yacht & Powercraft Design, April 2021, Solent University.

[12] IMOCA.org, The architectural choices of V and B MONBANA MAYENNE for the Vendée Globe 2024-2025 [accessed online: 06/03/2022]. https://www.imoca.org/fr/news/news/les-choix-architecturaux-de-v-and-b-monbana-mayenne

[13] Design of a 54ft offshore racing yacht for an Ocean Race type event, Timothée Villain-Amirat, submitted in part fulfilment of the Degree of Bachelor of Engineering with Honours in Yacht & Powercraft Design, 3rd May 2019, Solent University.

[14] ITTC 7.5-02-03-01.4 - 1978 ITTC Performance Prediction Method.

[15] www.sailingworld.com, How Heel Affects Speed and Handling [accessed online: 06/03/2022]. https://www.sailingworld.com/how-to/how-heel-affects-speed-and-handling/#:~:text=A%20general%20design%20rule%20is,waterline%20length%20or%20sailing%20length.

[16] www.sailingnews.com, The keel bulb on an IMOCA, description of this important counterweight [accessed online: 27/03/2022]. https://www.boatsnews.com/story/35523/the-keel-bulb-on-an-imoca-description-of-this-important-counterweight

[17] www.sailingnews.com, How does the keel of an IMOCA rock? [accessed online: 27/03/2022]. https://www.boatsnews.com/story/35642/how-does-the-keel-of-an-imoca-rock

[18] Course Au Large, Foils : les architectes s'expliquent [accessed online: 29/07/2022]. https://www.guillaumeverdier.com/wp-content/uploads/2015/03/FOIL_CAL66_Foils.pdf

A Appendix - Parametric study

Table 17: Main parameters of 40 current IMOCAs

Boat	Lh (m)	Bh (m)	Δ (t)	Max UP SA (m2)	Max DW SA (m2)
Maitre Coq IV	18.28	5.8	8	310	550
Apivia	18.28	5.85	8	350	560
Bureau Vallée 2	18.28	5.5	7.8	270	535
Yes We Cam!	18.28	5.85	8	300	620
Sea Explorer	18.28	5.7	7.6	290	490
Linkedout	18.28	5.85	8	320	430
Groupe Apicil	18.28	5.85	8.5	350	610
Prysmian Group	18.28	5.8	8	300	600
Omia, Water Family	18.28	5.85	8.4	296	700
V and B Mayenne	18.28	5.5	-	-	-
L'Occitane	18.28	5.5	7.8	270	535
Banque Populaire X	18.28	5.7	7.7	340	570
Charal	18.28	5.85	8	320	600
Pure Best Western®	18.28	5.8	9	270	560
La Mie Caline	18.28	5.65	7.9	300	610
DMG Mori	18.28	5.85	8	320	600
La Fabrique	18.28	5.85	-	290	580
Time For Oceans	18.28	5.5	8.5	340	550
Medallia	18.28	5.7	9	300	580
1 Planet 1 Ocean	18.28	5.3	8.9	240	470
Compagnie Du Lit	18.28	5.75	8.5	300	620
Campagne De France	18.25	5.5	9	330	600
Groupe Sétin	18.28	5.8	9	270	560
TSE 4MyPlanet	18.28	5.3	9	260	580
Stark	18.28	5.8	8.5	270	580
Merci	18.28	5.6	8.5	250	650
MACSF	18.28	5.7	8	300	650
Art & Fenêtres	18.28	5.85	7	320	570
Initiative-Cœur	18.28	5.7	8.5	280	600
Arkéa Paprec	18.28	5.7	8	260	600
Hugo Boss	18.28	5.4	7.6	330	630
PRB	18.28	5.5	-	300	600
Corum L'épargne	18.28	5.7	7.9	260	530
11th Hour Alaka'i	18.28	5.5	7.5	340	570
11th Hour Mãlama	18.28	5.5	10	280	600
Ebac	18.28	5.5	8.8	290	565
Fortinet	18.28	5.7	-	290	490
Kostum	18.28	5.85	-	300	600
No Limit 4 Us	18.28	5.65	-	-	-
Team Germany	18.28	5.85	8	330	620
Average	18.28	5.68	8.26	298.32	578.03

Table 18: Additional information for 40 current IMOCAs

Boat	Skipper	Sail Nb	Launch date	Foils	Mast
Maitre Coq IV	Yannick Bestaven	FRA 17	02/03/2015	Yes	Wing
Apivia	Charlie Dalin	FRA 79	05/08/2019	Yes	Wing
Bureau Vallée 2	Louis Burton	FRA 18	31/01/2020	Yes	Wing
Yes We Cam!	Jean Le Cam	FRA 01	29/05/2007	No	Wing
Sea Explorer	Boris Herrmann	MON 10	07/08/2015	Yes	Wing
Linkedout	Thomas Ruyant	FRA 59	07/09/2019	Yes	Wing
Groupe Apicil	Damien Seguin	FRA 1000	29/05/2008	No	Wing
Prysmian Group	Giancarlo Pedote	ITA 34	11/09/2015	Yes	Wing
Omia, Water Family	Benjamin Dutreux	FRA 09	25/06/2007	No	Classic
V and B Mayenne	Maxime Sorel	FRA 53	05/2022	Yes	Wing
L'Occitane	Armel Tripon	FRA 02	29/01/2020	Yes	Wing
Banque Pop. X	Clarisse Cremer	FRA 30	16/08/2011	No	Wing
Charal	Jérémie Beyou	FRA 08	20/08/2018	Yes	Wing
Pure Best Western®	Romain Attanasio	FRA 49	19/08/2008	No	Classic
La Mie Caline	Arnaud Boissieres	FRA 14	31/07/2007	Yes	Wing
DMG Mori	Kojiro Shiraishi	JPN 11	02/09/2019	Yes	Wing
La Fabrique	Alan Roura	SUI 07	01/08/2007	Yes	Wing
Time For Oceans	Stéphane Le Diraison	FRA 92	19/06/2007	Yes	Classic
Medallia	Pip Hare	GBR 777	03/07/1999	No	-
1 Planet 1 Ocean	Didac Costa	ESP 33	02/02/2000	No	-
Compagnie Du Lit	Clément Giraud	FRA 83	26/07/2006	No	Classic
Campagne De France	Miranda Merron	FRA 50	2006	No	-
Groupe Sétin	Manuel Cousin	FRA 71	03/02/2007	No	Wing
TSE 4MyPlanet	Alexia Barrier	FRA 72	31/01/1998	No	-
Stark	Ari Huusela	FIN 222	06/08/2007	No	-
Merci	Sébastien Destremau	FRA 69	15/01/2005	No	-
MACSF	Isabelle Joschke	FRA 27	06/08/2007	Yes	Wing
Art & Fenêtres	Fabrice Amedeo	FRA 56	18/08/2015	Yes	Wing
Initiative-Cœur	Samantha Davies	FRA 109	18/09/2010	Yes	Wing
Arkéa Paprec	Sébastien Simon	FRA 04	19/07/2019	Yes	Wing
Hugo Boss	Alex Thomson	GBR 99	01/10/2015	Yes	-
PRB	Kevin Escoffier	FRA 85	11/03/2021	Yes	-
Corum L'épargne	Nicolas Troussel	FRA 06	05/05/2020	Yes	Wing
11th Hour Alaka'i	Pascal Bidegorry	USA 11	01/09/2015	Yes	Wing
11th Hour Mãlama	Charlie Enright	USA 12	24/08/2021	Yes	Wing
Ebac	Antoine Cornic	FRA 1461	23/08/2005	No	Classic
Fortinet	Romain Attanasio	FRA 10	06/08/2015	Yes	-
Kostum	Louis Duc	FRA 83	30/09/2006	No	Wing
No Limit 4 Us	Tanguy Le Turquais	BEL 207	07/04/2014	No	-
Team Germany	Robert Stanjek	GER 21	02/09/2011	No	Classic

A.1 Races rankings for selection of the top most performing boats

Hereafter are presented the rankings of the latest major international IMOCA offshore races [5]. The top 5 of each ranking is highlighted in yellow, and the corresponding boats were selected as reference for the design (expect some old designs of the top 5 of the Vendée Globe 2016 edition, which are not highlighted). Note that the abbreviations ABD and DNS in parentheses respectively stand for abandonment and did not start.

Table 19: Rankings of the VG 2020 and Transat JV 2021

Vendée Globe 2020	**Jacques Vabre 2021**
MAITRE COQ IV	LINKEDOUT
APIVIA	APIVIA
BUREAU VALLÉE 2	CHARAL
YES WE CAM!	ARKÉA PAPREC
SEAEXPLORER	INITIATIVES-CŒUR
LINKEDOUT	PRYSMIAN GROUP
GROUPE APICIL	FORTINET BEST WESTERN
PRYSMIAN GROUP	CORUM
OMIA WATER FAMILY	MAITRE COQ IV
V AND B MAYENNE	NEXANS ART & FENÊTRES
L'OCCITANE	GROUPE APICIL
BANQUE POPULAIRE X	MACSF
CHARAL	11TH HOUR RACING TEAM MĀLAMA
PURE BEST WESTERN®	KOSTUM LANTANA PAYSAGE
LA MIE CÂLINE	TIME FOR OCEANS
DMG MORI GLOBAL ONE	LA MIE CÂLINE
LA FABRIQUE	COMPAGNIE DU LIT
TIME FOR OCEANS	GROUPE SÉTIN 4MYPLANET
MEDALLIA	LABORATOIRES DE BIARRITZ
ONE PLANET ONE OCEAN	EBAC
COMPAGNIE DU LIT	11TH HOUR RACING TEAM ALAKA'I *(ABD)*
CAMPAGNE DE FRANCE	BUREAU VALLÉE *(ABD)*
GROUPE SÉTIN	
TSE 4MYPLANET	
STARK	
INITIATIVES-CŒUR *(ABD)*	
ARKÉA PAPREC *(ABD)*	
MACSF *(ABD)*	
CORUM *(ABD)*	
MERCI *(ABD)*	
NEWREST ART & FENÊTRES *(ABD)*	
PRB *(ABD)*	
HUGO BOSS *(ABD)*	

Table 20: Rankings of the Rolex Fastnet Race 2021 and 2019

Rolex Fastnet Race 2021	**Rolex Fastnet Race 2019**
APIVIA	CHARAL
CHARAL	PRB
11TH HOUR RACING TEAM ALAKA'I	BANQUE POPULAIRE X
ARKÉA PAPREC	BUREAU VALLÉE 2
INITIATIVES-CŒUR	INITIATIVES-CŒUR
FORTINET BEST WESTERN	MAITRE COQ IV
GROUPE APICIL	MALIZIA II YACHT CLUB DE MONACO
PRYSMIAN GROUP	NEWREST ART & FENÊTRES
MACSF	PRYSMIAN GROUP
HUGO BOSS	LA FABRIQUE
COMPAGNIE DU LIT JILITI	GROUPE SETIN
THE MOUNTAIN MAN *(ABD)*	TIME FOR OCEANS
MAITRE COQ IV *(ABD)*	PIP HARE OCEAN RACING
	LA MIE CÂLINE ARTIPÔLE
	CAMPAGNE DE FRANCE
	GROUPE APICIL
	ROSALBA
	EYESEA.BE
	V AND B SAILING TOGETHER *(ABD)*
	ARKÉA PAPREC *(ABD)*

Table 21: Rankings of the Défi Azimut 2021 and 2020

Défi Azimut 2021	**Défi Azimut 2020**
APIVIA	CHARAL
11TH HOUR RACING TEAM ALAKA'I	INITIATIVES-CŒUR
LINKEDOUT	MACSF
BUREAU VALLÉE 2	BANQUE POPULAIRE X
ARKÉA PAPREC	PRB
INITIATIVES-CŒUR	ARKEA PAPREC
CORUM L'ÉPARGNE	SEAEXPLORER
MACSF	APIVIA
FORTINET BEST WESTERN	LINKEDOUT
GROUPE APICIL	GROUPE APICIL
LA MIE CÂLINE ARTISANS ARTIPÔLE	V AND B MAYENNE
COMPAGNIE DU LIT JILITI	L'OCCITANE EN PROVENCE
GROUPE SÉTIN 4MYPLANET *(ABD)*	OMIA WATER FAMILY
11TH HOUR RACING TEAM MĀLAMA *(ABD)*	LA FABRIQUE
	PURE BEST WESTERN®
	TIME FOR OCEANS
	CAMPAGNE DE FRANCE

Table 22: Rankings of the VG 2016 and Transat JV 2019

Vendée Globe 2016	**Jacques Vabre 2019**
BANQUE POPULAIRE VIII	APIVIA
HUGO BOSS	PRB
MAITRE COQ	CHARAL
ST MICHEL VIRBAC	11TH HOUR RACING ALAKA'I
QUÉGUINER LEUCÉMIE ESPOIR	LINKEDOUT
YES WE CAM!	BANQUE POPULAIRE X
BUREAU VALLÉE	INITIATIVES-CŒUR
SPIRIT OF HUNGARY	ARKÉA PAPREC
COMMEUNSEULHOMME	NEWREST ART & FENÊTRES
LA MIE CÂLINE	BUREAU VALLÉE 2
NEWREST MATMUT	MAITRE COQ IV
LA FABRIQUE	MALIZIA II YACHT CLUB DE MONACO
GREAT AMERICA IV	CORUM L'EPARGNE
ONE PLANET ONE OCEAN	GROUPE APICIL
FAMILLE MARY ETAMINE DU LYS	PRYSMIAN GROUP
FORESEIGHT NATURAL ENERGY	LA MIE CÂLINE ARTIPÔLE
NO WAY BACK	WATER FAMILY
MERCI	TIME FOR OCEANS
EDMOND DE ROTHSHILD *(ABD)*	LA FABRIQUE
LE SOUFFLE DU NORD *(ABD)*	GROUPE SETIN
INITIATIVES-CŒUR *(ABD)*	CAMPAGNE DE FRANCE *(ABD)*
SPIRIT OF YOUKOH *(ABD)*	PIP HARE OCEAN RACING *(ABD)*
SAFRAN II *(ABD)*	TSE 4MYPLANET
SMA *(ABD)*	ARIEL 2
CAMPAGNE DU LIT BOULOGNE *(ABD)*	VERS UN MONDE SANS SIDA
PRB *(ABD)*	MACSF *(ABD)*
KILCULLEN VOYAGER *(ABD)*	FORTIL *(DNS)*
BASTIDE OTIO *(ABD)*	HUGO BOSS *(ABD)*
MACSF *(ABD)*	

B Appendix - Velocity Prediction Program

B.1 Hull forms implemented in the VPP

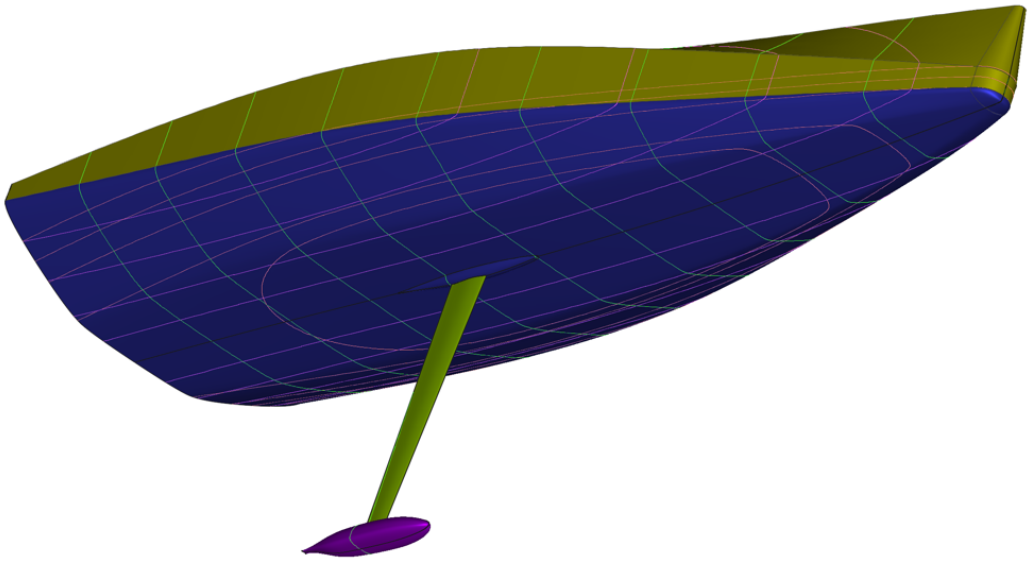

Figure 36: Reversed-engineered Maxsurf model of Hugo Boss

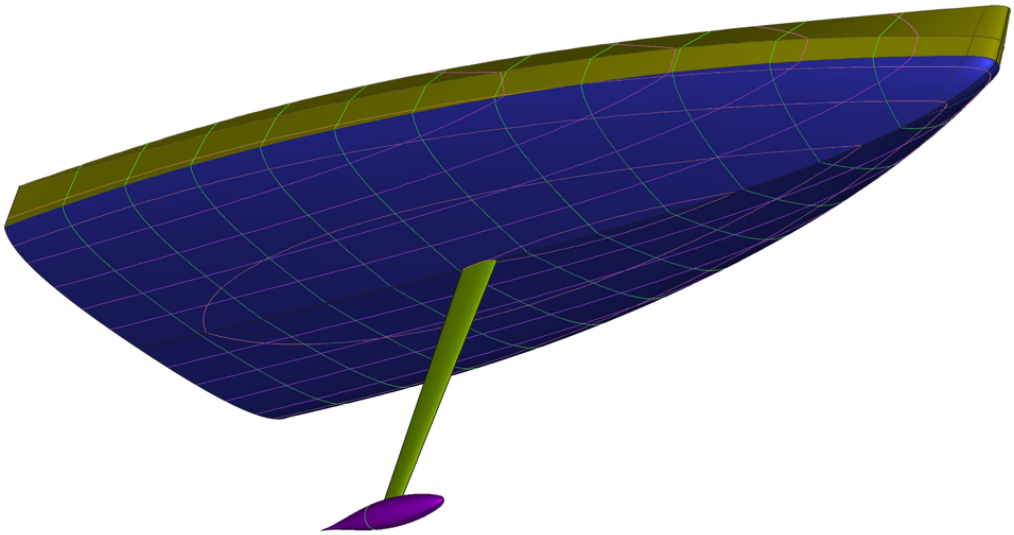

Figure 37: Reversed-engineered Maxsurf model of L'Occitane

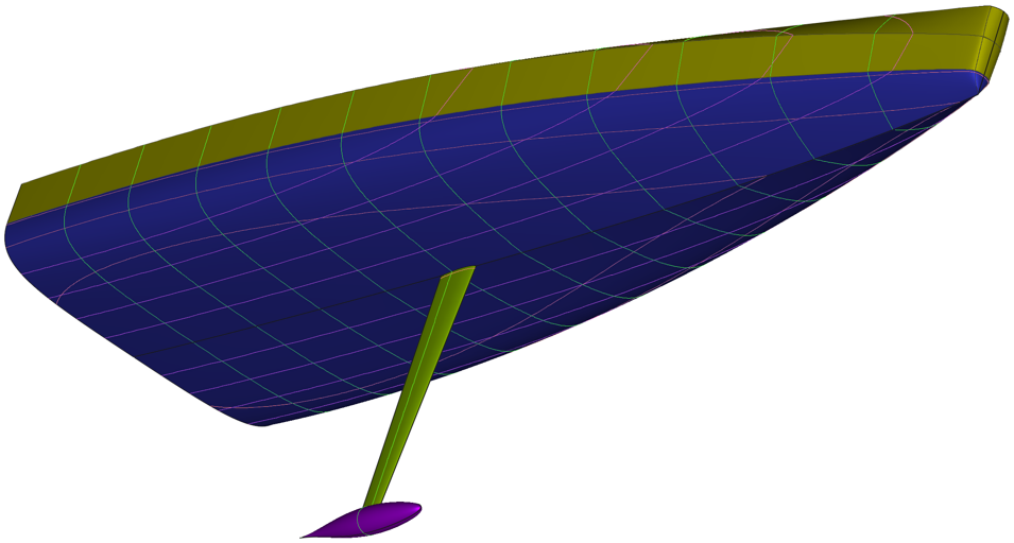

Figure 38: Maxsurf model of the 1^{st} design version

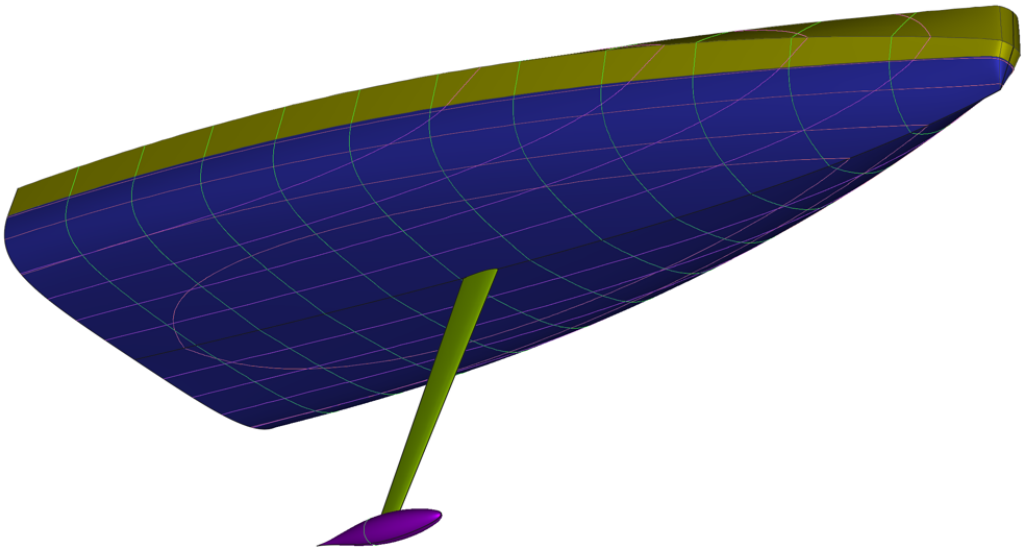

Figure 39: Maxsurf model of the final design version

B.2 Best boat speeds

Table 23: Best boat speeds in knots for Hugo Boss

	4	**6**	**8**	**10**	**14**	**16**	**20**	**25**	**30**	**35**
32	3.81	5.62	6.7	7.45	8.13	8.29	8.41	8.14	7.67	6.72
36	4.38	6.28	7.42	8.16	8.84	9.04	9.23	9.2	8.87	8.13
40	4.91	6.83	8.06	8.73	9.4	9.58	9.78	9.83	9.68	9.28
45	5.51	7.48	8.69	9.3	9.89	10.08	10.32	10.44	10.2	9.92
52	6.21	8.3	9.36	9.85	10.47	10.7	10.91	11.11	11.12	10.94
60	6.85	8.98	9.86	10.34	10.99	11.25	11.64	11.95	12.06	11.96
70	7.42	9.54	10.33	10.82	11.66	12.01	12.6	13.13	13.43	13.46
80	7.79	9.89	10.67	11.3	12.33	12.79	13.65	14.51	15.05	15.28
90	8.39	10.18	11.01	11.7	12.98	13.6	14.77	15.92	16.75	17.27
100	8.45	10.26	11.28	12.06	13.61	14.4	15.82	17.34	18.56	19.4
110	8.25	10.33	11.36	12.33	14.17	15.09	16.79	18.72	20.25	21.39
120	7.73	10.18	11.41	12.12	14.55	15.52	17.64	19.89	21.74	23.23
135	6.06	8.82	10.34	11.7	14.77	15.73	18.27	21.18	23.58	25.64
150	4.09	6.15	8.09	9.68	12.06	13.54	17.49	21.39	24.43	26.99
160	3.25	4.92	6.54	8.11	10.58	11.65	14.31	18.5	23.05	27.6
170	2.8	4.23	5.65	7.04	9.61	10.64	12.75	16.09	19.86	23.72
180	2.57	3.88	5.19	6.48	8.96	9.99	11.89	14.75	18.07	21.56
Up.Vmg	3.9	5.29	6.19	6.69	7.21	7.36	7.51	7.53	7.42	7.02
Dn.Vmg	4.33	6.24	7.5	8.53	10.93	12.39	15.39	18.27	22.62	26.08

Table 24: Best boat speeds in knots for L'Occitane

	4	**6**	**8**	**10**	**14**	**16**	**20**	**25**	**30**	**35**
32	3.81	5.74	6.95	7.67	8.32	8.48	8.63	8.56	8.21	7.71
36	4.39	6.44	7.59	8.28	8.95	9.15	9.37	9.4	9.21	8.71
40	4.93	7.01	8.16	8.8	9.47	9.66	9.91	10.02	9.93	9.64
45	5.54	7.59	8.71	9.35	9.99	10.22	10.55	10.75	10.53	10.29
52	6.27	8.3	9.37	9.92	10.67	10.95	11.2	11.47	11.54	11.42
60	6.92	8.93	9.9	10.5	11.23	11.54	12.07	12.52	12.73	12.71
70	7.47	9.5	10.46	11.03	12.03	12.48	13.27	14.05	14.51	14.68
80	7.78	9.87	10.85	11.55	12.84	13.46	14.58	15.63	16.55	16.94
90	8.31	10.22	11.22	12.04	13.66	14.44	15.82	17.32	18.2	18.77
100	8.33	10.32	11.49	12.41	14.4	15.3	17.11	18.58	19.72	20.55
110	8.19	10.38	11.6	12.73	15	16.11	17.97	19.72	21.14	22.24
120	7.68	9.99	11.64	12.54	15.39	16.75	18.67	20.7	22.4	23.81
135	6.07	8.52	10.16	11.69	15.48	16.73	19.13	21.66	23.96	25.88
150	4.07	6.15	8	9.48	12.09	13.71	17.88	21.98	24.69	27.01
160	3.23	4.91	6.54	8.04	10.51	11.65	14.47	18.65	22.71	27
170	2.79	4.22	5.65	7.03	9.5	10.59	12.81	16.29	19.84	23.44
180	2.56	3.87	5.19	6.48	8.85	9.9	11.9	14.87	18.19	21.41
Up.Vmg	3.93	5.39	6.25	6.74	7.27	7.43	7.61	7.68	7.62	7.28
Dn.Vmg	4.33	6.03	7.31	8.45	11.25	12.94	15.84	18.44	22.5	25.74

Table 25: Best boat speeds in knots for the 1^{st} design version

	4	**6**	**8**	**10**	**14**	**16**	**20**	**25**	**30**	**35**
32	3.7	5.63	6.81	7.56	8.32	8.5	8.68	8.51	8.24	7.3
36	4.25	6.32	7.46	8.27	9.02	9.22	9.43	9.4	9.32	8.45
40	4.77	6.89	8.11	8.85	9.52	9.69	9.92	10.02	9.95	9.71
45	5.39	7.49	8.74	9.4	9.98	10.17	10.45	10.62	10.46	10.28
52	6.1	8.27	9.41	9.91	10.54	10.78	11.02	11.17	11.23	11.24
60	6.75	8.97	9.89	10.39	11.04	11.3	11.64	12.11	12.31	11.99
70	7.3	9.53	10.36	10.85	11.69	12.07	12.72	13.23	13.66	13.97
80	7.59	9.87	10.69	11.31	12.37	12.87	13.84	14.85	15.55	15.94
90	8.27	10.16	11.02	11.7	13.03	13.72	15.01	16.35	17.44	18.18
100	8.33	10.25	11.22	12.02	13.69	14.54	16.11	17.91	19.33	20.36
110	8.12	10.3	11.35	12.22	14.26	15.24	17.15	19.3	21.03	22.39
120	7.41	9.88	11.35	12.29	14.6	15.62	18.02	20.47	22.52	24.21
135	5.79	8.34	10.01	11.24	14.4	16.11	18.63	21.57	24.27	26.53
150	3.99	5.98	7.82	9.4	11.65	12.98	16.69	21.93	25.04	27.61
160	3.2	4.83	6.41	7.92	10.34	11.35	13.77	17.92	22.5	27.23
170	2.78	4.18	5.58	6.93	9.46	10.44	12.42	15.63	19.36	23.24
180	2.54	3.84	5.13	6.39	8.8	9.83	11.62	14.32	17.6	21.09
Up.Vmg	3.82	5.31	6.22	6.78	7.32	7.47	7.64	7.69	7.63	7.3
Dn.Vmg	4.12	5.91	7.25	8.25	10.5	12.05	15.26	18.99	21.69	26.33

Table 26: Best boat speeds in knots for the final design version

	4	**6**	**8**	**10**	**14**	**16**	**20**	**25**	**30**	**35**
32	3.81	5.72	6.99	7.67	8.26	8.4	8.57	8.52	8.22	7.5
36	4.41	6.44	7.64	8.25	8.9	9.11	9.32	9.32	9.16	8.72
40	4.96	7.05	8.16	8.78	9.46	9.65	9.89	9.97	9.84	9.59
45	5.58	7.69	8.71	9.35	9.99	10.2	10.51	10.68	10.43	10.2
52	6.32	8.35	9.39	9.93	10.65	10.92	11.16	11.4	11.44	11.31
60	6.96	8.98	9.92	10.49	11.21	11.5	11.99	12.4	12.57	12.52
70	7.53	9.56	10.47	11.02	11.97	12.39	13.12	13.84	14.26	14.37
80	7.87	9.93	10.85	11.53	12.75	13.32	14.38	15.4	16.09	16.49
90	8.43	10.26	11.21	12	13.52	14.27	15.59	17.05	17.98	18.56
100	8.48	10.36	11.49	12.39	14.24	15.13	16.83	18.44	19.64	20.49
110	8.29	10.42	11.58	12.69	14.83	15.84	17.79	19.67	21.17	22.33
120	7.79	10.14	11.63	12.75	15.13	16.46	18.56	20.73	22.53	24.01
135	6.11	8.68	10.33	11.78	15.39	16.32	19.07	21.84	24.17	26.19
150	4.08	6.17	8.03	9.58	12.17	13.79	18.03	21.93	24.91	27.36
160	3.24	4.92	6.54	8.07	10.56	11.69	14.52	18.82	23.17	27.68
170	2.8	4.23	5.66	7.04	9.55	10.62	12.83	16.28	20	23.76
180	2.56	3.88	5.2	6.49	8.89	9.94	11.93	14.88	18.23	21.58
Up.Vmg	3.96	5.45	6.25	6.72	7.26	7.41	7.58	7.64	7.56	7.19
Dn.Vmg	4.36	6.14	7.42	8.55	11.3	12.89	15.95	18.97	22.9	26.26

B.3 Polar plots

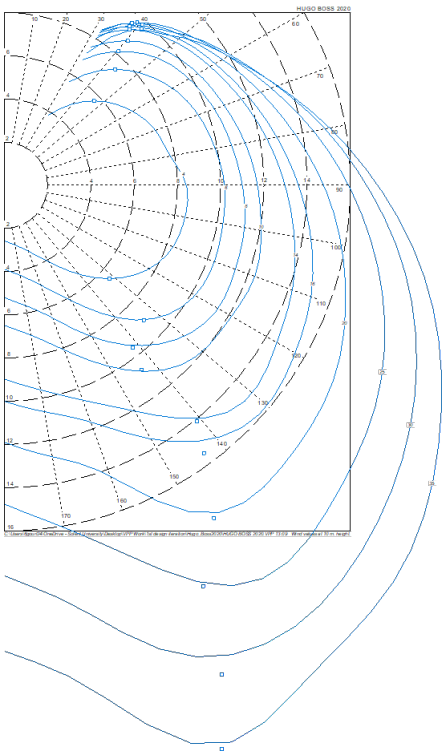

Figure 40: Polar plot for Hugo Boss

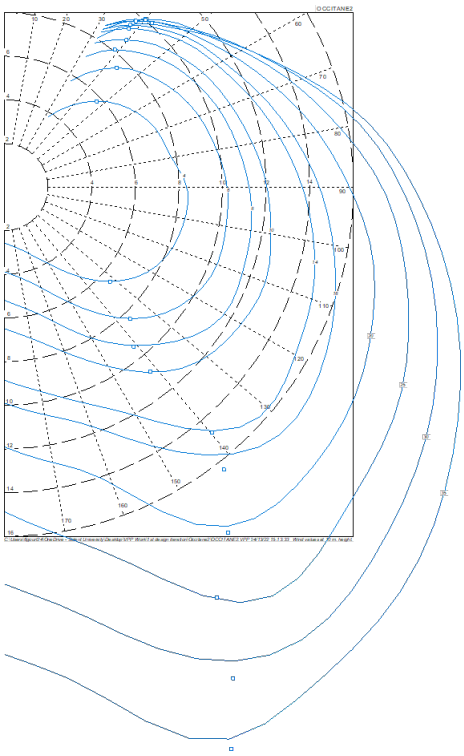

Figure 41: Polar plot for L'Occitane

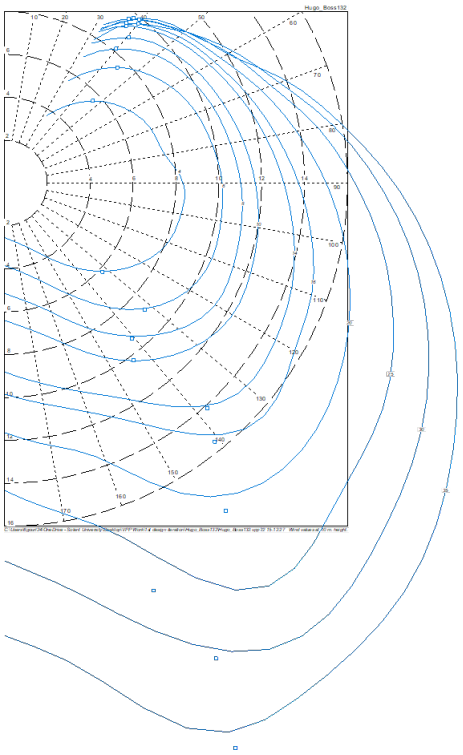

Figure 42: Polar plot for the 1^{st} design version

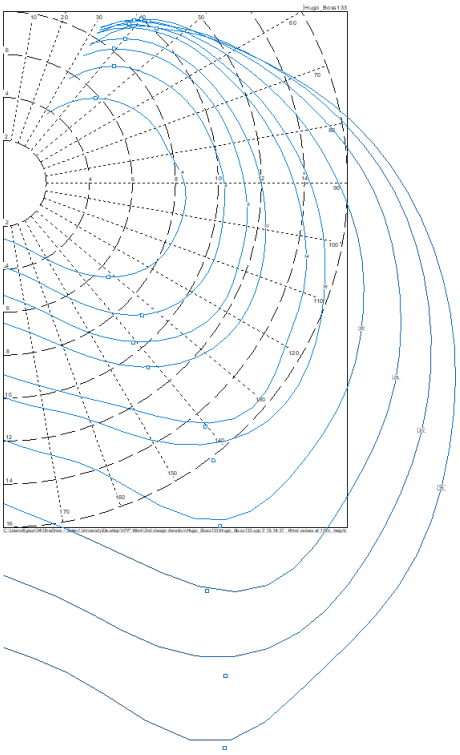

Figure 43: Polar plot for the final design version

B.4 Best keel cant angles

Table 27: Best keel cant angles in degrees for Hugo Boss

	4	**6**	**8**	**10**	**14**	**16**	**20**	**25**	**30**	**35**
32	0	0	0	38	38	38	38	38	38	0
36	0	0	38	38	38	38	38	38	38	38
40	0	0	38	38	38	38	38	38	38	38
45	0	38	38	38	38	38	38	38	38	38
52	0	38	38	38	38	38	38	38	38	38
60	0	38	38	38	38	38	38	38	38	38
70	0	38	38	38	38	38	38	38	38	38
80	0	38	38	38	38	38	38	38	38	38
90	38	38	38	38	38	38	38	38	38	38
100	38	38	38	38	38	38	38	38	38	38
110	0	38	38	38	38	38	38	38	38	38
120	0	38	38	38	38	38	38	38	38	38
135	0	0	0	38	38	38	38	38	38	38
150	0	0	0	0	0	38	38	38	38	38
160	0	0	0	0	0	0	0	38	38	38
170	0	0	0	0	0	0	0	0	0	0
180	38	38	38	38	38	0	0	0	0	0

Table 28: Best keel cant angles in degrees for L'Occitane

	4	**6**	**8**	**10**	**14**	**16**	**20**	**25**	**30**	**35**
32	0	0	0	38	38	38	38	38	38	0
36	0	0	38	38	38	38	38	38	38	38
40	0	0	38	38	38	38	38	38	38	38
45	0	0	38	38	38	38	38	38	38	38
52	0	38	38	38	38	38	38	38	38	38
60	0	38	38	38	38	38	38	38	38	38
70	0	38	38	38	38	38	38	38	38	38
80	0	38	38	38	38	38	38	38	38	38
90	38	38	38	38	38	38	38	38	38	38
100	0	38	38	38	38	38	38	38	38	38
110	0	38	38	38	38	38	38	38	38	38
120	0	38	38	38	38	38	38	38	38	38
135	0	0	0	38	38	38	38	38	38	38
150	0	0	0	0	0	0	38	38	38	38
160	0	0	0	0	0	0	0	0	38	38
170	0	0	0	38	38	38	0	0	0	0
180	38	38	38	38	38	38	38	0	38	38

Table 29: Best keel cant angles in degrees for the 1^{st} design version

	4	**6**	**8**	**10**	**14**	**16**	**20**	**25**	**30**	**35**
32	0	0	0	38	38	38	38	38	38	0
36	0	0	38	38	38	38	38	38	38	0
40	0	0	38	38	38	38	38	38	38	38
45	0	0	38	38	38	38	38	38	38	38
52	0	38	38	38	38	38	38	38	38	38
60	0	38	38	38	38	38	38	38	38	38
70	0	38	38	38	38	38	38	38	38	38
80	0	38	38	38	38	38	38	38	38	38
90	0	38	38	38	38	38	38	38	38	38
100	0	38	38	38	38	38	38	38	38	38
110	0	38	38	38	38	38	38	38	38	38
120	0	0	38	38	38	38	38	38	38	38
135	0	0	0	0	38	38	38	38	38	38
150	0	0	0	0	0	0	38	38	38	38
160	0	0	0	0	38	38	38	0	0	38
170	0	0	0	0	38	38	38	38	38	0
180	0	0	0	38	38	38	38	38	38	38

Table 30: Best keel cant angles in degrees for the final design version

	4	**6**	**8**	**10**	**14**	**16**	**20**	**25**	**30**	**35**
32	0	0	0	38	38	38	38	38	38	0
36	0	0	38	38	38	38	38	38	38	38
40	0	0	38	38	38	38	38	38	38	38
45	0	38	38	38	38	38	38	38	38	38
52	0	38	38	38	38	38	38	38	38	38
60	0	38	38	38	38	38	38	38	38	38
70	0	38	38	38	38	38	38	38	38	38
80	0	38	38	38	38	38	38	38	38	38
90	38	38	38	38	38	38	38	38	38	38
100	38	38	38	38	38	38	38	38	38	38
110	0	38	38	38	38	38	38	38	38	38
120	0	38	38	38	38	38	38	38	38	38
135	0	0	0	38	38	38	38	38	38	38
150	0	0	0	0	0	0	38	38	38	38
160	0	0	0	0	0	0	0	0	38	38
170	0	0	0	38	38	38	38	38	0	0
180	38	38	38	38	38	38	38	38	38	38

B.5 Best sail sets

Table 31: Best sail sets for Hugo Boss

	4	**6**	**8**	**10**	**14**	**16**	**20**	**25**	**30**	**35**
32	UPl	UPl	UPl	UPl	UPl	UPl	UPl	UPm	UPl	UPl
36	UPl	UPl	UPl	UPl	UPl	UPl	UPl	UPl	UPl	UPl
40	UPl	UPl	UPl	UPl	UPl	UPl	UPl	UPl	UPl	UPl
45	UPl	UPl	UPl	UPl	UPl	UPl	UPl	UPl	UPl	UPl
52	UPl	UPl	UPl	UPl	UPl	UPl	UPl	UPl	UPl	UPl
60	UPl	UPl	UPl	UPl	UPl	UPl	UPl	UPl	UPl	UPl
70	UPl	UPl	UPl	UPl	UPl	UPl	UPl	UPl	UPl	UPl
80	UPl	UPl	UPl	UPl	UPl	UPl	UPl	UPl	UPl	UPl
90	DWm	DWm	UPl	UPl	UPl	UPl	UPl	UPl	UPl	UPl
100	DWm	DWm	UPl	UPl	UPl	UPl	UPl	UPl	UPl	UPl
110	DWm	DWm	DWm	UPl	UPl	UPl	UPl	UPl	UPl	UPl
120	DWm	DWm	DWm	DWs	UPl	UPm	UPl	UPl	UPl	UPl
135	DWm	DWm	DWm	DWl	DWm	DWm	DWm	UPm	UPm	UPm
150	DWl	DWl	DWl	DWl	DWl	DWl	DWl	DWl	DWm	DWs
160	DWl	DWl	DWl	DWl	DWl	DWl	DWl	DWl	DWl	DWl
170	DWl	DWl	DWl	DWl	DWl	DWl	DWl	DWl	DWl	DWl
180	DWl	DWl	DWl	DWl	DWl	DWl	DWl	DWl	DWl	DWl

Table 32: Best sail sets for L'Occitane

	4	**6**	**8**	**10**	**14**	**16**	**20**	**25**	**30**	**35**
32	UPl	UPl	UPl	UPl	UPl	UPl	UPl	UPl	UPl	UPl
36	UPl	UPl	UPl	UPl	UPl	UPl	UPl	UPl	UPl	UPl
40	UPl	UPl	UPl	UPl	UPl	UPl	UPl	UPl	UPl	UPl
45	UPl	UPl	UPl	UPl	UPl	UPl	UPl	UPl	UPl	UPl
52	UPl	UPl	UPl	UPl	UPl	UPl	UPl	UPl	UPl	UPl
60	UPl	UPl	UPl	UPl	UPl	UPl	UPl	UPl	UPl	UPl
70	UPl	UPl	UPl	UPl	UPl	UPl	UPl	UPl	UPl	UPl
80	UPl	UPl	UPl	UPl	UPl	UPl	UPl	UPl	UPl	UPl
90	DWm	DWm	UPl	UPl	UPl	UPl	UPl	UPl	UPl	UPl
100	DWm	DWm	UPl	UPl	UPl	UPl	UPl	UPl	UPl	UPl
110	DWm	DWm	DWm	UPWl	UPl	UPl	UPl	UPl	UPl	UPl
120	DWm	DWm	DWm	DWm	UPl	UPl	UPl	UPl	UPl	UPl
135	DWm	DWm	DWm	DWl	DWm	DWm	DWm	UPl	UPl	UPm
150	DWl	DWl	DWl	DWl	DWl	DWl	DWl	DWl	DWm	DWm
160	DWl	DWl	DWl	DWl	DWl	DWl	DWl	DWl	DWl	DWl
170	DWl	DWl	DWl	DWl	DWl	DWl	DWl	DWl	DWl	DWl
180	DWl	DWl	DWl	DWl	DWl	DWl	DWl	DWl	DWl	DWl

Table 33: Best sail sets for the 1^{st} design version

	4	**6**	**8**	**10**	**14**	**16**	**20**	**25**	**30**	**35**
32	UPl	UPl	UPl	UPl	UPl	UPl	UPl	UPm	UPl	UPl
36	UPl	UPl	UPl	UPl	UPl	UPl	UPl	UPm	UPl	UPl
40	UPl	UPl	UPl	UPl	UPl	UPl	UPl	UPl	UPl	UPl
45	UPl	UPl	UPl	UPl	UPl	UPl	UPl	UPl	UPl	UPl
52	UPl	UPl	UPl	UPl	UPl	UPl	UPl	UPm	UPm	UPl
60	UPl	UPl	UPl	UPl	UPl	UPl	UPm	UPl	UPl	UPs
70	UPl	UPl	UPl	UPl	UPl	UPl	UPl	UPm	UPm	UPl
80	UPl	UPl	UPl	UPl	UPl	UPl	UPl	UPl	UPl	UPl
90	DWm	DWm	UPl	UPl	UPl	UPl	UPl	UPl	UPl	UPl
100	DWm	DWm	UPl	UPl	UPl	UPl	UPl	UPl	UPl	UPl
110	DWm	DWm	DWm	DWm	UPl	UPl	UPl	UPl	UPl	UPl
120	DWm	DWm	DWm	DWm	UPl	DWm	UPl	UPl	UPl	UPl
135	DWm	DWm	DWl	DWl	DWl	DWm	DWm	UPl	UPl	UPm
150	DWl	DWl	DWl	DWl	DWl	DWl	DWl	DWl	DWm	DWl
160	DWl	DWl	DWl	DWl	DWl	DWl	DWl	DWl	DWl	DWl
170	DWl	DWl	DWl	DWl	DWl	DWl	DWl	DWl	DWl	DWl
180	DWl	DWl	DWl	DWl	DWl	DWl	DWl	DWl	DWl	DWl

Table 34: Best sail sets for the final design version

	4	**6**	**8**	**10**	**14**	**16**	**20**	**25**	**30**	**35**
32	UPl	UPl	UPl	UPl	UPl	UPl	UPl	UPl	UPl	UPl
36	UPl	UPl	UPl	UPl	UPl	UPl	UPl	UPl	UPl	UPl
40	UPl	UPl	UPl	UPl	UPl	UPl	UPl	UPl	UPl	UPl
45	UPl	UPl	UPl	UPl	UPl	UPl	UPl	UPl	UPl	UPl
52	UPl	UPl	UPl	UPl	UPl	UPl	UPl	UPl	UPl	UPl
60	UPl	UPl	UPl	UPl	UPl	UPl	UPl	UPl	UPl	UPl
70	UPl	UPl	UPl	UPl	UPl	UPl	UPl	UPl	UPl	UPl
80	UPl	UPl	UPl	UPl	UPl	UPl	UPl	UPl	UPl	UPl
90	DWm	DWm	UPl	UPl	UPl	UPl	UPl	UPl	UPl	UPl
100	DWm	DWm	UPl	UPl	UPl	UPl	UPl	UPl	UPl	UPl
110	DWm	DWm	DWm	UPl	UPl	UPl	UPl	UPl	UPl	UPl
120	DWm	DWm	DWm	DWm	UPl	UPl	UPl	UPl	UPl	UPl
135	DWm	DWm	DWm	DWl	DWm	DWm	DWm	UPm	UPl	UPm
150	DWl	DWl	DWl	DWl	DWl	DWl	DWl	DWl	DWm	DWm
160	DWl	DWl	DWl	DWl	DWl	DWl	DWl	DWl	DWl	DWl
170	DWl	DWl	DWl	DWl	DWl	DWl	DWl	DWl	DWl	DWl
180	DWl	DWl	DWl	DWl	DWl	DWl	DWl	DWl	DWl	DWl

C Appendix - Theoretical model for foil predictions

Relevant parts of the Excel spreadsheet used for the predictions are presented below. Note that the yellow cells are input cells in which values are entered to base the calculations on. Proofs of the equations used in the model are also proposed.

C.1 3D lift and drag coefficients calculations for each foil sections

Table 35: Lift and drag coefficients of the foil sections for different angles of attack

			Foil section A			Foil section B			Foil section C			Foil section D		
AoA	Cl2D	Cd2D	Cdi	Cl3D	Cd3D	Cdi	Cl3D	Cd3D	Cdi	Cl3D	Cd3D	Cdi	Cl3D	Cd3D
0	0,48	0,004	0,006	0,25	0,010	0,006	0,26	0,010	0,004	0,10	0,008	0,006	0,18	0,010
0,25	0,51	0,004	0,007	0,26	0,011	0,007	0,28	0,011	0,005	0,11	0,009	0,006	0,19	0,011
0,5	0,53	0,004	0,008	0,28	0,012	0,007	0,29	0,012	0,005	0,12	0,009	0,007	0,20	0,011
0,75	0,56	0,004	0,008	0,29	0,013	0,008	0,31	0,013	0,006	0,12	0,010	0,008	0,21	0,012
1	0,59	0,004	0,009	0,30	0,013	0,009	0,32	0,013	0,006	0,13	0,011	0,009	0,22	0,013
1,25	0,62	0,004	0,010	0,32	0,014	0,010	0,34	0,014	0,007	0,13	0,011	0,009	0,23	0,014
1,5	0,64	0,004	0,011	0,33	0,015	0,011	0,35	0,015	0,007	0,14	0,012	0,010	0,24	0,015
1,75	0,66	0,005	0,012	0,34	0,016	0,012	0,36	0,016	0,008	0,14	0,013	0,011	0,25	0,016
2	0,68	0,005	0,012	0,35	0,017	0,012	0,37	0,017	0,008	0,15	0,014	0,012	0,26	0,017
2,25	0,70	0,006	0,013	0,36	0,019	0,013	0,38	0,019	0,009	0,15	0,015	0,012	0,26	0,018
2,5	0,72	0,006	0,014	0,37	0,020	0,013	0,39	0,020	0,009	0,16	0,016	0,013	0,27	0,019
2,75	0,73	0,007	0,014	0,38	0,021	0,014	0,40	0,021	0,010	0,16	0,017	0,013	0,27	0,021
3	0,75	0,008	0,015	0,39	0,023	0,015	0,41	0,023	0,010	0,16	0,018	0,014	0,28	0,022
3,25	0,77	0,009	0,016	0,40	0,024	0,016	0,42	0,024	0,011	0,17	0,019	0,015	0,29	0,023
3,5	0,79	0,009	0,017	0,41	0,026	0,017	0,43	0,025	0,011	0,17	0,020	0,016	0,30	0,025
3,75	0,82	0,009	0,018	0,42	0,027	0,018	0,45	0,027	0,012	0,18	0,021	0,017	0,31	0,026
4	0,84	0,009	0,019	0,44	0,028	0,019	0,46	0,028	0,013	0,18	0,022	0,018	0,32	0,027
4,25	0,87	0,010	0,020	0,45	0,030	0,020	0,47	0,030	0,014	0,19	0,023	0,019	0,33	0,028
4,5	0,89	0,010	0,021	0,46	0,031	0,021	0,49	0,031	0,014	0,20	0,024	0,020	0,33	0,030
4,75	0,92	0,010	0,022	0,47	0,033	0,022	0,50	0,032	0,015	0,20	0,026	0,021	0,34	0,031
5	0,94	0,011	0,023	0,49	0,034	0,023	0,51	0,034	0,016	0,21	0,027	0,022	0,35	0,033
5,25	0,97	0,011	0,025	0,50	0,036	0,025	0,53	0,035	0,017	0,21	0,028	0,023	0,36	0,034
5,5	0,99	0,011	0,026	0,51	0,037	0,026	0,54	0,037	0,018	0,22	0,029	0,024	0,37	0,035
5,75	1,01	0,011	0,027	0,52	0,039	0,027	0,55	0,038	0,019	0,22	0,030	0,026	0,38	0,037
6	1,04	0,012	0,028	0,54	0,040	0,028	0,57	0,040	0,019	0,23	0,031	0,027	0,39	0,039

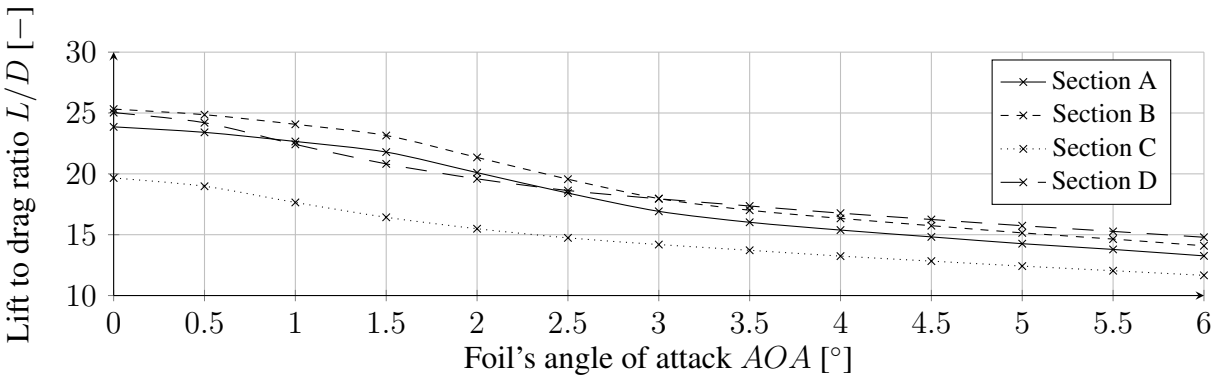

Figure 44: Lift to drag ratio of the foil sections as function of the AOA

C.2 First model version based on full displacement

C.2.1 Hydrodynamic forces calculation

Table 36: Hydrodynamic forces calculation for foil section A

Foil Section A														
Vb (kts)	Θ (°)	Υ (°)	Im. (%)	ξ (°)	η (°)	Vapp (m/s)	Lsec (N)	Dsec (N)	L (N)	D (N)	SF (N)	L contribution (%)	D contribution (%)	SF contribution (%)
10	0	0	0	0,0000	0,0000	5,1440	0	0	0	0	0	0	0	0
		1		0,1737	0,8290	5,1432	0	0	0	0	0	0	0	0
		2		0,3474	1,6582	5,1410	0	0	0	0	0	0	0	0
		3		0,5214	2,4877	5,1372	0	0	0	0	0	0	0	0
	5	0	0	0,0000	0,0000	5,1440	0	0	0	0	0	0	0	0
		1		0,2588	0,7500	5,1433	0	0	0	0	0	0	0	0
		2		0,5178	1,5003	5,1411	0	0	0	0	0	0	0	0
		3		0,7771	2,2509	5,1374	0	0	0	0	0	0	0	0
	15	0	76,02	0,0000	0,0000	5,1440	1810,35	90,05	1640,74	90,05	-765,09	24,94	22,18	23,82
		1		0,4227	0,6170	5,1434	1809,90	90,03	1639,68	103,37	-764,59	24,93	22,38	23,82
		2		0,8455	1,2343	5,1414	1808,54	89,96	1637,71	116,63	-763,68	24,93	22,53	23,83
		3		1,2688	1,8520	5,1382	1806,28	89,85	1634,84	129,80	-762,34	24,93	22,65	23,83
	25	0	100	0,0000	0,0000	5,1440	2381,51	118,46	1950,82	118,46	-1365,98	28,32	26,72	29,95
		1		0,5736	0,5302	5,1435	2381,02	118,44	1949,35	142,26	-1364,95	28,31	27,22	29,96
		2		1,1475	1,0606	5,1419	2379,56	118,37	1946,89	165,97	-1363,23	28,31	27,58	29,96
		3		1,7218	1,5915	5,1393	2377,13	118,24	1943,44	189,56	-1360,81	28,31	27,85	29,96
Vb (kts)	Θ (°)	Υ (°)	Im. (%)	ξ (°)	η (°)	Vapp (m/s)	Lsec (N)	Dsec (N)	L (N)	D (N)	SF (N)	L contribution (%)	D contribution (%)	SF contribution (%)
15	0	0	0	0,0000	0,0000	7,7160	0	0	0	0	0	0	0	0
		1		0,1737	0,8290	7,7149	0	0	0	0	0	0	0	0
		2		0,3474	1,6582	7,7114	0	0	0	0	0	0	0	0
		3		0,5214	2,4877	7,7057	0	0	0	0	0	0	0	0
	5	0	0	0,0000	0,0000	7,7160	0	0	0	0	0	0	0	0
		1		0,2588	0,7500	7,7149	0	0	0	0	0	0	0	0
		2		0,5178	1,5003	7,7116	0	0	0	0	0	0	0	0
		3		0,7771	2,2509	7,7061	0	0	0	0	0	0	0	0
	15	0	76,02	0,0000	0,0000	7,7160	4073,29	202,62	3691,66	202,62	-1721,45	24,94	22,18	23,82
		1		0,4227	0,6170	7,7150	4072,27	202,56	3689,28	232,59	-1720,34	24,94	22,38	23,82
		2		0,8455	1,2343	7,7121	4069,22	202,41	3684,85	262,41	-1718,28	24,93	22,53	23,83
		3		1,2688	1,8520	7,7073	4064,13	202,16	3678,39	292,04	-1715,26	24,94	22,66	23,83
	25	0	100	0,0000	0,0000	7,7160	5358,40	266,54	4389,34	266,54	-3073,45	28,32	26,72	29,95
		1		0,5736	0,5302	7,7152	5357,30	266,48	4386,04	320,09	-3071,14	28,31	27,22	29,96
		2		1,1475	1,0606	7,7128	5354,02	266,32	4380,50	373,44	-3067,26	28,32	27,58	29,96
		3		1,7218	1,5915	7,7089	5348,55	266,05	4372,75	426,50	-3061,83	28,32	27,86	29,96
Vb (kts)	Θ (°)	Υ (°)	Im. (%)	ξ (°)	η (°)	Vapp (m/s)	Lsec (N)	Dsec (N)	L (N)	D (N)	SF (N)	L contribution (%)	D contribution (%)	SF contribution (%)
20	0	0	0	0,0000	0,0000	10,2880	0	0	0	0	0	0	0	0
		1		0,1737	0,8290	10,2865	0	0	0	0	0	0	0	0
		2		0,3474	1,6582	10,2819	0	0	0	0	0	0	0	0
		3		0,5214	2,4877	10,2743	0	0	0	0	0	0	0	0
	5	0	0	0,0000	0,0000	10,2880	0	0	0	0	0	0	0	0
		1		0,2588	0,7500	10,2865	0	0	0	0	0	0	0	0
		2		0,5178	1,5003	10,2822	0	0	0	0	0	0	0	0
		3		0,7771	2,2509	10,2748	0	0	0	0	0	0	0	0
	15	0	76,02	0,0000	0,0000	10,2880	7241,41	360,20	6562,94	360,20	-3060,35	24,94	22,18	23,82
		1		0,4227	0,6170	10,2867	7239,59	360,11	6558,72	413,50	-3058,38	24,93	22,38	23,82
		2		0,8455	1,2343	10,2829	7234,16	359,84	6550,85	466,51	-3054,71	24,93	22,53	23,83
		3		1,2688	1,8520	10,2764	7225,11	359,39	6539,36	519,19	-3049,35	24,93	22,65	23,83
	25	0	100	0,0000	0,0000	10,2880	9526,04	473,85	7803,27	473,85	-5463,91	28,32	26,72	29,95
		1		0,5736	0,5302	10,2869	9524,09	473,75	7797,40	569,06	-5459,80	28,31	27,22	29,96
		2		1,1475	1,0606	10,2838	9518,25	473,46	7787,56	663,89	-5452,91	28,31	27,58	29,96
		3		1,7218	1,5915	10,2785	9508,53	472,98	7773,77	758,23	-5443,25	28,31	27,85	29,96
Vb (kts)	Θ (°)	Υ (°)	Im. (%)	ξ (°)	η (°)	Vapp (m/s)	Lsec (N)	Dsec (N)	L (N)	D (N)	SF (N)	L contribution (%)	D contribution (%)	SF contribution (%)
25	0	0	0	0,0000	0,0000	12,8600	0	0	0	0	0	0	0	0
		1		0,1737	0,8290	12,8581	0	0	0	0	0	0	0	0
		2		0,3474	1,6582	12,8524	0	0	0	0	0	0	0	0
		3		0,5214	2,4877	12,8429	0	0	0	0	0	0	0	0
	5	0	0	0,0000	0,0000	12,8600	0	0	0	0	0	0	0	0
		1		0,2588	0,7500	12,8582	0	0	0	0	0	0	0	0
		2		0,5178	1,5003	12,8527	0	0	0	0	0	0	0	0
		3		0,7771	2,2509	12,8436	0	0	0	0	0	0	0	0
	15	0	76,02	0,0000	0,0000	12,8600	11314,70	562,82	10254,60	562,82	-4781,80	24,94	22,18	23,82
		1		0,4227	0,6170	12,8584	11311,87	562,68	10247,99	646,09	-4778,72	24,93	22,38	23,82
		2		0,8455	1,2343	12,8536	11303,38	562,26	10235,70	728,93	-4772,99	24,93	22,53	23,83
		3		1,2688	1,8520	12,8455	11289,24	561,55	10217,75	811,23	-4764,61	24,93	22,65	23,83
	25	0	100	0,0000	0,0000	12,8600	14884,43	740,39	12192,61	740,39	-8537,36	28,32	26,72	29,95
		1		0,5736	0,5302	12,8587	14881,39	740,24	12183,44	889,15	-8530,94	28,31	27,22	29,96
		2		1,1475	1,0606	12,8547	14872,27	739,78	12168,07	1037,32	-8520,17	28,31	27,58	29,96
		3		1,7218	1,5915	12,8482	14857,07	739,03	12146,52	1184,73	-8505,08	28,31	27,85	29,96

Table 37: Hydrodynamic forces calculation for foil section B

Foil Section B														
Vb (kts)	Θ (°)	Υ (°)	Im. (%)	ξ (°)	η (°)	Vapp (m/s)	Lsec (N)	Dsec (N)	L (N)	D (N)	SF (N)	L contribution (%)	D contribution (%)	SF contribution (%)
10	0	0	0	0,0000	0,0000	5,1440	0	0	0	0	0	0	0	0
		1		0,0000	1,0000	5,1432	0	0	0	0	0	0	0	0
		2		0,0000	2,0000	5,1409	0	0	0	0	0	0	0	0
		3		0,0000	3,0000	5,1370	0	0	0	0	0	0	0	0
	5	0	6,84	0,0000	0,0000	5,1440	309,64	14,50	308,47	14,50	-26,99	95,71	89,78	69,91
		1		0,0872	0,9132	5,1432	309,55	14,50	308,35	14,97	-26,98	95,71	88,99	69,93
		2		0,1744	1,8265	5,1409	309,27	14,48	308,05	15,42	-26,95	95,71	88,25	69,95
		3		0,2617	2,7399	5,1370	308,80	14,46	307,56	15,87	-26,91	95,72	87,57	69,96
	15	0	100	0,0000	0,0000	5,1440	4530,28	212,15	4375,91	212,15	-1172,52	66,51	52,25	36,50
		1		0,2588	0,7500	5,1433	4528,99	212,09	4373,70	232,54	-1171,93	66,51	50,34	36,52
		2		0,5178	1,5003	5,1411	4525,13	211,91	4368,91	252,79	-1170,65	66,52	48,84	36,52
		3		0,7771	2,2509	5,1374	4518,70	211,61	4361,56	272,85	-1168,68	66,52	47,62	36,53
	25	0	100	0,0000	0,0000	5,1440	4530,28	212,15	4105,83	212,15	-1914,58	59,59	47,86	41,98
		1		0,4227	0,6170	5,1434	4529,15	212,10	4103,27	245,49	-1913,39	59,60	46,96	41,99
		2		0,8455	1,2343	5,1414	4525,75	211,94	4098,44	278,67	-1911,13	59,60	46,30	42,00
		3		1,2688	1,8520	5,1382	4520,09	211,67	4091,34	311,65	-1907,82	59,61	45,79	42,00
Vb (kts)	Θ (°)	Υ (°)	Im. (%)	ξ (°)	η (°)	Vapp (m/s)	Lsec (N)	Dsec (N)	L (N)	D (N)	SF (N)	L contribution (%)	D contribution (%)	SF contribution (%)
15	0	0	0	0,0000	0,0000	7,7160	0	0	0	0	0	0	0	0
		1		0,0000	1,0000	7,7148	0	0	0	0	0	0	0	0
		2		0,0000	2,0000	7,7113	0	0	0	0	0	0	0	0
		3		0,0000	3,0000	7,7054	0	0	0	0	0	0	0	0
	5	0	6,84	0,0000	0,0000	7,7160	696,70	32,63	694,05	32,63	-60,72	95,71	89,78	69,91
		1		0,0872	0,9132	7,7148	696,49	32,62	693,79	33,68	-60,70	95,71	88,99	69,93
		2		0,1744	1,8265	7,7113	695,85	32,59	693,10	34,70	-60,64	95,71	88,25	69,95
		3		0,2617	2,7399	7,7054	694,79	32,54	691,99	35,71	-60,54	95,71	87,56	69,96
	15	0	100	0,0000	0,0000	7,7160	10193,13	477,33	9845,81	477,33	-2638,18	66,51	52,25	36,50
		1		0,2588	0,7500	7,7148	10190,02	477,19	9840,62	523,21	-2636,79	66,51	50,34	36,52
		2		0,5178	1,5003	7,7113	10180,71	476,75	9829,25	568,72	-2633,74	66,51	48,83	36,52
		3		0,7771	2,2509	7,7054	10165,21	476,03	9811,70	613,80	-2629,04	66,51	47,62	36,52
	25	0	100	0,0000	0,0000	7,7160	10193,13	477,33	9238,11	477,33	-4307,80	59,59	47,86	41,98
		1		0,4227	0,6170	7,7148	10190,02	477,19	9231,86	552,33	-4304,89	59,60	46,96	41,99
		2		0,8455	1,2343	7,7113	10180,71	476,75	9219,48	626,88	-4299,11	59,60	46,30	41,99
		3		1,2688	1,8520	7,7054	10165,21	476,03	9201,00	700,86	-4290,50	59,59	45,78	41,99
Vb (kts)	Θ (°)	Υ (°)	Im. (%)	ξ (°)	η (°)	Vapp (m/s)	Lsec (N)	Dsec (N)	L (N)	D (N)	SF (N)	L contribution (%)	D contribution (%)	SF contribution (%)
20	0	0	0	0,0000	0,0000	10,2880	0	0	0	0	0	0	0	0
		1		0,0000	1,0000	10,2864	0	0	0	0	0	0	0	0
		2		0,0000	2,0000	10,2817	0	0	0	0	0	0	0	0
		3		0,0000	3,0000	10,2739	0	0	0	0	0	0	0	0
	5	0	6,84	0,0000	0,0000	10,2880	1238,58	58,00	1233,87	58,00	-107,95	95,71	89,78	69,91
		1		0,0872	0,9132	10,2864	1238,20	57,98	1233,40	59,87	-107,91	95,71	88,99	69,93
		2		0,1744	1,8265	10,2818	1237,08	57,93	1232,19	61,70	-107,80	95,71	88,25	69,95
		3		0,2617	2,7399	10,2740	1235,21	57,84	1230,24	63,48	-107,63	95,72	87,57	69,96
	15	0	100	0,0000	0,0000	10,2880	18121,12	848,59	17503,66	848,59	-4690,09	66,51	52,25	36,50
		1		0,2588	0,7500	10,2865	18115,97	848,35	17494,80	930,18	-4687,72	66,51	50,34	36,52
		2		0,5178	1,5003	10,2822	18100,53	847,63	17475,65	1011,14	-4682,59	66,52	48,84	36,52
		3		0,7771	2,2509	10,2748	18074,81	846,42	17446,23	1091,40	-4674,70	66,52	47,62	36,53
	25	0	100	0,0000	0,0000	10,2880	18121,12	848,59	16423,31	848,59	-7658,32	59,59	47,86	41,98
		1		0,4227	0,6170	10,2867	18116,58	848,38	16413,08	981,98	-7653,55	59,60	46,96	41,99
		2		0,8455	1,2343	10,2829	18102,99	847,74	16393,76	1114,69	-7644,53	59,60	46,30	42,00
		3		1,2688	1,8520	10,2764	18080,35	846,68	16365,35	1246,58	-7631,29	59,61	45,79	42,00
Vb (kts)	Θ (°)	Υ (°)	Im. (%)	ξ (°)	η (°)	Vapp (m/s)	Lsec (N)	Dsec (N)	L (N)	D (N)	SF (N)	L contribution (%)	D contribution (%)	SF contribution (%)
25	0	0	0	0,0000	0,0000	12,8600	0	0	0	0	0	0	0	0
		1		0,0000	1,0000	12,8580	0	0	0	0	0	0	0	0
		2		0,0000	2,0000	12,8522	0	0	0	0	0	0	0	0
		3		0,0000	3,0000	12,8424	0	0	0	0	0	0	0	0
	5	0	6,84	0,0000	0,0000	12,8600	1935,28	90,63	1927,91	90,63	-168,67	95,71	89,78	69,91
		1		0,0872	0,9132	12,8581	1934,69	90,60	1927,19	93,54	-168,61	95,71	88,99	69,93
		2		0,1744	1,8265	12,8522	1932,94	90,52	1925,30	96,40	-168,44	95,71	88,25	69,95
		3		0,2617	2,7399	12,8425	1930,02	90,38	1922,24	99,19	-168,17	95,72	87,57	69,96
	15	0	100	0,0000	0,0000	12,8600	28314,25	1325,93	27349,46	1325,93	-7328,27	66,51	52,25	36,50
		1		0,2588	0,7500	12,8582	28306,20	1325,55	27335,63	1453,40	-7324,56	66,51	50,34	36,52
		2		0,5178	1,5003	12,8527	28282,07	1324,42	27305,70	1579,91	-7316,54	66,52	48,84	36,52
		3		0,7771	2,2509	12,8436	28241,89	1322,54	27259,73	1705,31	-7304,22	66,52	47,62	36,53
	25	0	100	0,0000	0,0000	12,8600	28314,25	1325,93	25661,42	1325,93	-11966,12	59,59	47,86	41,98
		1		0,4227	0,6170	12,8584	28307,16	1325,60	25645,44	1534,34	-11958,67	59,60	46,96	41,99
		2		0,8455	1,2343	12,8536	28285,92	1324,60	25615,24	1741,70	-11944,58	59,60	46,30	42,00
		3		1,2688	1,8520	12,8455	28250,54	1322,94	25570,86	1947,78	-11923,89	59,61	45,79	42,00

Table 38: Hydrodynamic forces calculation for foil section C

Foil Section C														
Vb (kts)	Θ (°)	ϒ (°)	Im. (%)	ξ (°)	η (°)	Vapp (m/s)	Lsec (N)	Dsec (N)	L (N)	D (N)	SF (N)	L contribution (%)	D contribution (%)	SF contribution (%)
10	0	0	0	0,0000	0,0000	5,1440	0	0	0	0	0	0	0	0
		1		0,7071	0,5000	5,1436	0	0	0	0	0	0	0	0
		2		1,4145	1,0003	5,1424	0	0	0	0	0	0	0	0
		3		2,1223	1,5010	5,1405	0	0	0	0	0	0	0	0
	5	0	5,97	0,0000	0,0000	5,1440	18,07	1,65	13,84	1,65	11,61	4,29	10,22	30,09
		1		0,6428	0,5076	5,1435	18,06	1,65	13,82	1,85	11,60	4,29	11,01	30,07
		2		1,2859	1,0155	5,1422	18,05	1,65	13,80	2,05	11,58	4,29	11,75	30,05
		3		1,9294	1,5238	5,1399	18,04	1,65	13,77	2,25	11,55	4,28	12,43	30,04
	15	0	100	0,0000	0,0000	5,1440	302,81	27,66	262,24	27,66	151,40	3,99	6,81	4,71
		1		0,5000	0,5670	5,1434	302,74	27,65	261,96	30,29	151,24	3,98	6,56	4,71
		2		1,0003	1,1343	5,1416	302,53	27,63	261,54	32,91	151,00	3,98	6,36	4,71
		3		1,5010	1,7020	5,1387	302,18	27,60	260,98	35,50	150,68	3,98	6,20	4,71
	25	0	100	0,0000	0,0000	5,1440	302,81	27,66	284,54	27,66	103,57	4,13	6,24	2,27
		1		0,3421	0,6786	5,1433	302,72	27,65	284,31	29,46	103,48	4,13	5,64	2,27
		2		0,6843	1,3575	5,1412	302,48	27,63	283,91	31,24	103,33	4,13	5,19	2,27
		3		1,0269	2,0368	5,1378	302,07	27,59	283,35	33,00	103,13	4,13	4,85	2,27
Vb (kts)	Θ (°)	ϒ (°)	Im. (%)	ξ (°)	η (°)	Vapp (m/s)	Lsec (N)	Dsec (N)	L (N)	D (N)	SF (N)	L contribution (%)	D contribution (%)	SF contribution (%)
15	0	0	0	0,0000	0,0000	7,7160	0	0	0	0	0	0	0	0
		1		0,7071	0,5000	7,7154	0	0	0	0	0	0	0	0
		2		1,4145	1,0003	7,7137	0	0	0	0	0	0	0	0
		3		2,1223	1,5010	7,7107	0	0	0	0	0	0	0	0
	5	0	5,97	0,0000	0,0000	7,7160	40,65	3,71	31,14	3,71	26,13	4,29	10,22	30,09
		1		0,6428	0,5076	7,7154	40,65	3,71	31,10	4,17	26,10	4,29	11,01	30,07
		2		1,2859	1,0155	7,7137	40,63	3,71	31,05	4,62	26,05	4,29	11,75	30,05
		3		1,9294	1,5238	7,7107	40,60	3,71	30,99	5,07	26,00	4,29	12,44	30,04
	15	0	100	0,0000	0,0000	7,7160	681,31	62,23	590,03	62,23	340,66	3,99	6,81	4,71
		1		0,5000	0,5670	7,7154	681,21	62,22	589,45	68,16	340,32	3,98	6,56	4,71
		2		1,0003	1,1343	7,7137	680,90	62,19	588,64	74,06	339,85	3,98	6,36	4,71
		3		1,5010	1,7020	7,7107	680,38	62,15	587,61	79,93	339,26	3,98	6,20	4,71
	25	0	100	0,0000	0,0000	7,7160	681,31	62,23	640,22	62,23	233,02	4,13	6,24	2,27
		1		0,3421	0,6786	7,7154	681,21	62,22	639,77	66,29	232,86	4,13	5,64	2,27
		2		0,6843	1,3575	7,7137	680,90	62,19	639,09	70,32	232,61	4,13	5,19	2,27
		3		1,0269	2,0368	7,7107	680,38	62,15	638,20	74,32	232,28	4,13	4,85	2,27
Vb (kts)	Θ (°)	ϒ (°)	Im. (%)	ξ (°)	η (°)	Vapp (m/s)	Lsec (N)	Dsec (N)	L (N)	D (N)	SF (N)	L contribution (%)	D contribution (%)	SF contribution (%)
20	0	0	0	0,0000	0,0000	10,2880	0	0	0	0	0	0	0	0
		1		0,7071	0,5000	10,2872	0	0	0	0	0	0	0	0
		2		1,4145	1,0003	10,2849	0	0	0	0	0	0	0	0
		3		2,1223	1,5010	10,2810	0	0	0	0	0	0	0	0
	5	0	5,97	0,0000	0,0000	10,2880	72,27	6,60	55,36	6,60	46,45	4,29	10,22	30,09
		1		0,6428	0,5076	10,2871	72,26	6,60	55,29	7,41	46,40	4,29	11,01	30,07
		2		1,2859	1,0155	10,2843	72,22	6,60	55,19	8,21	46,31	4,29	11,75	30,05
		3		1,9294	1,5238	10,2797	72,15	6,59	55,07	9,01	46,21	4,28	12,43	30,04
	15	0	100	0,0000	0,0000	10,2880	1211,22	110,63	1048,95	110,63	605,61	3,99	6,81	4,71
		1		0,5000	0,5670	10,2868	1210,94	110,61	1047,83	121,17	604,97	3,98	6,56	4,71
		2		1,0003	1,1343	10,2833	1210,11	110,53	1046,16	131,63	604,00	3,98	6,36	4,71
		3		1,5010	1,7020	10,2774	1208,73	110,41	1043,93	142,00	602,71	3,98	6,20	4,71
	25	0	100	0,0000	0,0000	10,2880	1211,22	110,63	1138,18	110,63	414,26	4,13	6,24	2,27
		1		0,3421	0,6786	10,2866	1210,89	110,60	1137,23	117,83	413,92	4,13	5,64	2,27
		2		0,6843	1,3575	10,2825	1209,92	110,52	1135,63	124,95	413,34	4,13	5,19	2,27
		3		1,0269	2,0368	10,2756	1208,29	110,37	1133,38	131,98	412,52	4,13	4,85	2,27
Vb (kts)	Θ (°)	ϒ (°)	Im. (%)	ξ (°)	η (°)	Vapp (m/s)	Lsec (N)	Dsec (N)	L (N)	D (N)	SF (N)	L contribution (%)	D contribution (%)	SF contribution (%)
25	0	0	0	0,0000	0,0000	12,8600	0	0	0	0	0	0	0	0
		1		0,7071	0,5000	12,8590	0	0	0	0	0	0	0	0
		2		1,4145	1,0003	12,8561	0	0	0	0	0	0	0	0
		3		2,1223	1,5010	12,8512	0	0	0	0	0	0	0	0
	5	0	5,97	0,0000	0,0000	12,8600	112,92	10,31	86,50	10,31	72,58	4,29	10,22	30,09
		1		0,6428	0,5076	12,8589	112,90	10,31	86,39	11,58	72,49	4,29	11,01	30,07
		2		1,2859	1,0155	12,8554	112,84	10,31	86,24	12,83	72,37	4,29	11,75	30,05
		3		1,9294	1,5238	12,8497	112,74	10,30	86,05	14,08	72,20	4,28	12,43	30,04
	15	0	100	0,0000	0,0000	12,8600	1892,53	172,87	1638,98	172,87	946,27	3,99	6,81	4,71
		1		0,5000	0,5670	12,8585	1892,10	172,83	1637,24	189,33	945,26	3,98	6,56	4,71
		2		1,0003	1,1343	12,8541	1890,80	172,71	1634,62	205,67	943,75	3,98	6,36	4,71
		3		1,5010	1,7020	12,8468	1888,64	172,51	1631,14	221,87	941,74	3,98	6,20	4,71
	25	0	100	0,0000	0,0000	12,8600	1892,53	172,87	1778,40	172,87	647,28	4,13	6,24	2,27
		1		0,3421	0,6786	12,8583	1892,02	172,82	1776,92	184,11	646,75	4,13	5,64	2,27
		2		0,6843	1,3575	12,8531	1890,50	172,68	1774,42	195,23	645,84	4,13	5,19	2,27
		3		1,0269	2,0368	12,8444	1887,95	172,45	1770,91	206,23	644,56	4,13	4,85	2,27

Table 39: Hydrodynamic forces calculation for foil section D

Foil Section D														
Vb (kts)	Θ (°)	Υ (°)	Im. (%)	ξ (°)	η (°)	Vapp (m/s)	Lsec (N)	Dsec (N)	L (N)	D (N)	SF (N)	L contribution (%)	D contribution (%)	SF contribution (%)
10	0	0	0	0,0000	0,0000	5,1440	0	0	0	0	0	0	0	0
		1		1,0000	1,0000	5,1440	0	0	0	0	0	0	0	0
		2		2,0000	2,0000	5,1440	0	0	0	0	0	0	0	0
		3		3,0000	3,0000	5,1440	0	0	0	0	0	0	0	0
	5	0	0	0,0000	0,0000	5,1440	0	0	0	0	0	0	0	0
		1		0,9962	0,9132	5,1440	0	0	0	0	0	0	0	0
		2		1,9924	1,8265	5,1440	0	0	0	0	0	0	0	0
		3		2,9886	2,7399	5,1439	0	0	0	0	0	0	0	0
	15	0	89,59	0,0000	0,0000	5,1440	1162,62	76,16	300,91	76,16	1123,00	4,57	18,76	34,96
		1		0,9659	0,7500	5,1439	1162,59	76,15	300,53	95,74	1121,58	4,57	20,73	34,95
		2		1,9319	1,5003	5,1438	1162,52	76,15	300,05	115,29	1119,79	4,57	22,27	34,94
		3		2,8980	2,2509	5,1435	1162,40	76,14	299,47	134,80	1117,64	4,57	23,53	34,93
	25	0	100	0,0000	0,0000	5,1440	1297,74	85,01	548,45	85,01	1176,15	7,96	19,18	25,79
		1		0,9063	0,6170	5,1439	1297,67	85,00	547,78	105,52	1174,72	7,96	20,19	25,78
		2		1,8127	1,2343	5,1434	1297,45	84,99	546,92	125,98	1172,87	7,95	20,93	25,77
		3		2,7194	1,8520	5,1427	1297,10	84,97	545,86	146,38	1170,60	7,95	21,51	25,77
Vb (kts)	Θ (°)	Υ (°)	Im. (%)	ξ (°)	η (°)	Vapp (m/s)	Lsec (N)	Dsec (N)	L (N)	D (N)	SF (N)	L contribution (%)	D contribution (%)	SF contribution (%)
15	0	0	0	0,0000	0,0000	7,7160	0	0	0	0	0	0	0	0
		1		1,0000	1,0000	7,7160	0	0	0	0	0	0	0	0
		2		2,0000	2,0000	7,7160	0	0	0	0	0	0	0	0
		3		3,0000	3,0000	7,7160	0	0	0	0	0	0	0	0
	5	0	0	0,0000	0,0000	7,7160	0	0	0	0	0	0	0	0
		1		0,9962	0,9132	7,7160	0	0	0	0	0	0	0	0
		2		1,9924	1,8265	7,7160	0	0	0	0	0	0	0	0
		3		2,9886	2,7399	7,7159	0	0	0	0	0	0	0	0
	15	0	89,59	0,0000	0,0000	7,7160	2615,89	171,35	677,04	171,35	2526,75	4,57	18,76	34,96
		1		0,9659	0,7500	7,7159	2615,83	171,35	676,18	215,42	2523,55	4,57	20,73	34,95
		2		1,9319	1,5003	7,7157	2615,67	171,34	675,11	259,41	2519,53	4,57	22,27	34,94
		3		2,8980	2,2509	7,7153	2615,41	171,32	673,81	303,30	2514,69	4,57	23,53	34,93
	25	0	100	0,0000	0,0000	7,7160	2919,91	191,27	1234,01	191,27	2646,33	7,96	19,18	25,79
		1		0,9063	0,6170	7,7158	2919,75	191,26	1232,51	237,41	2643,12	7,96	20,19	25,78
		2		1,8127	1,2343	7,7152	2919,27	191,22	1230,56	283,45	2638,95	7,95	20,93	25,78
		3		2,7194	1,8520	7,7141	2918,48	191,17	1228,18	329,36	2633,84	7,95	21,51	25,78
Vb (kts)	Θ (°)	Υ (°)	Im. (%)	ξ (°)	η (°)	Vapp (m/s)	Lsec (N)	Dsec (N)	L (N)	D (N)	SF (N)	L contribution (%)	D contribution (%)	SF contribution (%)
20	0	0	0	0,0000	0,0000	10,2880	0	0	0	0	0	0	0	0
		1		1,0000	1,0000	10,2880	0	0	0	0	0	0	0	0
		2		2,0000	2,0000	10,2880	0	0	0	0	0	0	0	0
		3		3,0000	3,0000	10,2880	0	0	0	0	0	0	0	0
	5	0	0	0,0000	0,0000	10,2880	0	0	0	0	0	0	0	0
		1		0,9962	0,9132	10,2880	0	0	0	0	0	0	0	0
		2		1,9924	1,8265	10,2880	0	0	0	0	0	0	0	0
		3		2,9886	2,7399	10,2879	0	0	0	0	0	0	0	0
	15	0	89,59	0,0000	0,0000	10,2880	4650,46	304,63	1203,63	304,63	4492,00	4,57	18,76	34,96
		1		0,9659	0,7500	10,2879	4650,37	304,62	1202,10	382,97	4486,31	4,57	20,73	34,95
		2		1,9319	1,5003	10,2876	4650,08	304,60	1200,19	461,17	4479,17	4,57	22,27	34,94
		3		2,8980	2,2509	10,2871	4649,61	304,57	1197,88	539,21	4470,56	4,57	23,53	34,93
	25	0	100	0,0000	0,0000	10,2880	5190,95	340,03	2193,79	340,03	4704,59	7,96	19,18	25,79
		1		0,9063	0,6170	10,2877	5190,66	340,01	2191,12	422,06	4698,88	7,96	20,19	25,78
		2		1,8127	1,2343	10,2869	5189,82	339,95	2187,67	503,91	4691,47	7,95	20,93	25,77
		3		2,7194	1,8520	10,2855	5188,41	339,86	2183,43	585,52	4682,38	7,95	21,51	25,77
Vb (kts)	Θ (°)	Υ (°)	Im. (%)	ξ (°)	η (°)	Vapp (m/s)	Lsec (N)	Dsec (N)	L (N)	D (N)	SF (N)	L contribution (%)	D contribution (%)	SF contribution (%)
25	0	0	0	0,0000	0,0000	12,8600	0	0	0	0	0	0	0	0
		1		1,0000	1,0000	12,8600	0	0	0	0	0	0	0	0
		2		2,0000	2,0000	12,8600	0	0	0	0	0	0	0	0
		3		3,0000	3,0000	12,8600	0	0	0	0	0	0	0	0
	5	0	0	0,0000	0,0000	12,8600	0	0	0	0	0	0	0	0
		1		0,9962	0,9132	12,8600	0	0	0	0	0	0	0	0
		2		1,9924	1,8265	12,8599	0	0	0	0	0	0	0	0
		3		2,9886	2,7399	12,8599	0	0	0	0	0	0	0	0
	15	0	89,59	0,0000	0,0000	12,8600	7266,35	475,98	1880,67	475,98	7018,76	4,57	18,76	34,96
		1		0,9659	0,7500	12,8599	7266,20	475,97	1878,29	598,39	7009,86	4,57	20,73	34,95
		2		1,9319	1,5003	12,8595	7265,76	475,94	1875,29	720,58	6998,70	4,57	22,27	34,94
		3		2,8980	2,2509	12,8588	7265,02	475,89	1871,69	842,51	6985,25	4,57	23,53	34,93
	25	0	100	0,0000	0,0000	12,8600	8110,85	531,30	3427,79	531,30	7350,93	7,96	19,18	25,79
		1		0,9063	0,6170	12,8597	8110,41	531,27	3423,63	659,47	7341,99	7,96	20,19	25,78
		2		1,8127	1,2343	12,8586	8109,09	531,18	3418,23	787,36	7330,42	7,95	20,93	25,77
		3		2,7194	1,8520	12,8569	8106,88	531,04	3411,61	914,88	7316,22	7,95	21,51	25,77

Table 40: Hydrodynamic forces calculation for the entire foil

Entire Foil							
Vb (kts)	Θ (°)	ϒ (°)	Im. (%)	L (N)	D (N)	SF (N)	L/D
10	0	0	0	0	0	0	0
		1		0	0	0	0
		2		0	0	0	0
		3		0	0	0	0
	5	0	3,20	322,31	16,15	-15,37	19,96
		1		322,17	16,82	-15,38	19,15
		2		321,85	17,48	-15,37	18,41
		3		321,33	18,12	-15,36	17,73
	15	0	91,40	6579,79	406,01	-663,21	16,21
		1		6575,86	461,95	-663,70	14,23
		2		6568,21	517,61	-663,53	12,69
		3		6556,85	572,95	-662,70	11,44
	25	0	100	6889,64	443,28	-2000,84	15,54
		1		6884,71	522,73	-2000,14	13,17
		2		6876,15	601,86	-1998,16	11,42
		3		6863,98	680,58	-1994,91	10,09
Vb (kts)	Θ (°)	ϒ (°)	Im. (%)	L (N)	D (N)	SF (N)	L/D
15	0	0	0	0	0	0	0
		1		0	0	0	0
		2		0	0	0	0
		3		0	0	0	0
	5	0	3,20	725,19	36,34	-34,59	19,96
		1		724,89	37,84	-34,60	19,15
		2		724,15	39,32	-34,58	18,41
		3		722,98	40,78	-34,54	17,73
	15	0	91,40	14804,54	913,53	-1492,22	16,21
		1		14795,54	1039,39	-1493,26	14,23
		2		14777,85	1164,61	-1492,63	12,69
		3		14751,51	1289,07	-1490,35	11,44
	25	0	100	15501,68	997,37	-4501,90	15,54
		1		15490,17	1176,12	-4500,05	13,17
		2		15469,64	1354,08	-4494,81	11,42
		3		15440,12	1531,04	-4486,20	10,08
Vb (kts)	Θ (°)	ϒ (°)	Im. (%)	L (N)	D (N)	SF (N)	L/D
20	0	0	0	0	0	0	0
		1		0	0	0	0
		2		0	0	0	0
		3		0	0	0	0
	5	0	3,20	1289,23	64,60	-61,50	19,96
		1		1288,69	67,28	-61,51	19,15
		2		1287,39	69,91	-61,49	18,41
		3		1285,31	72,50	-61,42	17,73
	15	0	91,40	26319,18	1624,06	-2652,83	16,21
		1		26303,45	1847,81	-2654,82	14,23
		2		26272,85	2070,46	-2654,13	12,69
		3		26227,40	2291,79	-2650,78	11,44
	25	0	100	27558,55	1773,10	-8003,37	15,54
		1		27538,83	2090,92	-8000,55	13,17
		2		27504,62	2407,44	-7992,64	11,42
		3		27455,94	2722,32	-7979,64	10,09
Vb (kts)	Θ (°)	ϒ (°)	Im. (%)	L (N)	D (N)	SF (N)	L/D
25	0	0	0	0	0	0	0
		1		0	0	0	0
		2		0	0	0	0
		3		0	0	0	0
	5	0	3,20	2014,42	100,94	-96,09	19,96
		1		2013,59	105,12	-96,12	19,15
		2		2011,54	109,23	-96,08	18,41
		3		2008,29	113,28	-95,97	17,73
	15	0	91,40	41123,71	2537,59	-4145,04	16,21
		1		41099,14	2887,21	-4148,15	14,23
		2		41051,33	3235,09	-4147,08	12,69
		3		40980,31	3580,92	-4141,85	11,44
	25	0	100	43060,23	2770,48	-12505,26	15,54
		1		43029,43	3267,07	-12500,86	13,17
		2		42975,97	3761,62	-12488,50	11,42
		3		42899,90	4253,62	-12468,19	10,09

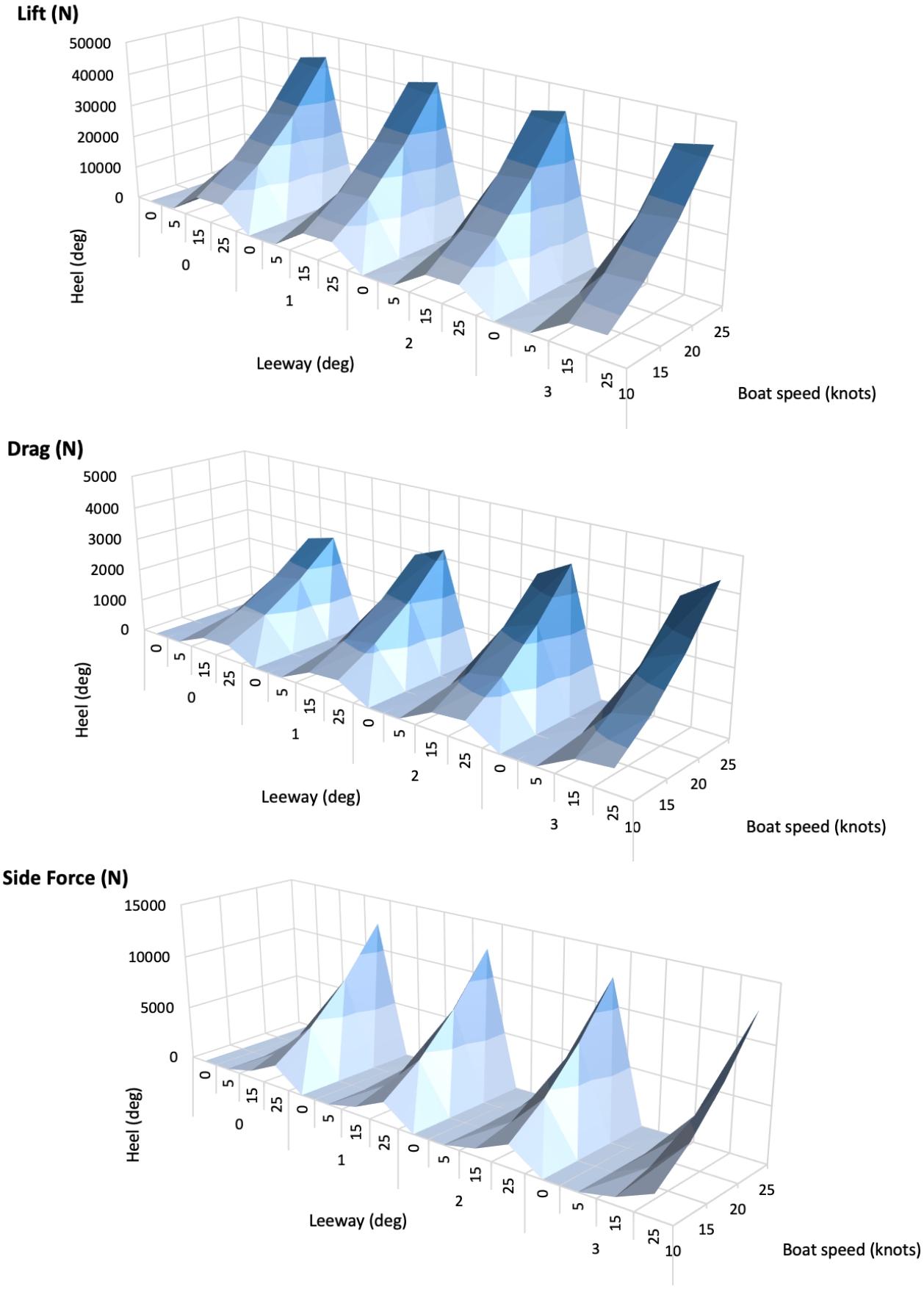

Figure 45: Foil's hydrodynamic forces for varying boat speed, heel and leeway angles

C.2.2 Foil righting moment calculation

For each heel angle considered, the equations derived to compute the horizontal center of lift x_i and vertical center of side force z_i of each foil section i (as shown in Figure 13), are respectively presented in Tables 41 and 42. When the foil sections are fully dry, these distances are not defined since no force exists (e.g. for $\theta = 0°$).

These equations were derived based on trigonometric considerations that relied on drawings such as the one presented in Figure 13. One drawing was done for each heeled case, and it was found that the immersion conditions of the sections (i.e. the way they cross the DWL) vary, leading to slightly different equations. The chord of the foil sections was assumed constant, leading to consider that the lifts L_i and side forces SF_i act on the middle of each immersed section, as drawn in Figure 13. Note that B is the boat's beam at foil's height (c.f. Figure 13).

Table 41: Equations derived to find the horizontal centers of lift on each foil section

θ (°)	x_i **(m)**
0	$\begin{cases} x_A = \emptyset \\ x_B = \emptyset \\ x_C = \emptyset \\ x_D = \emptyset \end{cases}$
5	$\begin{cases} x_A = \emptyset \\ x_B = \frac{B}{2}\cos\theta + s_A\cos(\alpha_A+\theta) + s_B^{dry}\cos(\alpha_B+\theta) + \frac{s_B^{wet}}{2}\cos(\alpha_B+\theta) \\ x_C = \frac{B}{2}\cos\theta + s_A\cos(\alpha_A+\theta) + s_B\cos(\alpha_B+\theta) + \frac{s_C^{wet}}{2}\cos(\alpha_C-\theta) \\ x_D = \emptyset \end{cases}$
15	$\begin{cases} x_A = \frac{B}{2}\cos\theta + s_A^{dry}\cos(\alpha_A+\theta) + \frac{s_A^{wet}}{2}cos(\alpha_A+\theta) \\ x_B = \frac{B}{2}\cos\theta + s_A\cos(\alpha_A+\theta) + \frac{s_B}{2}\cos(\alpha_B+\theta) \\ x_C = \frac{B}{2}\cos\theta + s_A\cos(\alpha_A+\theta) + s_B\cos(\alpha_B+\theta) + \frac{s_C}{2}\cos(\alpha_C-\theta) \\ x_D = \frac{B}{2}\cos\theta + s_A\cos(\alpha_A+\theta) + s_B\cos(\alpha_B+\theta) + s_C\cos(\alpha_C-\theta) + \frac{s_D^{wet}}{2}\cos(\alpha_D-\theta) \end{cases}$
25	$\begin{cases} x_A = \frac{B}{2}\cos\theta + \frac{s_A}{2}cos(\alpha_A+\theta) \\ x_B = \frac{B}{2}\cos\theta + s_A\cos(\alpha_A+\theta) + \frac{s_B}{2}\cos(\alpha_B+\theta) \\ x_C = \frac{B}{2}\cos\theta + s_A\cos(\alpha_A+\theta) + s_B\cos(\alpha_B+\theta) + \frac{s_C}{2}\cos(\alpha_C-\theta) \\ x_D = \frac{B}{2}\cos\theta + s_A\cos(\alpha_A+\theta) + s_B\cos(\alpha_B+\theta) + s_C\cos(\alpha_C-\theta) + \frac{s_D}{2}\cos(\alpha_D-\theta) \end{cases}$

Table 42: Equations derived to find the vertical centers of side force on each foil section

θ (°)	z_i **(m)**
0	$\begin{cases} z_A = \emptyset \\ z_B = \emptyset \\ z_C = \emptyset \\ z_D = \emptyset \end{cases}$
5	$\begin{cases} z_A = \emptyset \\ z_B = \frac{S_B^{wet}}{2}\sin(\alpha_B + \theta) \\ z_C = S_B^{wet}\sin(\alpha_B + \theta) - \frac{S_C^{wet}}{2}\sin(\alpha_C - \theta) \\ z_D = \emptyset \end{cases}$
15	$\begin{cases} z_A = \frac{S_A^{wet}}{2}\sin(\alpha_A + \theta) \\ z_B = s_A^{wet}\sin(\alpha_A + \theta) + \frac{s_B}{2}\sin(\alpha_B + \theta) \\ z_C = s_A^{wet}\sin(\alpha_A + \theta) + s_B\sin(\alpha_B + \theta) - \frac{s_C}{2}\sin(\alpha_C - \theta) \\ z_D = s_A^{wet}\sin(\alpha_A + \theta) + s_B\sin(\alpha_B + \theta) - s_C\sin(\alpha_C - \theta) - \frac{s_D^{wet}}{2}\sin(\alpha_D - \theta) \end{cases}$
25	$\begin{cases} z_A = \frac{S_A}{2}\sin(\alpha_A + \theta) \\ z_B = s_A\sin(\alpha_A + \theta) + \frac{s_B}{2}\sin(\alpha_B + \theta) \\ z_C = s_A\sin(\alpha_A + \theta) + s_B\sin(\alpha_B + \theta) - \frac{s_C}{2}\sin(\alpha_C - \theta) \\ z_D = s_A\sin(\alpha_A + \theta) + s_B\sin(\alpha_B + \theta) - s_C\sin(\alpha_C - \theta) - \frac{s_D}{2}\sin(\alpha_D - \theta) \end{cases}$

Table 43: Horizontal center of lift and vertical center of side force of each section

Heel Θ (°)	Foil section	Span si (m)	Dry span si_dry (m)	Immersed span si_wet (m)	xi (m)	zi (m)
0	A	1,00	1,00	0	0	0
	B	1,80	1,80	0	0	0
	C	0,30	0,30	0	0	0
	D	0,75	0,75	0	0	0
5	A	1,00	1,00	0	0	0
	B	1,80	1,68	0,12	4,99	0,01
	C	0,30	0,28	0,02	5,06	0,00
	D	0,75	0,75	0	0	0
15	A	1,00	0,24	0,76	2,78	0,16
	B	1,80	0	1,80	4,00	0,55
	C	0,30	0	0,30	5,00	0,71
	D	0,75	0,08	0,67	5,21	0,27
25	A	1,00	0	1,00	2,49	0,29
	B	1,80	0	1,80	3,72	0,95
	C	0,30	0	0,30	4,68	1,28
	D	0,75	0	0,75	4,98	0,89

Table 44: Foil righting moment and lever arm calculations

Entire Foil										
Speed (kts)	Heel Θ (deg)	Leeway Υ (deg)	L (N)	SF (N)	d1 (m)	d2 (m)	Added Moment Foil (N.m)	Static moment boat (N.m)	Revised GZ (m)	GZ (m)
10	0	0	0	0	0	0	0	0	0	0
		1	0	0	0	0	0		0	
		2	0	0	0	0	0		0	
		3	0	0	0	0	0		0	
	5	0	322,31	-15,37	4,99	0,0052	1609,03	48370,44	0,6479	0,627
		1	322,17	-15,38	4,99	0,0052	1608,37		0,6478	
		2	321,85	-15,37	4,99	0,0052	1606,73		0,6478	
		3	321,33	-15,36	4,99	0,0052	1604,14		0,6478	
	15	0	6579,79	-663,21	3,79	0,37	25183,29	115718,76	1,8264	1,500
		1	6575,86	-663,70	3,79	0,37	25168,32		1,8262	
		2	6568,21	-663,53	3,79	0,37	25139,07		1,8259	
		3	6556,85	-662,70	3,79	0,37	25095,57		1,8253	
	25	0	6889,64	-2000,84	3,51	0,75	25687,45	155371,72	2,3470	2,014
		1	6884,71	-2000,14	3,51	0,75	25669,32		2,3467	
		2	6876,15	-1998,16	3,51	0,75	25637,56		2,3463	
		3	6863,98	-1994,91	3,51	0,75	25592,22		2,3457	
Speed (kts)	Heel Θ (deg)	Leeway Υ (deg)	L (N)	SF (N)	d1 (m)	d2 (m)	Added Moment Foil (N.m)	Static moment boat (N.m)	Revised GZ (m)	GZ (m)
15	0	0	0	0	0	0	0	0	0	0
		1	0	0	0	0	0		0	
		2	0	0	0	0	0		0	
		3	0	0	0	0	0		0	
	5	0	725,19	-34,59	4,99	0,0052	3620,32	48370,44	0,6739	0,627
		1	724,89	-34,60	4,99	0,0052	3618,82		0,6739	
		2	724,15	-34,58	4,99	0,0052	3615,13		0,6739	
		3	722,98	-34,54	4,99	0,0052	3609,27		0,6738	
	15	0	14804,54	-1492,22	3,79	0,37	56662,40	115718,76	2,2345	1,500
		1	14795,54	-1493,26	3,79	0,37	56628,10		2,2340	
		2	14777,85	-1492,63	3,79	0,37	56560,47		2,2332	
		3	14751,51	-1490,35	3,79	0,37	56459,56		2,2319	
	25	0	15501,68	-4501,90	3,51	0,75	57796,76	155371,72	2,7632	2,014
		1	15490,17	-4500,05	3,51	0,75	57754,23		2,7626	
		2	15469,64	-4494,81	3,51	0,75	57677,60		2,7616	
		3	15440,12	-4486,20	3,51	0,75	57566,95		2,7602	
Speed (kts)	Heel Θ (deg)	Leeway Υ (deg)	L (N)	SF (N)	d1 (m)	d2 (m)	Added Moment Foil (N.m)	Static moment boat (N.m)	Revised GZ (m)	GZ (m)
20	0	0	0	0	0	0	0	0	0	0
		1	0	0	0	0	0		0	
		2	0	0	0	0	0		0	
		3	0	0	0	0	0		0	
	5	0	1289,23	-61,50	4,99	0,0052	6436,12	48370,44	0,7104	0,627
		1	1288,69	-61,51	4,99	0,0052	6433,46		0,7104	
		2	1287,39	-61,49	4,99	0,0052	6426,93		0,7103	
		3	1285,31	-61,42	4,99	0,0052	6416,54		0,7102	
	15	0	26319,18	-2652,83	3,79	0,37	100733,15	115718,76	2,8057	1,500
		1	26303,45	-2654,82	3,79	0,37	100673,26		2,8050	
		2	26272,85	-2654,13	3,79	0,37	100556,26		2,8035	
		3	26227,40	-2650,78	3,79	0,37	100382,28		2,8012	
	25	0	27558,55	-8003,37	3,51	0,75	102749,80	155371,72	3,3459	2,014
		1	27538,83	-8000,55	3,51	0,75	102677,27		3,3450	
		2	27504,62	-7992,64	3,51	0,75	102550,25		3,3433	
		3	27455,94	-7979,64	3,51	0,75	102368,87		3,3410	
Speed (kts)	Heel Θ (deg)	Leeway Υ (deg)	L (N)	SF (N)	d1 (m)	d2 (m)	Added Moment Foil (N.m)	Static moment boat (N.m)	Revised GZ (m)	GZ (m)
25	0	0	0	0	0	0	0	0	0	0
		1	0	0	0	0	0		0	
		2	0	0	0	0	0		0	
		3	0	0	0	0	0		0	
	5	0	2014,42	-96,09	4,99	0,0052	10056,44	48370,44	0,7574	0,627
		1	2013,59	-96,12	4,99	0,0052	10052,28		0,7573	
		2	2011,54	-96,08	4,99	0,0052	10042,08		0,7572	
		3	2008,29	-95,97	4,99	0,0052	10025,85		0,7570	
	15	0	41123,71	-4145,04	3,79	0,37	157395,55	115718,76	3,5402	1,500
		1	41099,14	-4148,15	3,79	0,37	157301,97		3,5390	
		2	41051,33	-4147,08	3,79	0,37	157119,16		3,5367	
		3	40980,31	-4141,85	3,79	0,37	156847,31		3,5331	
	25	0	43060,23	-12505,26	3,51	0,75	160546,57	155371,72	4,0951	2,014
		1	43029,43	-12500,86	3,51	0,75	160433,23		4,0936	
		2	42975,97	-12488,50	3,51	0,75	160234,76		4,0910	
		3	42899,90	-12468,19	3,51	0,75	159951,36		4,0874	

Table 45: Foil righting moment and lever arm calculations, keel canted

Entire Foil										
Speed (kts)	Heel Θ (deg)	Leeway Υ (deg)	L (N)	SF (N)	d1 (m)	d2 (m)	Added Moment Foil (N.m)	Static moment boat (N.m)	Revised GZ (m)	GZ (m)
10	0	0	0	0	0	0	0	81620,30	1,058	1,058
		1	0	0	0	0	0		1,058	
		2	0	0	0	0	0		1,058	
		3	0	0	0	0	0		1,058	
	5	0	322,31	-15,37	4,99	0,0052	1609,03	125207,70	1,6439	1,623
		1	322,17	-15,38	4,99	0,0052	1608,37		1,6438	
		2	321,85	-15,37	4,99	0,0052	1606,73		1,6438	
		3	321,33	-15,36	4,99	0,0052	1604,14		1,6438	
	15	0	6579,79	-663,21	3,79	0,37	25183,29	180289,83	2,6634	2,337
		1	6575,86	-663,70	3,79	0,37	25168,32		2,6632	
		2	6568,21	-663,53	3,79	0,37	25139,07		2,6629	
		3	6556,85	-662,70	3,79	0,37	25095,57		2,6623	
	25	0	6889,64	-2000,84	3,51	0,75	25687,45	209528,10	3,0490	2,716
		1	6884,71	-2000,14	3,51	0,75	25669,32		3,0487	
		2	6876,15	-1998,16	3,51	0,75	25637,56		3,0483	
		3	6863,98	-1994,91	3,51	0,75	25592,22		3,0477	
Speed (kts)	Heel Θ (deg)	Leeway Υ (deg)	L (N)	SF (N)	d1 (m)	d2 (m)	Added Moment Foil (N.m)	Static moment boat (N.m)	Revised GZ (m)	GZ (m)
15	0	0	0	0	0	0	0	81620,30	1,058	1,058
		1	0	0	0	0	0		1,058	
		2	0	0	0	0	0		1,058	
		3	0	0	0	0	0		1,058	
	5	0	725,19	-34,59	4,99	0,0052	3620,32	125207,70	1,6699	1,623
		1	724,89	-34,60	4,99	0,0052	3618,82		1,6699	
		2	724,15	-34,58	4,99	0,0052	3615,13		1,6699	
		3	722,98	-34,54	4,99	0,0052	3609,27		1,6698	
	15	0	14804,54	-1492,22	3,79	0,37	56662,40	180289,83	3,0715	2,337
		1	14795,54	-1493,26	3,79	0,37	56628,10		3,0710	
		2	14777,85	-1492,63	3,79	0,37	56560,47		3,0702	
		3	14751,51	-1490,35	3,79	0,37	56459,56		3,0689	
	25	0	15501,68	-4501,90	3,51	0,75	57796,76	209528,10	3,4652	2,716
		1	15490,17	-4500,05	3,51	0,75	57754,23		3,4646	
		2	15469,64	-4494,81	3,51	0,75	57677,60		3,4636	
		3	15440,12	-4486,20	3,51	0,75	57566,95		3,4622	
Speed (kts)	Heel Θ (deg)	Leeway Υ (deg)	L (N)	SF (N)	d1 (m)	d2 (m)	Added Moment Foil (N.m)	Static moment boat (N.m)	Revised GZ (m)	GZ (m)
20	0	0	0	0	0	0	0	81620,30	1,058	1,058
		1	0	0	0	0	0		1,058	
		2	0	0	0	0	0		1,058	
		3	0	0	0	0	0		1,058	
	5	0	1289,23	-61,50	4,99	0,0052	6436,12	125207,70	1,7064	1,623
		1	1288,69	-61,51	4,99	0,0052	6433,46		1,7064	
		2	1287,39	-61,49	4,99	0,0052	6426,93		1,7063	
		3	1285,31	-61,42	4,99	0,0052	6416,54		1,7062	
	15	0	26319,18	-2652,83	3,79	0,37	100733,15	180289,83	3,6427	2,337
		1	26303,45	-2654,82	3,79	0,37	100673,26		3,6420	
		2	26272,85	-2654,13	3,79	0,37	100556,26		3,6405	
		3	26227,40	-2650,78	3,79	0,37	100382,28		3,6382	
	25	0	27558,55	-8003,37	3,51	0,75	102749,80	209528,10	4,0479	2,716
		1	27538,83	-8000,55	3,51	0,75	102677,27		4,0470	
		2	27504,62	-7992,64	3,51	0,75	102550,25		4,0453	
		3	27455,94	-7979,64	3,51	0,75	102368,87		4,0430	
Speed (kts)	Heel Θ (deg)	Leeway Υ (deg)	L (N)	SF (N)	d1 (m)	d2 (m)	Added Moment Foil (N.m)	Static moment boat (N.m)	Revised GZ (m)	GZ (m)
25	0	0	0	0	0	0	0	81620,30	1,058	1,058
		1	0	0	0	0	0		1,058	
		2	0	0	0	0	0		1,058	
		3	0	0	0	0	0		1,058	
	5	0	2014,42	-96,09	4,99	0,0052	10056,44	125207,70	1,7534	1,623
		1	2013,59	-96,12	4,99	0,0052	10052,28		1,7533	
		2	2011,54	-96,08	4,99	0,0052	10042,08		1,7532	
		3	2008,29	-95,97	4,99	0,0052	10025,85		1,7530	
	15	0	41123,71	-4145,04	3,79	0,37	157395,55	180289,83	4,3772	2,337
		1	41099,14	-4148,15	3,79	0,37	157301,97		4,3760	
		2	41051,33	-4147,08	3,79	0,37	157119,16		4,3737	
		3	40980,31	-4141,85	3,79	0,37	156847,31		4,3701	
	25	0	43060,23	-12505,26	3,51	0,75	160546,57	209528,10	4,7971	2,716
		1	43029,43	-12500,86	3,51	0,75	160433,23		4,7956	
		2	42975,97	-12488,50	3,51	0,75	160234,76		4,7930	
		3	42899,90	-12468,19	3,51	0,75	159951,36		4,7894	

C.3 Second model version based on reduced displacement

C.3.1 Hydrodynamic forces calculation

Table 46: Hydrodynamic forces calculation for foil section A

Foil Section A														
Vb (kts)	Θ (°)	Υ (°)	Im. (%)	ξ (deg)	η (deg)	Vapp (m/s)	L_section (N)	D_section (N)	L (N)	D (N)	SF (N)	Lift contribution (%)	Drag contribution (%)	SF contribution (%)
10	0	0	0	0,0000	0,0000	5,1440	0	0	0	0	0	0	0	0
		1		0,1737	0,8290	5,1432	0	0	0	0	0	0	0	0
		2		0,3474	1,6582	5,1410	0	0	0	0	0	0	0	0
		3		0,5214	2,4877	5,1372	0	0	0	0	0	0	0	0
	5	0	0	0,0000	0,0000	5,1440	0	0	0	0	0	0	0	0
		1		0,2588	0,7500	5,1433	0	0	0	0	0	0	0	0
		2		0,5178	1,5003	5,1411	0	0	0	0	0	0	0	0
		3		0,7771	2,2509	5,1374	0	0	0	0	0	0	0	0
	15	0	70,22	0,0000	0,0000	5,1440	1672,27	83,18	1515,59	83,18	-706,73	23,52	20,99	22,72
		1		0,4227	0,6170	5,1434	1671,85	83,16	1514,62	95,49	-706,28	23,52	21,20	22,72
		2		0,8455	1,2343	5,1414	1670,60	83,10	1512,80	107,73	-705,43	23,52	21,36	22,72
		3		1,2688	1,8520	5,1382	1668,51	83,00	1510,15	119,90	-704,19	23,52	21,49	22,72
	25	0	100	0,0000	0,0000	5,1440	2381,51	118,46	1950,82	118,46	-1365,98	28,32	26,72	29,95
		1		0,5736	0,5302	5,1435	2381,02	118,44	1949,35	142,26	-1364,95	28,31	27,22	29,96
		2		1,1475	1,0606	5,1419	2379,56	118,37	1946,89	165,97	-1363,23	28,31	27,58	29,96
		3		1,7218	1,5915	5,1393	2377,13	118,24	1943,44	189,56	-1360,81	28,31	27,85	29,96
Vb (kts)	Θ (°)	Υ (°)	Im. (%)	ξ (deg)	η (deg)	Vapp (m/s)	L_section (N)	D_section (N)	L (N)	D (N)	SF (N)	Lift contribution (%)	Drag contribution (%)	SF contribution (%)
15	0	0	0	0,0000	0,0000	7,7160	0	0	0	0	0	0	0	0
		1		0,1737	0,8290	7,7149	0	0	0	0	0	0	0	0
		2		0,3474	1,6582	7,7114	0	0	0	0	0	0	0	0
		3		0,5214	2,4877	7,7057	0	0	0	0	0	0	0	0
	5	0	0	0,0000	0,0000	7,7160	0	0	0	0	0	0	0	0
		1		0,2588	0,7500	7,7149	0	0	0	0	0	0	0	0
		2		0,5178	1,5003	7,7116	0	0	0	0	0	0	0	0
		3		0,7771	2,2509	7,7061	0	0	0	0	0	0	0	0
	15	0	65,77	0,0000	0,0000	7,7160	3524,06	187,16	3193,88	187,16	-1489,33	22,40	21,11	21,82
		1		0,4227	0,6170	7,7150	3523,17	187,11	3191,74	213,09	-1488,33	22,39	21,19	21,82
		2		0,8455	1,2343	7,7121	3520,53	186,97	3187,84	238,88	-1486,51	22,39	21,26	21,82
		3		1,2688	1,8520	7,7073	3516,13	186,74	3182,16	264,50	-1483,87	22,39	21,31	21,83
	25	0	100	0,0000	0,0000	7,7160	5358,40	266,54	4389,34	266,54	-3073,45	28,32	26,72	29,95
		1		0,5736	0,5302	7,7152	5357,30	266,48	4386,04	320,09	-3071,14	28,31	27,22	29,96
		2		1,1475	1,0606	7,7128	5354,02	266,32	4380,50	373,44	-3067,26	28,32	27,58	29,96
		3		1,7218	1,5915	7,7089	5348,55	266,05	4372,75	426,50	-3061,83	28,32	27,86	29,96
Vb (kts)	Θ (°)	Υ (°)	Im. (%)	ξ (deg)	η (deg)	Vapp (m/s)	L_section (N)	D_section (N)	L (N)	D (N)	SF (N)	Lift contribution (%)	Drag contribution (%)	SF contribution (%)
20	0	0	0	0,0000	0,0000	10,2880	0	0	0	0	0	0	0	0
		1		0,1737	0,8290	10,2865	0	0	0	0	0	0	0	0
		2		0,3474	1,6582	10,2819	0	0	0	0	0	0	0	0
		3		0,5214	2,4877	10,2743	0	0	0	0	0	0	0	0
	5	0	0	0,0000	0,0000	10,2880	0	0	0	0	0	0	0	0
		1		0,2588	0,7500	10,2865	0	0	0	0	0	0	0	0
		2		0,5178	1,5003	10,2822	0	0	0	0	0	0	0	0
		3		0,7771	2,2509	10,2748	0	0	0	0	0	0	0	0
	15	0	57,81	0,0000	0,0000	10,2880	5506,72	273,92	4990,78	273,92	-2327,24	20,28	18,24	20,10
		1		0,4227	0,6170	10,2867	5505,34	273,85	4987,56	314,44	-2325,74	20,28	18,46	20,10
		2		0,8455	1,2343	10,2829	5501,21	273,64	4981,58	354,76	-2322,95	20,28	18,63	20,10
		3		1,2688	1,8520	10,2764	5494,33	273,30	4972,84	394,82	-2318,88	20,28	18,77	20,10
	25	0	100	0,0000	0,0000	10,2880	9526,04	473,85	7803,27	473,85	-5463,91	28,32	26,72	29,95
		1		0,5736	0,5302	10,2869	9524,09	473,75	7797,40	569,06	-5459,80	28,31	27,22	29,96
		2		1,1475	1,0606	10,2838	9518,25	473,46	7787,56	663,89	-5452,91	28,31	27,58	29,96
		3		1,7218	1,5915	10,2785	9508,53	472,98	7773,77	758,23	-5443,25	28,31	27,85	29,96
Vb (kts)	Θ (°)	Υ (°)	Im. (%)	ξ (deg)	η (deg)	Vapp (m/s)	L_section (N)	D_section (N)	L (N)	D (N)	SF (N)	Lift contribution (%)	Drag contribution (%)	SF contribution (%)
25	0	0	0	0,0000	0,0000	12,8600	0	0	0	0	0	0	0	0
		1		0,1737	0,8290	12,8581	0	0	0	0	0	0	0	0
		2		0,3474	1,6582	12,8524	0	0	0	0	0	0	0	0
		3		0,5214	2,4877	12,8429	0	0	0	0	0	0	0	0
	5	0	0	0,0000	0,0000	12,8600	0	0	0	0	0	0	0	0
		1		0,2588	0,7500	12,8582	0	0	0	0	0	0	0	0
		2		0,5178	1,5003	12,8527	0	0	0	0	0	0	0	0
		3		0,7771	2,2509	12,8436	0	0	0	0	0	0	0	0
	15	0	44,62	0,0000	0,0000	12,8600	6642,03	330,39	6019,72	330,39	-2807,04	16,49	14,97	16,85
		1		0,4227	0,6170	12,8584	6640,37	330,31	6015,84	379,27	-2805,23	16,49	15,18	16,85
		2		0,8455	1,2343	12,8536	6635,38	330,06	6008,63	427,90	-2801,87	16,49	15,36	16,85
		3		1,2688	1,8520	12,8455	6627,08	329,65	5998,09	476,21	-2796,96	16,49	15,50	16,85
	25	0	100	0,0000	0,0000	12,8600	14884,43	740,39	12192,61	740,39	-8537,36	28,32	26,72	29,95
		1		0,5736	0,5302	12,8587	14881,39	740,24	12183,44	889,15	-8530,94	28,31	27,22	29,96
		2		1,1475	1,0606	12,8547	14872,27	739,78	12168,07	1037,32	-8520,17	28,31	27,58	29,96
		3		1,7218	1,5915	12,8482	14857,07	739,03	12146,52	1184,73	-8505,08	28,31	27,85	29,96

Table 47: Hydrodynamic forces calculation for foil section B

Foil Section B														
Vb (kts)	Θ (°)	ϒ (°)	Im. (%)	ξ (deg)	η (deg)	Vapp (m/s)	L_section (N)	D_section (N)	L (N)	D (N)	SF (N)	Lift contribution (%)	Drag contribution (%)	SF contribution (%)
10	0	0	0	0,0000	0,0000	5,1440	0	0	0	0	0	0	0	0
		1		0,0000	1,0000	5,1432	0	0	0	0	0	0	0	0
		2		0,0000	2,0000	5,1409	0	0	0	0	0	0	0	0
		3		0,0000	3,0000	5,1370	0	0	0	0	0	0	0	0
	5	0	6,67	0,0000	0,0000	5,1440	302,09	14,15	300,94	14,15	-26,33	95,71	89,78	69,92
		1		0,0872	0,9132	5,1432	302,00	14,14	300,83	14,60	-26,32	95,71	88,99	69,94
		2		0,1744	1,8265	5,1409	301,73	14,13	300,54	15,05	-26,29	95,71	88,25	69,95
		3		0,2617	2,7399	5,1370	301,27	14,11	300,06	15,48	-26,25	95,72	87,57	69,97
	15	0	100	0,0000	0,0000	5,1440	4530,28	212,15	4375,91	212,15	-1172,52	67,91	53,54	37,69
		1		0,2588	0,7500	5,1433	4528,99	212,09	4373,70	232,54	-1171,93	67,92	51,63	37,70
		2		0,5178	1,5003	5,1411	4525,13	211,91	4368,91	252,79	-1170,65	67,93	50,12	37,71
		3		0,7771	2,2509	5,1374	4518,70	211,61	4361,56	272,85	-1168,68	67,93	48,90	37,71
	25	0	100	0,0000	0,0000	5,1440	4530,28	212,15	4105,83	212,15	-1914,58	59,59	47,86	41,98
		1		0,4227	0,6170	5,1434	4529,15	212,10	4103,27	245,49	-1913,39	59,60	46,96	41,99
		2		0,8455	1,2343	5,1414	4525,75	211,94	4098,44	278,67	-1911,13	59,60	46,30	42,00
		3		1,2688	1,8520	5,1382	4520,09	211,67	4091,34	311,65	-1907,82	59,61	45,79	42,00
Vb (kts)	Θ (°)	ϒ (°)	Im. (%)	ξ (deg)	η (deg)	Vapp (m/s)	L_section (N)	D_section (N)	L (N)	D (N)	SF (N)	Lift contribution (%)	Drag contribution (%)	SF contribution (%)
15	0	0	0	0,0000	0,0000	7,7160	0	0	0	0	0	0	0	0
		1		0,0000	1,0000	7,7148	0	0	0	0	0	0	0	0
		2		0,0000	2,0000	7,7113	0	0	0	0	0	0	0	0
		3		0,0000	3,0000	7,7054	0	0	0	0	0	0	0	0
	5	0	5,68	0,0000	0,0000	7,7160	579,14	27,12	576,94	27,12	-50,48	95,71	89,78	69,91
		1		0,0872	0,9132	7,7148	578,96	27,11	576,72	27,99	-50,46	95,71	88,99	69,93
		2		0,1744	1,8265	7,7113	578,43	27,09	576,15	28,85	-50,41	95,71	88,25	69,95
		3		0,2617	2,7399	7,7054	577,55	27,05	575,23	29,68	-50,33	95,71	87,56	69,96
	15	0	100	0,0000	0,0000	7,7160	10193,13	477,33	9845,81	477,33	-2638,18	69,04	53,84	38,65
		1		0,2588	0,7500	7,7148	10190,02	477,19	9840,62	523,21	-2636,79	69,04	52,04	38,66
		2		0,5178	1,5003	7,7113	10180,71	476,75	9829,25	568,72	-2633,74	69,05	50,61	38,67
		3		0,7771	2,2509	7,7054	10165,21	476,03	9811,70	613,80	-2629,04	69,05	49,45	38,67
	25	0	100	0,0000	0,0000	7,7160	10193,13	477,33	9238,11	477,33	-4307,80	59,59	47,86	41,98
		1		0,4227	0,6170	7,7148	10190,02	477,19	9231,86	552,33	-4304,89	59,60	46,96	41,99
		2		0,8455	1,2343	7,7113	10180,71	476,75	9219,48	626,88	-4299,11	59,60	46,30	41,99
		3		1,2688	1,8520	7,7054	10165,21	476,03	9201,00	700,86	-4290,50	59,59	45,78	41,99
Vb (kts)	Θ (°)	ϒ (°)	Im. (%)	ξ (deg)	η (deg)	Vapp (m/s)	L_section (N)	D_section (N)	L (N)	D (N)	SF (N)	Lift contribution (%)	Drag contribution (%)	SF contribution (%)
20	0	0	0	0,0000	0,0000	10,2880	0	0	0	0	0	0	0	0
		1		0,0000	1,0000	10,2864	0	0	0	0	0	0	0	0
		2		0,0000	2,0000	10,2817	0	0	0	0	0	0	0	0
		3		0,0000	3,0000	10,2739	0	0	0	0	0	0	0	0
	5	0	5,30	0,0000	0,0000	10,2880	959,61	44,94	955,96	44,94	-83,64	95,71	89,78	69,91
		1		0,0872	0,9132	10,2864	959,32	44,92	955,60	46,38	-83,60	95,71	88,98	69,93
		2		0,1744	1,8265	10,2818	958,45	44,88	954,67	47,80	-83,52	95,71	88,25	69,95
		3		0,2617	2,7399	10,2740	957,01	44,82	953,15	49,19	-83,39	95,71	87,57	69,96
	15	0	100	0,0000	0,0000	10,2880	18121,12	848,59	17503,66	848,59	-4690,09	71,14	56,51	40,50
		1		0,2588	0,7500	10,2865	18115,97	848,35	17494,80	930,18	-4687,72	71,15	54,61	40,51
		2		0,5178	1,5003	10,2822	18100,53	847,63	17475,65	1011,14	-4682,59	71,15	53,11	40,52
		3		0,7771	2,2509	10,2748	18074,81	846,42	17446,23	1091,40	-4674,70	71,16	51,89	40,52
	25	0	100	0,0000	0,0000	10,2880	18121,12	848,59	16423,31	848,59	-7658,32	59,59	47,86	41,98
		1		0,4227	0,6170	10,2867	18116,58	848,38	16413,08	981,98	-7653,55	59,60	46,96	41,99
		2		0,8455	1,2343	10,2829	18102,99	847,74	16393,76	1114,69	-7644,53	59,60	46,30	42,00
		3		1,2688	1,8520	10,2764	18080,35	846,68	16365,35	1246,58	-7631,29	59,61	45,79	42,00
Vb (kts)	Θ (°)	ϒ (°)	Im. (%)	ξ (deg)	η (deg)	Vapp (m/s)	L_section (N)	D_section (N)	L (N)	D (N)	SF (N)	Lift contribution (%)	Drag contribution (%)	SF contribution (%)
25	0	0	0	0,0000	0,0000	12,8600	0	0	0	0	0	0	0	0
		1		0,0000	1,0000	12,8580	0	0	0	0	0	0	0	0
		2		0,0000	2,0000	12,8522	0	0	0	0	0	0	0	0
		3		0,0000	3,0000	12,8424	0	0	0	0	0	0	0	0
	5	0	3,90	0,0000	0,0000	12,8600	1103,47	51,67	1099,27	51,67	-96,17	95,70	89,78	69,91
		1		0,0872	0,9132	12,8581	1103,14	51,66	1098,86	53,34	-96,14	95,71	88,98	69,93
		2		0,1744	1,8265	12,8522	1102,14	51,61	1097,78	54,97	-96,04	95,71	88,25	69,94
		3		0,2617	2,7399	12,8425	1100,47	51,53	1096,04	56,56	-95,89	95,71	87,56	69,95
	15	0	100	0,0000	0,0000	12,8600	28314,25	1325,93	27349,46	1325,93	-7328,27	74,92	60,06	43,98
		1		0,2588	0,7500	12,8582	28306,20	1325,55	27335,63	1453,40	-7324,56	74,93	58,19	43,99
		2		0,5178	1,5003	12,8527	28282,07	1324,42	27305,70	1579,91	-7316,54	74,93	56,70	44,00
		3		0,7771	2,2509	12,8436	28241,89	1322,54	27259,73	1705,31	-7304,22	74,94	55,49	44,01
	25	0	100	0,0000	0,0000	12,8600	28314,25	1325,93	25661,42	1325,93	-11966,12	59,59	47,86	41,98
		1		0,4227	0,6170	12,8584	28307,16	1325,60	25645,44	1534,34	-11958,67	59,60	46,96	41,99
		2		0,8455	1,2343	12,8536	28285,92	1324,60	25615,24	1741,70	-11944,58	59,60	46,30	42,00
		3		1,2688	1,8520	12,8455	28250,54	1322,94	25570,86	1947,78	-11923,89	59,61	45,79	42,00

Table 48: Hydrodynamic forces calculation for foil section C

Foil Section C														
Vb (kts)	Θ (°)	Υ (°)	Im. (%)	ξ (deg)	η (deg)	Vapp (m/s)	L_section (N)	D_section (N)	L (N)	D (N)	SF (N)	Lift contribution (%)	Drag contribution (%)	SF contribution (%)
10	0	0	0	0,0000	0,0000	5,1440	0	0	0	0	0	0	0	0
		1		0,7071	0,5000	5,1436	0	0	0	0	0	0	0	0
		2		1,4145	1,0003	5,1424	0	0	0	0	0	0	0	0
		3		2,1223	1,5010	5,1405	0	0	0	0	0	0	0	0
	5	0	5,82	0,0000	0,0000	5,1440	17,62	1,61	13,50	1,61	11,33	4,29	10,22	30,08
		1		0,6428	0,5076	5,1435	17,62	1,61	13,48	1,81	11,31	4,29	11,01	30,06
		2		1,2859	1,0155	5,1422	17,61	1,61	13,46	2,00	11,29	4,29	11,75	30,05
		3		1,9294	1,5238	5,1399	17,59	1,61	13,43	2,20	11,27	4,28	12,43	30,03
	15	0	100	0,0000	0,0000	5,1440	302,81	27,66	262,24	27,66	151,40	4,07	6,98	4,87
		1		0,5000	0,5670	5,1434	302,74	27,65	261,96	30,29	151,24	4,07	6,72	4,87
		2		1,0003	1,1343	5,1416	302,53	27,63	261,54	32,91	151,00	4,07	6,52	4,86
		3		1,5010	1,7020	5,1387	302,18	27,60	260,98	35,50	150,68	4,06	6,36	4,86
	25	0	100	0,0000	0,0000	5,1440	302,81	27,66	284,54	27,66	103,57	4,13	6,24	2,27
		1		0,3421	0,6786	5,1433	302,72	27,65	284,31	29,46	103,48	4,13	5,64	2,27
		2		0,6843	1,3575	5,1412	302,48	27,63	283,91	31,24	103,33	4,13	5,19	2,27
		3		1,0269	2,0368	5,1378	302,07	27,59	283,35	33,00	103,13	4,13	4,85	2,27
Vb (kts)	Θ (°)	Υ (°)	Im. (%)	ξ (deg)	η (deg)	Vapp (m/s)	L_section (N)	D_section (N)	L (N)	D (N)	SF (N)	Lift contribution (%)	Drag contribution (%)	SF contribution (%)
15	0	0	0	0,0000	0,0000	7,7160	0	0	0	0	0	0	0	0
		1		0,7071	0,5000	7,7154	0	0	0	0	0	0	0	0
		2		1,4145	1,0003	7,7137	0	0	0	0	0	0	0	0
		3		2,1223	1,5010	7,7107	0	0	0	0	0	0	0	0
	5	0	4,96	0,0000	0,0000	7,7160	33,79	3,09	25,89	3,09	21,72	4,29	10,22	30,09
		1		0,6428	0,5076	7,7154	33,79	3,09	25,85	3,46	21,69	4,29	11,01	30,07
		2		1,2859	1,0155	7,7137	33,77	3,08	25,81	3,84	21,66	4,29	11,75	30,05
		3		1,9294	1,5238	7,7107	33,75	3,08	25,76	4,22	21,61	4,29	12,44	30,04
	15	0	100	0,0000	0,0000	7,7160	681,31	62,23	590,03	62,23	340,66	4,14	7,02	4,99
		1		0,5000	0,5670	7,7154	681,21	62,22	589,45	68,16	340,32	4,14	6,78	4,99
		2		1,0003	1,1343	7,7137	680,90	62,19	588,64	74,06	339,85	4,13	6,59	4,99
		3		1,5010	1,7020	7,7107	680,38	62,15	587,61	79,93	339,26	4,14	6,44	4,99
	25	0	100	0,0000	0,0000	7,7160	681,31	62,23	640,22	62,23	233,02	4,13	6,24	2,27
		1		0,3421	0,6786	7,7154	681,21	62,22	639,77	66,29	232,86	4,13	5,64	2,27
		2		0,6843	1,3575	7,7137	680,90	62,19	639,09	70,32	232,61	4,13	5,19	2,27
		3		1,0269	2,0368	7,7107	680,38	62,15	638,20	74,32	232,28	4,13	4,85	2,27
Vb (kts)	Θ (°)	Υ (°)	Im. (%)	ξ (deg)	η (deg)	Vapp (m/s)	L_section (N)	D_section (N)	L (N)	D (N)	SF (N)	Lift contribution (%)	Drag contribution (%)	SF contribution (%)
20	0	0	0	0,0000	0,0000	10,2880	0	0	0	0	0	0	0	0
		1		0,7071	0,5000	10,2872	0	0	0	0	0	0	0	0
		2		1,4145	1,0003	10,2849	0	0	0	0	0	0	0	0
		3		2,1223	1,5010	10,2810	0	0	0	0	0	0	0	0
	5	0	4,62	0,0000	0,0000	10,2880	56,00	5,11	42,90	5,11	36,00	4,29	10,22	30,09
		1		0,6428	0,5076	10,2871	55,99	5,11	42,84	5,74	35,95	4,29	11,02	30,07
		2		1,2859	1,0155	10,2843	55,96	5,11	42,77	6,36	35,89	4,29	11,75	30,05
		3		1,9294	1,5238	10,2797	55,91	5,11	42,67	6,98	35,81	4,29	12,43	30,04
	15	0	100	0,0000	0,0000	10,2880	1211,22	110,63	1048,95	110,63	605,61	4,26	7,37	5,23
		1		0,5000	0,5670	10,2868	1210,94	110,61	1047,83	121,17	604,97	4,26	7,11	5,23
		2		1,0003	1,1343	10,2833	1210,11	110,53	1046,16	131,63	604,00	4,26	6,91	5,23
		3		1,5010	1,7020	10,2774	1208,73	110,41	1043,93	142,00	602,71	4,26	6,75	5,22
	25	0	100	0,0000	0,0000	10,2880	1211,22	110,63	1138,18	110,63	414,26	4,13	6,24	2,27
		1		0,3421	0,6786	10,2866	1210,89	110,60	1137,23	117,83	413,92	4,13	5,64	2,27
		2		0,6843	1,3575	10,2825	1209,92	110,52	1135,63	124,95	413,34	4,13	5,19	2,27
		3		1,0269	2,0368	10,2756	1208,29	110,37	1133,38	131,98	412,52	4,13	4,85	2,27
Vb (kts)	Θ (°)	Υ (°)	Im. (%)	ξ (deg)	η (deg)	Vapp (m/s)	L_section (N)	D_section (N)	L (N)	D (N)	SF (N)	Lift contribution (%)	Drag contribution (%)	SF contribution (%)
25	0	0	0	0,0000	0,0000	12,8600	0	0	0	0	0	0	0	0
		1		0,7071	0,5000	12,8590	0	0	0	0	0	0	0	0
		2		1,4145	1,0003	12,8561	0	0	0	0	0	0	0	0
		3		2,1223	1,5010	12,8512	0	0	0	0	0	0	0	0
	5	0	3,40	0,0000	0,0000	12,8600	64,41	5,88	49,34	5,88	41,40	4,30	10,22	30,09
		1		0,6428	0,5076	12,8589	64,40	5,88	49,28	6,60	41,35	4,29	11,02	30,07
		2		1,2859	1,0155	12,8554	64,36	5,88	49,19	7,32	41,28	4,29	11,75	30,06
		3		1,9294	1,5238	12,8497	64,31	5,87	49,08	8,03	41,18	4,29	12,44	30,05
	15	0	100	0,0000	0,0000	12,8600	1892,53	172,87	1638,98	172,87	946,27	4,49	7,83	5,68
		1		0,5000	0,5670	12,8585	1892,10	172,83	1637,24	189,33	945,26	4,49	7,58	5,68
		2		1,0003	1,1343	12,8541	1890,80	172,71	1634,62	205,67	943,75	4,49	7,38	5,68
		3		1,5010	1,7020	12,8468	1888,64	172,51	1631,14	221,87	941,74	4,48	7,22	5,67
	25	0	100	0,0000	0,0000	12,8600	1892,53	172,87	1778,40	172,87	647,28	4,13	6,24	2,27
		1		0,3421	0,6786	12,8583	1892,02	172,82	1776,92	184,11	646,75	4,13	5,64	2,27
		2		0,6843	1,3575	12,8531	1890,50	172,68	1774,42	195,23	645,84	4,13	5,19	2,27
		3		1,0269	2,0368	12,8444	1887,95	172,45	1770,91	206,23	644,56	4,13	4,85	2,27

Table 49: Hydrodynamic forces calculation for foil section D

Foil Section D														
Vb (kts)	Θ (°)	Υ (°)	Im. (%)	ξ (deg)	η (deg)	Vapp (m/s)	L_section (N)	D_section (N)	L (N)	D (N)	SF (N)	Lift contribution (%)	Drag contribution (%)	SF contribution (%)
10	0	0	0	0,0000	0,0000	5,1440	0	0	0	0	0	0	0	0
		1		1,0000	1,0000	5,1440	0	0	0	0	0	0	0	0
		2		2,0000	2,0000	5,1440	0	0	0	0	0	0	0	0
		3		3,0000	3,0000	5,1440	0	0	0	0	0	0	0	0
	5	0	0	0,0000	0,0000	5,1440	0	0	0	0	0	0	0	0
		1		0,9962	0,9132	5,1440	0	0	0	0	0	0	0	0
		2		1,9924	1,8265	5,1440	0	0	0	0	0	0	0	0
		3		2,9886	2,7399	5,1439	0	0	0	0	0	0	0	0
	15	0	86,20	0,0000	0,0000	5,1440	1118,61	73,27	289,52	73,27	1080,50	4,49	18,49	34,73
		1		0,9659	0,7500	5,1439	1118,59	73,27	289,15	92,12	1079,13	4,49	20,45	34,71
		2		1,9319	1,5003	5,1438	1118,52	73,27	288,69	110,93	1077,41	4,49	21,99	34,70
		3		2,8980	2,2509	5,1435	1118,41	73,26	288,14	129,70	1075,34	4,49	23,25	34,70
	25	0	100	0,0000	0,0000	5,1440	1297,74	85,01	548,45	85,01	1176,15	7,96	19,18	25,79
		1		0,9063	0,6170	5,1439	1297,67	85,00	547,78	105,52	1174,72	7,96	20,19	25,78
		2		1,8127	1,2343	5,1434	1297,45	84,99	546,92	125,98	1172,87	7,95	20,93	25,77
		3		2,7194	1,8520	5,1427	1297,10	84,97	545,86	146,38	1170,60	7,95	21,51	25,77
Vb (kts)	Θ (°)	Υ (°)	Im. (%)	ξ (deg)	η (deg)	Vapp (m/s)	L_section (N)	D_section (N)	L (N)	D (N)	SF (N)	Lift contribution (%)	Drag contribution (%)	SF contribution (%)
15	0	0	0	0,0000	0,0000	7,7160	0	0	0	0	0	0	0	0
		1		1,0000	1,0000	7,7160	0	0	0	0	0	0	0	0
		2		2,0000	2,0000	7,7160	0	0	0	0	0	0	0	0
		3		3,0000	3,0000	7,7160	0	0	0	0	0	0	0	0
	5	0	0	0,0000	0,0000	7,7160	0	0	0	0	0	0	0	0
		1		0,9962	0,9132	7,7160	0	0	0	0	0	0	0	0
		2		1,9924	1,8265	7,7160	0	0	0	0	0	0	0	0
		3		2,9886	2,7399	7,7159	0	0	0	0	0	0	0	0
	15	0	83,59	0,0000	0,0000	7,7160	2440,89	159,89	631,75	159,89	2357,72	4,43	18,03	34,54
		1		0,9659	0,7500	7,7159	2440,84	159,89	630,95	201,01	2354,73	4,43	19,99	34,53
		2		1,9319	1,5003	7,7157	2440,69	159,88	629,94	242,05	2350,98	4,43	21,54	34,52
		3		2,8980	2,2509	7,7153	2440,44	159,86	628,73	283,01	2346,46	4,42	22,80	34,51
	25	0	100	0,0000	0,0000	7,7160	2919,91	191,27	1234,01	191,27	2646,33	7,96	19,18	25,79
		1		0,9063	0,6170	7,7158	2919,75	191,26	1232,51	237,41	2643,12	7,96	20,19	25,78
		2		1,8127	1,2343	7,7152	2919,27	191,22	1230,56	283,45	2638,95	7,95	20,93	25,78
		3		2,7194	1,8520	7,7141	2918,48	191,17	1228,18	329,36	2633,84	7,95	21,51	25,78
Vb (kts)	Θ (°)	Υ (°)	Im. (%)	ξ (deg)	η (deg)	Vapp (m/s)	L_section (N)	D_section (N)	L (N)	D (N)	SF (N)	Lift contribution (%)	Drag contribution (%)	SF contribution (%)
20	0	0	0	0,0000	0,0000	10,2880	0	0	0	0	0	0	0	0
		1		1,0000	1,0000	10,2880	0	0	0	0	0	0	0	0
		2		2,0000	2,0000	10,2880	0	0	0	0	0	0	0	0
		3		3,0000	3,0000	10,2880	0	0	0	0	0	0	0	0
	5	0	0	0,0000	0,0000	10,2880	0	0	0	0	0	0	0	0
		1		0,9962	0,9132	10,2880	0	0	0	0	0	0	0	0
		2		1,9924	1,8265	10,2880	0	0	0	0	0	0	0	0
		3		2,9886	2,7399	10,2879	0	0	0	0	0	0	0	0
	15	0	78,94	0,0000	0,0000	10,2880	4097,80	268,42	1060,59	268,42	3958,17	4,31	17,88	34,18
		1		0,9659	0,7500	10,2879	4097,72	268,42	1059,25	337,46	3953,16	4,31	19,81	34,16
		2		1,9319	1,5003	10,2876	4097,47	268,40	1057,56	406,37	3946,86	4,31	21,34	34,15
		3		2,8980	2,2509	10,2871	4097,05	268,37	1055,53	475,13	3939,28	4,31	22,59	34,15
	25	0	100	0,0000	0,0000	10,2880	5190,95	340,03	2193,79	340,03	4704,59	7,96	19,18	25,79
		1		0,9063	0,6170	10,2877	5190,66	340,01	2191,12	422,06	4698,88	7,96	20,19	25,78
		2		1,8127	1,2343	10,2869	5189,82	339,95	2187,67	503,91	4691,47	7,95	20,93	25,77
		3		2,7194	1,8520	10,2855	5188,41	339,86	2183,43	585,52	4682,38	7,95	21,51	25,77
Vb (kts)	Θ (°)	Υ (°)	Im. (%)	ξ (deg)	η (deg)	Vapp (m/s)	L_section (N)	D_section (N)	L (N)	D (N)	SF (N)	Lift contribution (%)	Drag contribution (%)	SF contribution (%)
25	0	0	0	0,0000	0,0000	12,8600	0	0	0	0	0	0	0	0
		1		1,0000	1,0000	12,8600	0	0	0	0	0	0	0	0
		2		2,0000	2,0000	12,8600	0	0	0	0	0	0	0	0
		3		3,0000	3,0000	12,8600	0	0	0	0	0	0	0	0
	5	0	0	0,0000	0,0000	12,8600	0	0	0	0	0	0	0	0
		1		0,9962	0,9132	12,8600	0	0	0	0	0	0	0	0
		2		1,9924	1,8265	12,8599	0	0	0	0	0	0	0	0
		3		2,9886	2,7399	12,8599	0	0	0	0	0	0	0	0
	15	0	71,23	0,0000	0,0000	12,8600	5777,63	378,46	1495,36	378,46	5580,76	4,10	17,14	33,49
		1		0,9659	0,7500	12,8599	5777,51	378,45	1493,47	475,79	5573,69	4,09	19,05	33,48
		2		1,9319	1,5003	12,8595	5777,16	378,43	1491,09	572,95	5564,81	4,09	20,56	33,47
		3		2,8980	2,2509	12,8588	5776,57	378,39	1488,22	669,90	5554,12	4,09	21,80	33,46
	25	0	100	0,0000	0,0000	12,8600	8110,85	531,30	3427,79	531,30	7350,93	7,96	19,18	25,79
		1		0,9063	0,6170	12,8597	8110,41	531,27	3423,63	659,47	7341,99	7,96	20,19	25,78
		2		1,8127	1,2343	12,8586	8109,09	531,18	3418,23	787,36	7330,42	7,95	20,93	25,77
		3		2,7194	1,8520	12,8569	8106,88	531,04	3411,61	914,88	7316,22	7,95	21,51	25,77

Table 50: Hydrodynamic forces calculation for the entire foil

Entire Foil							
Vb (kts)	Heel Θ (°)	Leeway ϒ (°)	Immersion (%)	L (N)	D (N)	SF (N)	L/D
10	0	0	0	0	0	0	0
		1		0	0	0	0
		2		0	0	0	0
		3		0	0	0	0
	5	0	3,12	314,44	15,76	-15,00	19,96
		1		314,31	16,41	-15,01	19,16
		2		314,00	17,05	-15,00	18,42
		3		313,49	17,68	-14,98	17,73
	15	0	89,10	6443,26	396,26	-647,35	16,26
		1		6439,43	450,44	-647,84	14,30
		2		6431,94	504,36	-647,67	12,75
		3		6420,82	557,95	-646,85	11,51
	25	0	100	6889,64	443,28	-2000,84	15,54
		1		6884,71	522,73	-2000,14	13,17
		2		6876,15	601,86	-1998,16	11,42
		3		6863,98	680,58	-1994,91	10,09
Vb (kts)	Θ (°)	ϒ (°)	Im. (%)	L (N)	D (N)	SF (N)	L/D
15	0	0	0	0	0	0	0
		1		0	0	0	0
		2		0	0	0	0
		3		0	0	0	0
	5	0	2,66	602,82	30,21	-28,75	19,96
		1		602,57	31,46	-28,76	19,15
		2		601,96	32,69	-28,75	18,41
		3		600,98	33,90	-28,71	17,73
	15	0	87,34	14261,47	886,62	-1429,14	16,09
		1		14252,77	1005,48	-1430,07	14,18
		2		14235,67	1123,72	-1429,42	12,67
		3		14210,21	1241,24	-1427,18	11,45
	25	0	100	15501,68	997,37	-4501,90	15,54
		1		15490,17	1176,12	-4500,05	13,17
		2		15469,64	1354,08	-4494,81	11,42
		3		15440,12	1531,04	-4486,20	10,08
Vb (kts)	Θ (°)	ϒ (°)	Im. (%)	L (N)	D (N)	SF (N)	L/D
20	0	0	0	0	0	0	0
		1		0	0	0	0
		2		0	0	0	0
		3		0	0	0	0
	5	0	2,48	998,86	50,05	-47,64	19,96
		1		998,45	52,13	-47,65	19,15
		2		997,43	54,16	-47,64	18,41
		3		995,82	56,17	-47,58	17,73
	15	0	84,19	24603,97	1501,57	-2453,55	16,39
		1		24589,44	1703,25	-2455,33	14,44
		2		24560,95	1903,90	-2454,68	12,90
		3		24518,53	2103,34	-2451,59	11,66
	25	0	100	27558,55	1773,10	-8003,37	15,54
		1		27538,83	2090,92	-8000,55	13,17
		2		27504,62	2407,44	-7992,64	11,42
		3		27455,94	2722,32	-7979,64	10,09
Vb (kts)	Θ (°)	ϒ (°)	Im. (%)	L (N)	D (N)	SF (N)	L/D
25	0	0	0	0	0	0	0
		1		0	0	0	0
		2		0	0	0	0
		3		0	0	0	0
	5	0	1,83	1148,61	57,56	-54,77	19,96
		1		1148,14	59,94	-54,79	19,15
		2		1146,97	62,29	-54,77	18,41
		3		1145,12	64,59	-54,71	17,73
	15	0	78,96	36503,53	2207,64	-3608,28	16,54
		1		36482,17	2497,79	-3610,84	14,61
		2		36440,05	2786,43	-3609,85	13,08
		3		36377,19	3073,29	-3605,32	11,84
	25	0	100	43060,23	2770,48	-12505,26	15,54
		1		43029,43	3267,07	-12500,86	13,17
		2		42975,97	3761,62	-12488,50	11,42
		3		42899,90	4253,62	-12468,19	10,09

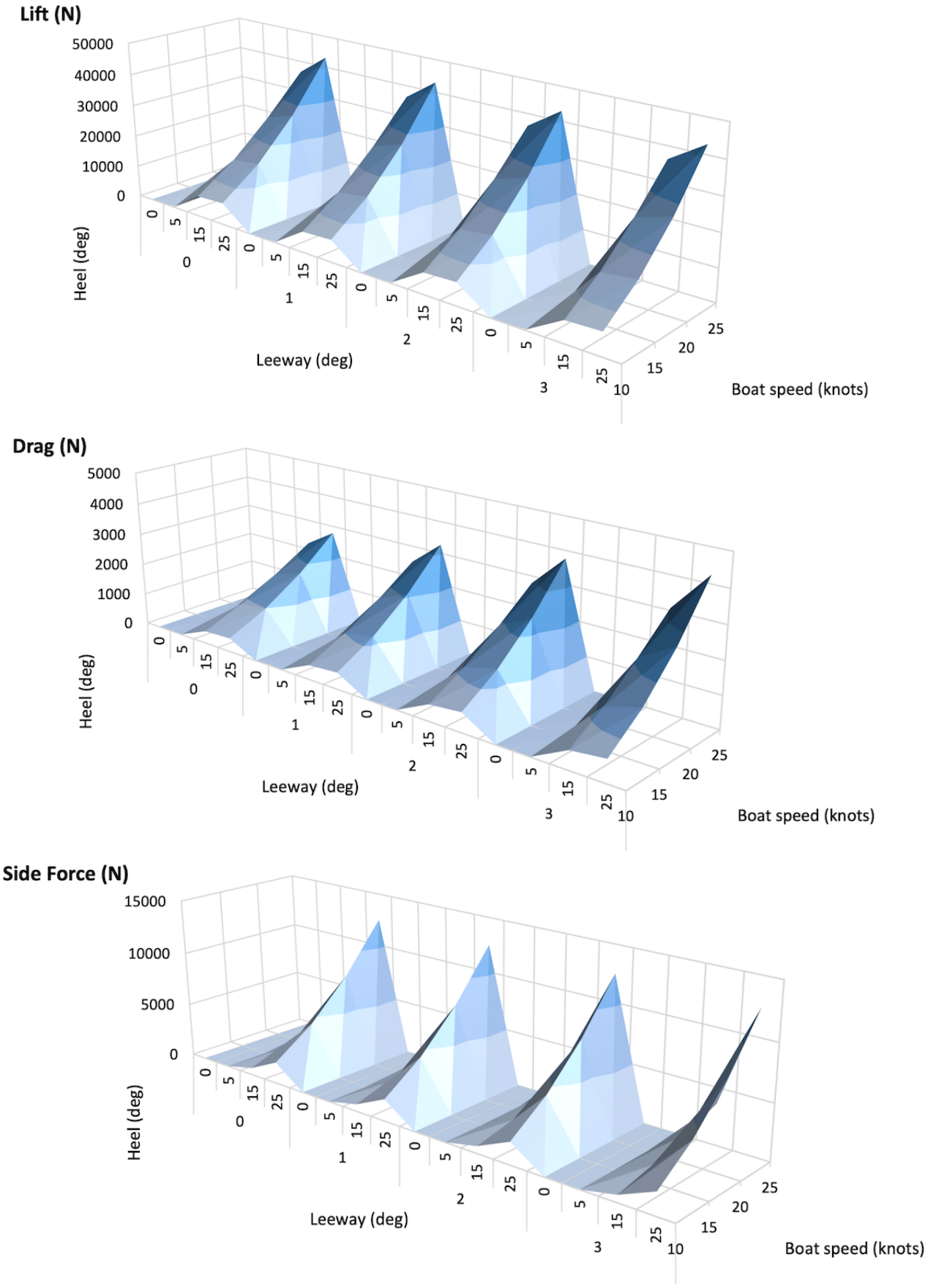

Figure 46: Foil's hydrodynamic forces for varying boat speed, heel and leeway angles

C.3.2 Foil righting moment calculation

Table 51: Horizontal center of lift and vertical center of side force of each section

Speed (kts)	Heel Θ (deg)	Foil section	Span si (m)	Dry span si_dry (m)	Immersed span si_wet (m)	xi (m)	zi (m)
10	0	A	1,00	1,00	0	0	0
		B	1,80	1,80	0	0	0
		C	0,30	0,30	0	0	0
		D	0,75	0,75	0	0	0
	5	A	1,00	1,00	0	0	0
		B	1,80	1,68	0,120	4,99	0,0052
		C	0,30	0,28	0,017	5,06	0,0048
		D	0,75	0,75	0	0	0
	15	A	1,00	0,30	0,70	2,81	0,15
		B	1,80	0,00	1,80	4,00	0,53
		C	0,30	0,00	0,30	5,00	0,69
		D	0,75	0,10	0,65	5,21	0,25
	25	A	1,00	0,00	1,00	2,49	0,29
		B	1,80	0,00	1,80	3,72	0,95
		C	0,30	0,00	0,30	4,68	1,28
		D	0,75	0,00	0,75	4,98	0,89
15	0	A	1,00	1,00	0	0	0
		B	1,80	1,80	0	0	0
		C	0,30	0,30	0	0	0
		D	0,75	0,75	0	0	0
	5	A	1,00	1,00	0	0	0
		B	1,80	1,70	0,102	5,00	0,0045
		C	0,30	0,29	0,015	5,06	0,0041
		D	0,75	0,75	0	0	0
	15	A	1,00	0,34	0,66	2,83	0,14
		B	1,80	0,00	1,80	4,00	0,51
		C	0,30	0,00	0,30	5,00	0,67
		D	0,75	0,12	0,63	5,21	0,23
	25	A	1,00	0,00	1,00	2,49	0,29
		B	1,80	0,00	1,80	3,72	0,95
		C	0,30	0,00	0,30	4,68	1,28
		D	0,75	0,00	0,75	4,98	0,89
20	0	A	1,00	1,00	0	0	0
		B	1,80	1,80	0	0	0
		C	0,30	0,30	0	0	0
		D	0,75	0,75	0	0	0
	5	A	1,00	1,00	0	0	0
		B	1,80	1,70	0,095	5,00	0,0042
		C	0,30	0,29	0,014	5,06	0,0038
		D	0,75	0,75	0	0	0
	15	A	1,00	0,42	0,58	2,87	0,12
		B	1,80	0,00	1,80	4,00	0,48
		C	0,30	0,00	0,30	5,00	0,64
		D	0,75	0,16	0,59	5,20	0,20
	25	A	1,00	0,00	1,00	2,49	0,29
		B	1,80	0,00	1,80	3,72	0,95
		C	0,30	0,00	0,30	4,68	1,28
		D	0,75	0,00	0,75	4,98	0,89
25	0	A	1,00	1,00	0	0	0
		B	1,80	1,80	0	0	0
		C	0,30	0,30	0	0	0
		D	0,75	0,75	0	0	0
	5	A	1,00	1,00	0	0	0
		B	1,80	1,73	0,070	5,02	0,0031
		C	0,30	0,29	0,010	5,05	0,0028
		D	0,75	0,75	0	0	0
	15	A	1,00	0,55	0,45	2,93	0,09
		B	1,80	0,00	1,80	4,00	0,42
		C	0,30	0,00	0,30	5,00	0,58
		D	0,75	0,22	0,53	5,20	0,14
	25	A	1,00	0,00	1,00	2,49	0,29
		B	1,80	0,00	1,80	3,72	0,95
		C	0,30	0,00	0,30	4,68	1,28
		D	0,75	0,00	0,75	4,98	0,89

Table 52: Foil righting moment and lever arm calculations

Entire Foil										
Speed (kts)	Heel Θ (deg)	Leeway Υ (deg)	L (N)	SF (N)	d1 (m)	d2 (m)	Added Moment Foil (N.m)	Static moment boat (N.m)	Revised GZ (m)	GZ (m)
10	0	0	0	0	0	0	0	0	0	0
		1	0	0	0	0	0		0	
		2	0	0	0	0	0		0	
		3	0	0	0	0	0		0	
	5	0	314,44	-15,00	4,99	0,0051	1570,22	48370,44	0,6474	0,627
		1	314,31	-15,01	4,99	0,0051	1569,57		0,6473	
		2	314,00	-15,00	4,99	0,0051	1567,98		0,6473	
		3	313,49	-14,98	4,99	0,0051	1565,45		0,6473	
	15	0	6443,26	-647,35	3,81	0,35	24797,82	115718,76	1,8214	1,500
		1	6439,43	-647,84	3,81	0,35	24783,11		1,8213	
		2	6431,94	-647,67	3,81	0,35	24754,33		1,8209	
		3	6420,82	-646,85	3,81	0,35	24711,51		1,8203	
	25	0	6889,64	-2000,84	3,51	0,75	25687,45	155371,72	2,3470	2,014
		1	6884,71	-2000,14	3,51	0,75	25669,32		2,3467	
		2	6876,15	-1998,16	3,51	0,75	25637,56		2,3463	
		3	6863,98	-1994,91	3,51	0,75	25592,22		2,3457	
Speed (kts)	Heel Θ (deg)	Leeway Υ (deg)	L (N)	SF (N)	d1 (m)	d2 (m)	Added Moment Foil (N.m)	Static moment boat (N.m)	Revised GZ (m)	GZ (m)
15	0	0	0	0	0	0	0	0	0	0
		1	0	0	0	0	0		0	
		2	0	0	0	0	0		0	
		3	0	0	0	0	0		0	
	5	0	602,82	-28,75	5,00	0,0044	3015,33	48370,44	0,6661	0,627
		1	602,57	-28,76	5,00	0,0044	3014,08		0,6661	
		2	601,96	-28,75	5,00	0,0044	3011,02		0,6660	
		3	600,98	-28,71	5,00	0,0044	3006,13		0,6660	
	15	0	14261,47	-1429,14	3,83	0,34	55120,25	115718,76	2,2145	1,500
		1	14252,77	-1430,07	3,83	0,34	55086,77		2,2141	
		2	14235,67	-1429,42	3,83	0,34	55020,79		2,2132	
		3	14210,21	-1427,18	3,83	0,34	54922,37		2,2119	
	25	0	15501,68	-4501,90	3,51	0,75	57796,76	155371,72	2,7632	2,014
		1	15490,17	-4500,05	3,51	0,75	57754,23		2,7626	
		2	15469,64	-4494,81	3,51	0,75	57677,60		2,7616	
		3	15440,12	-4486,20	3,51	0,75	57566,95		2,7602	
Speed (kts)	Heel Θ (deg)	Leeway Υ (deg)	L (N)	SF (N)	d1 (m)	d2 (m)	Added Moment Foil (N.m)	Static moment boat (N.m)	Revised GZ (m)	GZ (m)
20	0	0	0	0	0	0	0	0	0	0
		1	0	0	0	0	0		0	
		2	0	0	0	0	0		0	
		3	0	0	0	0	0		0	
	5	0	998,86	-47,64	5,06	0,0041	5050,07	48370,44	0,6925	0,627
		1	998,45	-47,65	5,06	0,0041	5047,98		0,6924	
		2	997,43	-47,64	5,06	0,0041	5042,86		0,6924	
		3	995,82	-47,58	5,06	0,0041	5034,71		0,6923	
	15	0	24603,97	-2453,55	3,86	0,32	95811,60	115718,76	2,7420	1,500
		1	24589,44	-2455,33	3,86	0,32	95755,07		2,7412	
		2	24560,95	-2454,68	3,86	0,32	95644,07		2,7398	
		3	24518,53	-2451,59	3,86	0,32	95478,74		2,7376	
	25	0	27558,55	-8003,37	3,51	0,75	102749,80	155371,72	3,3459	2,014
		1	27538,83	-8000,55	3,51	0,75	102677,27		3,3450	
		2	27504,62	-7992,64	3,51	0,75	102550,25		3,3433	
		3	27455,94	-7979,64	3,51	0,75	102368,87		3,3410	
Speed (kts)	Heel Θ (deg)	Leeway Υ (deg)	L (N)	SF (N)	d1 (m)	d2 (m)	Added Moment Foil (N.m)	Static moment boat (N.m)	Revised GZ (m)	GZ (m)
25	0	0	0	0	0	0	0	0	0	0
		1	0	0	0	0	0		0	
		2	0	0	0	0	0		0	
		3	0	0	0	0	0		0	
	5	0	1148,61	-54,77	5,05	0,0030	5805,51	48370,44	0,7023	0,627
		1	1148,14	-54,79	5,05	0,0030	5803,11		0,7022	
		2	1146,97	-54,77	5,05	0,0030	5797,23		0,7021	
		3	1145,12	-54,71	5,05	0,0030	5787,86		0,7020	
	15	0	36503,53	-3608,28	3,91	0,28	143910,54	115718,76	3,3654	1,500
		1	36482,17	-3610,84	3,91	0,28	143826,17		3,3643	
		2	36440,05	-3609,85	3,91	0,28	143659,82		3,3622	
		3	36377,19	-3605,32	3,91	0,28	143411,67		3,3590	
	25	0	43060,23	-12505,26	3,51	0,75	160546,57	155371,72	4,0951	2,014
		1	43029,43	-12500,86	3,51	0,75	160433,23		4,0936	
		2	42975,97	-12488,50	3,51	0,75	160234,76		4,0910	
		3	42899,90	-12468,19	3,51	0,75	159951,36		4,0874	

Table 53: Foil righting moment and lever arm calculations, keel canted

Entire Foil										
Speed (kts)	Heel Θ (deg)	Leeway Υ (deg)	L (N)	SF (N)	d1 (m)	d2 (m)	Added Moment Foil (N.m)	Static moment boat (N.m)	Revised GZ (m)	GZ (m)
10	0	0	0	0	0	0	0	81620,30	1,058	1,058
		1	0	0	0	0	0		1,058	
		2	0	0	0	0	0		1,058	
		3	0	0	0	0	0		1,058	
	5	0	314,44	-15,00	4,99	0,0051	1570,22	125207,70	1,6434	1,623
		1	314,31	-15,01	4,99	0,0051	1569,57		1,6433	
		2	314,00	-15,00	4,99	0,0051	1567,98		1,6433	
		3	313,49	-14,98	4,99	0,0051	1565,45		1,6433	
	15	0	6443,26	-647,35	3,81	0,35	24797,82	180289,83	2,6584	2,337
		1	6439,43	-647,84	3,81	0,35	24783,11		2,6583	
		2	6431,94	-647,67	3,81	0,35	24754,33		2,6579	
		3	6420,82	-646,85	3,81	0,35	24711,51		2,6573	
	25	0	6889,64	-2000,84	3,51	0,75	25687,45	209528,10	3,0490	2,716
		1	6884,71	-2000,14	3,51	0,75	25669,32		3,0487	
		2	6876,15	-1998,16	3,51	0,75	25637,56		3,0483	
		3	6863,98	-1994,91	3,51	0,75	25592,22		3,0477	
Speed (kts)	Heel Θ (deg)	Leeway Υ (deg)	L (N)	SF (N)	d1 (m)	d2 (m)	Added Moment Foil (N.m)	Static moment boat (N.m)	Revised GZ (m)	GZ (m)
15	0	0	0	0	0	0	0	81620,30	1,058	1,058
		1	0	0	0	0	0		1,058	
		2	0	0	0	0	0		1,058	
		3	0	0	0	0	0		1,058	
	5	0	602,82	-28,75	5,00	0,0044	3015,33	125207,70	1,6621	1,623
		1	602,57	-28,76	5,00	0,0044	3014,08		1,6621	
		2	601,96	-28,75	5,00	0,0044	3011,02		1,6620	
		3	600,98	-28,71	5,00	0,0044	3006,13		1,6620	
	15	0	14261,47	-1429,14	3,83	0,34	55120,25	180289,83	3,0515	2,337
		1	14252,77	-1430,07	3,83	0,34	55086,77		3,0511	
		2	14235,67	-1429,42	3,83	0,34	55020,79		3,0502	
		3	14210,21	-1427,18	3,83	0,34	54922,37		3,0489	
	25	0	15501,68	-4501,90	3,51	0,75	57796,76	209528,10	3,4652	2,716
		1	15490,17	-4500,05	3,51	0,75	57754,23		3,4646	
		2	15469,64	-4494,81	3,51	0,75	57677,60		3,4636	
		3	15440,12	-4486,20	3,51	0,75	57566,95		3,4622	
Speed (kts)	Heel Θ (deg)	Leeway Υ (deg)	L (N)	SF (N)	d1 (m)	d2 (m)	Added Moment Foil (N.m)	Static moment boat (N.m)	Revised GZ (m)	GZ (m)
20	0	0	0	0	0	0	0	81620,30	1,058	1,058
		1	0	0	0	0	0		1,058	
		2	0	0	0	0	0		1,058	
		3	0	0	0	0	0		1,058	
	5	0	998,86	-47,64	5,06	0,0041	5050,07	125207,70	1,6885	1,623
		1	998,45	-47,65	5,06	0,0041	5047,98		1,6884	
		2	997,43	-47,64	5,06	0,0041	5042,86		1,6884	
		3	995,82	-47,58	5,06	0,0041	5034,71		1,6883	
	15	0	24603,97	-2453,55	3,86	0,32	95811,60	180289,83	3,5790	2,337
		1	24589,44	-2455,33	3,86	0,32	95755,07		3,5782	
		2	24560,95	-2454,68	3,86	0,32	95644,07		3,5768	
		3	24518,53	-2451,59	3,86	0,32	95478,74		3,5746	
	25	0	27558,55	-8003,37	3,51	0,75	102749,80	209528,10	4,0479	2,716
		1	27538,83	-8000,55	3,51	0,75	102677,27		4,0470	
		2	27504,62	-7992,64	3,51	0,75	102550,25		4,0453	
		3	27455,94	-7979,64	3,51	0,75	102368,87		4,0430	
Speed (kts)	Heel Θ (deg)	Leeway Υ (deg)	L (N)	SF (N)	d1 (m)	d2 (m)	Added Moment Foil (N.m)	Static moment boat (N.m)	Revised GZ (m)	GZ (m)
25	0	0	0	0	0	0	0	81620,30	1,058	1,058
		1	0	0	0	0	0		1,058	
		2	0	0	0	0	0		1,058	
		3	0	0	0	0	0		1,058	
	5	0	1148,61	-54,77	5,05	0,0030	5805,51	125207,70	1,6983	1,623
		1	1148,14	-54,79	5,05	0,0030	5803,11		1,6982	
		2	1146,97	-54,77	5,05	0,0030	5797,23		1,6981	
		3	1145,12	-54,71	5,05	0,0030	5787,86		1,6980	
	15	0	36503,53	-3608,28	3,91	0,28	143910,54	180289,83	4,2024	2,337
		1	36482,17	-3610,84	3,91	0,28	143826,17		4,2013	
		2	36440,05	-3609,85	3,91	0,28	143659,82		4,1992	
		3	36377,19	-3605,32	3,91	0,28	143411,67		4,1960	
	25	0	43060,23	-12505,26	3,51	0,75	160546,57	209528,10	4,7971	2,716
		1	43029,43	-12500,86	3,51	0,75	160433,23		4,7956	
		2	42975,97	-12488,50	3,51	0,75	160234,76		4,7930	
		3	42899,90	-12468,19	3,51	0,75	159951,36		4,7894	

Immersions with foil influence on displacement

Vb = 10 kts

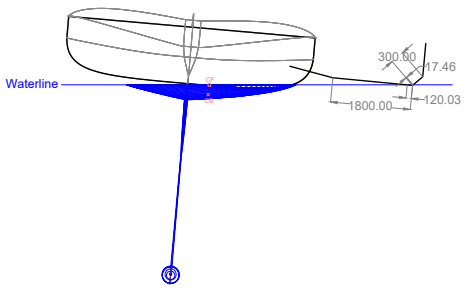

Heel angle = 5 degrees

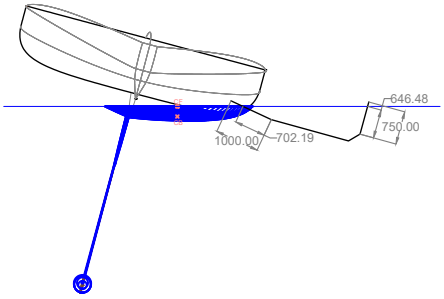

Heel angle = 15 degrees

Vb = 15 kts

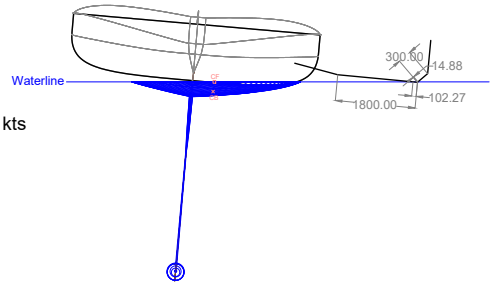

Heel angle = 5 degrees

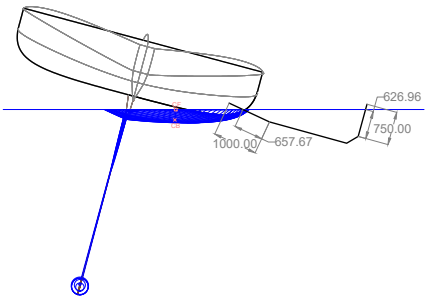

Heel angle = 15 degrees

Vb = 20 kts

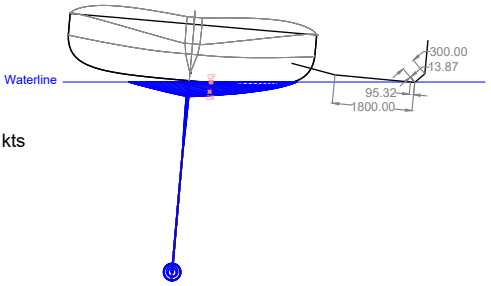

Heel angle = 5 degrees

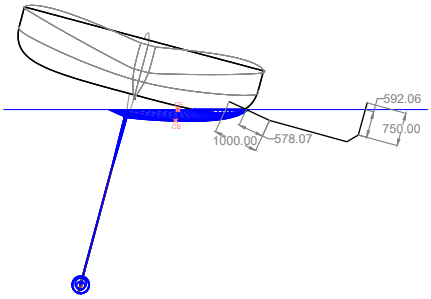

Heel angle = 15 degrees

Vb = 25 kts

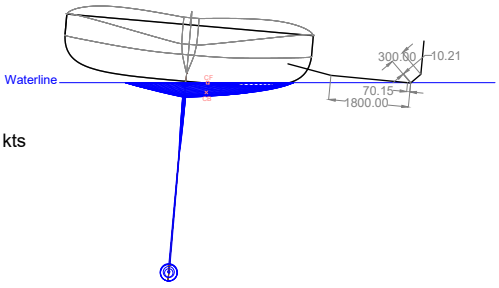

Heel angle = 5 degrees

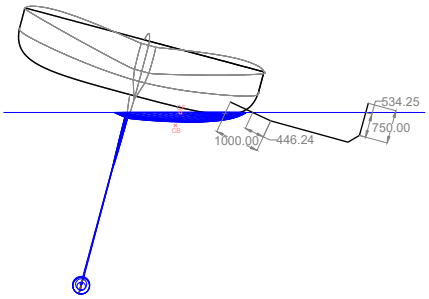

Heel angle = 15 degrees

Vb = 35 kts

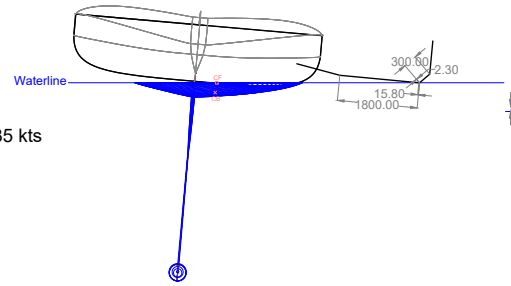

Heel angle = 5 degrees

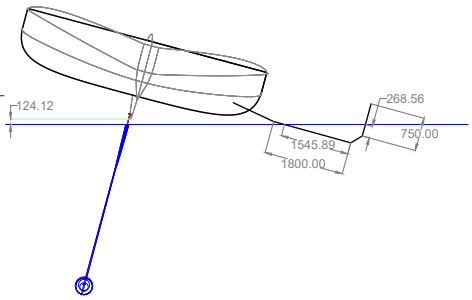

Heel angle = 15 degrees

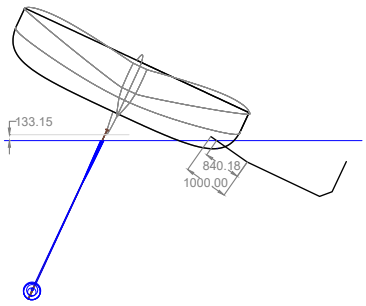

Heel angle = 25 degrees

SOLENT UNIVERSITY	Issue date: 12/05/2022	Scale: 1:170 (A4)	File name: Immersions.dwg
	Drawn by: Lazare GOURNAY	Units: mm	Projection method: Body Plan
	Drawing number: 00		**Drawing title: Foil sections' immersions**
		Sheet: 1 of 1	

C.4 Proofs and demonstrations of the equations used

The demonstrations of the equations used to compute the hydrodynamic forces in the model are presented. They were proposed with the help of Prof. Barkley to explain how the equations were derived.

C.4.1 Apparent velocity of the flow relative to the boat's centreline V_{app}

Consider a yacht with a foil at an angle α to the waterplane, as shown below.

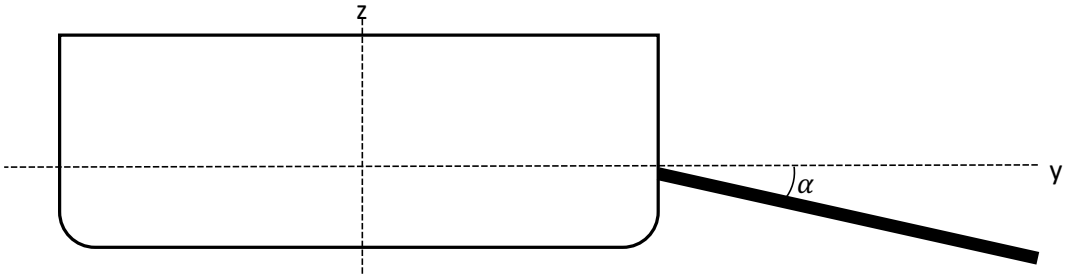

Figure 47: Angle of the foil to the waterline in the (yz) plane

The boat sails at a velocity V_b and at a leeway angle γ. As shown in Figure 48, the flow velocities parallel and perpendicular to the boat's CL, and in the waterplane, are respectively given by:

$$\begin{cases} V_b \times \cos\gamma \\ V_b \times \sin\gamma \end{cases}$$

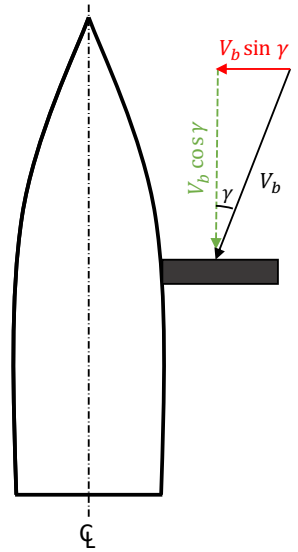

Figure 48: Change in velocity of the flow due to leeway angle

Now consider the heel angle θ of the boat, which adds up to the angle α in the case of a downward foil section, s.t. $(\theta + \alpha)$. A sketch of a 3D view is depicted in Figure 49, in which the two previous velocity components, respectively in the direction of the boat, and perpendicular to it, are represented.

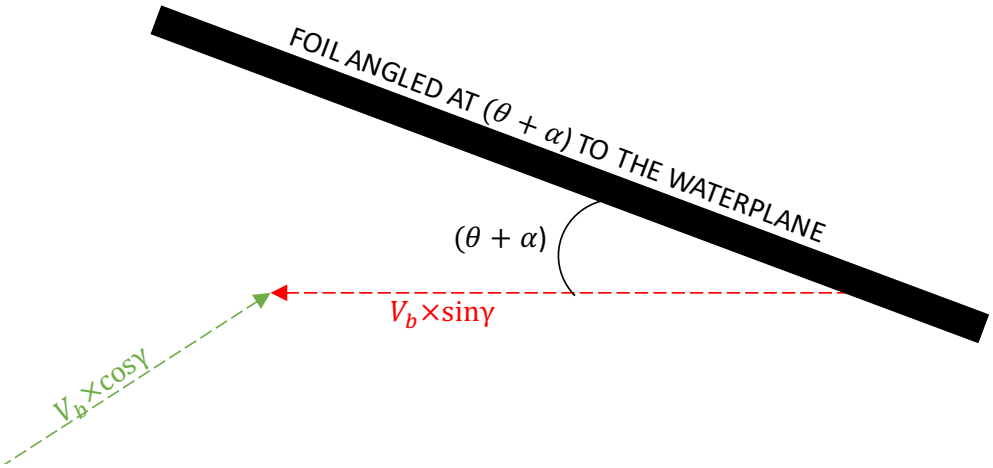

Figure 49: View of resolved velocity vectors in the waterplane

If one resolves $V_b \times \sin\gamma$ perpendicular to the plane of the foil, the vector becomes $V_b \times \sin\gamma \times \sin(\theta + \alpha)$, which is represented in Figure 50.

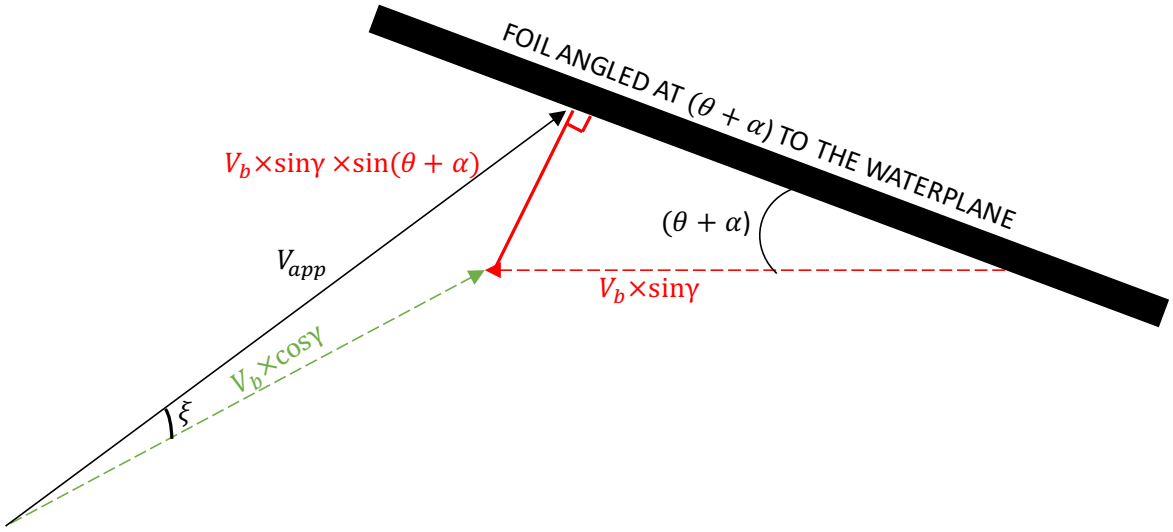

Figure 50: Projection of the velocity $V_b \times \sin\gamma$ perpendicular to the plane of the foil

Based on Figure 50, the apparent velocity of the flow on the foil V_{app} can be expressed s.t:

$$V_{app} = \sqrt{(V_b \times sin\gamma \times sin(\alpha + \theta))^2 + (V_b \times cos\gamma)^2}$$

C.4.2 Apparent angle of attack of the foil ξ

The apparent angle of attack in the plane perpendicular to the foil section ξ, is represented in Figure 50. It can be expressed from trigonometry as follows:

$$\xi = \tan^{-1}\left(\frac{V_b \sin\gamma \sin(\alpha+\theta)}{V_b \cos\gamma}\right)$$

The terms V_b cancel out, leading to equation 8 used in section 4.

C.4.3 Apparent leeway angle in the plane of the foil η

There is also a change of inflow to the foil due to the angle $(\theta + \alpha)$. This is depicted in the Figure 51, with the resulting apparent leeway angle becoming $(\gamma - \eta)$.

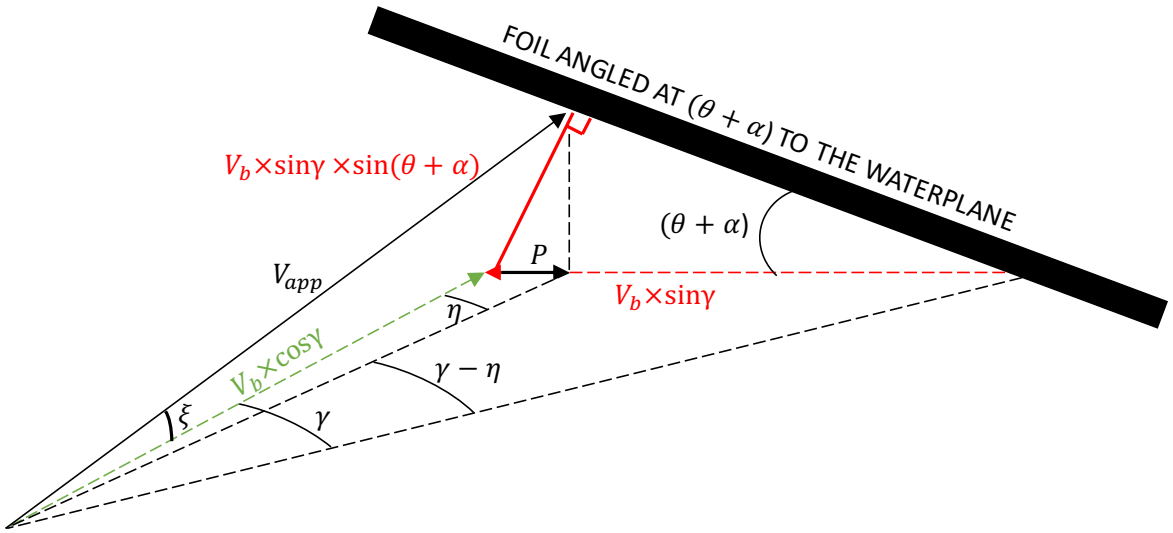

Figure 51: Sketch to visualise the derivation of η

It is seen on Figure 51 that trigonometry can be used to write η s.t:

$$\eta = \tan^{-1}\left(\frac{P}{V_b \cos\gamma}\right)$$

Where: $P = V_b \sin\gamma \sin(\theta+\alpha)\sin(\theta+\alpha)$.

Hence, η can be re-written as:

$$\eta = \tan^{-1}\left(\tan\gamma \sin^2(\theta+\alpha)\right)$$

C.4.4 Lift and drag forces L and D

Consider the lift and drag $L_{section}$ and $D_{section}$ calculated in the directions relative to the foil section. Since the flow direction has been rotated through the apparent angle of attack ξ, the lift and drag forces have been resolved perpendicular and parallel to this modified inflow. Therefore, these need to be resolved vertically and horizontally to the waterplane, as shown in Figure 52.

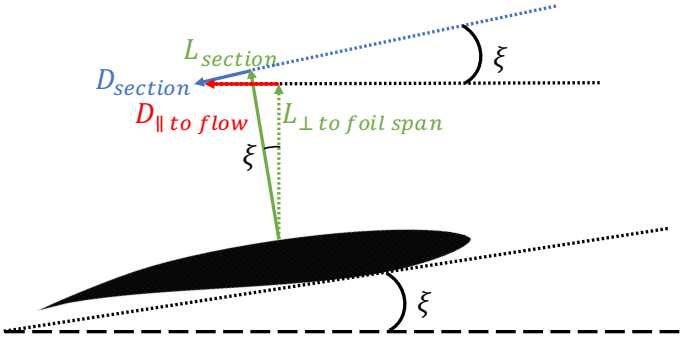

Figure 52: Sketch to visualise the projection of $L_{section}$ into vertical lift $L_{\perp\ to\ foil\ span}$

Using Figure 52, the vertical lift perpendicular to the span of the foil can be found s.t:

$$L_{\perp\ to\ foil\ span} = L_{section} \times \cos\xi - D_{section} \times \sin\xi$$

As shown in Figure 53, one must then account for the angle of the section to the waterplane $(\alpha + \theta)$, and resolve the lift force perpendicular to the waterplane, s.t:

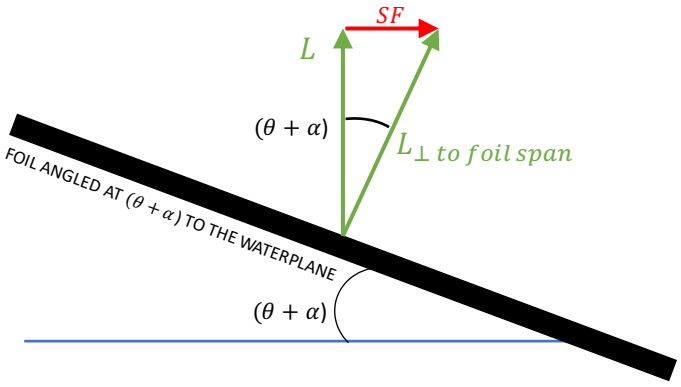

Figure 53: Sketch to visualise the horizontal side force SF and the projection of $L_{\perp\ to\ foil\ span}$ into vertical lift L

$$L = L_{\perp\ to\ foil\ span} \times \cos(\alpha + \theta)$$

Therefore, one gets:

$$L = (L_{section} \times \cos\xi - D_{section} \times \sin\xi) \times \cos(\alpha + \theta)$$

Similarly using Figure 52, the drag D parallel to the flow can be found using the following expression:

$$D_{\parallel to\, flow} = (L_{section} \sin\xi + D_{section} \cos\xi)$$

This drag is in the direction of the inflow, which is at an angle $(\gamma - \eta)$ to the boat's CL (c.f. Figure 51). Therefore, this needs to be resolved parallel to the CL, as:

$$D = D_{\parallel to\, flow} \times \cos(\gamma - \eta)$$

$$D = (L_{section} \sin\xi + D_{section} \cos\xi) \times \cos(\gamma - \eta)$$

C.4.5 Side force SF

As shown in Figure 53, the lift component perpendicular to the span of the foil also produces a side force. It is given as:

$$SF = (L_{section} \cos\xi - D_{section} \sin\xi) \times \sin(\alpha + \theta)$$

D Appendix - Manufacturing of the model scale hull form

Figure 54: CNC milled polystyrene hull

Figure 55: Glass fiber application on the hull

Figure 56: Primer and paint application on the hull

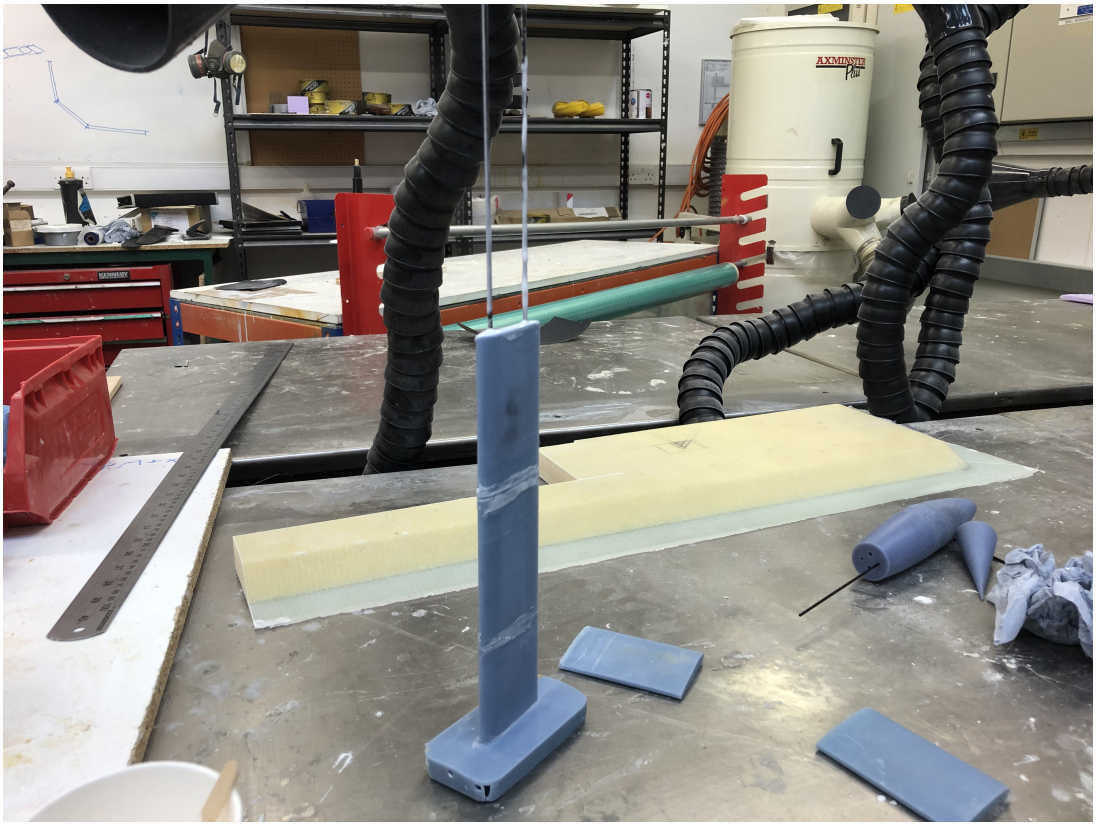

Figure 57: Assembly of the 3D printed appendages

Figure 58: Stiffening of the keel

Figure 59: New keel shaped in plywood

Figure 60: Stiffening of the foil

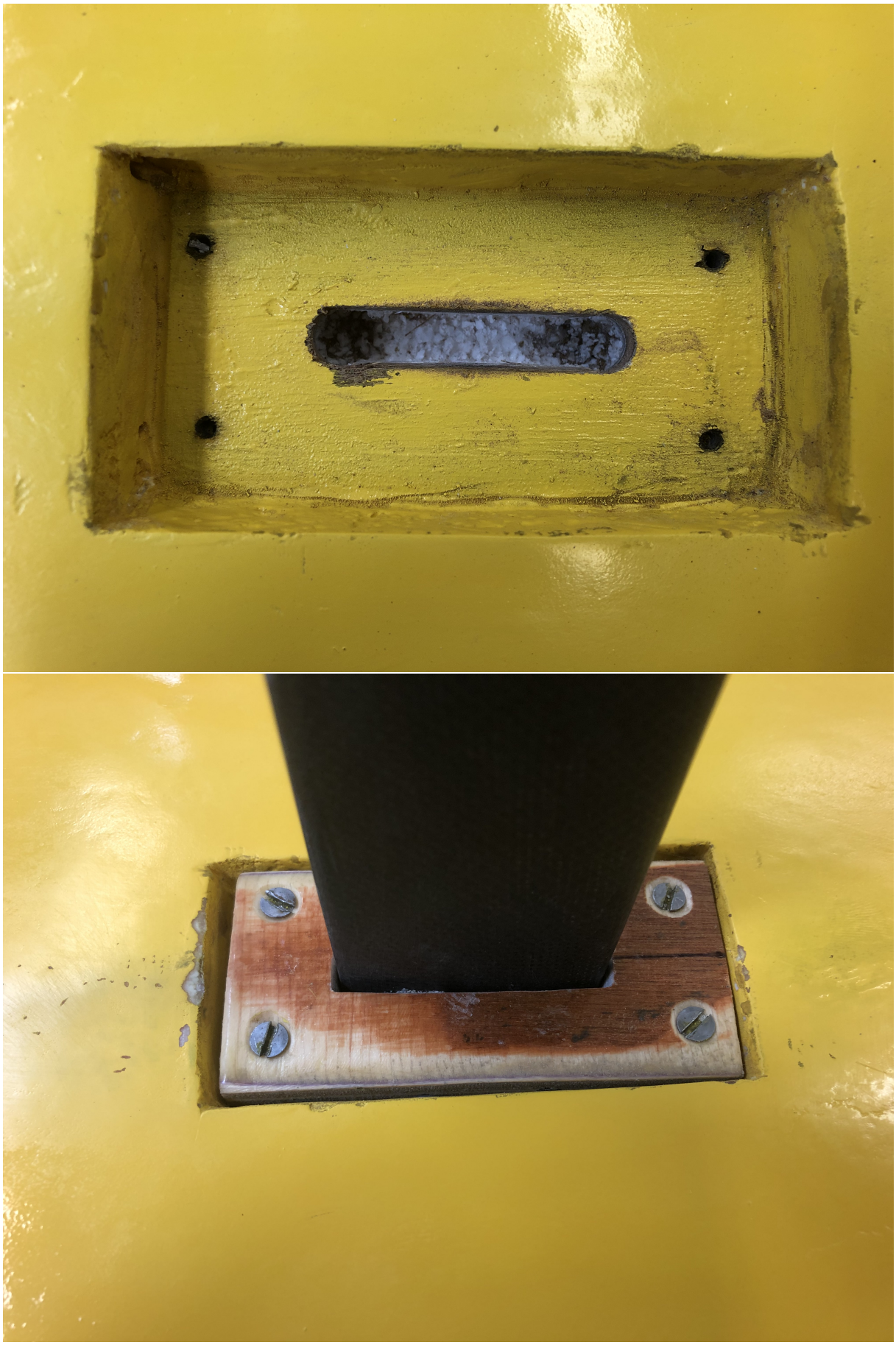

Figure 61: Keel fixation system

Figure 62: Model hull testing configurations

E Appendix - Tank test results

The Excel spreadsheet of Jan-Malte Nagel, third year student at Solent University, was used to scale the resistance data in order to gain time to perform other tasks. Help was received from Giles Barkley to perform the effective draft calculations.

E.1 Upright tests

Table 54: Input data for ITTC 78 calculations

Dimensions								
		Scale Factor	10			Reynolds Number LWL	100	%
		Model Data				Full Size Data		
Environment		Water Density	1000	kg/m3		Water Density	1025	kg/m3
		Water Viscosity	0,00114	Ns/m2		Water Viscosity	0,00119	Ns/m2
Hull Dimensions		Hull Length	1,829	m		Hull Length	18,288	m
		Hull Canoe body Tc	0,031	m		Hull Canoe body Tc	0,31	m
		Hull WSA	0,573	m2		Hull WSA	57,334	m2
		Form Factor	1,21			Form Factor	1,21	
Keel Dimensions		Keel Span	0,380	m		Keel Span	3,8	m
		Keel Chord	0,050	m		Keel Chord	0,5	m
		Keel t/c Ratio	0,2			Keel t/c Ratio	0,2	
		Keel Form Factor	1,496			Keel Form Factor	1,496	
		Draft to keel bottomTk	0,45	m		Draft to keel bottomTk	4,52	m
Bulb Dimensions		Bulb Length	0,270	m		Bulb Length	2,7	m
		Bulb Profile t/c Ratio	0,15			Bulb Profile t/c Ratio	0,15	
		Bulb Plan t/c Ratio	0,15			Bulb Plan t/c Ratio	0,15	
		Bulb WSA	0,0224	m2		Bulb WSA	2,24	m2
		Bulb Form Factor	1,225			Bulb Form Factor	1,225	

Table 55: Form factor calculation using Prohaska method

Prohaska Plot Calculation											
Run No	Speed	Froude Number	Reynolds Number	ITTC 57 Cf	Overall Drag	Keel Drag	Bulb Drag	Hull Drag	Ct	Fn^4/Cf	Ct/Cf
-	m/s	-	-	-	N	N	N	N	-	-	-
1	0,64	0,15	1,02E+06	0,0047	0,85	0,14	0,04	0,66	0,0057	0,110	1,221
2	0,83	0,19	1,32E+06	0,0044	1,30	0,22	0,06	1,02	0,0052	0,326	1,179
3	1,03	0,24	1,66E+06	0,0042	2,09	0,32	0,10	1,67	0,0055	0,836	1,300
4	1,22	0,29	1,96E+06	0,0041	2,95	0,43	0,13	2,39	0,0056	1,702	1,372
5	1,41	0,33	2,27E+06	0,0040	3,76	0,55	0,17	3,05	0,0053	3,142	1,345
6	1,61	0,38	2,58E+06	0,0039	5,30	0,68	0,21	4,41	0,0060	5,376	1,546
7	1,81	0,43	2,90E+06	0,0038	6,57	0,83	0,26	5,48	0,0058	8,815	1,553
8	2,02	0,48	3,23E+06	0,0037	8,23	1,00	0,31	6,92	0,0059	13,917	1,611
9	2,23	0,53	3,57E+06	0,0036	10,00	1,18	0,37	8,45	0,0060	21,043	1,646
10	2,44	0,58	3,92E+06	0,0036	11,56	1,39	0,43	9,74	0,0057	31,131	1,602
11	2,67	0,63	4,29E+06	0,0035	13,35	1,62	0,51	11,22	0,0055	45,378	1,567
Form Factor (1+k)	1,2117										

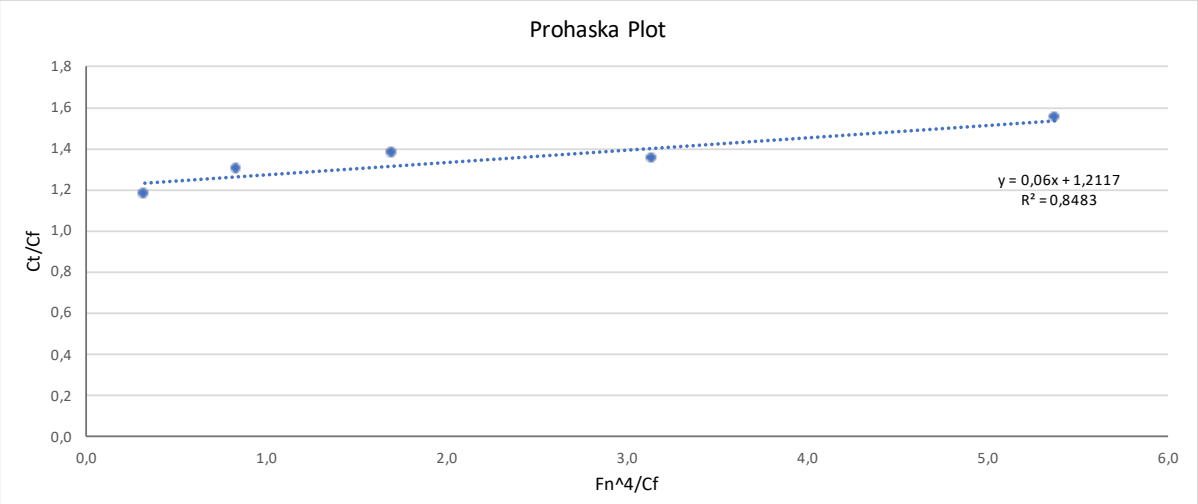

Table 56: Measured upright resistance data

RECORDED TOW TANK MODEL RESULTS FROM DYNAMOMETER									
Model Speed	Recorded Speed	Recorded Drag	Sideforce 1	Sideforce 2	Total side force	Roll moment	Heave	Pitch	Total Sideforce
kts	m/s	N	N	N	N	N.m	mm	mm	N
1,240	0,638	0,8510	0,0537	-0,0010	0,0527	-0,0070	0,2170	0,0966	0,053
1,604	0,825	1,3022	-0,0736	-0,0934	-0,1670	0,0034	-0,0440	0,1390	-0,167
2,006	1,032	2,0899	0,0545	-0,0786	-0,0241	-0,0056	-0,4879	0,2283	-0,024
2,376	1,222	2,9459	-0,0847	0,1811	0,0964	0,0050	-1,0184	0,3090	0,096
2,749	1,414	3,7598	-0,8171	0,6159	-0,2012	0,0202	-1,6534	0,3696	-0,201
3,124	1,607	5,2960	0,0856	-0,4030	-0,3174	0,0450	-3,0300	0,4911	-0,317
3,515	1,808	6,5655	-0,4107	-0,0410	-0,4517	0,0686	-3,0879	0,4307	-0,452
3,919	2,016	8,2308	-0,0900	-0,3807	-0,4708	0,0724	-2,7270	0,7894	-0,471
4,325	2,225	9,9999	-0,5652	0,3245	-0,2407	0,0704	-1,2387	1,0897	-0,241
4,749	2,443	11,5605	-0,5015	-0,1506	-0,6521	0,0561	0,2777	1,2220	-0,652
5,196	2,673	13,3471	-0,1502	-0,6101	-0,7603	0,0576	1,1343	1,4982	-0,760
5,655	2,909	15,3499	-2,5058	0,1878	-2,3180	0,1913	1,9890	1,5631	-2,318
6,129	3,153	17,7561	-1,7722	-3,1589	-4,9311	0,7570	3,4431	1,6447	-4,931
6,586	3,388	19,8816	-2,7985	-3,1177	-5,9162	0,8857	4,2889	1,4891	-5,916
7,063	3,633	23,0887	-5,1915	-2,4035	-7,5951	1,2238	5,3675	1,6621	-7,595
7,609	3,914	27,3272	-8,2308	-2,4412	-10,6720	1,7792	3,4142	1,6738	-10,672
8,188	4,212	31,3145	-8,4070	-5,6872	-14,0942	2,4532	5,3886	1,5515	-14,094
8,756	4,504	34,8350	-15,2220	-7,7293	-22,9513	4,4443	7,5638	1,9825	-22,951

Table 57: Upright resistance ITTC 78 calculations, model scale data

Model Scale Data							
Overall							
Speed	Speed	Froude Number	Hull Viscous Drag	Hull Wave Drag	Keel Viscous Drag	Bulb Viscous Drag	Total Model Drag
kts	m/s	-	N	N	N	N	N
1,24	0,638	0,151	0,6585	0,0061	0,1449	0,0414	0,851
1,60	0,825	0,195	1,0423	-0,0264	0,2217	0,0647	1,302
2,01	1,032	0,244	1,5566	0,1159	0,3219	0,0955	2,090
2,38	1,222	0,289	2,1086	0,2817	0,4274	0,1282	2,946
2,75	1,414	0,334	2,7416	0,3060	0,5466	0,1656	3,760
3,12	1,607	0,379	3,4525	0,9575	0,6787	0,2073	5,296
3,51	1,808	0,427	4,2705	1,2109	0,8290	0,2550	6,565
3,92	2,016	0,476	5,1988	1,7250	0,9979	0,3090	8,231
4,33	2,225	0,525	6,2140	2,2372	1,1810	0,3678	10,000
4,75	2,443	0,577	7,3595	2,3813	1,3858	0,4338	11,561
5,20	2,673	0,631	8,6625	2,5588	1,6171	0,5088	13,347
5,66	2,909	0,687	10,0988	2,7898	1,8702	0,5911	15,350
6,13	3,153	0,744	11,6881	3,2377	2,1484	0,6819	17,756
6,59	3,388	0,800	13,3180	3,3568	2,4320	0,7748	19,882
7,06	3,633	0,858	15,1195	4,3482	2,7438	0,8772	23,089
7,61	3,914	0,924	17,3130	5,8914	3,1212	1,0016	27,327
8,19	4,212	0,994	19,7859	6,8426	3,5444	1,1416	31,314
8,76	4,504	1,063	22,3541	7,2127	3,9816	1,2865	34,835
Hull							
Speed	Speed	Froude Number	Reynolds Number	Friction Coefficient	Friction Drag	Viscous Drag	Wave Drag
kts	m/s	-	-	-	N	N	N
1,24	0,638	0,151	1,02E+06	4,66E-03	0,5442	0,6585	0,0061
1,60	0,825	0,195	1,32E+06	4,41E-03	0,8614	1,0423	-0,0264
2,01	1,032	0,244	1,66E+06	4,21E-03	1,2865	1,5566	0,1159
2,38	1,222	0,289	1,96E+06	4,07E-03	1,7426	2,1086	0,2817
2,75	1,414	0,334	2,27E+06	3,95E-03	2,2658	2,7416	0,3060
3,12	1,607	0,379	2,58E+06	3,85E-03	2,8533	3,4525	0,9575
3,51	1,808	0,427	2,90E+06	3,77E-03	3,5293	4,2705	1,2109
3,92	2,016	0,476	3,23E+06	3,69E-03	4,2965	5,1988	1,7250
4,33	2,225	0,525	3,57E+06	3,62E-03	5,1355	6,2140	2,2372
4,75	2,443	0,577	3,92E+06	3,55E-03	6,0822	7,3595	2,3813
5,20	2,673	0,631	4,29E+06	3,50E-03	7,1591	8,6625	2,5588
5,66	2,909	0,687	4,67E+06	3,44E-03	8,3461	10,0988	2,7898
6,13	3,153	0,744	5,06E+06	3,39E-03	9,6596	11,6881	3,2377
6,59	3,388	0,800	5,44E+06	3,34E-03	11,0066	13,3180	3,3568
7,06	3,633	0,858	5,83E+06	3,30E-03	12,4955	15,1195	4,3482
7,61	3,914	0,924	6,28E+06	3,26E-03	14,3082	17,3130	5,8914
8,19	4,212	0,994	6,76E+06	3,22E-03	16,3520	19,7859	6,8426
8,76	4,504	1,063	7,23E+06	3,18E-03	18,4745	22,3541	7,2127
Keel							
Speed	Speed	Froude Number	Reynolds Number	Friction Coefficient	Friction Drag	Viscous Drag	
kts	m/s	-	-	-	N	N	
1,240	0,638	0,151	2,8E+04	1,25E-02	0,0969	0,1449	
1,604	0,825	0,195	3,6E+04	1,15E-02	0,1482	0,2217	
2,006	1,032	0,244	4,5E+04	1,06E-02	0,2152	0,3219	
2,376	1,222	0,289	5,4E+04	1,01E-02	0,2857	0,4274	
2,749	1,414	0,334	6,2E+04	9,62E-03	0,3654	0,5466	
3,124	1,607	0,379	7,0E+04	9,25E-03	0,4537	0,6787	
3,515	1,808	0,427	7,9E+04	8,92E-03	0,5542	0,8290	
3,919	2,016	0,476	8,8E+04	8,64E-03	0,6671	0,9979	
4,325	2,225	0,525	9,8E+04	8,39E-03	0,7894	1,1810	
4,749	2,443	0,577	1,1E+05	8,17E-03	0,9264	1,3858	
5,196	2,673	0,631	1,2E+05	7,96E-03	1,0809	1,6171	
5,655	2,909	0,687	1,3E+05	7,78E-03	1,2501	1,8702	
6,129	3,153	0,744	1,4E+05	7,60E-03	1,4361	2,1484	
6,586	3,388	0,800	1,5E+05	7,45E-03	1,6257	2,4320	
7,063	3,633	0,858	1,6E+05	7,31E-03	1,8341	2,7438	
7,609	3,914	0,924	1,7E+05	7,17E-03	2,0864	3,1212	
8,188	4,212	0,994	1,8E+05	7,03E-03	2,3693	3,5444	
8,756	4,504	1,063	2,0E+05	6,91E-03	2,6615	3,9816	
Bulb							
Speed	Speed	Froude Number	Reynolds Number	Friction Coefficient	Friction Drag	Viscous Drag	
kts	m/s	-	-	-	N	N	
1,240	0,638	0,151	1,5E+05	7,42E-03	0,0338	0,0414	
1,604	0,825	0,195	2,0E+05	6,93E-03	0,0528	0,0647	
2,006	1,032	0,244	2,4E+05	6,53E-03	0,0779	0,0955	
2,376	1,222	0,289	2,9E+05	6,26E-03	0,1047	0,1282	
2,749	1,414	0,334	3,3E+05	6,04E-03	0,1352	0,1656	
3,124	1,607	0,379	3,8E+05	5,85E-03	0,1692	0,2073	
3,515	1,808	0,427	4,3E+05	5,69E-03	0,2082	0,2550	
3,919	2,016	0,476	4,8E+05	5,54E-03	0,2522	0,3090	
4,325	2,225	0,525	5,3E+05	5,41E-03	0,3002	0,3678	
4,749	2,443	0,577	5,8E+05	5,30E-03	0,3542	0,4338	
5,196	2,673	0,631	6,3E+05	5,19E-03	0,4153	0,5088	
5,655	2,909	0,687	6,9E+05	5,09E-03	0,4825	0,5911	
6,129	3,153	0,744	7,5E+05	5,00E-03	0,5567	0,6819	
6,586	3,388	0,800	8,0E+05	4,92E-03	0,6325	0,7748	
7,063	3,633	0,858	8,6E+05	4,84E-03	0,7161	0,8772	
7,609	3,914	0,924	9,3E+05	4,77E-03	0,8177	1,0016	
8,188	4,212	0,994	1,0E+06	4,69E-03	0,9319	1,1416	
8,756	4,504	1,063	1,1E+06	4,62E-03	1,0502	1,2865	

Table 58: Upright resistance ITTC 78 calculations, full scale data

Full Scale Data							
Overall							
Speed	Speed	Froude Number	Hull Viscous Drag	Hull Wave Drag	Keel Viscous Drag	Bulb Viscous Drag	Total Drag
kts	m/s	-	kN	kN	kN	kN	kN
3,92	2,018	0,151	0,3585	0,0063	0,0573	0,0197	0,442
5,07	2,609	0,195	0,5759	-0,0271	0,0906	0,0314	0,671
6,34	3,263	0,244	0,8707	0,1188	0,1353	0,0472	1,172
7,51	3,864	0,289	1,1901	0,2887	0,1831	0,0642	1,726
8,69	4,471	0,334	1,5591	0,3137	0,2380	0,0838	2,194
9,88	5,082	0,379	1,9760	0,9815	0,2996	0,1059	3,363
11,11	5,717	0,427	2,4584	1,2412	0,3704	0,1313	4,201
12,39	6,375	0,476	3,0086	1,7681	0,4508	0,1603	5,388
13,68	7,036	0,525	3,6130	2,2931	0,5386	0,1921	6,637
15,02	7,725	0,577	4,2977	2,4409	0,6377	0,2280	7,604
16,43	8,453	0,631	5,0796	2,6228	0,7504	0,2689	8,722
17,88	9,199	0,687	5,9446	2,8596	0,8747	0,3141	9,993
19,38	9,971	0,744	6,9051	3,3186	1,0121	0,3643	11,600
20,83	10,714	0,8	7,8930	3,4408	1,1530	0,4157	12,902
22,33	11,489	0,858	8,9881	4,4569	1,3087	0,4727	15,226
24,06	12,377	0,924	10,3252	6,0387	1,4982	0,5422	18,404
25,89	13,320	0,994	11,8371	7,0136	1,7119	0,6206	21,183
27,69	14,243	1,063	13,4114	7,3931	1,9338	0,7022	23,440
Hull							
Speed	Speed	Froude Number	Reynolds Number	Friction Coefficient	Friction Drag	Viscous Drag	Wave Drag
kts	m/s	-	-	-	N	N	N
3,92	2,018	0,151	3,2E+07	2,48E-03	296,31	358,53	6,27
5,07	2,609	0,195	4,1E+07	2,38E-03	475,95	575,90	-27,05
6,34	3,263	0,244	5,1E+07	2,30E-03	719,61	870,73	118,81
7,51	3,864	0,289	6,1E+07	2,24E-03	983,54	1190,08	288,73
8,69	4,471	0,334	7,0E+07	2,19E-03	1288,49	1559,08	313,65
9,88	5,082	0,379	8,0E+07	2,15E-03	1633,05	1976,00	981,48
11,11	5,717	0,427	9,0E+07	2,12E-03	2031,74	2458,40	1241,21
12,39	6,375	0,476	1,0E+08	2,08E-03	2486,45	3008,61	1768,14
13,68	7,036	0,525	1,1E+08	2,05E-03	2985,94	3612,99	2293,09
15,02	7,725	0,577	1,2E+08	2,03E-03	3551,85	4297,74	2440,88
16,43	8,453	0,631	1,3E+08	2,00E-03	4198,04	5079,63	2622,77
17,88	9,199	0,687	1,4E+08	1,98E-03	4912,93	5944,64	2859,59
19,38	9,971	0,744	1,6E+08	1,95E-03	5706,67	6905,08	3318,62
20,83	10,714	0,8	1,7E+08	1,93E-03	6523,14	7893,00	3440,77
22,33	11,489	0,858	1,8E+08	1,92E-03	7428,16	8988,08	4456,90
24,06	12,377	0,924	1,9E+08	1,90E-03	8533,22	10325,19	6038,68
25,89	13,320	0,994	2,1E+08	1,88E-03	9782,69	11837,05	7013,64
27,69	14,243	1,063	2,2E+08	1,86E-03	11083,78	13411,37	7393,05
Keel							
Speed	Speed	Froude Number	Reynolds Number	Friction Coefficient	Friction Drag	Viscous Drag	
kts	m/s	-	-	-	N	N	
3,92	2,02	0,151	8,7E+05	4,83E-03	38,32	57,33	
5,07	2,61	0,195	1,1E+06	4,57E-03	60,59	90,64	
6,34	3,26	0,244	1,4E+06	4,36E-03	90,42	135,27	
7,51	3,86	0,289	1,7E+06	4,21E-03	122,41	183,12	
8,69	4,47	0,334	1,9E+06	4,09E-03	159,08	237,98	
9,88	5,08	0,379	2,2E+06	3,98E-03	200,24	299,56	
11,11	5,72	0,427	2,5E+06	3,89E-03	247,59	370,40	
12,39	6,38	0,476	2,7E+06	3,81E-03	301,31	450,77	
13,68	7,04	0,525	3,0E+06	3,73E-03	360,04	538,63	
15,02	7,73	0,577	3,3E+06	3,67E-03	426,30	637,74	
16,43	8,45	0,631	3,6E+06	3,61E-03	501,64	750,45	
17,88	9,20	0,687	4,0E+06	3,55E-03	584,67	874,66	
19,38	9,97	0,744	4,3E+06	3,49E-03	676,53	1012,09	
20,83	10,71	0,8	4,6E+06	3,45E-03	770,71	1152,98	
22,33	11,49	0,858	4,9E+06	3,40E-03	874,80	1308,70	
24,06	12,38	0,924	5,3E+06	3,36E-03	1001,50	1498,25	
25,89	13,32	0,994	5,7E+06	3,31E-03	1144,33	1711,92	
27,69	14,24	1,063	6,1E+06	3,27E-03	1292,63	1933,77	
Bulb							
Speed	Speed	Froude Number	Reynolds Number	Friction Coefficient	Friction Drag	Viscous Drag	
kts	m/s	-	-	-	N	N	
3,92	2,02	0,151	4,7E+06	3,44E-03	16,06	19,67	
5,07	2,61	0,195	6,1E+06	3,28E-03	25,62	31,38	
6,34	3,26	0,244	7,6E+06	3,15E-03	38,50	47,16	
7,51	3,86	0,289	9,0E+06	3,06E-03	52,40	64,19	
8,69	4,47	0,334	1,0E+07	2,98E-03	68,39	83,78	
9,88	5,08	0,379	1,2E+07	2,91E-03	86,41	105,86	
11,11	5,72	0,427	1,3E+07	2,86E-03	107,21	131,33	
12,39	6,38	0,476	1,5E+07	2,80E-03	130,87	160,31	
13,68	7,04	0,525	1,6E+07	2,76E-03	156,80	192,08	
15,02	7,73	0,577	1,8E+07	2,72E-03	186,12	228,00	
16,43	8,45	0,631	2,0E+07	2,68E-03	219,54	268,93	
17,88	9,20	0,687	2,1E+07	2,64E-03	256,44	314,14	
19,38	9,97	0,744	2,3E+07	2,61E-03	297,35	364,25	
20,83	10,71	0,8	2,5E+07	2,58E-03	339,37	415,72	
22,33	11,49	0,858	2,7E+07	2,55E-03	385,87	472,70	
24,06	12,38	0,924	2,9E+07	2,52E-03	442,58	542,16	
25,89	13,32	0,994	3,1E+07	2,49E-03	506,61	620,60	
27,69	14,24	1,063	3,3E+07	2,46E-03	573,19	702,16	

E.2 Heeled and yawed tests

Table 59: Measured heeled and yawed resistance data - no foil

RECORDED TOW TANK MODEL RESULTS FROM DYNAMOMETER NO FOIL													
Run No.	Heel Angle	Leeway Angle	CLOCK Number	Model Speed	Recorded Speed	Drag	Sideforce 1	Sideforce 2	Recorded roll moment	Heave	Pitch	Total Sideforce	Side Force Sqd
	deg	deg	-	m/s	m/s	N	N	N	N.m	mm	deg	N	N^2
19	0	1	197	0,813	0,820	1,2971	0,5255	0,0696	-0,2234	0,5379	0,1191	0,5950	0,3540
20	0	1	405	1,627	1,627	5,1463	1,7906	0,5007	-0,4772	-2,4104	0,1347	2,2913	5,2501
21	0	1	600	2,440	2,443	11,9443	6,3844	1,9475	-1,7497	-3,3511	0,4580	8,3320	69,4216
22	0	1	770	3,253	3,244	19,6850	17,6118	8,5949	-5,4579	-0,2955	0,7432	26,2066	686,7875
23	0	1,5	197	0,813	0,821	1,1680	0,6114	0,4870	-0,1922	0,8924	0,2598	1,0983	1,2064
24	0	1,5	405	1,627	1,627	5,0733	4,5947	2,2877	-1,5437	-2,4797	0,2121	6,8824	47,3678
25	0	1,5	600	2,440	2,443	11,4235	12,7899	5,4943	-3,9758	-2,4120	0,5281	18,2842	334,3123
26	0	1,5	770	3,253	3,240	19,7540	26,2129	11,5207	-8,1855	0,2864	0,7589	37,7336	1423,8246
29	0	2	197	0,813	0,822	1,2680	1,4780	0,5829	-0,5156	0,9701	-0,3056	2,0610	4,2475
30	0	2	405	1,627	1,628	5,1075	6,4424	2,6281	-2,0111	-2,5074	-0,2400	9,0705	82,2731
31	0	2	600	2,440	2,443	11,5178	16,1639	6,6662	-5,0259	-2,5067	0,5866	22,8301	521,2126
32	0	2	770	3,253	3,244	19,8280	29,7272	14,4804	-9,3841	0,8789	0,5613	44,2076	1954,3154
33	0	2,5	197	0,813	0,821	1,2686	1,8490	0,8014	-0,4567	1,3667	-0,3223	2,6504	7,0247
34	0	2,5	405	1,627	1,628	5,0918	7,6349	3,3034	-2,4706	-2,0846	-0,3228	10,9383	119,6473
35	0	2,5	600	2,440	2,445	11,7670	18,4186	7,6250	-5,7476	-2,1949	0,4933	26,0436	678,2686
36	0	2,5	770	3,253	3,247	20,2842	35,0755	15,1715	-10,7496	0,8796	0,4312	50,2470	2524,7620
Run No.	Heel Angle	Leeway Angle	CLOCK Number	Model Speed	Recorded Speed	Drag	Sideforce 1	Sideforce 2	Recorded roll moment	Heave	Pitch	Total Sideforce	Side Force Sqd
	deg	deg	-	m/s	m/s	N	N	N	N.m	mm	deg	N	N^2
51	5	1	197	0,813	0,820	1,1304	0,5626	0,2790	2,7648	2,8811	-1,3867	0,8416	0,7083
52	5	1	405	1,627	1,626	5,1248	2,1717	1,0957	2,0876	-0,5600	-1,3233	3,2674	10,6757
53	5	1	600	2,440	2,439	11,3265	7,6952	2,5912	0,4846	-0,9467	-0,1932	10,2864	105,8092
54	5	1	770	3,253	3,240	18,9521	22,0515	8,3835	-3,6436	3,2364	-0,0472	30,4350	926,2868
50	5	1,5	197	0,813	0,821	1,1733	0,8596	0,3007	2,6473	2,6812	-1,3804	1,1604	1,3464
49	5	1,5	405	1,627	1,626	5,1262	5,0193	2,0930	1,1330	-0,2561	-1,3740	7,1123	50,5851
48	5	1,5	600	2,440	2,439	10,9103	13,7241	5,1573	-1,5727	-0,3497	0,0619	18,8814	356,5061
47	5	1,5	770	3,253	3,240	18,8556	28,8578	11,6562	-6,2282	3,4240	0,0240	40,5140	1641,3850
43	5	2	197	0,813	0,820	1,2250	1,3447	0,5619	2,5966	2,9009	-1,2002	1,9066	3,6352
44	5	2	405	1,627	1,627	5,0649	6,8581	2,1969	0,6179	-0,6706	-1,1563	9,0550	81,9927
45	5	2	600	2,440	2,438	11,0455	16,6575	6,5242	-2,5917	0,0621	0,1818	23,1818	537,3949
46	5	2	770	3,253	3,238	18,8539	31,2501	13,4339	-7,2453	3,7477	0,0712	44,6839	1996,6527
41	5	2,5	197	0,813	0,821	1,1747	1,7291	0,8556	2,4062	2,6790	-1,2060	2,5847	6,6806
40	5	2,5	405	1,627	1,626	5,0980	8,1050	3,2532	0,1150	-0,5279	-1,0271	11,3582	129,0087
39	5	2,5	600	2,440	2,440	11,1979	19,0733	7,4032	-3,3031	0,5963	0,3604	26,4765	701,0066
38	5	2,5	770	3,253	3,243	19,2828	36,5657	16,3511	-9,1177	4,4076	0,3243	52,9168	2800,1856
Run No.	Heel Angle	Leeway Angle	CLOCK Number	Model Speed	Recorded Speed	Drag	Sideforce 1	Sideforce 2	Recorded roll moment	Heave	Pitch	Total Sideforce	Side Force Sqd
	deg	deg	-	m/s	m/s	N	N	N	N.m	mm	deg	N	N^2
58	15	1	197	0,813	0,821	1,0698	0,7898	0,0780	6,5053	12,7971	-4,3567	0,8678	0,7530
57	15	1	405	1,627	1,625	4,8887	5,0058	0,2839	4,8096	10,1744	-4,2870	5,2897	27,9811
56	15	1	600	2,440	2,439	10,6829	10,7611	0,2197	3,2728	9,1068	-3,6605	10,9808	120,5786
55	15	1	770	3,253	3,241	17,4804	22,6972	5,4203	-1,0544	13,5553	-2,8655	28,1175	790,5944
66	15	1,5	197	0,813	0,821	1,1362	0,8403	0,1500	6,5239	12,9801	-4,3874	0,9902	0,9806
65	15	1,5	405	1,627	1,626	4,8052	4,0853	0,6228	4,8951	9,7151	-4,2231	4,7081	22,1657
64	15	1,5	600	2,440	2,436	10,2824	12,3307	2,4170	1,9079	9,6329	-3,7788	14,7476	217,4923
63	15	1,5	770	3,253	3,242	17,7044	27,1186	8,2596	-3,5323	15,0391	-2,9500	35,3782	1251,6170
68	15	2	197	0,813	0,820	1,2249	0,8200	0,2559	6,4280	11,0648	-1,3257	1,0759	1,1575
69	15	2	405	1,627	1,626	4,5317	5,0027	1,6334	4,3225	8,3473	-1,6801	6,6361	44,0374
70	15	2	600	2,440	2,445	10,1977	15,7145	3,8874	0,6341	9,2501	0,0216	19,6019	384,2333
71	15	2	770	3,253	3,246	17,3955	29,1925	9,7458	-4,5851	14,5747	0,5914	38,9383	1516,1912
75	15	2,5	197	0,813	0,861	1,8289	2,0385	0,8077	5,7269	12,2638	-1,6259	2,8462	8,1007
74	15	2,5	405	1,627	1,626	4,6278	7,3918	2,0369	3,3161	9,4048	-1,3634	9,4287	88,8998
73	15	2,5	600	2,440	2,441	10,4848	19,0887	4,7397	-0,7346	10,7504	-0,2929	23,8284	567,7903
72	15	2,5	770	3,253	3,247	17,5006	32,3188	11,3220	-6,2052	15,3409	0,5000	43,6408	1904,5203
Run No.	Heel Angle	Leeway Angle	CLOCK Number	Model Speed	Recorded Speed	Drag	Sideforce 1	Sideforce 2	Recorded roll moment	Heave	Pitch	Total Sideforce	Side Force Sqd
	deg	deg	-	m/s	m/s	N	N	N	N.m	mm	deg	N	N^2
93	25	1	197	0,813	0,820	1,2797	0,2554	-0,1759	8,3345	27,4657	-1,7178	0,0796	0,0063
94	25	1	405	1,627	1,625	4,6520	1,9497	-1,2936	7,6727	24,1274	-1,5486	0,6561	0,4305
95	25	1	600	2,440	2,441	10,4755	7,8684	-3,5868	6,7791	22,3403	-0,9078	4,2816	18,3320
96	25	1	770	3,253	3,247	17,8560	19,0508	-2,9491	3,5891	24,1600	-0,9542	16,1017	259,2654
92	25	1,5	197	0,813	0,820	1,2762	0,4580	-0,1488	8,2565	27,5569	-1,5976	0,3092	0,0956
91	25	1,5	405	1,627	1,625	4,6606	2,8223	-1,2978	7,3075	23,9721	-1,5124	1,5245	2,3240
90	25	1,5	600	2,440	2,442	10,3292	9,5431	-3,2861	5,8926	22,5517	-0,9348	6,2570	39,1499
89	25	1,5	770	3,253	3,243	18,0363	22,8027	-1,6664	1,9547	25,0823	-0,5164	21,1363	446,7432
84	25	2	197	0,813	0,820	1,2125	0,7235	-0,1609	8,1141	27,9548	-0,9033	0,5626	0,3165
86	25	2	405	1,627	1,624	4,7083	3,6731	-1,4072	7,1358	24,4115	-1,5165	2,2659	5,1341
87	25	2	600	2,440	2,442	10,7606	12,5663	-2,7333	4,6791	23,7526	-1,0367	9,8330	96,6873
88	25	2	770	3,253	3,247	17,2980	26,5411	0,8586	-0,7455	27,1968	-0,2109	27,3997	750,7447
76	25	2,5	197	0,813	0,820	1,2764	0,6194	0,1486	7,9768	27,6336	-1,8212	0,7680	0,5898
77	25	2,5	405	1,627	1,625	4,9120	6,5532	-0,1361	5,5729	24,8615	-1,6791	6,4172	41,1803
78	25	2,5	600	2,440	2,442	10,3197	19,7115	0,5342	0,8709	26,2413	-0,5768	20,2457	409,8876
79	25	2,5	770	3,253	3,244	18,4703	35,7441	4,0981	-5,1151	30,9929	-0,1045	39,8422	1587,4017

Table 60: Measured heeled and yawed resistance data - with foil

RECORDED TOW TANK MODEL RESULTS FROM DYNAMOMETER WITH FOIL													
Run No.	Heel Angle deg	Leeway Angle deg	CLOCK Number -	Model Speed m/s	Recorded Speed m/s	Drag N	Sideforce 1 N	Sideforce 2 N	Recorded roll moment N.m	Heave mm	Pitch deg	Total Sideforce N	Side Force Sqd N^2
1	10	1	405	1,627	1,626	5,2414	4,2588	0,7836	3,7829	2,8188	0,1384	5,0423	25,4251
2	10	1	600	2,440	2,438	11,0633	9,8901	4,5299	3,2366	4,7534	0,6985	14,4200	207,9367
3	10	1	770	3,253	3,222	18,9558	22,0289	11,7445	-0,8561	9,1222	1,5510	33,7734	1140,6439
22	10	1,5	405	1,627	1,627	5,2824	4,7259	1,6741	3,1464	3,1714	0,8845	6,4000	40,9597
23	10	1,5	600	2,440	2,437	11,4098	13,3252	6,0943	1,8463	5,5581	1,4662	19,4195	377,1178
24	10	1,5	770	3,253	3,219	19,3643	26,1076	12,0402	-2,5064	9,4742	2,2210	38,1478	1455,2569
106	10	2	405	1,627	1,627	5,2507	6,6806	1,6645	2,3561	2,0291	1,8168	8,3451	69,6404
105	10	2	600	2,440	2,438	11,4645	16,0746	7,1434	0,7311	3,9486	2,4323	23,2180	539,0769
104	10	2	770	3,253	3,223	19,4131	27,8461	14,9153	-3,1112	8,8843	2,6548	42,7614	1828,5373
121	10	2,5	405	1,627	1,627	5,2894	8,1019	2,6340	1,7482	2,7847	0,8017	10,7359	115,2593
120	10	2,5	600	2,440	2,440	11,4469	18,2197	8,3269	-0,0167	6,1747	1,8686	26,5466	704,7209
119	10	2,5	770	3,253	3,229	19,2429	31,7108	16,8545	-4,8717	11,6771	2,1927	48,5653	2358,5845
Run No.	Heel Angle deg	Leeway Angle deg	CLOCK Number -	Model Speed m/s	Recorded Speed m/s	Drag N	Sideforce 1 N	Sideforce 2 N	Recorded roll moment N.m	Heave mm	Pitch deg	Total Sideforce N	Side Force Sqd N^2
6	15	1	405	1,627	1,626	5,2647	2,8750	0,3236	5,3393	9,1586	-0,1715	3,1985	10,2305
7	15	1	600	2,440	2,442	11,4388	9,1858	2,6898	5,4706	11,3368	0,2743	11,8755	141,0277
8	15	1	770	3,253	3,225	16,5485	18,4388	9,6380	3,7858	20,4312	0,5098	28,0768	788,3056
29	15	1,5	405	1,627	1,627	5,1736	4,2145	0,4732	4,4847	9,1782	0,1814	4,6877	21,9742
28	15	1,5	600	2,440	2,435	11,0251	11,6659	4,0018	4,0135	11,5782	0,7109	15,6676	245,4746
27	15	1,5	770	3,253	3,223	16,2093	20,5750	11,5710	2,1312	21,1794	0,9770	32,1460	1033,3627
111	15	2	405	1,627	1,626	5,3653	5,5824	1,0454	3,7110	8,2697	0,6986	6,6278	43,9277
110	15	2	600	2,440	2,441	11,2281	14,7996	5,9145	2,4738	11,5200	1,4222	20,7141	429,0752
109	15	2	770	3,253	3,186	14,8810	23,5176	12,1405	0,6589	20,8970	2,1225	35,6581	1271,5029
126	15	2,5	405	1,627	1,626	5,2742	7,6842	2,0597	2,7646	8,6587	-0,5309	9,7438	94,9424
125	15	2,5	600	2,440	2,442	11,5209	17,5684	6,4871	1,4747	12,5446	1,2055	24,0555	578,6676
124	15	2,5	770	3,253	3,227	16,5164	27,0761	14,4168	-1,1526	22,7931	1,4161	41,4929	1721,6616
Run No.	Heel Angle deg	Leeway Angle deg	CLOCK Number -	Model Speed m/s	Recorded Speed m/s	Drag N	Sideforce 1 N	Sideforce 2 N	Recorded roll moment N.m	Heave mm	Pitch deg	Total Sideforce N	Side Force Sqd N^2
35	25	1	405	1,627	1,626	4,9545	1,9637	-1,1586	6,9035	23,7981	-1,3151	0,8051	0,6481
33	25	1	600	2,440	2,437	11,4643	8,6192	-2,7261	6,1674	21,4506	-0,8193	5,8932	34,7297
32	25	1	770	3,253	3,224	17,9559	11,4186	-0,9615	7,3870	26,6293	0,1194	10,4571	109,3505
19	25	1,5	405	1,627	1,627	5,3199	4,7380	-0,9186	6,0536	24,0081	-1,6109	3,8193	14,5872
17	25	1,5	600	2,440	2,438	11,9676	13,5630	-2,0941	4,2428	23,0729	-0,6859	11,4690	131,5368
18	25	1,5	770	3,253	3,217	18,5664	21,6985	1,5415	2,4352	28,5017	-1,0130	23,2400	540,0953
116	25	2	405	1,627	1,626	5,3313	4,4886	-0,6394	5,5838	22,7658	-0,6152	3,8493	14,8170
115	25	2	600	2,440	2,441	11,7026	14,8085	-0,9126	2,9416	22,3114	-0,2355	13,8959	193,0963
114	25	2	770	3,253	3,227	18,6640	23,7451	3,2631	0,8824	28,1893	0,4741	27,0081	729,4396
132	25	2,5	405	1,627	1,627	5,3160	6,4374	-0,2890	4,6233	22,9515	-1,2793	6,1484	37,8026
131	25	2,5	600	2,440	2,438	11,9549	19,1940	0,8854	0,7763	23,3986	-0,6057	20,0794	403,1827
130	25	2,5	770	3,253	3,219	19,3257	29,8580	4,2843	-1,8273	29,0561	0,5610	34,1423	1165,6966

Table 61: T_e calculations from heeled resistance, model scale data

Model Scale Data													
0 degrees Heel													
Run No	Froude No	Speed	Leeway	Viscous Drag	Wave+Heel+Induced Drag	Total Drag	SF	SF^2	L/D Ratio	Rupright + Rheel	Slope Rt/Fh^2	Te	Te/Tk
-	-	m/s	deg	N	N	N	N	N^2	-	N	-	m	-
19	0,19	1,594	1,0	1,31	-0,05	1,26	0,60	0,354	0,47	1,23	5,79E-03	0,286	0,633
20	0,19	3,163	1,5	1,32	-0,12	1,20	1,10	1,206	0,92	1,23	5,79E-03	0,286	0,632
21	0,19	4,749	2,0	1,32	-0,05	1,27	2,06	4,248	1,63	1,23	5,79E-03	0,285	0,632
22	0,19	6,306	2,5	1,32	-0,05	1,27	2,65	7,025	2,09	1,23	5,79E-03	0,286	0,632
23	0,38	1,596	1,0	4,44	0,61	5,05	2,29	5,250	0,45	5,05	4,56E-04	0,513	1,137
24	0,38	3,163	1,5	4,44	0,64	5,07	6,88	47,368	1,36	5,05	4,56E-04	0,513	1,137
25	0,38	4,749	2,0	4,44	0,67	5,11	9,07	82,273	1,78	5,05	4,56E-04	0,513	1,136
26	0,38	6,299	2,5	4,44	0,65	5,09	10,94	119,647	2,15	5,05	4,56E-04	0,513	1,136
29	0,58	1,598	1,0	9,18	2,36	11,54	8,33	69,422	0,72	11,43	3,24E-04	0,405	0,898
30	0,58	3,165	1,5	9,18	2,24	11,42	18,28	334,312	1,60	11,43	3,24E-04	0,405	0,898
31	0,58	4,749	2,0	9,18	2,34	11,52	22,83	521,213	1,98	11,43	3,24E-04	0,405	0,898
32	0,58	6,306	2,5	9,19	2,57	11,77	26,04	678,269	2,21	11,43	3,24E-04	0,405	0,897
33	0,77	1,596	1,0	15,28	4,40	19,69	26,21	686,787	1,33	19,39	3,02E-04	0,317	0,701
34	0,76	3,165	1,5	15,25	4,51	19,75	37,73	1423,825	1,91	19,39	3,02E-04	0,317	0,702
35	0,77	4,753	2,0	15,28	4,55	19,83	44,21	1954,315	2,23	19,39	3,02E-04	0,317	0,701
36	0,77	6,312	2,5	15,31	4,98	20,28	50,25	2524,762	2,48	19,39	3,02E-04	0,316	0,701
5 degrees heel													
Run No	Froude No	Speed	Leeway	Viscous Drag	Wave+Heel+Induced Drag	Total Drag	SF	SF^2	L/D Ratio	Rupright + Rheel	Slope Rt/Fh^2	Te	Te/Tk
-	-	m/s	deg	N	N	N	N	N^2	-	N	-	m	-
24	0,19	1,596	1,0	1,32	-0,19	1,13	0,84	0,708	0,74	1,16	6,19E-03	0,276	0,612
25	0,19	3,161	1,5	1,32	-0,14	1,17	1,16	1,346	0,99	1,16	6,19E-03	0,276	0,612
26	0,19	4,741	2,0	1,32	-0,09	1,22	1,91	3,635	1,56	1,16	6,19E-03	0,276	0,612
27	0,19	6,299	2,5	1,32	-0,14	1,17	2,58	6,681	2,20	1,16	6,19E-03	0,276	0,612
40	0,38	1,596	1,0	4,43	0,69	5,12	3,27	10,676	0,64	5,10	4,80E-04	0,501	1,109
41	0,38	3,161	1,5	4,43	0,70	5,13	7,11	50,585	1,39	5,10	4,80E-04	0,501	1,109
42	0,38	4,741	2,0	4,44	0,63	5,06	9,05	81,993	1,79	5,10	4,80E-04	0,501	1,109
43	0,38	6,299	2,5	4,43	0,77	5,20	11,36	129,009	2,19	5,10	4,80E-04	0,501	1,109
56	0,58	1,596	1,0	9,15	1,85	11,00	10,29	105,809	0,94	10,90	3,37E-04	0,398	0,883
57	0,58	3,163	1,5	9,15	1,76	10,91	18,88	356,506	1,73	10,90	3,37E-04	0,398	0,883
58	0,58	4,740	2,0	9,15	1,90	11,05	23,18	537,395	2,10	10,90	3,37E-04	0,399	0,883
59	0,58	6,295	2,5	9,16	2,04	11,20	26,48	701,007	2,36	10,90	3,37E-04	0,398	0,882
72	0,76	1,596	1,0	15,25	3,70	18,95	30,43	926,287	1,61	18,66	1,76E-04	0,415	0,918
73	0,76	3,161	1,5	15,25	3,61	18,86	40,51	1641,385	2,15	18,66	1,76E-04	0,415	0,918
74	0,76	4,743	2,0	15,23	3,62	18,85	44,68	1996,653	2,37	18,66	1,76E-04	0,415	0,919
75	0,77	6,304	2,5	15,27	4,01	19,28	52,92	2800,186	2,74	18,66	1,76E-04	0,414	0,918
15 degrees heel													
Run No	Froude No	Speed	Leeway	Viscous Drag	Wave+Heel+Induced Drag	Total Drag	SF	SF^2	L/D Ratio	Rupright + Rheel	Slope Rt/Fh^2	Te	Te/Tk
-	-	m/s	deg	N	N	N	N	N^2	-	N	-	m	-
28	0,19	1,596	1,0	1,32	-0,25	1,07	0,87	0,753	0,81	1,10	1,31E-02	0,190	0,421
29	0,19	3,159	1,5	1,32	-0,18	1,14	0,99	0,981	0,87	1,10	1,31E-02	0,190	0,421
30	0,19	4,741	2,0	1,31	-0,19	1,12	1,08	1,157	0,96	1,10	1,31E-02	0,190	0,422
31	0,20	6,301	2,5	1,43	-0,23	1,20	2,85	8,100	2,37	1,10	1,31E-02	0,181	0,402
44	0,38	1,596	1,0	4,43	0,46	4,89	5,29	27,981	1,08	4,75	4,42E-03	0,165	0,366
45	0,38	3,161	1,5	4,43	0,37	4,81	4,71	22,166	0,98	4,75	4,42E-03	0,165	0,365
46	0,38	4,736	2,0	4,43	0,56	4,99	6,64	44,037	1,33	4,75	4,42E-03	0,165	0,365
47	0,38	6,302	2,5	4,43	0,70	5,13	9,43	88,900	1,84	4,75	4,42E-03	0,165	0,365
60	0,58	1,594	1,0	9,15	1,13	10,28	10,98	120,579	1,07	10,19	3,83E-04	0,374	0,828
61	0,58	3,161	1,5	9,13	1,15	10,28	14,75	217,492	1,43	10,19	3,83E-04	0,374	0,829
62	0,58	4,753	2,0	9,19	1,01	10,20	19,60	384,233	1,92	10,19	3,83E-04	0,373	0,826
63	0,58	6,310	2,5	9,17	1,32	10,48	23,83	567,790	2,27	10,19	3,83E-04	0,374	0,828
76	0,77	1,674	1,0	15,26	2,22	17,48	28,12	790,594	1,61	17,30	1,80E-04	0,410	0,909
77	0,77	3,161	1,5	15,26	2,24	17,50	35,38	1251,617	2,02	17,30	1,80E-04	0,410	0,908
78	0,77	4,745	2,0	15,30	2,20	17,50	38,94	1516,191	2,23	17,30	1,80E-04	0,410	0,907
79	0,77	6,312	2,5	15,31	2,39	17,70	43,64	1904,520	2,47	17,30	1,80E-04	0,410	0,907
25 degrees heel													
Run No	Froude No	Speed	Leeway	Viscous Drag	Wave+Heel+Induced Drag	Total Drag	SF	SF^2	L/D Ratio	Rupright + Rheel	Slope Rt/Fh^2	Te	Te/Tk
-	-	m/s	deg	N	N	N	N	N^2	-	N	-	m	-
32	0,19	1,594	1,0	1,31	-0,03	1,28	0,08	0,006	0,06	1,28	1,99E-02	0,190	0,422
33	0,19	3,159	1,5	1,31	-0,04	1,28	0,31	0,096	0,24	1,28	1,99E-02	0,190	0,422
34	0,19	4,745	2,0	1,31	-0,03	1,28	0,56	0,316	0,44	1,28	1,99E-02	0,190	0,422
35	0,19	6,312	2,5	1,31	-0,02	1,29	0,77	0,590	0,60	1,28	1,99E-02	0,190	0,422
48	0,38	1,594	1,0	4,43	0,23	4,65	0,66	0,431	0,14	4,66	6,25E-03	0,165	0,366
49	0,38	3,159	1,5	4,43	0,24	4,66	1,52	2,324	0,33	4,66	6,25E-03	0,165	0,366
50	0,38	4,747	2,0	4,42	0,29	4,71	2,27	5,134	0,48	4,66	6,25E-03	0,165	0,366
51	0,38	6,304	2,5	4,43	0,49	4,91	6,42	41,180	1,31	4,66	6,25E-03	0,165	0,366
64	0,58	1,594	1,0	9,17	1,31	10,48	4,28	18,332	0,41	10,49	3,59E-04	0,374	0,828
65	0,58	3,157	1,5	9,17	1,16	10,33	6,26	39,150	0,61	10,49	3,59E-04	0,374	0,827
66	0,58	4,747	2,0	9,17	1,59	10,76	9,83	96,687	0,91	10,49	3,59E-04	0,374	0,827
67	0,58	6,312	2,5	9,17	1,43	10,60	20,25	409,888	1,91	10,49	3,59E-04	0,374	0,827
80	0,77	1,594	1,0	15,31	2,55	17,86	16,10	259,265	0,90	17,84	4,32E-04	0,410	0,907
81	0,77	3,159	1,5	15,27	2,76	18,04	21,14	446,743	1,17	17,84	4,32E-04	0,410	0,908
82	0,77	4,747	2,0	15,31	2,99	18,30	27,40	750,745	1,50	17,84	4,32E-04	0,410	0,907
83	0,77	6,306	2,5	15,28	3,19	18,47	39,84	1587,402	2,16	17,84	4,32E-04	0,410	0,908

Table 62: T_e calculations from heeled resistance, full scale data

Full Scale Data														
0 degrees Heel														
Run No	Froude No	Speed	Leeway	Viscous Drag	Wave+Heel+Induced Drag	Total Drag	SF	SF^2	L/D Ratio	Rupright + Rheel	Rheel	Slope Rt/Fh^2	Te	Te/Tk
-	-	m/s	deg	kN	kN	kN	kN	kN^2	-	kN	kN	-	m	-
19	0,19	2,593	1,0	0,69	-0,06	0,63	0,61	0,372	0,96	0,60	-0,07	5,47E-03	2,905	0,644
20	0,19	2,596	1,5	0,69	-0,12	0,57	1,13	1,267	1,97	0,60	-0,07	5,47E-03	2,902	0,643
21	0,19	2,599	2,0	0,69	-0,05	0,64	2,11	4,463	3,30	0,60	-0,07	5,47E-03	2,898	0,642
22	0,19	2,596	2,5	0,69	-0,05	0,64	2,72	7,380	4,23	0,60	-0,07	5,47E-03	2,902	0,643
23	0,38	5,145	1,0	2,44	0,63	3,06	2,35	5,516	0,77	3,07	-0,43	4,23E-04	5,266	1,166
24	0,38	5,145	1,5	2,44	0,65	3,09	7,05	49,766	2,28	3,07	-0,43	4,23E-04	5,266	1,166
25	0,38	5,148	2,0	2,44	0,68	3,12	9,30	86,438	2,98	3,07	-0,43	4,23E-04	5,263	1,166
26	0,38	5,148	2,5	2,44	0,67	3,11	11,21	125,704	3,61	3,07	-0,43	4,23E-04	5,263	1,166
29	0,58	7,725	1,0	5,16	2,42	7,59	8,54	72,936	1,13	7,48	-0,12	3,09E-04	4,105	0,909
30	0,58	7,725	1,5	5,16	2,30	7,46	18,74	351,237	2,51	7,48	-0,12	3,09E-04	4,105	0,909
31	0,58	7,725	2,0	5,16	2,40	7,56	23,40	547,599	3,10	7,48	-0,12	3,09E-04	4,105	0,909
32	0,58	7,732	2,5	5,17	2,64	7,81	26,69	712,606	3,42	7,48	-0,12	3,09E-04	4,101	0,908
33	0,77	10,258	1,0	8,73	4,51	13,24	26,86	721,556	2,03	12,95	0,85	2,88E-04	3,203	0,709
34	0,76	10,246	1,5	8,71	4,62	13,33	38,68	1495,906	2,90	12,95	0,85	2,88E-04	3,207	0,710
35	0,77	10,258	2,0	8,73	4,66	13,39	45,31	2053,253	3,38	12,95	0,85	2,88E-04	3,203	0,709
36	0,77	10,268	2,5	8,74	5,10	13,85	51,50	2652,578	3,72	12,95	0,85	2,88E-04	3,200	0,709
5 degrees heel														
Run No	Froude No	Speed	Leeway	Viscous Drag	Wave+Heel+Induced Drag	Total Drag	Side Force	Side Force^2	Lift / Drag Ratio	Rupright + Rheel	Rheel	Slope Rt/Fh^2	Te	Te/Tk
-	-	m/s	deg	kN	kN	kN	kN	kN^2	-	kN	kN	-	m	-
24	0,19	2,596	1,0	0,69	-0,19	0,50	0,86	0,744	1,72	0,53	-0,14	6,04E-03	2,763	0,612
25	0,19	2,596	1,5	0,69	-0,15	0,54	1,19	1,415	2,19	0,53	-0,14	6,04E-03	2,763	0,612
26	0,19	2,596	2,0	0,69	-0,09	0,60	1,95	3,819	3,27	0,53	-0,14	6,04E-03	2,763	0,612
27	0,19	2,596	2,5	0,69	-0,15	0,55	2,65	7,019	4,86	0,53	-0,14	6,04E-03	2,763	0,612
40	0,38	5,142	1,0	2,43	0,71	3,15	3,35	11,216	1,06	3,12	-0,38	4,64E-04	5,030	1,114
41	0,38	5,142	1,5	2,43	0,71	3,15	7,29	53,146	2,32	3,12	-0,38	4,64E-04	5,030	1,114
42	0,38	5,145	2,0	2,44	0,65	3,08	9,28	86,144	3,01	3,12	-0,38	4,64E-04	5,027	1,113
43	0,38	5,142	2,5	2,43	0,79	3,22	11,64	135,540	3,62	3,12	-0,38	4,64E-04	5,030	1,114
56	0,58	7,713	1,0	5,15	1,89	7,04	10,54	111,166	1,50	6,94	-0,66	3,26E-04	3,999	0,886
57	0,58	7,713	1,5	5,15	1,80	6,95	19,35	374,554	2,78	6,94	-0,66	3,26E-04	3,999	0,886
58	0,58	7,710	2,0	5,14	1,95	7,09	23,76	564,601	3,35	6,94	-0,66	3,26E-04	4,001	0,886
59	0,58	7,716	2,5	5,15	2,09	7,24	27,14	736,495	3,75	6,94	-0,66	3,26E-04	3,998	0,885
72	0,76	10,246	1,0	8,71	3,80	12,51	31,20	973,180	2,49	12,22	0,12	1,67E-04	4,208	0,932
73	0,76	10,246	1,5	8,71	3,70	12,41	41,53	1724,480	3,35	12,22	0,12	1,67E-04	4,208	0,932
74	0,76	10,239	2,0	8,70	3,71	12,41	45,80	2097,733	3,69	12,22	0,12	1,67E-04	4,210	0,933
75	0,77	10,255	2,5	8,72	4,11	12,83	54,24	2941,945	4,23	12,22	0,12	1,67E-04	4,204	0,931
15 degrees heel														
Run No	Froude No	Speed	Leeway	Viscous Drag	Wave+Heel+Induced Drag	Total Drag	Side Force	Side Force^2	Lift / Drag Ratio	Rupright + Rheel	Rheel	Slope Rt/Fh^2	Te	Te/Tk
-	-	m/s	deg	kN	kN	kN	kN	kN^2	-	kN	kN	-	m	-
28	0,19	2,596	1,0	0,69	-0,25	0,44	0,89	0,791	2,03	0,47	-0,20	5,34E-03	2,936	0,650
29	0,19	2,596	1,5	0,69	-0,19	0,51	1,01	1,030	2,01	0,47	-0,20	5,34E-03	2,936	0,650
30	0,19	2,593	2,0	0,69	-0,20	0,49	1,10	1,216	2,25	0,47	-0,20	5,34E-03	2,940	0,651
31	0,20	2,723	2,5	0,75	-0,24	0,52	2,92	8,510	5,65	0,47	-0,20	5,34E-03	2,800	0,620
44	0,38	5,139	1,0	2,43	0,47	2,91	5,42	29,398	1,87	2,76	-0,74	4,30E-03	1,654	0,366
45	0,38	5,142	1,5	2,43	0,38	2,82	4,83	23,288	1,71	2,76	-0,74	4,30E-03	1,653	0,366
46	0,38	5,142	2,0	2,43	0,58	3,01	6,80	46,267	2,26	2,76	-0,74	4,30E-03	1,653	0,366
47	0,38	5,142	2,5	2,43	0,71	3,15	9,66	93,400	3,07	2,76	-0,74	4,30E-03	1,653	0,366
60	0,58	7,713	1,0	5,15	1,16	6,31	11,26	126,683	1,78	6,22	-1,38	3,44E-04	3,894	0,863
61	0,58	7,703	1,5	5,14	1,18	6,32	15,12	228,503	2,39	6,22	-1,38	3,44E-04	3,899	0,864
62	0,58	7,732	2,0	5,17	1,03	6,20	20,09	403,685	3,24	6,22	-1,38	3,44E-04	3,885	0,860
63	0,58	7,719	2,5	5,16	1,35	6,51	24,42	596,535	3,75	6,22	-1,38	3,44E-04	3,891	0,862
76	0,77	10,249	1,0	8,71	2,28	10,99	28,82	830,618	2,62	10,83	-1,27	1,55E-04	4,369	0,968
77	0,77	10,252	1,5	8,72	2,30	11,02	36,26	1314,980	3,29	10,83	-1,27	1,55E-04	4,368	0,967
78	0,77	10,265	2,0	8,74	2,25	10,99	39,91	1592,948	3,63	10,83	-1,27	1,55E-04	4,363	0,966
79	0,77	10,268	2,5	8,74	2,45	11,20	44,73	2000,937	3,99	10,83	-1,27	1,55E-04	4,361	0,966
25 degrees heel														
Run No	Froude No	Speed	Leeway	Viscous Drag	Wave+Heel+Induced Drag	Total Drag	Side Force	Side Force^2	Lift / Drag Ratio	Rupright + Rheel	Rheel	Slope Rt/Fh^2	Te	Te/Tk
-	-	m/s	deg	kN	kN	kN	kN	kN^2	-	kN	kN	-	m	-
32	0,19	2,593	1,0	0,69	-0,04	0,65	0,08	0,007	0,12	0,65	-0,02	1,94E-02	1,542	0,342
33	0,19	2,593	1,5	0,69	-0,04	0,65	0,32	0,100	0,49	0,65	-0,02	1,94E-02	1,542	0,342
34	0,19	2,593	2,0	0,69	-0,04	0,65	0,58	0,332	0,88	0,65	-0,02	1,94E-02	1,542	0,342
35	0,19	2,593	2,5	0,69	-0,03	0,67	0,79	0,620	1,18	0,65	-0,02	1,94E-02	1,542	0,342
48	0,38	5,139	1,0	2,43	0,23	2,66	0,67	0,452	0,25	2,67	-0,83	6,08E-03	1,391	0,308
49	0,38	5,139	1,5	2,43	0,24	2,67	1,56	2,442	0,58	2,67	-0,83	6,08E-03	1,391	0,308
50	0,38	5,136	2,0	2,43	0,29	2,72	2,32	5,394	0,85	2,67	-0,83	6,08E-03	1,392	0,308
51	0,38	5,139	2,5	2,43	0,50	2,93	6,58	43,265	2,25	2,67	-0,83	6,08E-03	1,391	0,308
64	0,58	7,719	1,0	5,16	1,34	6,50	4,39	19,260	0,68	6,51	-1,09	3,46E-04	3,879	0,859
65	0,58	7,722	1,5	5,16	1,19	6,35	6,41	41,132	1,01	6,51	-1,09	3,46E-04	3,878	0,859
66	0,58	7,722	2,0	5,16	1,63	6,79	10,08	101,582	1,48	6,51	-1,09	3,46E-04	3,878	0,859
67	0,58	7,722	2,5	5,16	1,46	6,62	20,75	430,638	3,13	6,51	-1,09	3,46E-04	3,878	0,859
80	0,77	10,268	1,0	8,74	2,61	11,36	16,50	272,391	1,45	11,34	-0,76	4,26E-04	2,631	0,583
81	0,77	10,255	1,5	8,72	2,83	11,56	21,66	469,360	1,87	11,34	-0,76	4,26E-04	2,634	0,583
82	0,77	10,268	2,0	8,74	3,07	11,81	28,08	788,751	2,38	11,34	-0,76	4,26E-04	2,631	0,583
83	0,77	10,258	2,5	8,73	3,27	12,00	40,84	1667,764	3,40	11,34	-0,76	4,26E-04	2,633	0,583

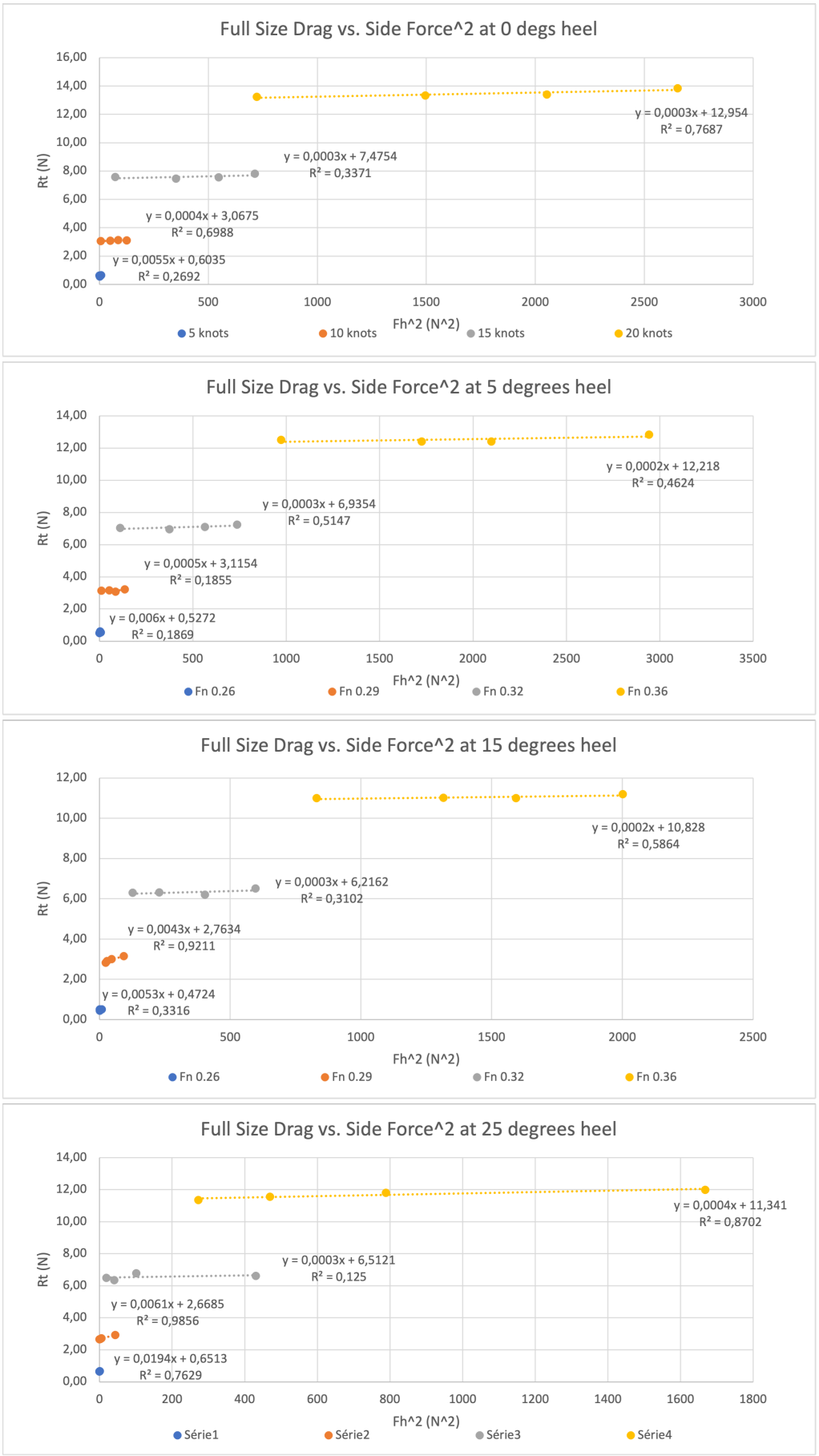

Figure 63: Full size graphs to determine T_e from experimental data - no foil

Table 63: ITTC 78 calculations for heeled resistance, 10 and 15 degrees of heel

10 deg Heel											
Full Scale Resistance Calcs											
Froude Number	Speed	Hull Rn	Hull Cf	Hull Rv	Keel Rn	Keel Cf	Keel Rv	Bulb Rn	Bulb Cf	Bulb Rv	Total Rv
-	m/s	-	-	N	-	-	N	-	-	N	N
0,194	2,60	4,09E+07	2,38E-03	570,76	1,12E+06	4,58E-03	89,86	6,04E+06	3,28E-03	31,10	691,72
0,194	2,60	4,09E+07	2,38E-03	570,76	1,12E+06	4,58E-03	89,86	6,04E+06	3,28E-03	31,10	691,72
0,194	2,60	4,09E+07	2,38E-03	570,76	1,12E+06	4,58E-03	89,86	6,04E+06	3,28E-03	31,10	691,72
0,194	2,60	4,09E+07	2,38E-03	570,76	1,12E+06	4,58E-03	89,86	6,04E+06	3,28E-03	31,10	691,72
0,384	5,14	8,10E+07	2,15E-03	2019,50	2,21E+06	3,97E-03	305,97	1,20E+07	2,91E-03	108,16	2433,63
0,384	5,14	8,10E+07	2,15E-03	2019,50	2,21E+06	3,97E-03	305,97	1,20E+07	2,91E-03	108,16	2433,63
0,384	5,15	8,10E+07	2,15E-03	2021,81	2,22E+06	3,97E-03	306,31	1,20E+07	2,91E-03	108,28	2436,39
0,384	5,14	8,10E+07	2,15E-03	2019,50	2,21E+06	3,97E-03	305,97	1,20E+07	2,91E-03	108,16	2433,63
0,576	7,71	1,21E+08	2,03E-03	4284,68	3,32E+06	3,67E-03	635,85	1,79E+07	2,72E-03	227,31	5147,85
0,576	7,71	1,21E+08	2,03E-03	4284,68	3,32E+06	3,67E-03	635,85	1,79E+07	2,72E-03	227,31	5147,85
0,576	7,71	1,21E+08	2,03E-03	4281,42	3,32E+06	3,67E-03	635,38	1,79E+07	2,72E-03	227,14	5143,94
0,576	7,72	1,22E+08	2,03E-03	4287,95	3,32E+06	3,67E-03	636,32	1,79E+07	2,72E-03	227,48	5151,75
0,765	10,25	1,61E+08	1,95E-03	7263,65	4,41E+06	3,48E-03	1063,28	2,38E+07	2,59E-03	382,94	8709,87
0,765	10,25	1,61E+08	1,95E-03	7263,65	4,41E+06	3,48E-03	1063,28	2,38E+07	2,59E-03	382,94	8709,87
0,764	10,24	1,61E+08	1,95E-03	7255,31	4,41E+06	3,48E-03	1062,09	2,38E+07	2,59E-03	382,51	8699,91
0,766	10,26	1,62E+08	1,95E-03	7276,17	4,42E+06	3,48E-03	1065,06	2,38E+07	2,59E-03	383,60	8724,83
Model Scale Resistance Calcs											
Froude Number	Speed	Hull Rn	Hull Cf	Hull Rv	Keel Rn	Keel Cf	Keel Rv	Bulb Rn	Bulb Cf	Bulb Rv	Total Rv
-	m/s	-	-	N	-	-	N	-	-	N	N
0,194	0,821	1,32E+06	4,42E-03	1,03	3,60E+04	1,15E-02	0,22	1,94E+05	6,93E-03	0,06	1,32
0,194	0,821	1,32E+06	4,42E-03	1,03	3,60E+04	1,15E-02	0,22	1,94E+05	6,93E-03	0,06	1,32
0,194	0,821	1,32E+06	4,42E-03	1,03	3,60E+04	1,15E-02	0,22	1,94E+05	6,93E-03	0,06	1,32
0,194	0,821	1,32E+06	4,42E-03	1,03	3,60E+04	1,15E-02	0,22	1,94E+05	6,93E-03	0,06	1,32
0,384	1,626	2,61E+06	3,85E-03	3,53	7,13E+04	9,21E-03	0,69	3,85E+05	5,83E-03	0,21	4,43
0,384	1,626	2,61E+06	3,85E-03	3,53	7,13E+04	9,21E-03	0,69	3,85E+05	5,83E-03	0,21	4,43
0,384	1,627	2,61E+06	3,84E-03	3,53	7,14E+04	9,21E-03	0,69	3,85E+05	5,83E-03	0,21	4,44
0,384	1,626	2,61E+06	3,85E-03	3,53	7,13E+04	9,21E-03	0,69	3,85E+05	5,83E-03	0,21	4,43
0,576	2,439	3,91E+06	3,56E-03	7,34	1,07E+05	8,17E-03	1,38	5,78E+05	5,30E-03	0,43	9,15
0,576	2,439	3,91E+06	3,56E-03	7,34	1,07E+05	8,17E-03	1,38	5,78E+05	5,30E-03	0,43	9,15
0,576	2,438	3,91E+06	3,56E-03	7,33	1,07E+05	8,17E-03	1,38	5,77E+05	5,30E-03	0,43	9,15
0,576	2,440	3,91E+06	3,56E-03	7,34	1,07E+05	8,17E-03	1,38	5,78E+05	5,30E-03	0,43	9,16
0,765	3,240	5,20E+06	3,37E-03	12,28	1,42E+05	7,55E-03	2,25	7,67E+05	4,97E-03	0,72	15,25
0,765	3,240	5,20E+06	3,37E-03	12,28	1,42E+05	7,55E-03	2,25	7,67E+05	4,97E-03	0,72	15,25
0,764	3,238	5,19E+06	3,37E-03	12,27	1,42E+05	7,55E-03	2,25	7,67E+05	4,97E-03	0,71	15,23
0,766	3,243	5,20E+06	3,37E-03	12,30	1,42E+05	7,54E-03	2,26	7,68E+05	4,97E-03	0,72	15,27

15 deg Heel											
Full Scale Resistance Calcs											
Froude Number	Speed	Hull Rn	Hull Cf	Hull Rv	Keel Rn	Keel Cf	Keel Rv	Bulb Rn	Bulb Cf	Bulb Rv	Total Rv
-	m/s	-	-	N	-	-	N	-	-	N	N
0,194	2,60	4,09E+07	2,38E-03	570,76	1,12E+06	4,58E-03	89,86	6,04E+06	3,28E-03	31,10	691,72
0,194	2,60	4,09E+07	2,38E-03	570,76	1,12E+06	4,58E-03	89,86	6,04E+06	3,28E-03	31,10	691,72
0,194	2,59	4,08E+07	2,38E-03	569,48	1,12E+06	4,58E-03	89,67	6,03E+06	3,28E-03	31,03	690,18
0,203	2,72	4,29E+07	2,36E-03	623,13	1,17E+06	4,53E-03	97,83	6,33E+06	3,25E-03	33,91	754,88
0,384	5,14	8,09E+07	2,15E-03	2017,20	2,21E+06	3,97E-03	305,63	1,20E+07	2,91E-03	108,03	2430,87
0,384	5,14	8,10E+07	2,15E-03	2019,50	2,21E+06	3,97E-03	305,97	1,20E+07	2,91E-03	108,16	2433,63
0,384	5,14	8,10E+07	2,15E-03	2019,50	2,21E+06	3,97E-03	305,97	1,20E+07	2,91E-03	108,16	2433,63
0,384	5,14	8,10E+07	2,15E-03	2019,50	2,21E+06	3,97E-03	305,97	1,20E+07	2,91E-03	108,16	2433,63
0,576	7,71	1,21E+08	2,03E-03	4284,68	3,32E+06	3,67E-03	635,85	1,79E+07	2,72E-03	227,31	5147,85
0,575	7,70	1,21E+08	2,03E-03	4274,90	3,32E+06	3,67E-03	634,44	1,79E+07	2,72E-03	226,80	5136,14
0,577	7,73	1,22E+08	2,03E-03	4304,28	3,33E+06	3,67E-03	638,68	1,80E+07	2,72E-03	228,34	5171,30
0,576	7,72	1,22E+08	2,03E-03	4291,21	3,32E+06	3,67E-03	636,79	1,80E+07	2,72E-03	227,65	5155,66
0,765	10,25	1,61E+08	1,95E-03	7267,82	4,41E+06	3,48E-03	1063,87	2,38E+07	2,59E-03	383,16	8714,86
0,765	10,25	1,61E+08	1,95E-03	7271,99	4,42E+06	3,48E-03	1064,47	2,38E+07	2,59E-03	383,38	8719,84
0,766	10,26	1,62E+08	1,95E-03	7288,69	4,42E+06	3,48E-03	1066,85	2,39E+07	2,59E-03	384,25	8739,79
0,767	10,27	1,62E+08	1,95E-03	7292,87	4,42E+06	3,48E-03	1067,45	2,39E+07	2,59E-03	384,47	8744,78
Model Scale Resistance Calcs											
Froude Number	Speed	Hull Rn	Hull Cf	Hull Rv	Keel Rn	Keel Cf	Keel Rv	Bulb Rn	Bulb Cf	Bulb Rv	Total Rv
-	m/s	-	-	N	-	-	N	-	-	N	N
0,194	0,821	1,32E+06	4,42E-03	1,03	3,60E+04	1,15E-02	0,22	1,94E+05	6,93E-03	0,06	1,32
0,194	0,821	1,32E+06	4,42E-03	1,03	3,60E+04	1,15E-02	0,22	1,94E+05	6,93E-03	0,06	1,32
0,194	0,820	1,32E+06	4,42E-03	1,03	3,60E+04	1,15E-02	0,22	1,94E+05	6,94E-03	0,06	1,31
0,203	0,861	1,38E+06	4,38E-03	1,13	3,78E+04	1,13E-02	0,24	2,04E+05	6,85E-03	0,07	1,43
0,384	1,625	2,61E+06	3,85E-03	3,52	7,13E+04	9,21E-03	0,69	3,85E+05	5,83E-03	0,21	4,43
0,384	1,626	2,61E+06	3,85E-03	3,53	7,13E+04	9,21E-03	0,69	3,85E+05	5,83E-03	0,21	4,43
0,384	1,626	2,61E+06	3,85E-03	3,53	7,13E+04	9,21E-03	0,69	3,85E+05	5,83E-03	0,21	4,43
0,384	1,626	2,61E+06	3,85E-03	3,53	7,13E+04	9,21E-03	0,69	3,85E+05	5,83E-03	0,21	4,43
0,576	2,439	3,91E+06	3,56E-03	7,34	1,07E+05	8,17E-03	1,38	5,78E+05	5,30E-03	0,43	9,15
0,575	2,436	3,91E+06	3,56E-03	7,32	1,07E+05	8,18E-03	1,38	5,77E+05	5,30E-03	0,43	9,13
0,577	2,445	3,92E+06	3,55E-03	7,37	1,07E+05	8,17E-03	1,39	5,79E+05	5,30E-03	0,43	9,19
0,576	2,441	3,92E+06	3,56E-03	7,35	1,07E+05	8,17E-03	1,38	5,78E+05	5,30E-03	0,43	9,17
0,765	3,241	5,20E+06	3,37E-03	12,29	1,42E+05	7,55E-03	2,25	7,68E+05	4,97E-03	0,72	15,26
0,765	3,242	5,20E+06	3,37E-03	12,29	1,42E+05	7,54E-03	2,25	7,68E+05	4,97E-03	0,72	15,26
0,766	3,246	5,21E+06	3,37E-03	12,32	1,42E+05	7,54E-03	2,26	7,69E+05	4,97E-03	0,72	15,30
0,767	3,247	5,21E+06	3,37E-03	12,33	1,42E+05	7,54E-03	2,26	7,69E+05	4,97E-03	0,72	15,31

Table 64: ITTC 78 calculations for heeled resistance, 25 degrees of heel

25 deg Heel												
Full Size Resistance Calcs												
Run No	Froude Number	Speed	Hull Rn	Hull Cf	Hull Rv	Keel Rn	Keel Cf	Keel Rv	Bulb Rn	Bulb Cf	Bulb Rv	Total Rv
-	-	m/s	-	-	N	-	-	N	-	-	N	N
32	0,194	2,59	4,08E+07	2,38E-03	569,48	1,12E+06	4,58E-03	89,67	6,03E+06	3,28E-03	31,03	690,18
33	0,194	2,59	4,08E+07	2,38E-03	569,48	1,12E+06	4,58E-03	89,67	6,03E+06	3,28E-03	31,03	690,18
34	0,194	2,59	4,08E+07	2,38E-03	569,48	1,12E+06	4,58E-03	89,67	6,03E+06	3,28E-03	31,03	690,18
35	0,194	2,59	4,08E+07	2,38E-03	569,48	1,12E+06	4,58E-03	89,67	6,03E+06	3,28E-03	31,03	690,18
48	0,384	5,14	8,09E+07	2,15E-03	2017,20	2,21E+06	3,97E-03	305,63	1,20E+07	2,91E-03	108,03	2430,87
49	0,384	5,14	8,09E+07	2,15E-03	2017,20	2,21E+06	3,97E-03	305,63	1,20E+07	2,91E-03	108,03	2430,87
50	0,383	5,14	8,09E+07	2,15E-03	2014,90	2,21E+06	3,97E-03	305,29	1,19E+07	2,91E-03	107,91	2428,11
51	0,384	5,14	8,09E+07	2,15E-03	2017,20	2,21E+06	3,97E-03	305,63	1,20E+07	2,91E-03	108,03	2430,87
64	0,576	7,72	1,22E+08	2,03E-03	4291,21	3,32E+06	3,67E-03	636,79	1,80E+07	2,72E-03	227,65	5155,66
65	0,577	7,72	1,22E+08	2,03E-03	4294,48	3,33E+06	3,67E-03	637,27	1,80E+07	2,72E-03	227,83	5159,57
66	0,577	7,72	1,22E+08	2,03E-03	4294,48	3,33E+06	3,67E-03	637,27	1,80E+07	2,72E-03	227,83	5159,57
67	0,577	7,72	1,22E+08	2,03E-03	4294,48	3,33E+06	3,67E-03	637,27	1,80E+07	2,72E-03	227,83	5159,57
80	0,767	10,27	1,62E+08	1,95E-03	7292,87	4,42E+06	3,48E-03	1067,45	2,39E+07	2,59E-03	384,47	8744,78
81	0,766	10,26	1,62E+08	1,95E-03	7276,17	4,42E+06	3,48E-03	1065,06	2,38E+07	2,59E-03	383,60	8724,83
82	0,767	10,27	1,62E+08	1,95E-03	7292,87	4,42E+06	3,48E-03	1067,45	2,39E+07	2,59E-03	384,47	8744,78
83	0,766	10,26	1,62E+08	1,95E-03	7280,34	4,42E+06	3,48E-03	1065,66	2,39E+07	2,59E-03	383,81	8729,81
Model Resistance Calcs												
Run No.	Froude Number	Speed	Hull Rn	Hull Cf	Hull Rv	Keel Rn	Keel Cf	Keel Rv	Bulb Rn	Bulb Cf	Bulb Rv	Total Rv
-	-	m/s	-	-	N	-	-	N	-	-	N	N
32	0,194	0,82	1,32E+06	4,42E-03	1,03	3,60E+04	1,15E-02	0,22	1,94E+05	6,94E-03	0,06	1,31
33	0,194	0,82	1,32E+06	4,42E-03	1,03	3,60E+04	1,15E-02	0,22	1,94E+05	6,94E-03	0,06	1,31
34	0,194	0,82	1,32E+06	4,42E-03	1,03	3,60E+04	1,15E-02	0,22	1,94E+05	6,94E-03	0,06	1,31
35	0,194	0,82	1,32E+06	4,42E-03	1,03	3,60E+04	1,15E-02	0,22	1,94E+05	6,94E-03	0,06	1,31
48	0,384	1,63	2,61E+06	3,85E-03	3,52	7,13E+04	9,21E-03	0,69	3,85E+05	5,83E-03	0,21	4,43
49	0,384	1,63	2,61E+06	3,85E-03	3,52	7,13E+04	9,21E-03	0,69	3,85E+05	5,83E-03	0,21	4,43
50	0,383	1,62	2,61E+06	3,85E-03	3,52	7,12E+04	9,22E-03	0,69	3,85E+05	5,84E-03	0,21	4,42
51	0,384	1,63	2,61E+06	3,85E-03	3,52	7,13E+04	9,21E-03	0,69	3,85E+05	5,83E-03	0,21	4,43
64	0,576	2,44	3,92E+06	3,56E-03	7,35	1,07E+05	8,17E-03	1,38	5,78E+05	5,30E-03	0,43	9,17
65	0,577	2,44	3,92E+06	3,56E-03	7,35	1,07E+05	8,17E-03	1,38	5,78E+05	5,30E-03	0,43	9,17
66	0,577	2,44	3,92E+06	3,56E-03	7,35	1,07E+05	8,17E-03	1,38	5,78E+05	5,30E-03	0,43	9,17
67	0,577	2,44	3,92E+06	3,56E-03	7,35	1,07E+05	8,17E-03	1,38	5,78E+05	5,30E-03	0,43	9,17
80	0,767	3,25	5,21E+06	3,37E-03	12,33	1,42E+05	7,54E-03	2,26	7,69E+05	4,97E-03	0,72	15,31
81	0,766	3,24	5,20E+06	3,37E-03	12,30	1,42E+05	7,54E-03	2,26	7,68E+05	4,97E-03	0,72	15,27
82	0,767	3,25	5,21E+06	3,37E-03	12,33	1,42E+05	7,54E-03	2,26	7,69E+05	4,97E-03	0,72	15,31
83	0,766	3,24	5,20E+06	3,37E-03	12,31	1,42E+05	7,54E-03	2,26	7,68E+05	4,97E-03	0,72	15,28

E.3 Comparison of foil predictions and experimental results

E.3.1 Righting (or roll) moment due to the foil

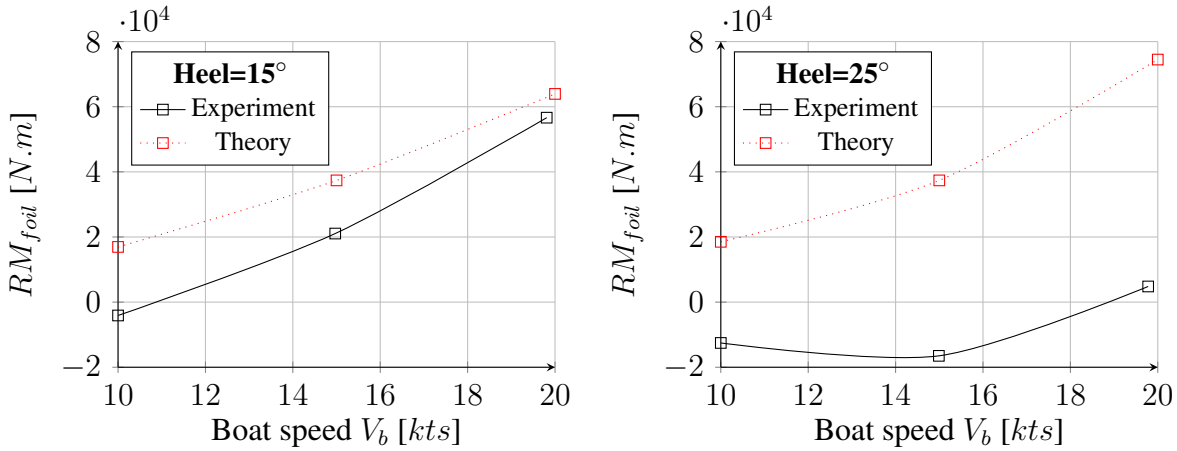

Figure 64: Comparison of experimental and theoretical foil RM, leeway=1.5°

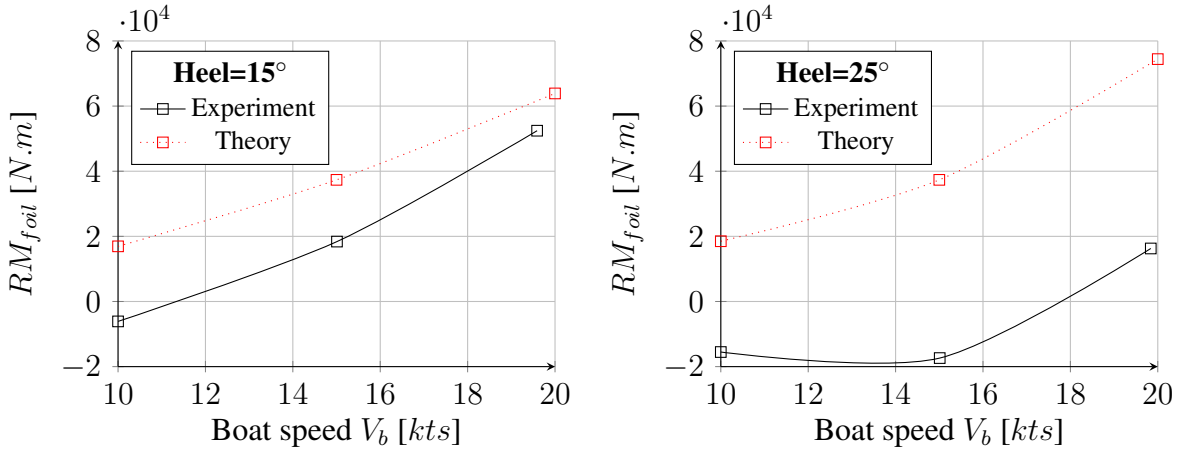

Figure 65: Comparison of experimental and theoretical foil RM, leeway=2°

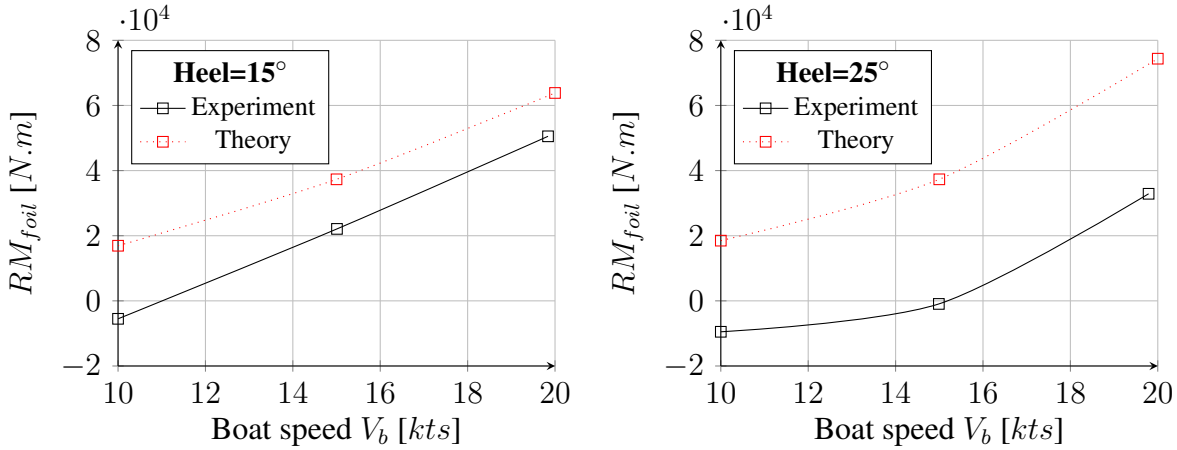

Figure 66: Comparison of experimental and theoretical foil RM, leeway=2.5°

E.3.2 Revised righting lever of the boat with foils

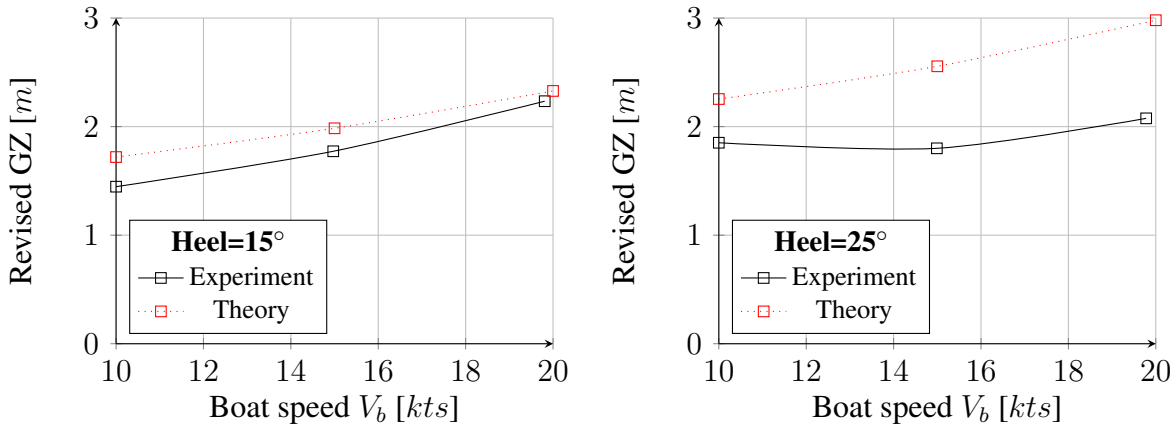

Figure 67: Comparison of experimental and theoretical revised GZ, leeway=1.5°

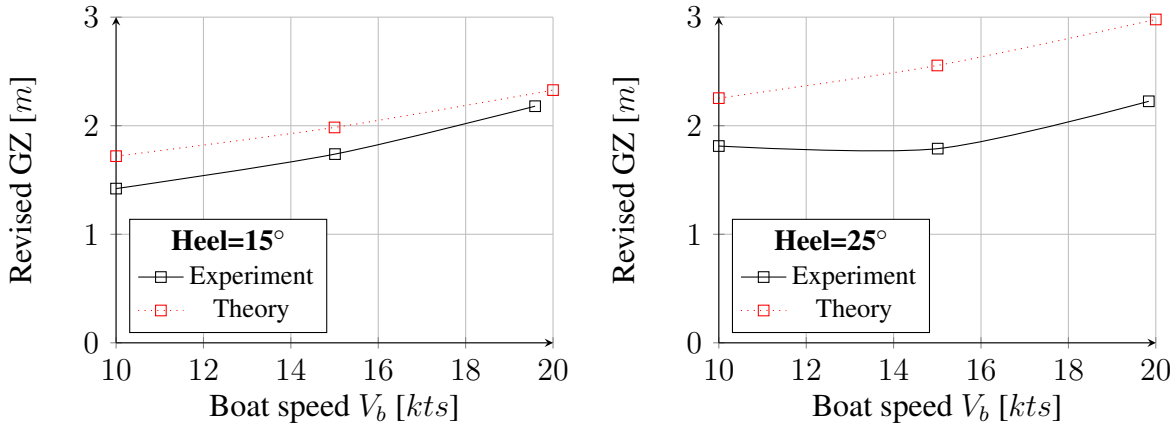

Figure 68: Comparison of experimental and theoretical revised GZ, leeway=2°

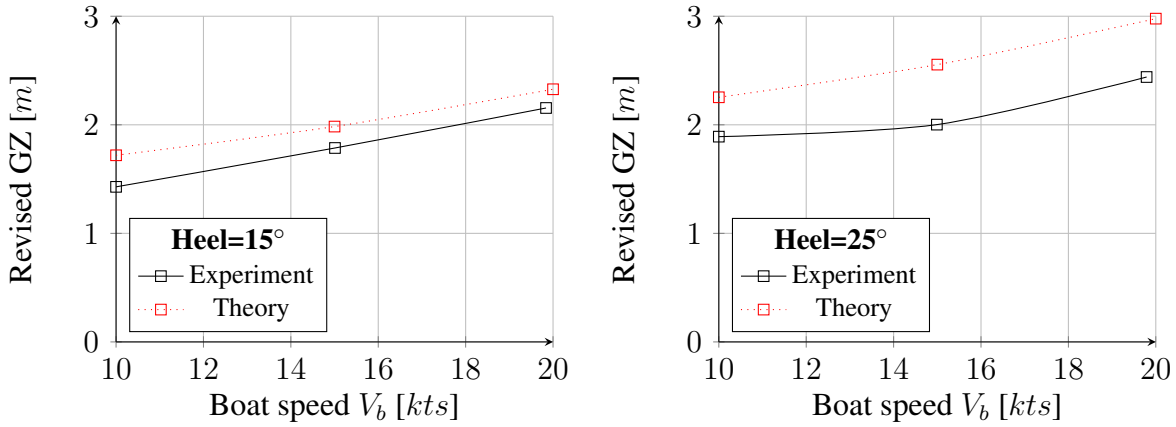

Figure 69: Comparison of experimental and theoretical revised GZ, leeway=2.5°

E.3.3 Heave due to foil

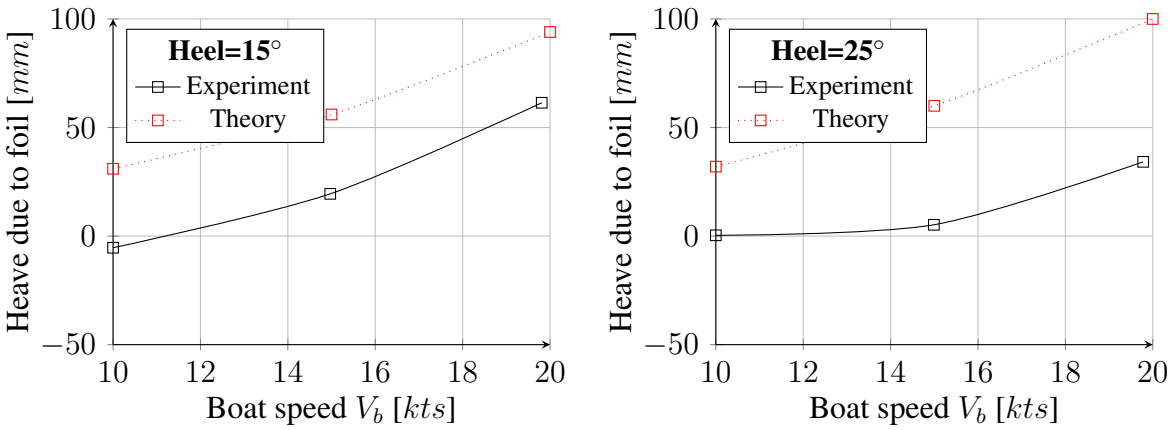

Figure 70: Comparison of experimental and theoretical heave due to foil, leeway=1.5°

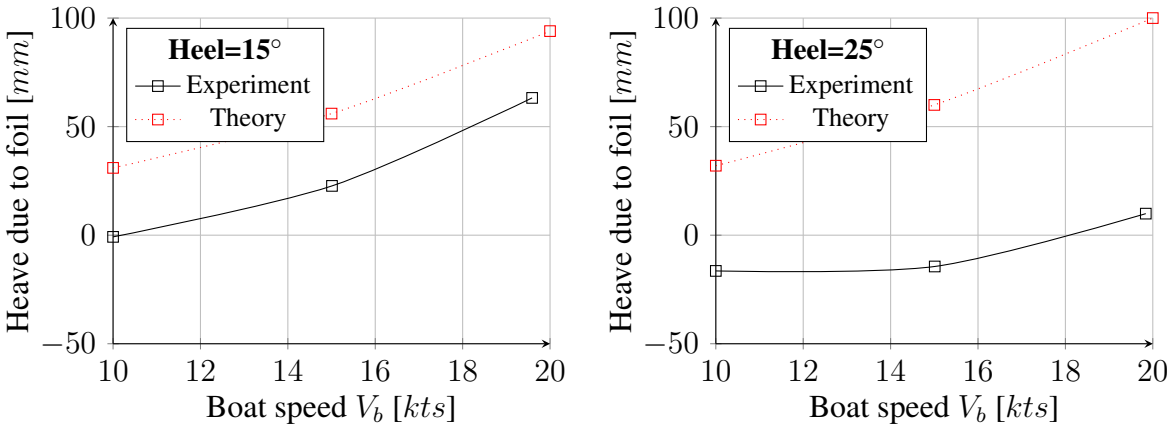

Figure 71: Comparison of experimental and theoretical heave due to foil, leeway=2°

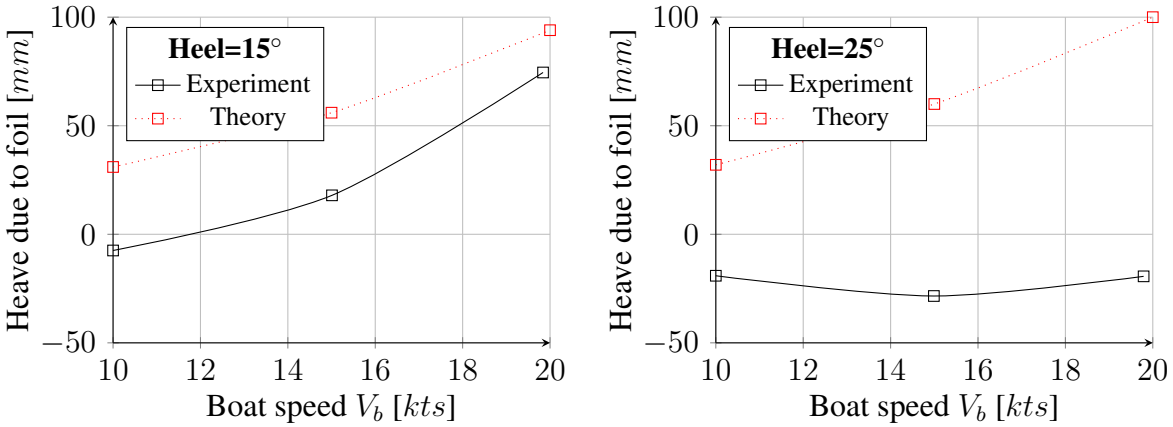

Figure 72: Comparison of experimental and theoretical heave due to foil, leeway=2.5°

E.3.4 Drag due to foil

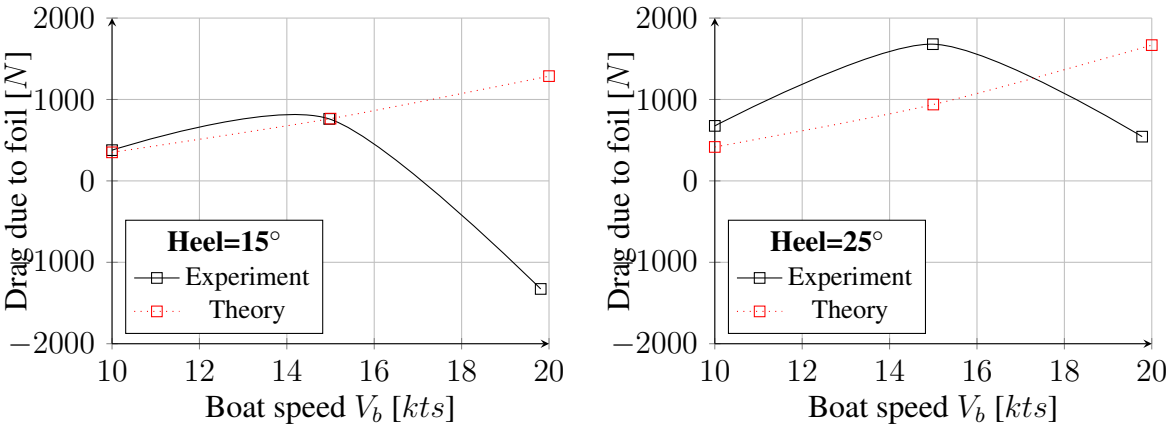

Figure 73: Comparison of experimental and theoretical drag due to foil, leeway=1.5°

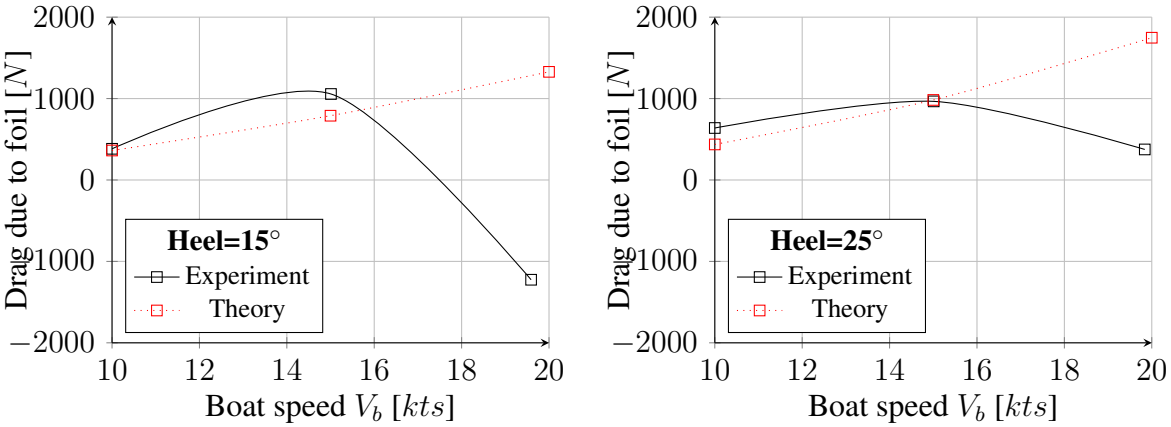

Figure 74: Comparison of experimental and theoretical drag due to foil, leeway=2°

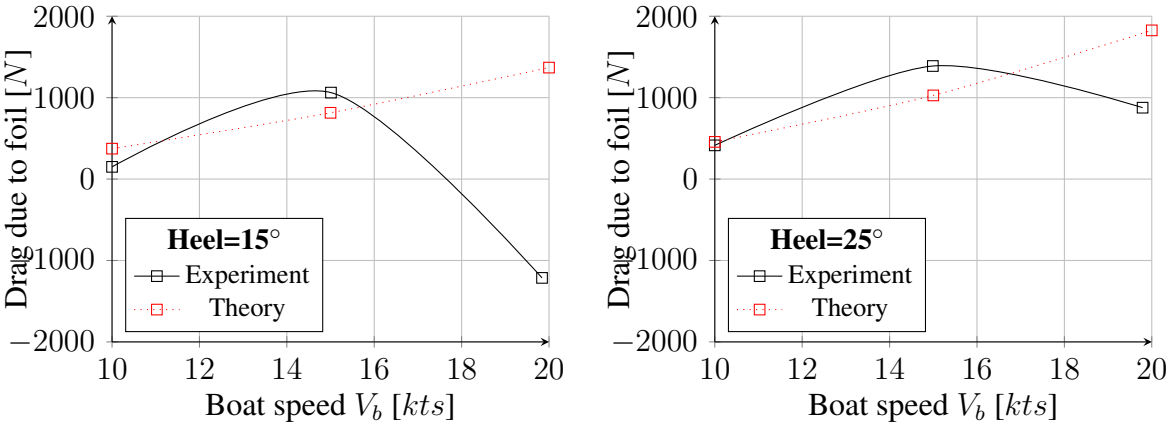

Figure 75: Comparison of experimental and theoretical drag due to foil, leeway=2.5°

E.3.5 Side force due to foil

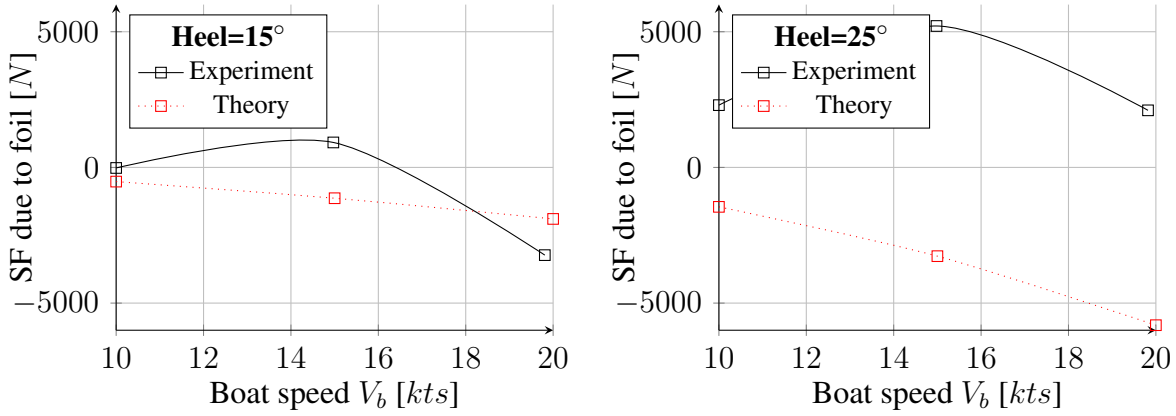

Figure 76: Comparison of experimental and theoretical SF due to foil, leeway=1.5°

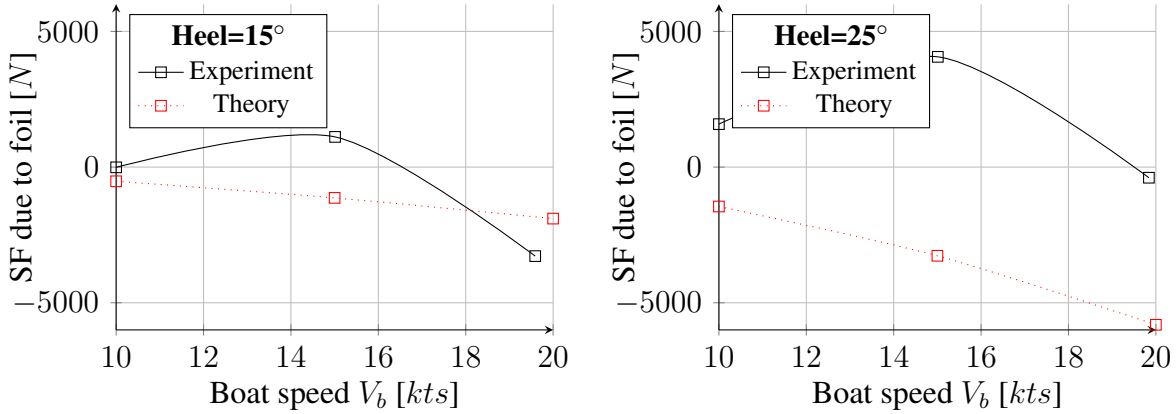

Figure 77: Comparison of experimental and theoretical SF due to foil, leeway=2°

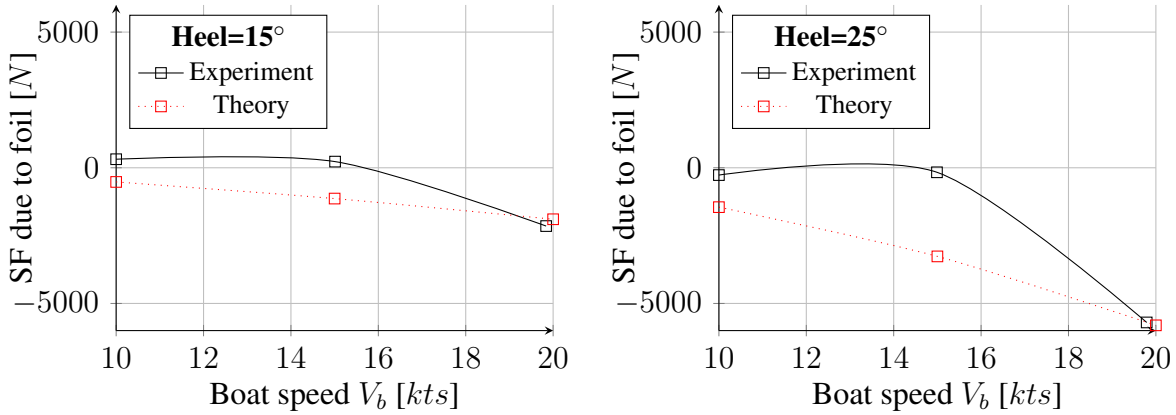

Figure 78: Comparison of experimental and theoretical SF due to foil, leeway=2.5°

E.3.6 Angle of attack of the foil to the horizontal waterplane

Figure 79 shows the experimental angle of attack of the foil relative to the horizontal waterplane. It was found by adding the pitch measured during the tests with foil, to the original 2 degrees of AOA to the horizontal waterplane when the boat is at rest.

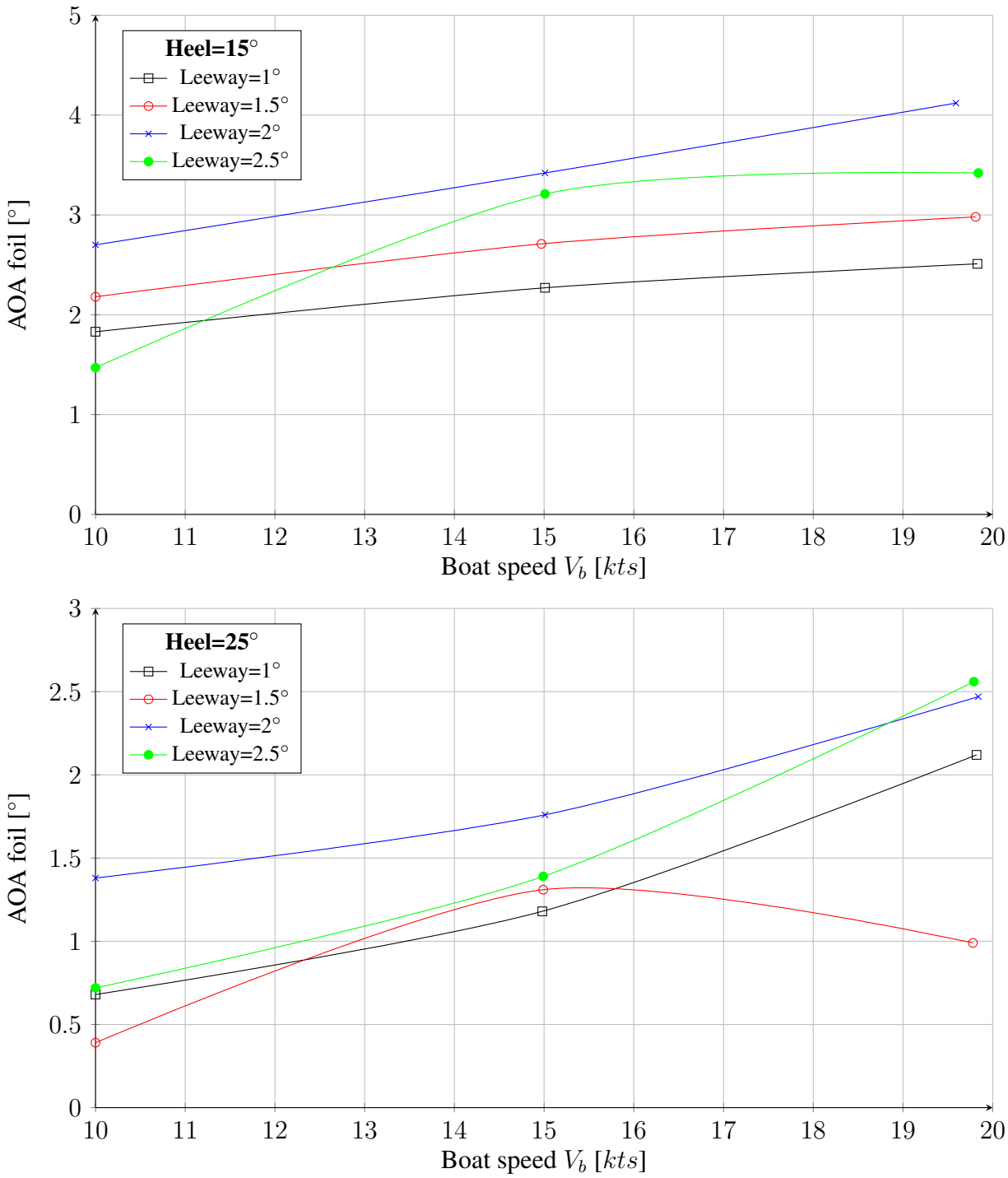

Figure 79: Variation of the foil's experimental AOA to the horizontal waterplane

F Appendix - Pictures of the tank tests

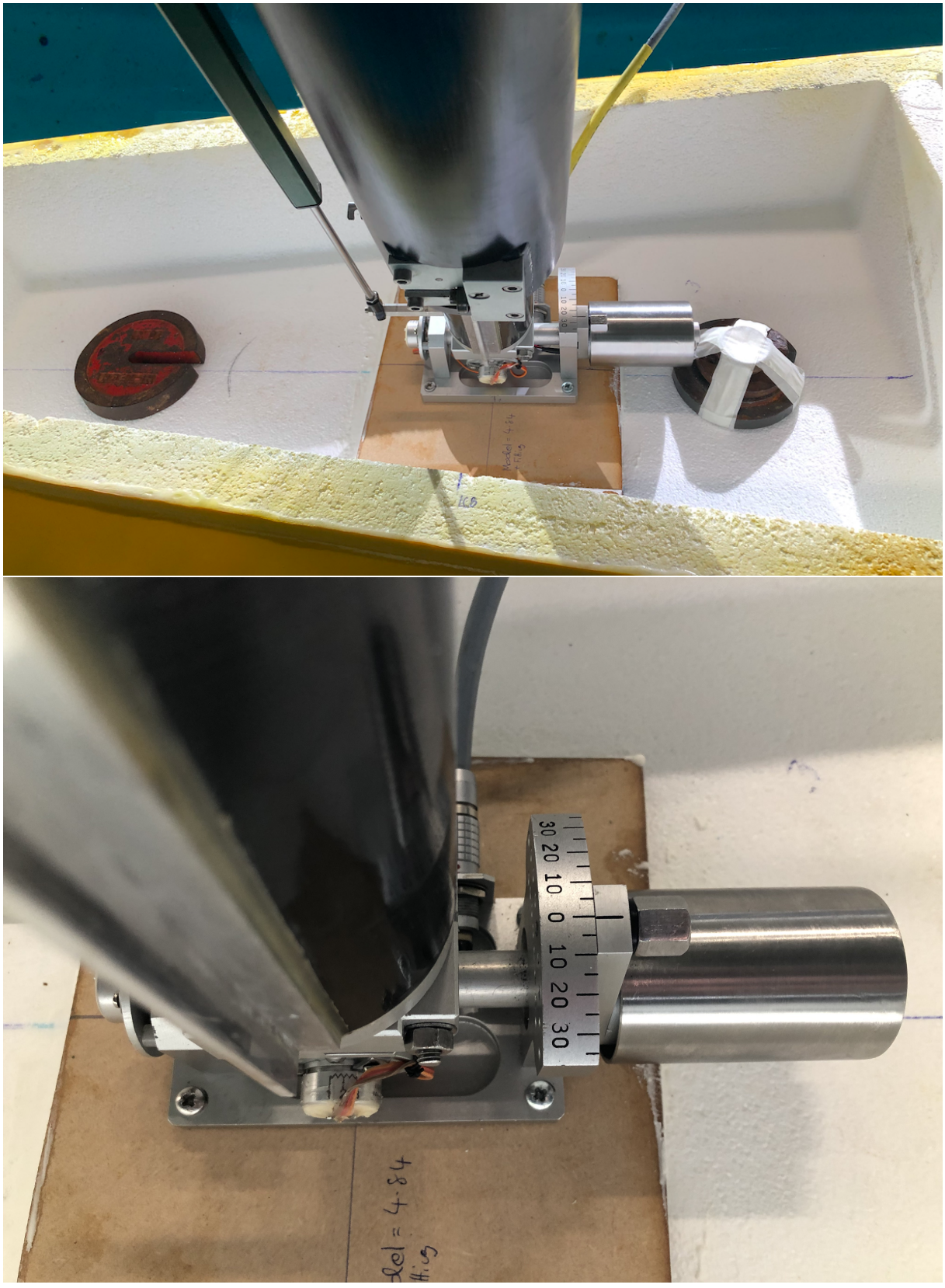

Figure 80: Heel fitting and weights

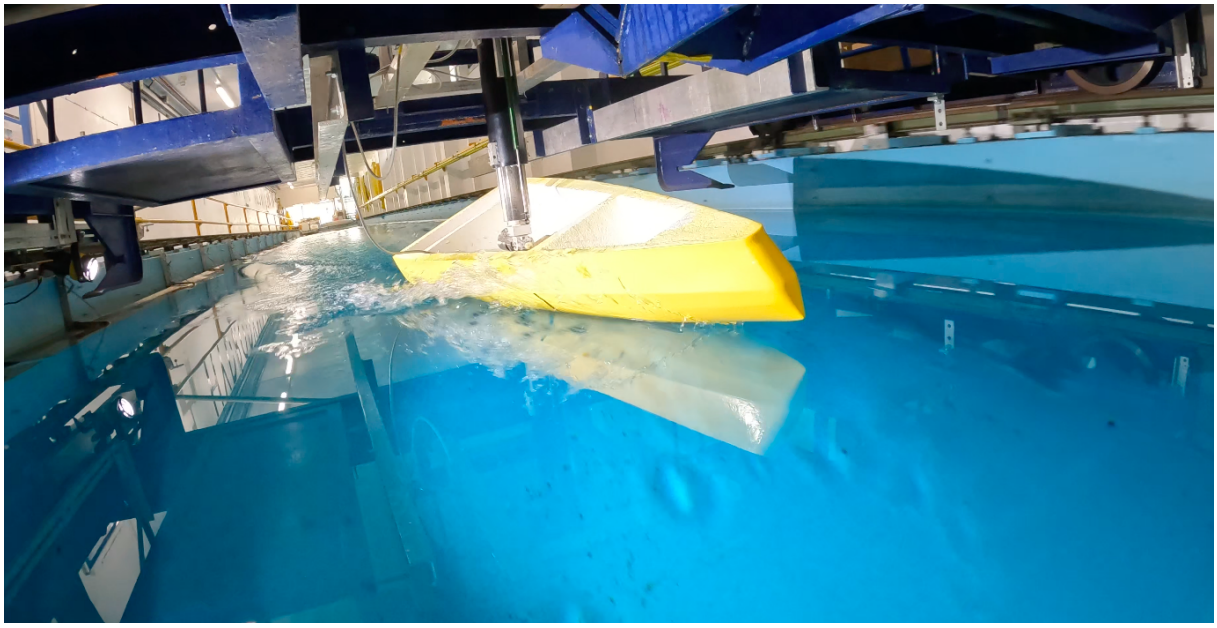

Figure 81: Test without foil, carriage speed=3.25 m/s, heel=25°, leeway=2°

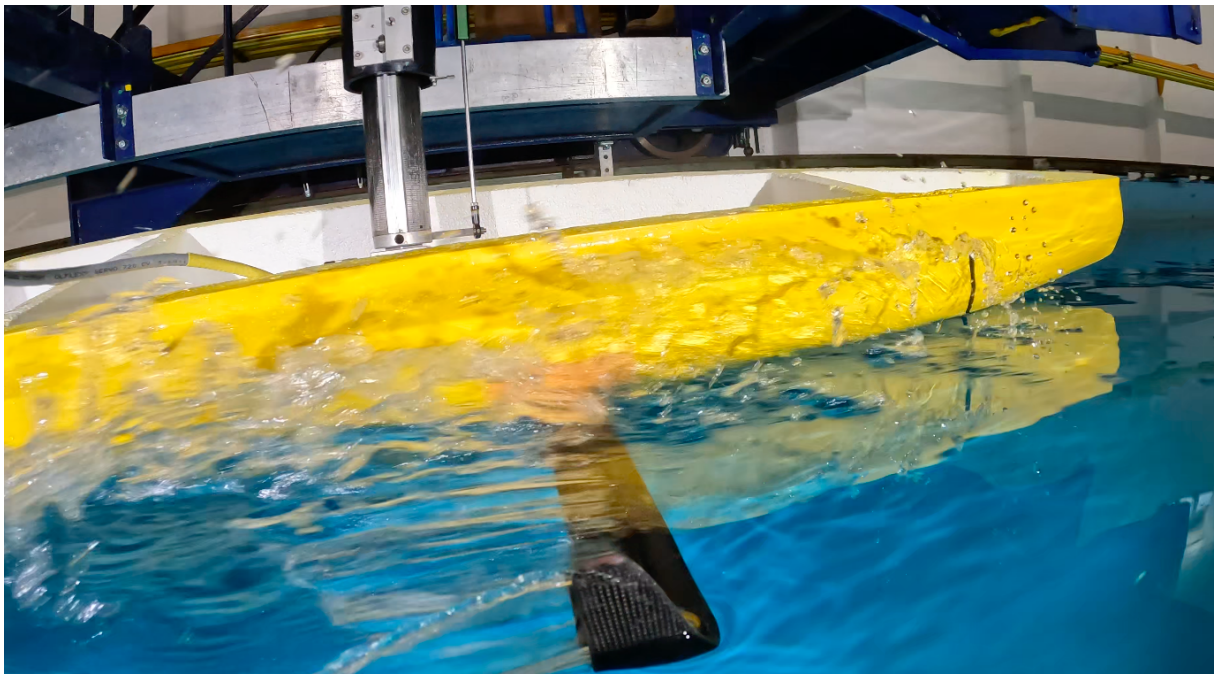

Figure 82: Ventilation on the foil, carriage speed=3.25 m/s, heel=10°, leeway=2°

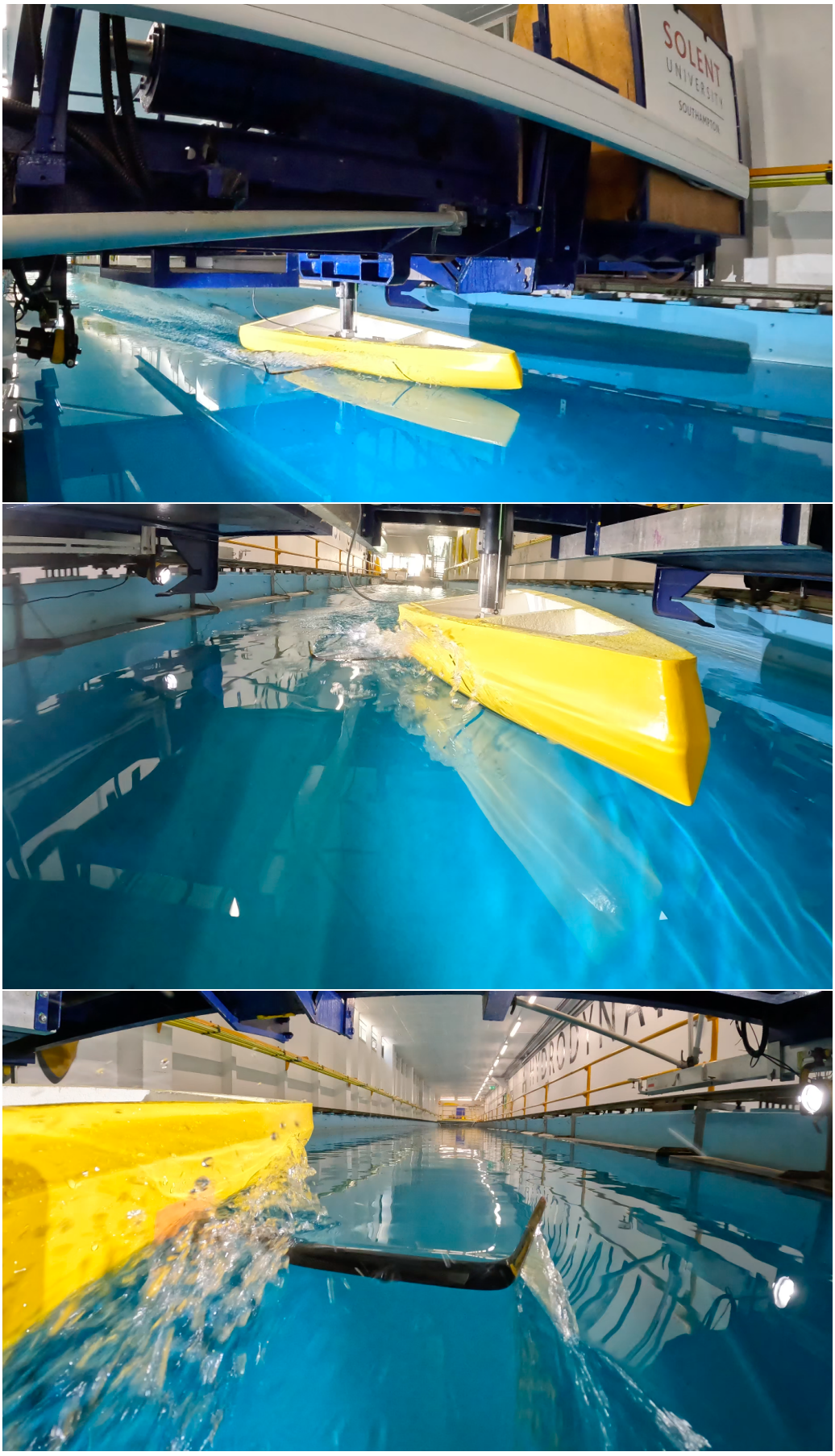

Figure 83: Test with foil, carriage speed=3.25 m/s, heel=10°, leeway=2°

G Appendix - Direct experimental VPP analyses

Table 65: Best boat speeds in knots - No foil

	4	**6**	**8**	**10**	**14**	**16**	**20**	**25**	**30**	**35**
40	4.12	5.7	6.62	7.45	8.65	8.82	8.97	8.88	8.8	9.06
45	4.73	6.21	7.36	8.57	9.26	9.44	9.69	9.76	9.28	8.46
52	5.31	6.87	8.6	9.25	10.1	10.78	11.45	11.65	11.77	11.77
60	5.74	7.81	9.21	9.9	11.46	11.74	12.35	12.85	13.13	13.22
70	6.1	8.74	9.81	11.13	12.29	12.76	13.57	14.41	14.96	15.24
75	6.22	8.92	10.21	11.39	12.71	13.24	14.24	15.23	15.84	16.19
80	6.29	9.03	10.67	11.73	13.12	13.74	14.92	15.97	16.67	17.11
90	7.04	9.06	11.36	12.36	14	14.82	16.11	17.33	18.17	18.72
100	7.07	9.69	11.7	12.77	14.76	15.65	17.1	18.45	19.49	20.47
110	6.83	9.61	11.86	13.07	15.33	16.29	17.91	19.46	21	21.96
120	6.46	9.15	11.73	13.21	15.72	16.77	18.52	20.55	22.05	23.14
135	5.34	7.24	9.29	11.23	15.81	17.13	19.09	21.45	23.3	24.86
140	4.73	6.54	8.79	9.87	13.8	16.48	19.2	21.68	23.43	25.1
150	3.18	5.28	6.65	8.48	10.96	12.35	15.77	19.89	23.52	26.18
160	2.58	4.27	5.7	6.91	9.48	10.67	13.04	16.43	20.08	23.38
165	2.43	3.99	5.4	6.57	9.12	10.14	12.48	15.61	18.74	22.22
170	2.32	3.8	5.19	6.35	8.85	9.81	12.1	15.03	18.11	21.2
180	2.21	3.61	4.97	6.1	8.53	9.47	11.65	14.36	17.37	20.28

Table 66: Best boat speeds in knots - Foil, experiment

	4	**6**	**8**	**10**	**14**	**16**	**20**	**25**	**30**	**35**
40	4.28	6.04	7.02	7.93	8.8	8.98	9.2	9.31	9.26	9.06
45	4.83	6.5	7.71	8.65	9.26	9.45	9.75	9.97	10	9.66
52	5.36	7.1	8.61	9.17	9.85	10.17	10.71	10.95	11.09	11.03
60	5.78	7.91	9.11	9.67	10.57	11.02	11.63	12.07	12.3	12.34
70	6.11	8.62	9.58	10.27	11.58	12.01	12.7	13.34	13.79	14.03
75	6.21	8.78	9.8	10.66	11.97	12.44	13.23	14.08	14.73	15.12
80	6.27	8.87	10.03	11.02	12.34	12.85	13.8	14.9	15.69	16.22
90	7.08	9.37	10.65	11.66	13.07	13.73	15.08	16.48	17.68	18.61
100	7.06	9.51	11.02	12.06	13.72	14.61	16.22	18.03	19.97	21.14
110	6.81	9.41	11.2	12.34	14.32	15.36	17.27	19.52	21.35	22.41
120	6.46	9.04	10.94	12.48	14.79	15.92	18.12	20.8	22.37	23.62
135	5.34	7.24	9.37	10.88	14.57	16.31	18.79	21.55	23.3	25.38
140	4.73	6.54	8.79	9.97	13.15	15.27	18.59	21.79	23.7	25.68
150	3.18	5.28	6.65	8.48	10.96	12.28	15.37	19.15	22.82	25.92
160	2.58	4.27	5.7	6.91	9.48	10.67	13.04	16.43	19.74	22.93
165	2.43	3.99	5.4	6.57	9.12	10.14	12.48	15.61	18.74	21.96
170	2.32	3.8	5.19	6.35	8.85	9.81	12.1	15.03	18.11	21.2
180	2.21	3.61	4.97	6.1	8.53	9.47	11.65	14.36	17.37	20.28

Table 67: Best boat speeds in knots - Foil, experiment+RM

	4	**6**	**8**	**10**	**14**	**16**	**20**	**25**	**30**	**35**
40	4.28	6.12	7.29	8.4	9.1	9.29	9.54	9.7	9.7	9.54
45	4.85	6.59	8.16	8.93	9.56	9.8	10.22	10.55	10.64	10.28
52	5.39	7.23	8.87	9.44	10.3	10.71	11.17	11.57	11.74	11.72
60	5.81	8.16	9.35	10.03	11.14	11.56	12.17	12.68	12.96	13.06
70	6.14	8.74	9.87	10.78	12.07	12.54	13.34	14.19	14.81	15.13
75	6.24	8.87	10.15	11.18	12.48	13	13.98	15.07	15.78	16.23
80	6.3	8.94	10.43	11.5	12.87	13.47	14.69	15.88	16.75	17.43
90	7.15	8.95	11.13	12.12	13.71	14.55	15.99	17.48	18.72	20.08
100	7.1	9.69	11.46	12.52	14.48	15.46	17.12	18.95	20.82	21.82
110	6.83	9.49	11.6	12.81	15.11	16.17	18.09	20.54	22.02	23.11
120	6.46	9.08	11.14	12.91	15.54	16.7	18.87	21.46	22.99	24.38
135	5.34	7.24	9.37	10.93	14.89	16.89	19.57	22.11	23.92	26.11
140	4.73	6.54	8.79	9.97	13.18	15.38	18.98	22.29	24.32	26.52
150	3.18	5.28	6.65	8.48	10.96	12.28	15.37	19.16	22.85	26.33
160	2.58	4.27	5.7	6.91	9.48	10.67	13.04	16.43	19.73	22.91
165	2.43	3.99	5.4	6.57	9.12	10.14	12.48	15.61	18.74	21.95
170	2.32	3.8	5.19	6.35	8.85	9.81	12.1	15.03	18.11	21.2
180	2.21	3.61	4.97	6.1	8.53	9.47	11.65	14.36	17.37	20.28

Table 68: Best boat speeds in knots - Foil, theory+RM

	4	**6**	**8**	**10**	**14**	**16**	**20**	**25**	**30**	**35**
40	4.37	6.16	7.68	8.89	9.76	10.08	10.61	11.03	11.19	11.15
45	4.94	6.65	8.6	9.37	10.46	10.9	11.49	11.91	12.12	12.17
52	5.4	7.32	9.2	10.02	11.43	11.84	12.45	12.83	13.17	13.33
60	5.82	8.29	9.72	10.92	12.26	12.59	13.38	14.25	14.91	15.28
70	6.15	8.81	10.37	11.77	13.1	13.73	15.01	16.22	17.16	17.85
75	6.34	8.92	10.67	12.06	13.59	14.37	15.79	17.18	18.26	19.16
80	6.39	8.99	10.87	12.37	14.11	15.02	16.53	18.08	19.44	20.64
90	7.18	9.83	11.84	13.04	15.24	16.2	17.92	20.03	21.44	22.32
100	7.12	9.81	12.09	13.47	16.01	17.12	19.09	21.38	22.66	23.73
110	6.97	9.54	12.02	13.72	16.6	17.82	20.27	22.27	23.74	25.21
120	6.46	9.1	11.25	13.35	16.76	18.27	20.88	22.97	24.79	26.76
135	5.34	7.24	9.37	10.96	15.04	17.33	21	23.56	25.82	28.28
140	4.73	6.54	8.79	9.97	13.19	15.42	19.16	23.16	26.18	28.85
150	3.18	5.28	6.65	8.48	10.96	12.28	15.26	19.16	22.84	26.57
160	2.58	4.27	5.7	6.91	9.48	10.67	13.04	16.43	19.73	22.91
165	2.43	3.99	5.4	6.57	9.12	10.14	12.48	15.61	18.74	21.95
170	2.32	3.8	5.19	6.35	8.85	9.81	12.1	15.03	18.11	21.2
180	2.21	3.61	4.97	6.1	8.53	9.47	11.65	14.36	17.37	20.28

Table 69: Best boat speeds in knots - Foil, median+RM

	4	**6**	**8**	**10**	**14**	**16**	**20**	**25**	**30**	**35**
40	4.37	6.14	7.5	8.7	9.44	9.66	10.04	10.34	10.43	10.31
45	4.86	6.63	8.44	9.18	9.99	10.33	10.92	11.33	11.48	11.45
52	5.39	7.28	9.06	9.74	10.92	11.35	11.92	12.24	12.48	12.54
60	5.81	8.24	9.56	10.49	11.8	12.1	12.79	13.43	13.89	14.13
70	6.14	8.78	10.18	11.39	12.59	13.13	14.16	15.27	16.02	16.52
75	6.24	8.9	10.48	11.66	13.03	13.66	14.94	16.15	17.08	17.77
80	6.39	8.97	10.72	11.97	13.47	14.24	15.66	17.03	18.12	19.01
90	7.17	9.74	11.54	12.6	14.49	15.43	16.99	18.67	20.4	21.4
100	7.11	9.77	11.81	13.01	15.3	16.31	18.13	20.44	21.84	22.81
110	6.84	9.52	11.87	13.28	15.89	17.03	19.12	21.51	22.91	24.14
120	6.46	9.09	11.21	13.19	16.28	17.54	19.95	22.26	23.89	25.55
135	5.34	7.24	9.37	10.95	14.98	17.19	20.51	22.86	24.86	27.09
140	4.73	6.54	8.79	9.97	13.19	15.41	19.12	22.84	25.25	27.73
150	3.18	5.28	6.65	8.48	10.96	12.28	15.36	19.16	22.84	26.53
160	2.58	4.27	5.7	6.91	9.48	10.67	13.04	16.43	19.73	22.91
165	2.43	3.99	5.4	6.57	9.12	10.14	12.48	15.61	18.74	21.95
170	2.32	3.8	5.19	6.35	8.85	9.81	12.1	15.03	18.11	21.2
180	2.21	3.61	4.97	6.1	8.53	9.47	11.65	14.36	17.37	20.28

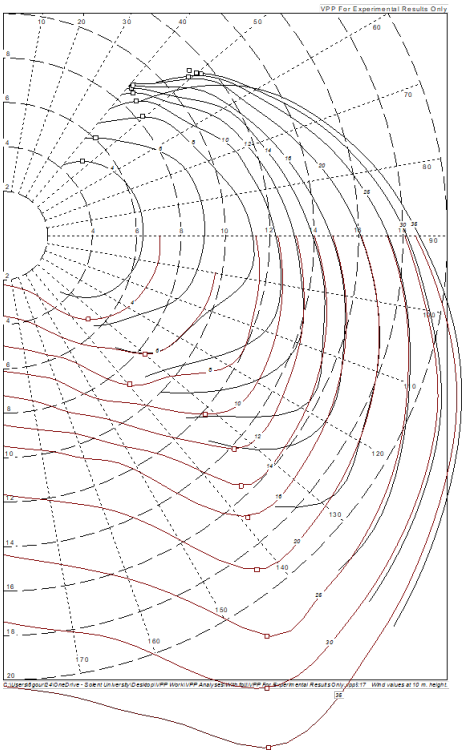

Figure 84: Polar plot - No foil

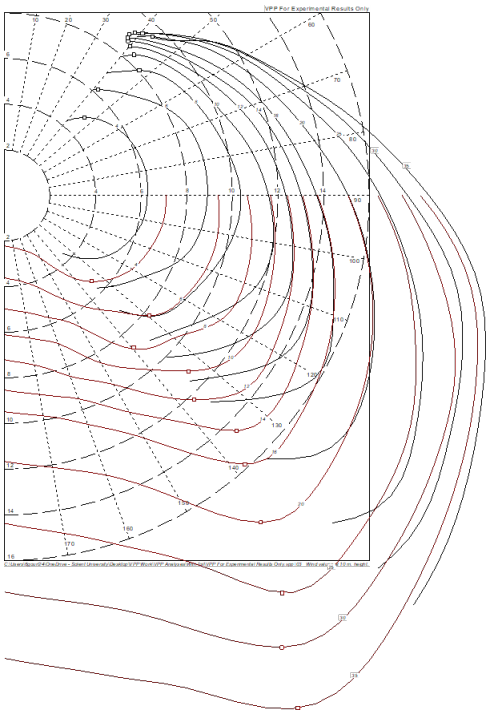

Figure 85: Polar plot - Foil, experiment

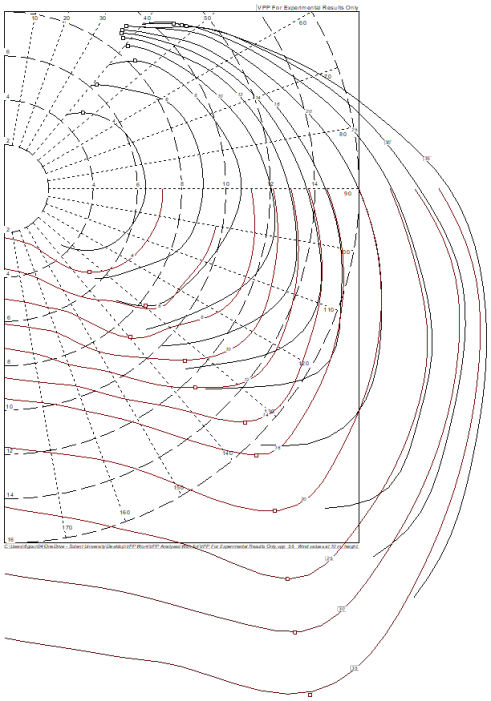

Figure 86: Polar plot - Foil, experiment+RM

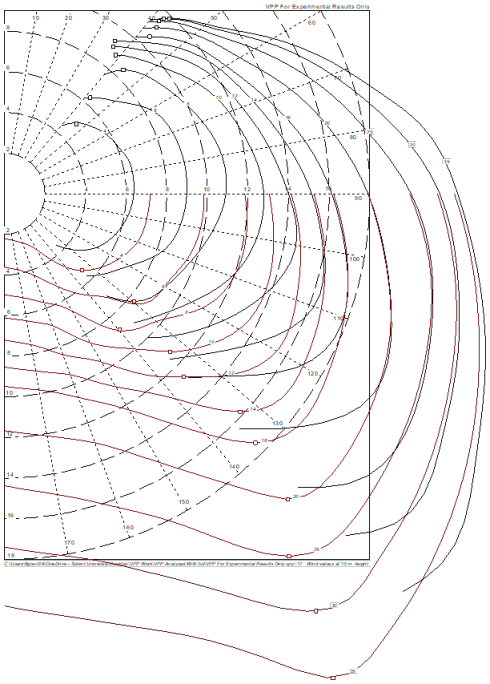

Figure 87: Polar plot - Foil, theory+RM

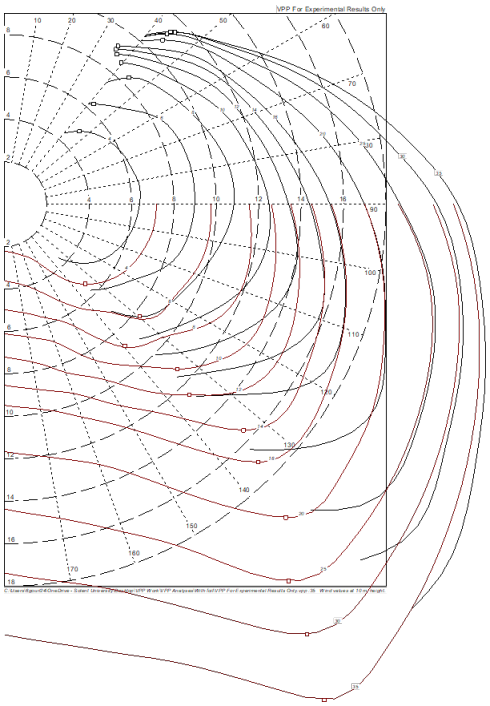

Figure 88: Polar plot - Foil, median+RM

G.1 Best heel angles

Table 70: Best heel angles in degrees - No foil

	4	6	8	10	14	16	20	25	30	35
40	4.21	8.82	13.3	17.19	22.71	23.1	23.75	24.48	-	-
45	5.07	10.22	15.59	19.73	23.62	24.01	24.76	25.72	-	25.26
52	5.61	12.34	18.22	21.44	24.89	26.41	26.98	27.43	29.35	35
60	5.82	14.79	19.65	22.64	25.47	24.97	25.19	25.97	27.36	29.87
70	5.61	15.34	20.62	24.5	24.02	23.95	24.08	24.8	26.07	28.11
75	5.34	14.45	21.39	24.15	23.62	23.54	23.75	24.48	25.75	27.72
80	4.5	13.25	22.17	23.83	23.29	23.27	23.47	24.25	25.48	27.35
90	8.98	10.44	22.82	23.28	22.7	22.61	22.83	23.88	25.02	26.59
100	7.34	17.17	22.07	22.86	22.23	22.19	22.46	23.59	24.56	25.81
110	5.31	13.18	21.02	22.53	21.88	21.88	22.63	23.35	24.26	25.51
120	3.24	8.26	16.63	21.26	21.63	21.63	22.49	23.17	24.03	25.15
130	1.92	4.05	6.51	12.17	21.43	21.47	21.9	23.06	23.87	24.9
135	1.33	2.38	3.95	6.92	17.64	21.44	21.89	22.5	23.59	24.86
140	0.8	1.5	2.71	3.44	8.42	13.58	21.19	22.54	23.41	24.41
150	0.2	0.51	0.83	1.32	2.38	3.05	5.76	10.16	16.2	23.29
160	0.09	0.2	0.35	0.56	1.11	1.46	2.33	3.61	6.09	8.94
165	0.07	0.14	0.25	0.4	0.79	1.07	1.7	2.65	3.82	6.05
170	0.05	0.1	0.16	0.26	0.52	0.71	1.12	1.77	2.54	3.44
180	0	0.01	0.01	0.01	0.03	0.04	0.06	0.1	0.15	0.2

Table 71: Best heel angles in degrees - Foil, experiment

	4	6	8	10	14	16	20	25	30	35
40	4.21	12.15	17.81	21.82	25.18	25.54	26.27	27.21	28.18	29.13
45	5.22	13.1	19.24	22.9	25.34	25.69	26.42	27.4	28.45	28.8
52	5.72	14.02	20.69	23.69	25.46	25.62	25.79	25.93	26.99	28.39
60	5.88	15.12	21.42	24.15	24.26	24.15	24.34	25.02	26.09	27.55
70	5.62	14.95	21.73	23.96	23.34	23.32	23.66	24.5	25.71	27.28
75	5.34	13.98	21.71	23.55	23.02	23.11	23.53	24.46	25.85	27.65
80	4.97	12.77	22.03	23.2	22.87	22.98	23.46	24.62	26.44	28.71
90	9.21	18.41	22.15	22.62	22.32	22.42	23.63	25.9	29.28	31.9
100	7.31	17.7	21.24	22.27	22.04	22.28	24.41	28.53	32.51	33.44
110	5.28	12.47	20.04	21.97	21.88	22.36	25.78	31.62	33	33.61
120	3.24	8	13.49	20.44	21.8	22.52	27.35	32.58	33.46	34.07
130	1.92	4.05	6.3	10.36	21.2	22.79	27.07	25.31	33.11	34.58
135	1.33	2.38	3.95	6.38	13.74	19.16	27.59	31.4	32.96	31
140	0.8	1.5	2.71	3.44	7.49	11.01	19.29	31.07	33.58	34.45
150	0.2	0.51	0.83	1.32	2.38	3.05	5.62	9.75	15.66	23.1
160	0.09	0.2	0.35	0.56	1.11	1.46	2.33	3.61	6.2	9.13
165	0.07	0.14	0.25	0.4	0.79	1.07	1.7	2.65	3.82	6.15
170	0.05	0.1	0.16	0.26	0.52	0.71	1.12	1.77	2.54	3.44
180	0	0.01	0.01	0.01	0.03	0.04	0.06	0.1	0.15	0.2

Table 72: Best heel angles in degrees - Foil, experiment+RM

	4	**6**	**8**	**10**	**14**	**16**	**20**	**25**	**30**	**35**
40	3.77	9.57	15.69	19.24	22.36	22.69	23.39	24.46	25.82	27.21
45	4.18	10.24	17.09	20.12	22.54	22.86	23.31	23.94	25.18	26.29
52	5.02	10.95	18.25	20.87	22.37	22.26	22.35	22.44	23.34	24.8
60	5.15	12	18.92	21.35	21.23	21.17	21.33	21.83	22.64	23.89
70	4.46	11.56	19.29	21.06	20.66	20.67	20.97	21.66	22.74	24.28
75	4.27	10.83	19.26	20.78	20.49	20.57	20.95	21.88	23.37	25.7
80	4.03	9.98	17.94	20.57	20.41	20.51	21.03	22.38	24.8	28.37
90	7.59	8.14	19.53	20.19	20.07	20.26	21.23	24.87	29.73	32.31
100	6.23	13.84	18.85	19.97	19.99	20.41	22.86	29.01	32.09	32.8
110	4.24	9.82	17.91	19.56	20.02	20.68	24.94	31.52	32.51	33.27
120	2.9	6.72	10.81	17.07	20.07	20.97	27.24	31.86	33.01	33.77
130	1.72	3.63	5.48	8.42	18.6	21.23	27.09	29.96	29.92	34.33
135	1.2	2.13	3.54	5.56	11.16	16.17	27.74	30.21	32.11	27.85
140	0.72	1.34	2.43	3.08	6.34	8.88	15.56	27.61	32.87	34.06
150	0.18	0.45	0.74	1.19	2.13	2.74	4.26	7.91	12.1	18.69
160	0.08	0.18	0.31	0.5	0.99	1.31	2.08	3.23	5.37	7.48
165	0.06	0.13	0.22	0.36	0.71	0.96	1.52	2.38	3.42	5.34
170	0.04	0.09	0.15	0.24	0.46	0.63	1.01	1.59	2.27	3.08
180	0	0	0.01	0.01	0.02	0.04	0.06	0.09	0.13	0.18

Table 73: Best heel angles in degrees - Foil, theory+RM

	4	**6**	**8**	**10**	**14**	**16**	**20**	**25**	**30**	**35**
40	3.46	8.05	14.09	18.08	22.73	23.82	23.8	24.04	24.56	25.3
45	3.84	8.49	15.59	19.13	23.08	23.24	23.23	23.51	24	24.68
52	4.14	8.98	16.4	20.16	22.74	22.68	22.73	22.66	23.12	23.74
60	4.25	9.67	16.05	20.46	22.3	21.92	22.02	22.42	23.08	23.91
70	4.1	9.32	15.05	20.43	21.58	21.61	22.03	23.24	25.24	27.38
75	3.93	8.86	14.32	21.06	21.47	21.58	22.39	24.53	27.38	29.47
80	3.7	8.31	13.33	20.91	21.41	21.71	23.03	26.31	29.34	30.51
90	6.67	13.31	18.64	20.73	21.5	22.18	25.15	29.63	30.21	30.83
100	5.63	10.73	18.01	20.11	21.83	23.07	27.59	29.7	30.38	31.11
110	3.9	8.23	13.76	19.21	22.22	24.1	29.14	29.76	30.53	31.36
120	2.66	6	8.96	13.05	26.73	24.8	28.42	29.82	30.71	31.64
130	1.58	3.33	5.03	7.27	14.46	19.34	28.09	28.53	29.36	31.07
135	1.1	1.95	3.25	5.1	9.2	12.47	20.98	28.6	29.48	30.41
140	0.66	1.23	2.23	2.83	5.7	7.58	11.73	19.07	28.35	30.84
150	0.16	0.42	0.68	1.09	1.95	2.51	3.91	6.87	9.65	13.37
160	0.08	0.16	0.29	0.46	0.91	1.2	1.91	2.97	4.28	6.55
165	0.06	0.12	0.2	0.33	0.65	0.88	1.4	2.18	3.14	4.27
170	0.04	0.08	0.13	0.22	0.43	0.58	0.92	1.46	2.09	2.83
180	0	0	0.01	0.01	0.02	0.03	0.05	0.09	0.12	0.16

Table 74: Best heel angles in degrees - Foil, median+RM

	4	**6**	**8**	**10**	**14**	**16**	**20**	**25**	**30**	**35**
40	3.64	8.69	14.89	18.75	23.01	23.38	23.91	24.37	25.16	26.26
45	4.04	9.21	16.39	19.7	23.27	23.2	23.2	23.58	24.29	25.34
52	4.36	9.77	17.6	20.57	22.54	22.45	22.52	22.52	23.13	24
60	4.47	10.6	18.41	20.9	21.96	21.57	21.68	22.09	22.72	23.58
70	4.31	10.2	17.39	20.72	21.15	21.15	21.44	22.3	23.63	25.44
75	4.13	9.65	16.36	21.26	20.99	21.07	21.59	22.94	25.26	27.93
80	3.89	9	15.1	21.08	20.92	21.08	21.92	24.12	27.55	30.08
90	7.09	14.86	19.1	20.74	20.76	21.15	22.87	27.74	30.87	31.57
100	5.93	11.92	18.46	20.32	20.87	21.6	25.49	30.35	31.18	31.98
110	4.1	8.9	15.63	19.4	21.06	22.2	27.75	30.5	31.47	32.39
120	2.8	6.34	9.72	14.63	21.23	22.76	28.68	30.66	31.84	32.86
130	1.66	3.51	5.27	7.78	16.21	22.09	28.28	29.06	25.41	33.46
135	1.16	2.06	3.42	5.34	10.01	13.98	24.56	29.2	30.53	31.95
140	0.7	1.3	2.35	2.98	6.02	8.14	13.2	22.68	31.05	32.66
150	0.17	0.44	0.71	1.15	2.06	2.64	4.11	7.33	10.6	15.34
160	0.08	0.17	0.3	0.48	0.96	1.27	2.01	3.13	5.17	6.98
165	0.06	0.12	0.21	0.34	0.68	0.92	1.47	2.3	3.31	5.14
170	0.04	0.08	0.14	0.23	0.45	0.61	0.97	1.53	2.19	2.97
180	0	0	0.01	0.01	0.02	0.03	0.06	0.09	0.13	0.17

G.2 Best leeway angles

Table 75: Best leeway angles in degrees - No foil

	4	**6**	**8**	**10**	**14**	**16**	**20**	**25**	**30**	**35**
40	3.37	3.4	4.16	4.48	4.1	4.2	4.49	4.96	5.94	-
45	2.97	3.37	4.09	3.8	3.81	3.9	4.1	4.4	5.4	6.56
52	2.62	3.45	3.49	3.5	3.48	3.31	3.21	3.46	3.64	4.06
60	2.33	3.31	3.27	3.24	2.84	2.9	2.84	2.87	2.99	3.2
70	2.04	2.69	3.03	2.69	2.5	2.42	2.32	2.26	2.3	2.44
75	1.91	2.35	2.88	2.62	2.31	2.22	2.07	2	2.04	2.17
80	1.79	2.03	2.68	2.45	2.14	2.02	1.85	1.78	1.81	1.91
90	2.51	1.56	2.57	2.32	1.96	1.82	1.64	1.4	1.39	1.47
100	2.09	2.76	2.33	2.1	1.69	1.55	1.35	1.06	0.98	1.03
110	1.76	1.94	2.13	1.92	1.48	1.33	0.94	0.71	0.69	0.84
120	1.56	1.41	1.57	2.06	1.31	1.13	0.7	0.44	0.53	0.66
130	1.28	1.17	1.09	0.9	1.52	0.97	0.6	0.29	0.38	0.51
135	1.13	1.11	1.11	0.86	0.75	1.01	0.5	0.3	0.28	0.45
140	0.98	0.97	0.97	0.96	0.5	0.2	0.31	0.24	0.33	0.45
150	0.74	0.72	0.73	0.73	0.7	0.64	0.1	-1.23	-1.19	0.15
160	0.66	0.61	0.61	0.62	0.63	0.61	0.49	0.16	-1.02	-1.32
165	0.62	0.58	0.57	0.58	0.59	0.59	0.48	0.22	-0.29	-1.08
170	0.58	0.54	0.54	0.54	0.55	0.56	0.45	0.23	-0.22	-0.63
180	0.46	0.46	0.46	0.46	0.46	0.46	0.37	0.19	-0.21	-0.77

Table 76: Best leeway angles in degrees - Foil, experiment

	4	**6**	**8**	**10**	**14**	**16**	**20**	**25**	**30**	**35**
40	3.5	4.07	4.03	4.01	4.29	4.46	4.88	5.55	6.43	7.56
45	3.11	3.72	3.68	3.69	4.06	4.21	4.55	5.08	5.81	7.04
52	2.72	3.31	3.3	3.5	3.76	3.74	3.61	3.94	4.29	4.93
60	2.39	2.89	3.14	3.3	3.23	3.07	2.98	3.05	3.24	3.56
70	2.04	2.47	2.95	3.03	2.55	2.47	2.37	2.35	2.41	2.56
75	1.89	2.25	2.84	2.74	2.34	2.24	2.13	2.06	2.08	2.18
80	1.75	2.02	2.78	2.51	2.14	2.04	1.9	1.81	1.84	1.94
90	2.58	2.79	2.65	2.34	2.01	1.89	1.51	1.5	1.62	1.73
100	2.09	2.63	2.37	2.1	1.73	1.58	1.28	1.42	1.6	1.64
110	1.7	1.92	2.16	1.9	1.5	1.35	1.17	1.46	1.5	1.52
120	1.56	1.28	1.5	1.73	1.3	1.18	1.13	1.42	1.44	1.46
130	1.28	1.02	0.89	0.75	1.11	1.04	1.17	0.74	1.34	1.41
135	1.13	1.11	1.11	0.61	0.46	0.66	1.15	1.34	1.39	1.14
140	0.98	0.97	0.97	0.96	0.19	-0.07	0.15	1.27	1.39	1.41
150	0.74	0.72	0.73	0.73	0.7	0.64	-0.21	-1.44	-1.38	0.25
160	0.66	0.61	0.61	0.62	0.63	0.61	0.49	0.16	-1.44	-1.92
165	0.62	0.58	0.57	0.58	0.59	0.59	0.48	0.22	-0.29	-1.57
170	0.58	0.54	0.54	0.54	0.55	0.56	0.45	0.23	-0.22	-0.63
180	0.46	0.46	0.46	0.46	0.46	0.46	0.37	0.19	-0.21	-0.77

Table 77: Best leeway angles in degrees - Foil, experiment+RM

	4	**6**	**8**	**10**	**14**	**16**	**20**	**25**	**30**	**35**
40	3.2	4.01	4.02	3.67	3.88	4.01	4.33	4.86	5.65	6.73
45	3.05	3.65	3.51	3.46	3.68	3.78	3.88	4.07	4.54	5.81
52	2.7	3.2	3.21	3.28	3.26	3.14	3.06	3.33	3.58	4.02
60	2.38	2.7	3.05	3.05	2.82	2.73	2.68	2.72	2.85	3.08
70	2.04	2.27	2.84	2.67	2.34	2.27	2.15	2.08	2.1	2.21
75	1.9	2.06	2.7	2.46	2.16	2.06	1.9	1.8	1.84	1.97
80	1.76	1.85	2.42	2.29	1.98	1.86	1.67	1.6	1.69	1.84
90	2.52	1.46	2.44	2.18	1.84	1.69	1.53	1.41	1.63	1.73
100	2.08	2.42	2.23	1.96	1.56	1.42	1.15	1.46	1.58	1.6
110	1.73	1.77	2.08	1.78	1.34	1.21	1.11	1.46	1.49	1.52
120	1.56	1.29	1.28	1.53	1.16	1.05	1.15	1.39	1.43	1.45
130	1.28	1.27	0.92	0.69	0.9	0.9	1.2	1.31	1.14	1.4
135	1.13	1.11	1.11	0.66	0.21	0.31	1.19	1.28	1.36	0.9
140	0.98	0.97	0.97	0.96	0.25	-0.12	-0.52	1.03	1.36	1.4
150	0.74	0.72	0.73	0.73	0.7	0.64	-0.06	-1.28	-1.82	-0.65
160	0.66	0.61	0.61	0.62	0.63	0.61	0.49	0.16	-1.3	-1.7
165	0.62	0.58	0.57	0.58	0.59	0.59	0.48	0.22	-0.29	-1.43
170	0.58	0.54	0.54	0.54	0.55	0.56	0.45	0.23	-0.22	-0.63
180	0.46	0.46	0.46	0.46	0.46	0.46	0.37	0.19	-0.21	-0.77

Table 78: Best leeway angles in degrees - Foil, theory+RM

	4	**6**	**8**	**10**	**14**	**16**	**20**	**25**	**30**	**35**
40	3.2	3.93	4.26	3.99	4.34	4.43	4.31	4.37	4.66	5.17
45	2.85	3.57	3.74	3.85	3.85	3.69	3.59	3.66	3.85	4.17
52	2.67	3.11	3.47	3.62	3.16	3.08	3.01	3.22	3.32	3.51
60	2.36	2.58	3.12	3.09	2.7	2.78	2.67	2.58	2.57	2.66
70	2.04	2.16	2.61	2.63	2.41	2.29	2.09	2.01	2.04	2.11
75	1.96	1.97	2.34	2.56	2.21	2.06	1.88	1.85	1.92	1.97
80	1.85	1.79	2.07	2.4	2.02	1.86	1.72	1.76	1.84	1.84
90	2.49	2.82	2.59	2.3	1.85	1.75	1.73	1.67	1.65	1.67
100	2.08	2.25	2.39	2.08	1.63	1.56	1.5	1.52	1.52	1.55
110	1.84	1.72	1.82	1.9	1.46	1.45	1.44	1.41	1.42	1.44
120	1.56	1.31	1.19	1.22	1.68	1.35	1.44	1.31	1.32	1.34
130	1.28	1.27	0.95	0.71	0.46	0.7	1.33	1.28	1.27	1.21
135	1.13	1.11	1.11	0.69	0.14	-0.14	0.48	1.23	1.23	1.24
140	0.98	0.97	0.97	0.96	0.3	-0.07	-1.01	-0.14	1.09	1.22
150	0.74	0.72	0.73	0.73	0.7	0.64	0.42	-1.15	-1.74	-1.74
160	0.66	0.61	0.61	0.62	0.63	0.61	0.49	0.16	-1.12	-1.55
165	0.62	0.58	0.57	0.58	0.59	0.59	0.48	0.22	-0.29	-1.24
170	0.58	0.54	0.54	0.54	0.55	0.56	0.45	0.23	-0.22	-0.63
180	0.46	0.46	0.46	0.46	0.46	0.46	0.37	0.19	-0.21	-0.77

Table 79: Best leeway angles in degrees - Foil, median+RM

	4	**6**	**8**	**10**	**14**	**16**	**20**	**25**	**30**	**35**
40	3.2	3.97	4.17	3.83	4.15	4.27	4.49	4.7	5.18	6.02
45	3.04	3.6	3.62	3.67	3.9	3.81	3.68	3.77	4.04	4.51
52	2.67	3.15	3.4	3.48	3.19	3.08	3.02	3.26	3.43	3.71
60	2.36	2.63	3.23	3.07	2.68	2.75	2.68	2.66	2.71	2.85
70	2.04	2.2	2.77	2.57	2.38	2.29	2.12	2.01	2.03	2.12
75	1.9	2	2.49	2.5	2.19	2.07	1.87	1.8	1.86	1.96
80	1.85	1.81	2.21	2.34	2.01	1.86	1.67	1.66	1.78	1.87
90	2.5	2.85	2.51	2.24	1.84	1.7	1.6	1.58	1.67	1.69
100	2.08	2.32	2.31	2.02	1.58	1.47	1.34	1.54	1.54	1.57
110	1.73	1.73	1.95	1.84	1.38	1.31	1.34	1.42	1.45	1.48
120	1.56	1.3	1.22	1.35	1.23	1.18	1.44	1.34	1.38	1.41
130	1.28	1.27	0.94	0.7	0.66	0.99	1.31	1.28	0.76	1.36
135	1.13	1.11	1.11	0.67	0.15	0.03	0.93	1.24	1.28	1.32
140	0.98	0.97	0.97	0.96	0.28	-0.1	-0.89	0.5	1.27	1.32
150	0.74	0.72	0.73	0.73	0.7	0.64	-0.04	-1.21	-1.81	-1.44
160	0.66	0.61	0.61	0.62	0.63	0.61	0.49	0.16	-1.27	-1.62
165	0.62	0.58	0.57	0.58	0.59	0.59	0.48	0.22	-0.29	-1.39
170	0.58	0.54	0.54	0.54	0.55	0.56	0.45	0.23	-0.22	-0.63
180	0.46	0.46	0.46	0.46	0.46	0.46	0.37	0.19	-0.21	-0.77

G.3 Proposal of an optimised foil design

Figure 89: Optimisation of the foil

Figure 90: Optimised foil design

H Appendix - Rhinoceros® renders

Figure 91: Union Solidaire at sea - render 1

Figure 92: Union Solidaire at sea - render 2

Figure 93: Union Solidaire at sea - render 3

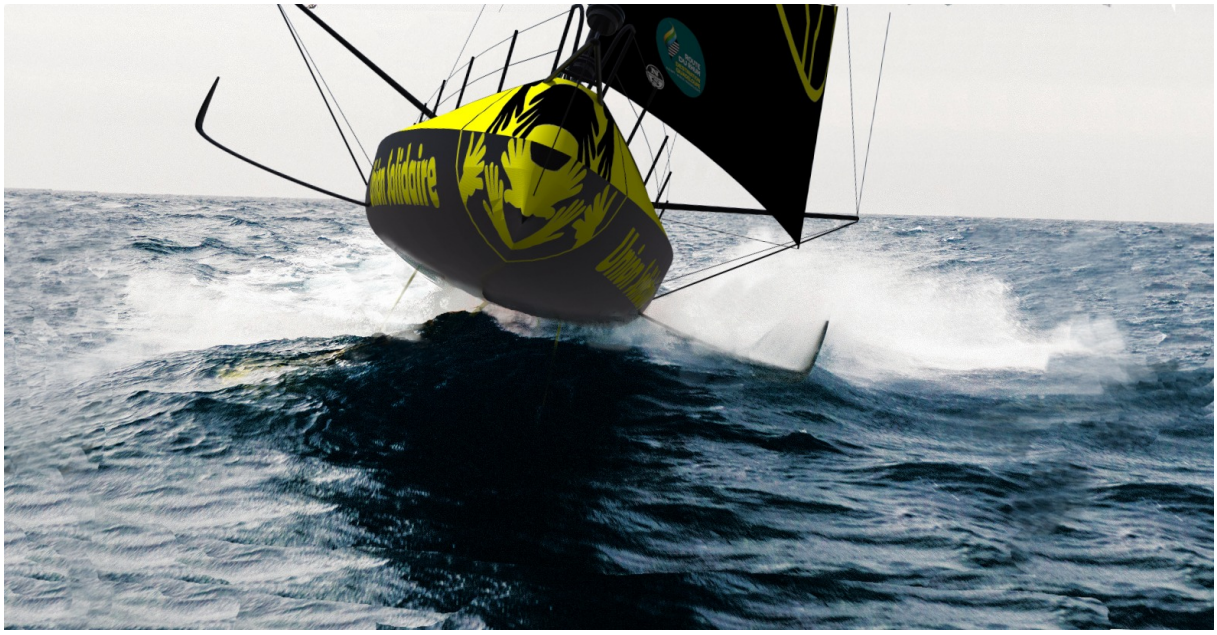

Figure 94: Union Solidaire at sea - render 4

Figure 95: Union Solidaire at sea - render 5

Figure 96: Union Solidaire at sea - render 6

I Appendix - Autocad® drawings

The positions of the design grid elements drawn on the lines plan (drawing 01) are given relative to the zero point, which is located at the height of the DWL, on the centreline (CL), and at AP.

Table 80: Position of the design grid elements from the zero point

Element	Position (m)	
AP	0	X, Longitudinal
ST1	0.961	X, Longitudinal
ST2	1.924	X, Longitudinal
ST3	2.886	X, Longitudinal
ST4	3.848	X, Longitudinal
ST5	4.81	X, Longitudinal
ST6	5.772	X, Longitudinal
ST7	6.734	X, Longitudinal
ST8	7.696	X, Longitudinal
ST9	8.658	X, Longitudinal
ST10	9.62	X, Longitudinal
ST11	10.582	X, Longitudinal
ST12	11.545	X, Longitudinal
ST13	12.507	X, Longitudinal
ST14	13.469	X, Longitudinal
ST15	14.431	X, Longitudinal
ST16	15.393	X, Longitudinal
ST17	16.355	X, Longitudinal
FP	16.58	X, Longitudinal
ST18	17.317	X, Longitudinal
CL	0	Y, Transversal
B1	0.56	Y, Transversal
B2	1.12	Y, Transversal
B3	1.68	Y, Transversal
B4	2.24	Y, Transversal
WL1	-0.118	Z, Vertical
WL2	-0.018	Z, Vertical
DWL	0	Z, Vertical
WL3	0.064	Z, Vertical
WL4	0.384	Z, Vertical
WL5	0.705	Z, Vertical
D1	0	CL height
D2	0.5	CL height
D3	1	CL height

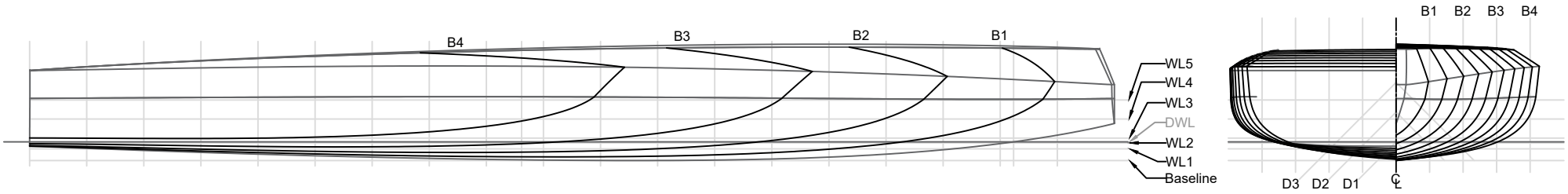

AP ST1 ST2 ST3 ST4 ST5 ST6 ST7 ST8 MS ST9 ST10 ST11 ST12 ST13 ST14 ST15 ST16 ST17 FP ST18

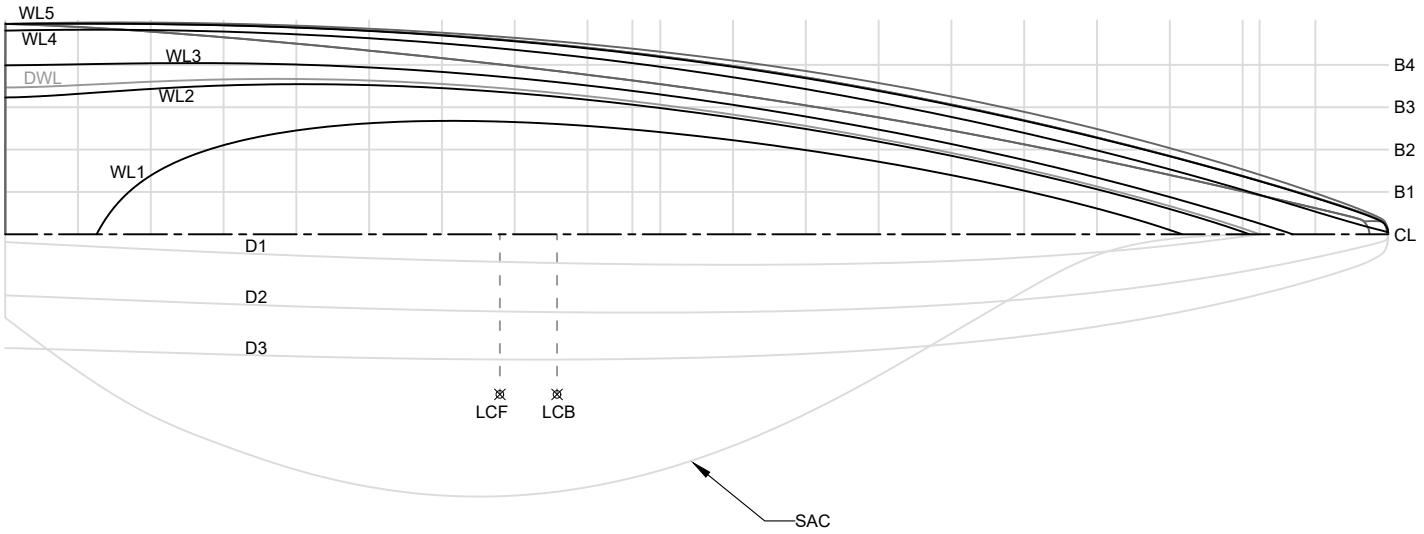

Hydrostatics		
LOA hull	18.28	m
LWL	16.58	m
BOA hull	5.60	m
BWL	4.11	m
Tc	0.31	m
Displacement Hull	7.67	m^3
Displacement Appendages	0.38	m^3
LCB % of LWL	43.85	%
LCF % of LWL	39.44	%
WSA	50.55	m^2
WPA	49.70	m^2
SA max hull	0.69	m^2
CP	0.64	-

SOLENT UNIVERSITY

Issue date: 31/03/2022	Scale: 1:100 (A4)	File name: Lines_Plan_IMOCA.dwg
Drawn by: Lazare GOURNAY	Units: mm	Projection method: Multiple
Drawing number: 01		**Drawing title: Lines Plan IMOCA**
	Sheet: 1 of 1	

Heeled at 10 degrees:

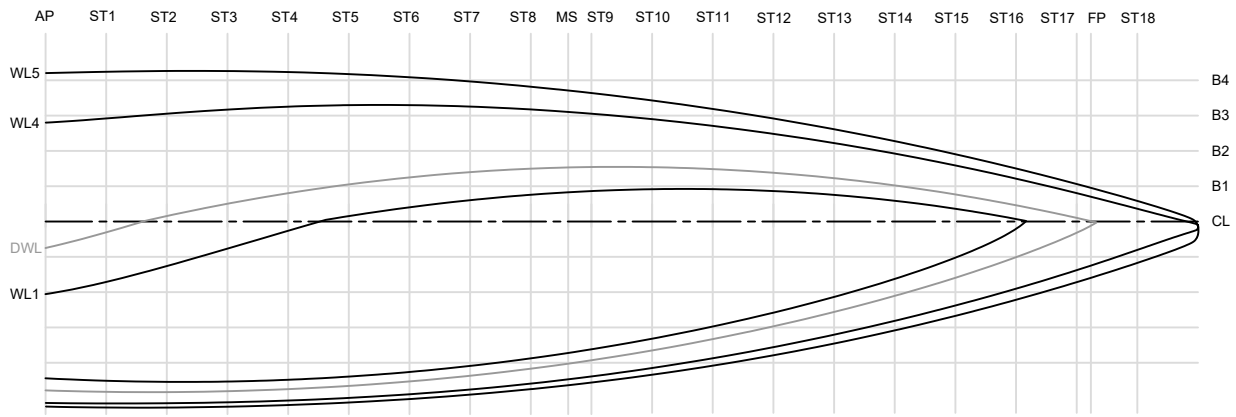

Heeled at 15 degrees:

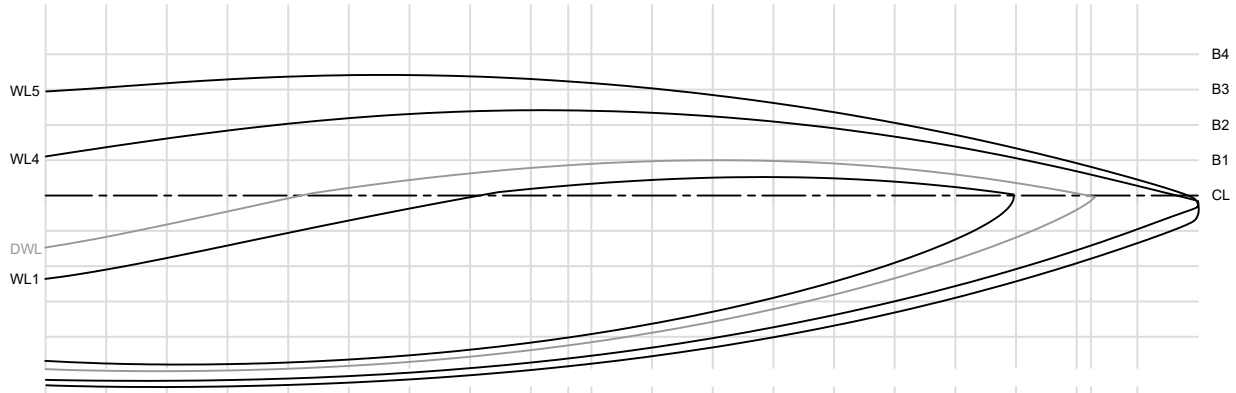

Heeled at 25 degrees:

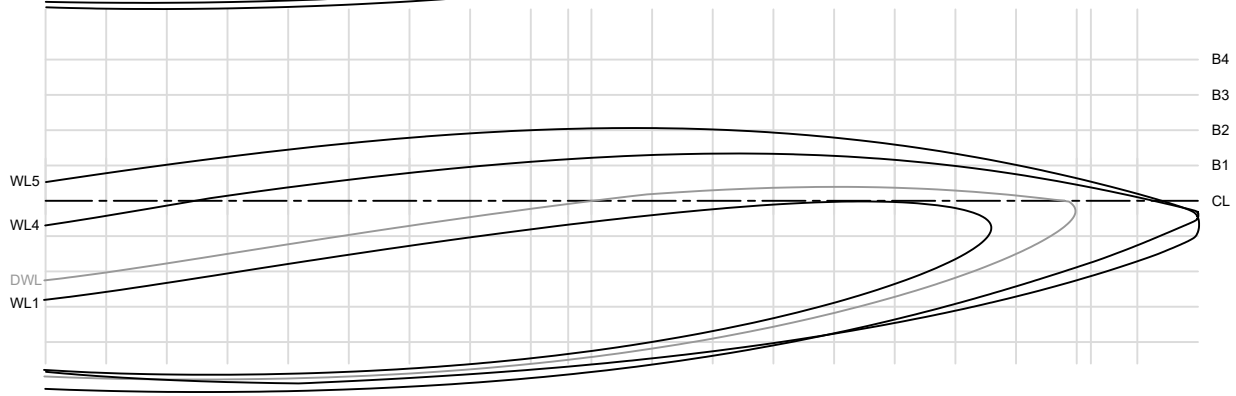

SOLENT UNIVERSITY

Issue date: 03/04/2022	Scale: 1:120 (A4)	File name: Heeled_Water_Lines_IMOCA.dwg
Drawn by: Lazare GOURNAY	Units: mm	Projection method: Plan View
Drawing number: 02		**Drawing title: Heeled Waterlines IMOCA**
	Sheet: 1 of 1	

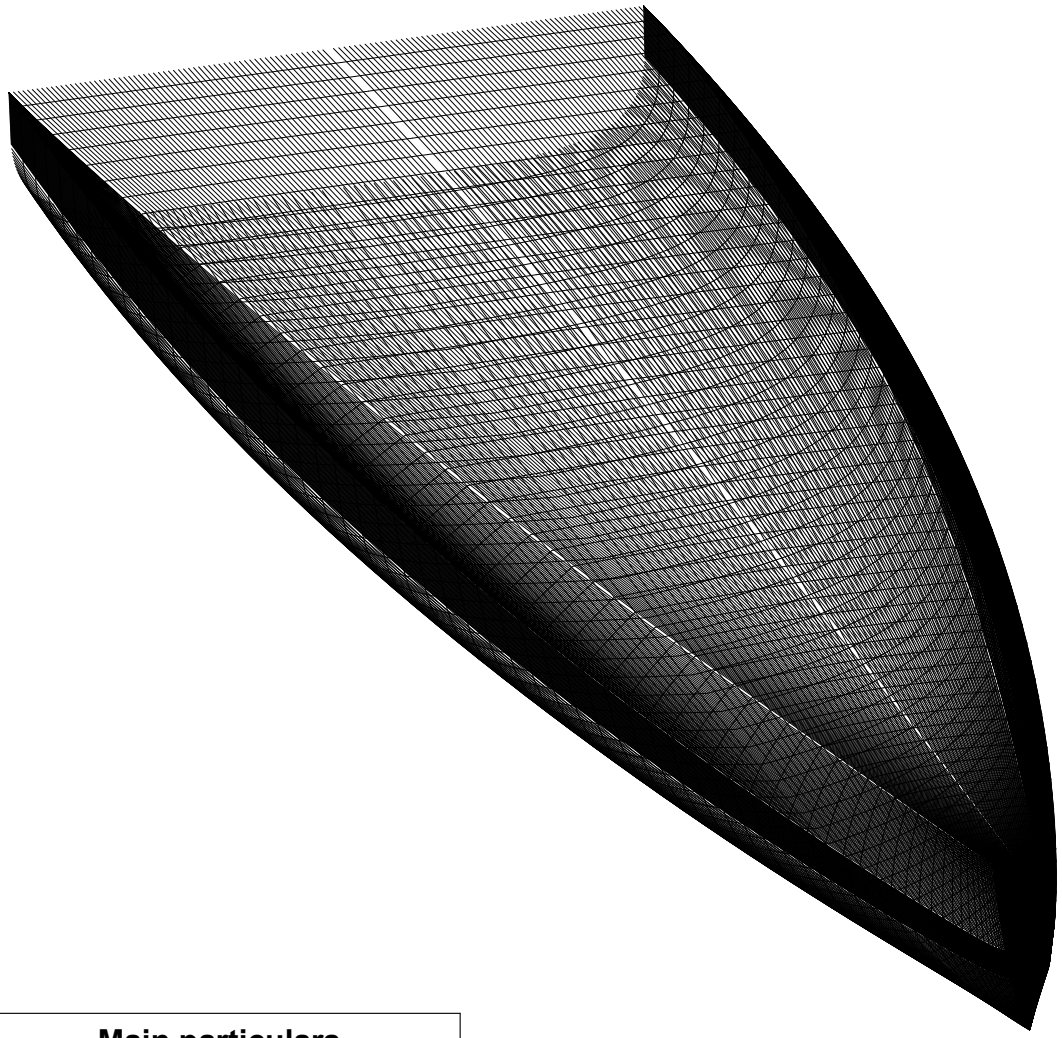

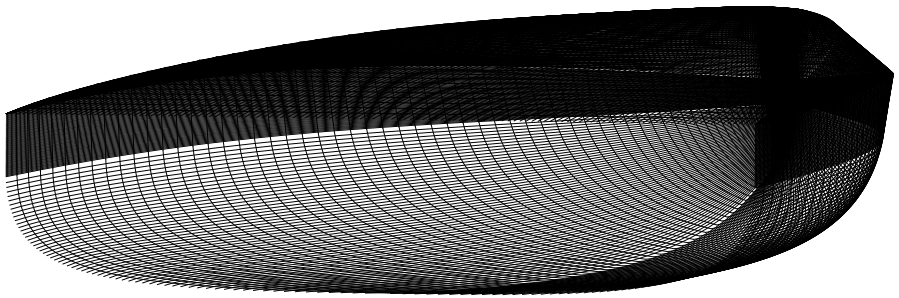

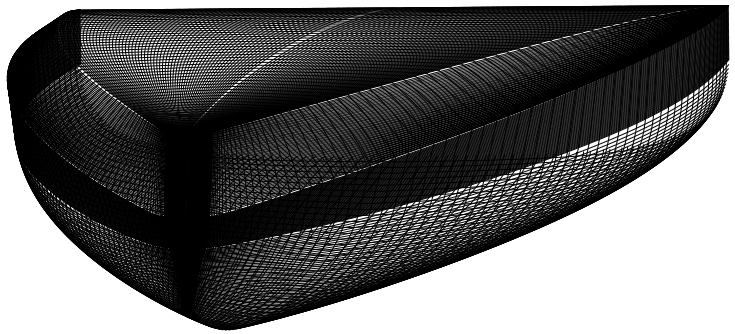

Main particulars		
LOA hull	18.28	m
LWL	16.58	m
BOA hull	5.60	m
BWL	4.11	m
Tc	0.31	m
Displacement Hull	7.67	m^3
Displacement Appendages	0.38	m^3
LCB % of LWL	43.85	%
LCF % of LWL	39.44	%
WSA	50.55	m^2
WPA	49.70	m^2
SA max hull	0.69	m^2
CP	0.64	-

SOLENT UNIVERSITY

Issue date: 04/04/2022	Scale: 1:50 (A4)	File name: Parametrics_IMOCA.dwg
Drawn by: Lazare GOURNAY	Units: mm	Projection method: Perspective
Drawing number: 03		**Drawing title: IMOCA Hull Form**
	Sheet: 1 of 1	

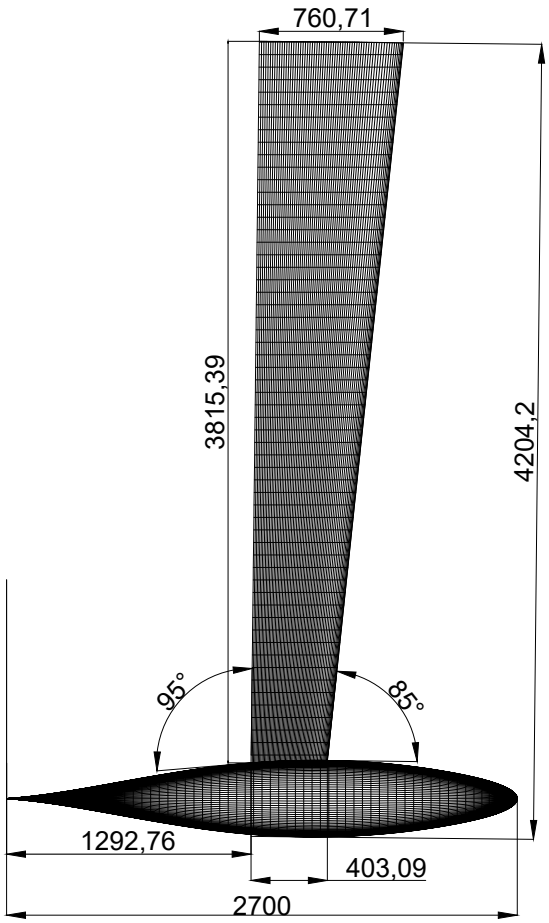

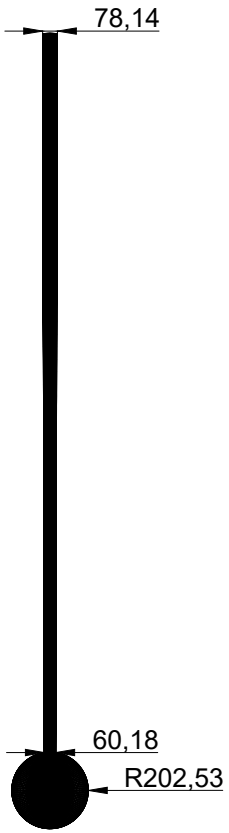

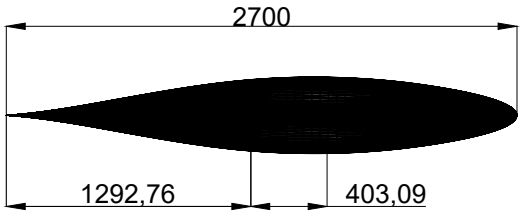

Main particulars

Keel profile	NACA0010	-
Total draft	4.20	m
Bulb radius	0.20	m
Bulb span	2.70	m
Keel span	3.82	m
Longitudinal angle	6.00	deg
Displacement Keel	0.10	m^3
Displacement Bulb	0.22	m^3
Assumed density Keel	2000.00	kg/m^3
Assumed density Bulb	11343.00	kg/m^3
3D true area keel	4.54	m^2
3D true area bulb	2.24	m^2

SOLENT UNIVERSITY

Issue date: 05/04/2022	Scale: 1:40 (A4)	File name: Parametrics_Keel.dwg
Drawn by: Lazare GOURNAY	Units: mm	Projection method: Multiple
Drawing number: 04		**Drawing title: IMOCA Keel**
	Sheet: 1 of 1	

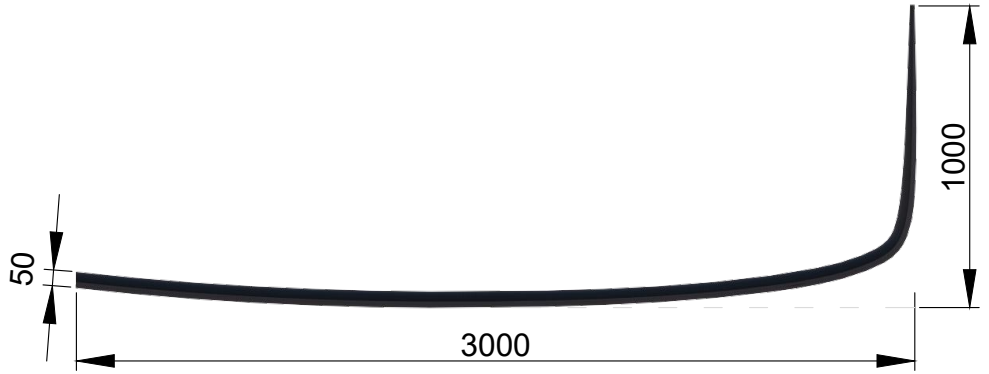

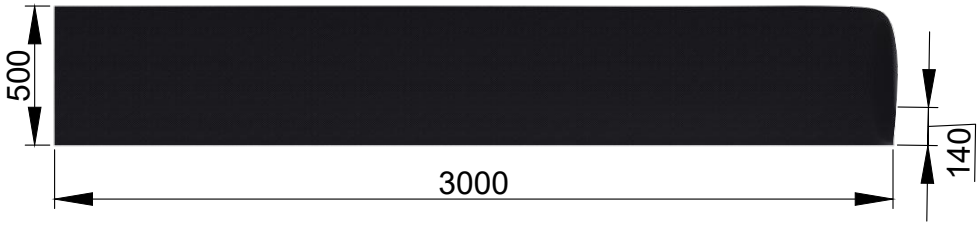

Foil characteristics		
Section	Eppler 817	-
Material	Carbon	-
Total span	3.85	m
Horizontal span	3.00	m
Chord	0.5	m
Tip chord	0.14	m
Max. thickness	0.05	m
Vertical position on hull from DWL	0.557	m
Longitudinal position on hull from AP	8.00	m
Total developed area	3.62	m^2
Assumed weight	0.03	t
Assumed density	2000	kg/m^3
Displacement	0.04	m^3

SOLENT UNIVERSITY

Issue date: 29/05/2022	Format: A4	File name: foil.dwg
Drawn by: Lazare GOURNAY	Units: mm	Projection method: Multiple
Drawing number: 05		**Drawing title: Foils**
	Sheet: 1 of 1	

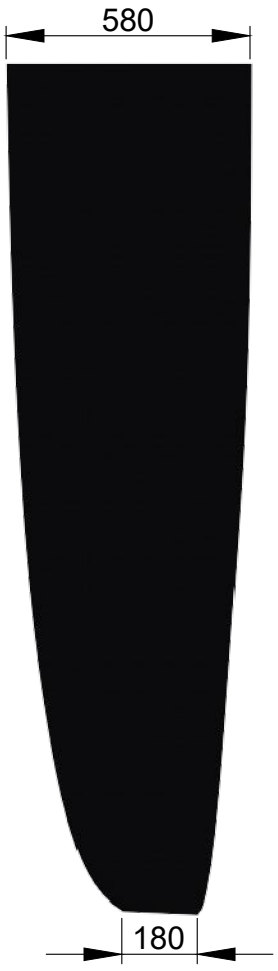

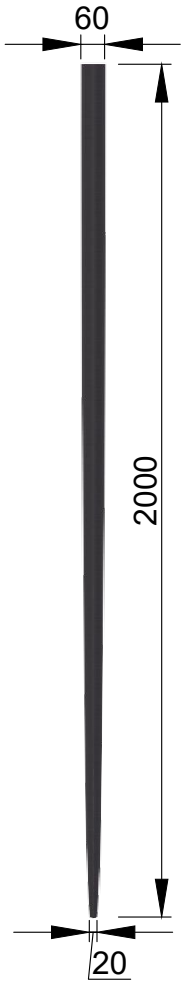

Rudder characteristics		
Section	NACA0063	-
Material	Carbon	-
Total span	2.00	m
Root chord	0.58	m
Tip chord	0.18	m
Root thickness	0.06	m
Tip thickness	0.02	m
Total developed area	1.98	m^2
Assumed weight	0.03	t
Assumed density	2000	kg/m^3
Displacement	0.015	m^3

SOLENT UNIVERSITY

Issue date: 08/07/2022	Format: A4	File name: Rudder.dwg
Drawn by: Lazare GOURNAY	Units: mm	Projection method: Multiple
Drawing number: 06		**Drawing title: Rudders**
	Sheet: 1 of 1	

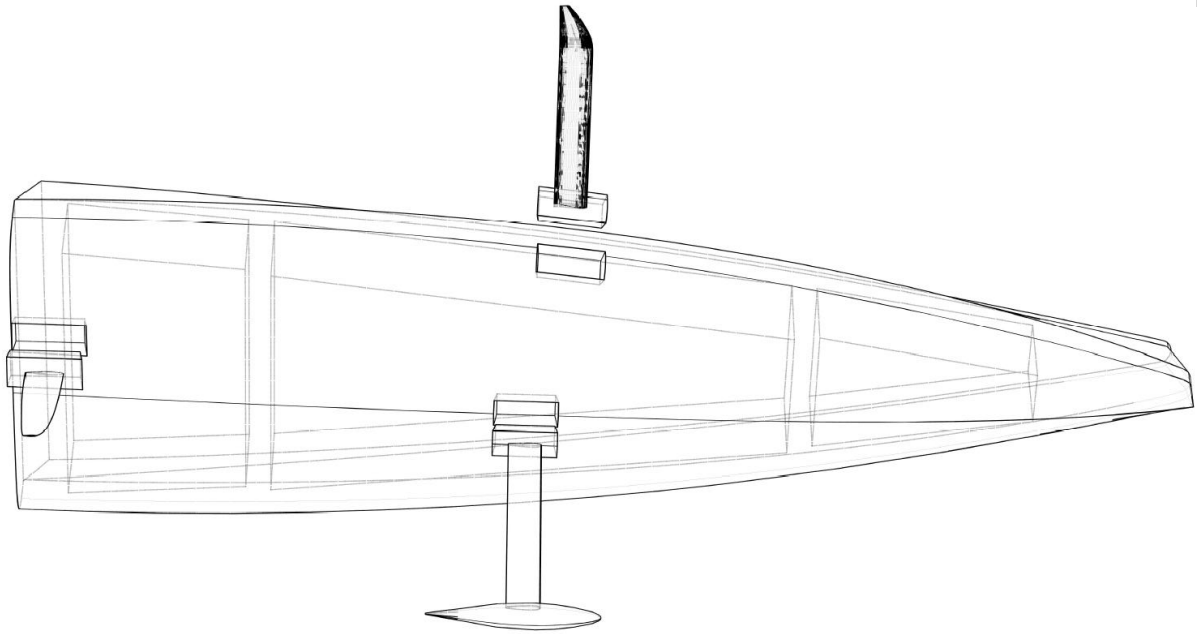

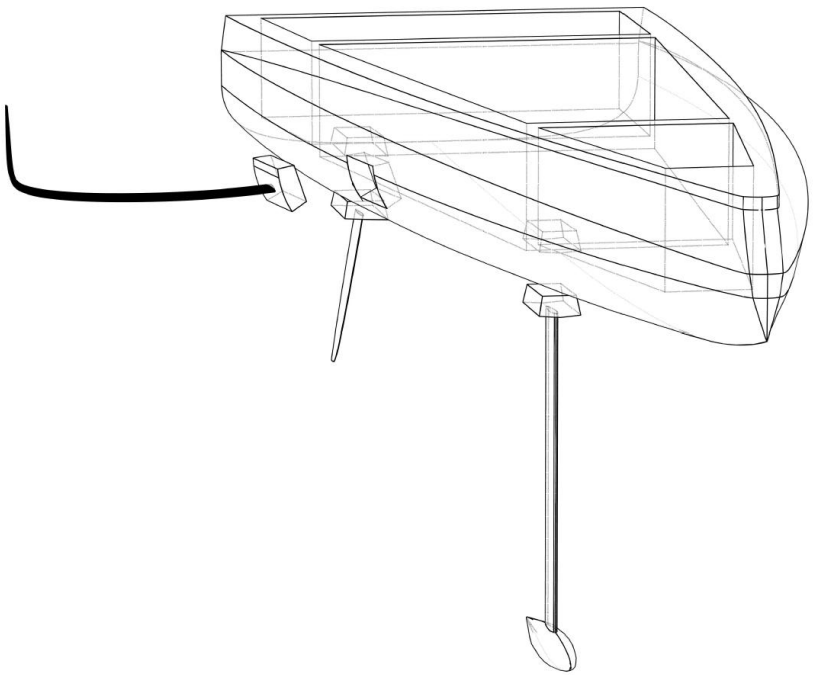

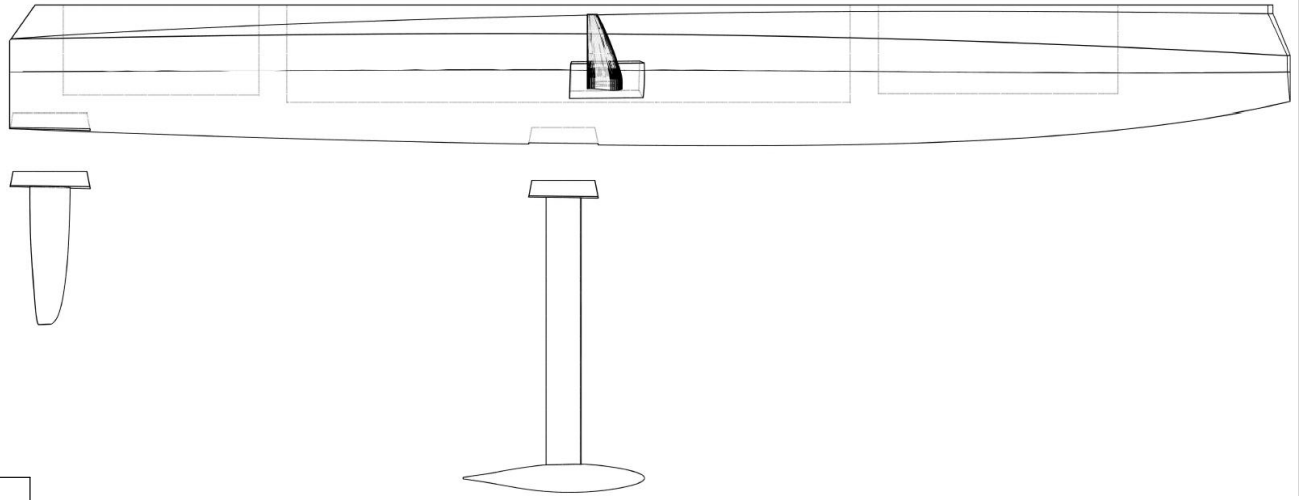

Model characteristics		
Scale	1:10	-
Length	1.8	m
Beam	0.56	m
Material	Polystyrene	-
Manufacturing process hull	CNC milling	-
Manufacturing process appendages	3D printing	-

SOLENT UNIVERSITY

Issue date: 21/05/2022	Format: A4	File name: model_hull.dwg
Drawn by: Lazare GOURNAY	Units: mm	Projection method: Perspective
Drawing number: 07		**Drawing title: Model hull to CNC**
	Sheet: 1 of 1	

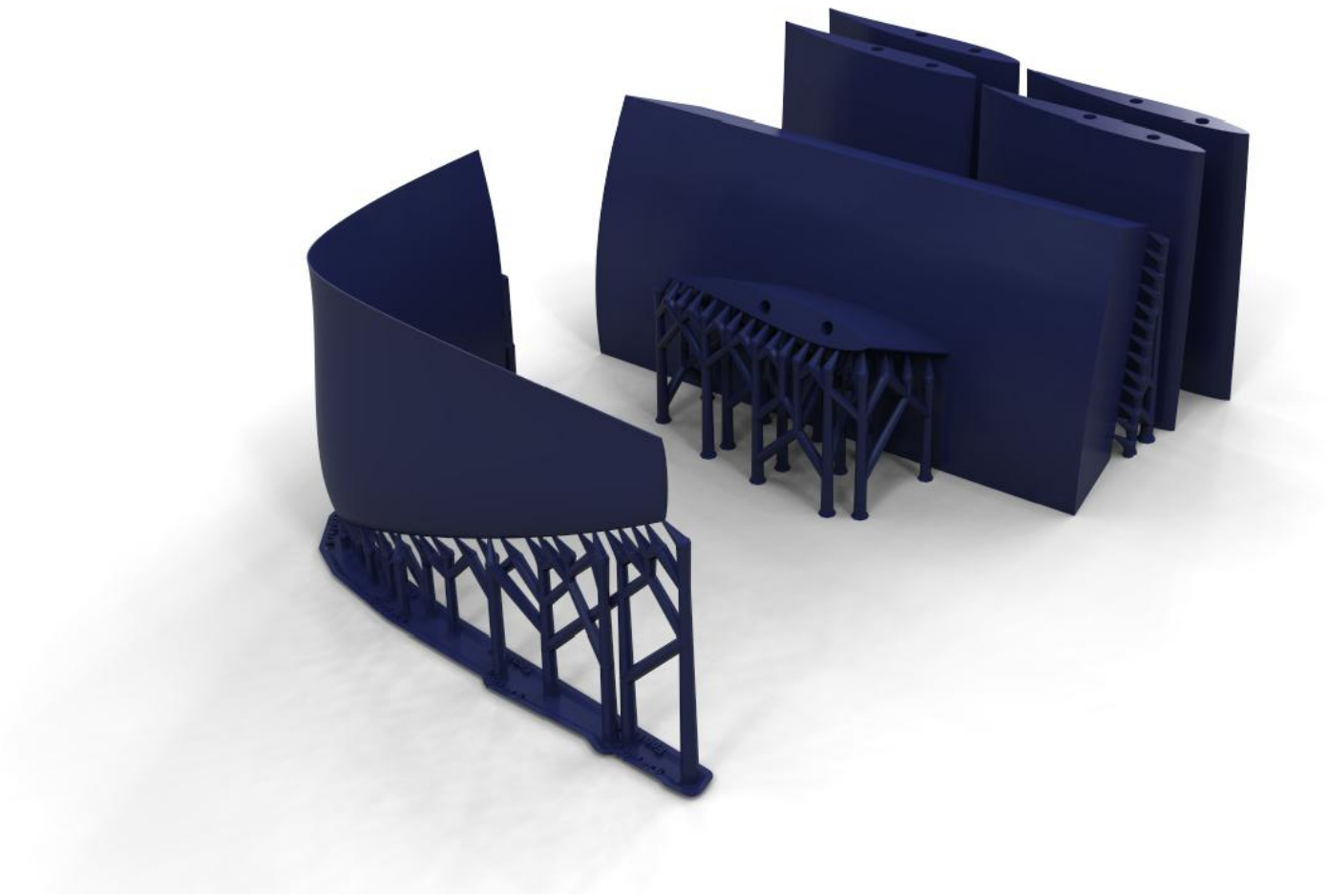

Model foil characteristics		
Section	Eppler 817	-
Scale	1:10	-
Material	Plastic	-
Total span	0.385	m
Horizontal span	0.3	m
Base chord	0.05	m
Tip chord	0.014	m
Max. thickness	0.005	m
Vertical position on model hull from DWL	0.056	m
Longitudinal position on model hull from AP	0.8	m

SOLENT UNIVERSITY

Issue date: 29/05/2022	Format: (A4)	File name: 3D_foil.dwg
Drawn by: Lazare GOURNAY	Units: mm	Projection method: Perspective
Drawing number: 08		**Drawing title: 3D printed foil**
	Sheet: 1 of 4	

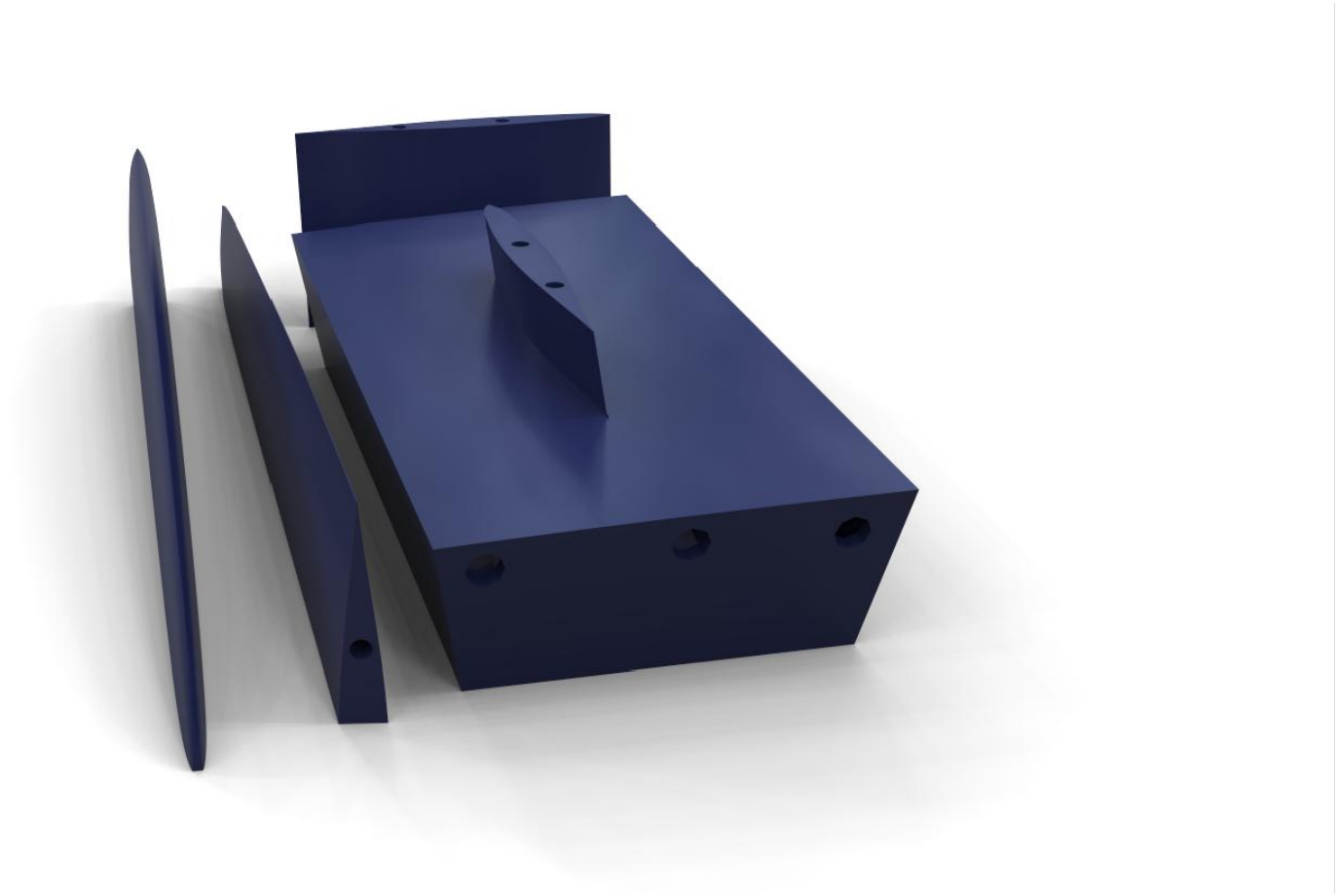

Model rudder characteristics		
Section	NACA0063	-
Scale	1:10	-
Material	Plastic	-
Span	0.2	m
Base chord	0.06	m
Tip chord	0.02	m
Max. thickness	0.01	m

SOLENT UNIVERSITY

Issue date: 29/05/2022	Format: (A4)	File name: 3D_rudder.dwg
Drawn by: Lazare GOURNAY	Units: mm	Projection method: Perspective
Drawing number: 09		**Drawing title: 3D printed rudder**
	Sheet: 2 of 4	

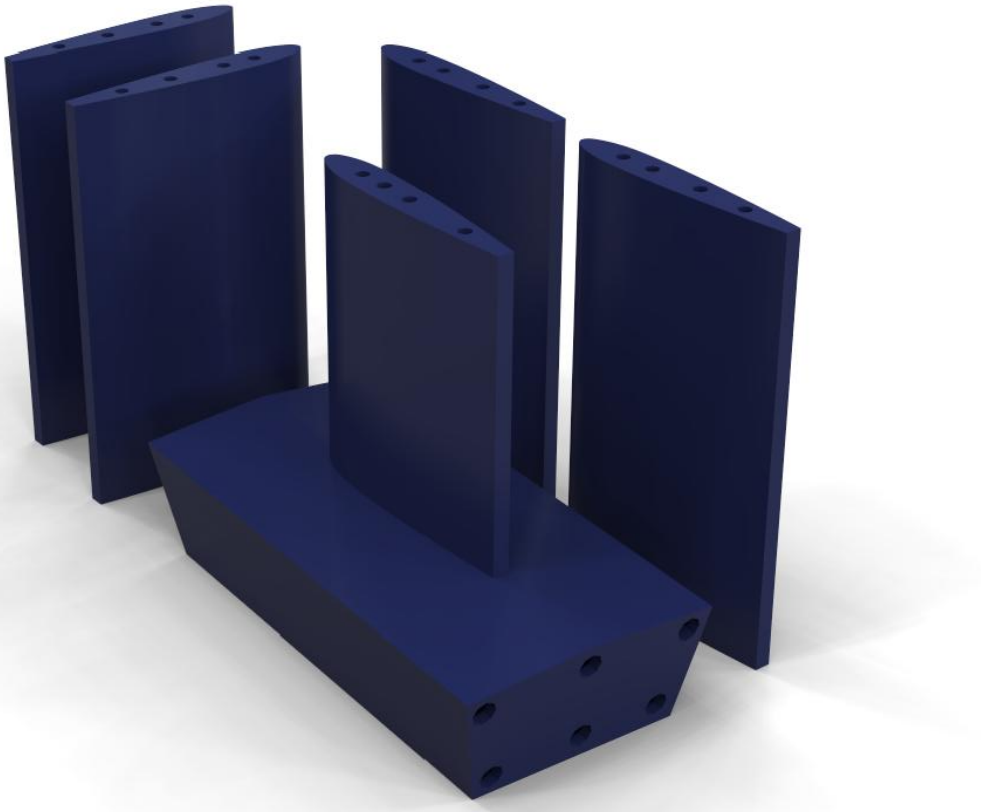

Model keel characteristics		
Section	NACA0010	-
Scale	1:10	-
Material	Plastic	-
Span	0.38	m
Base chord	0.05	m
Tip chord	0.05	m
Max. thickness	0.01	m
Longitudinal position on model hull from AP	0.77	m

SOLENT UNIVERSITY

Issue date: 29/05/2022	Format: (A4)	File name: 3D_keel.dwg
Drawn by: Lazare GOURNAY	Units: mm	Projection method: Perspective
Drawing number: 10		**Drawing title: 3D printed keel**
	Sheet: 3 of 4	

Model bulb characteristics		
Section	NACA65-015	-
Scale	1:10	-
Material	Plastic	-
Max. radius	0.02	m
Span	0.27	m

SOLENT UNIVERSITY

Issue date: 29/05/2022	Format: (A4)	File name: 3D_bulb.dwg
Drawn by: Lazare GOURNAY	Units: mm	Projection method: Perspective
Drawing number: 11		**Drawing title: 3D printed bulb**
	Sheet: 4 of 4	

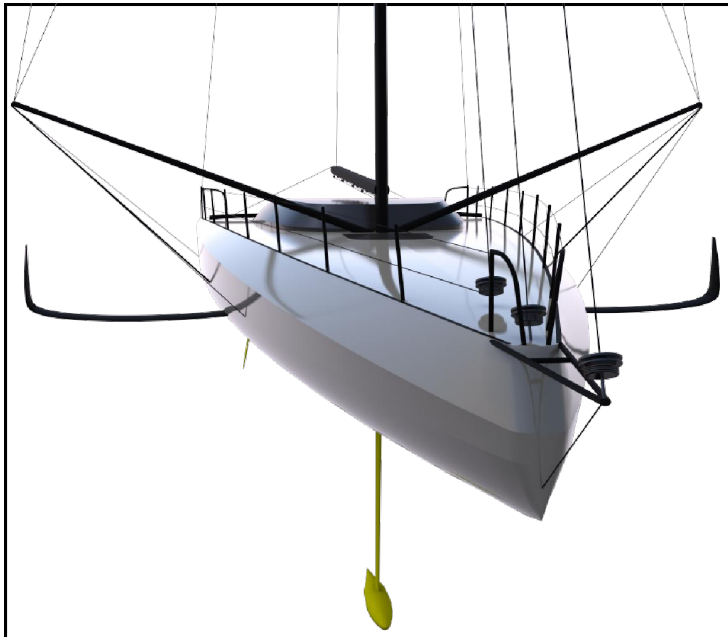

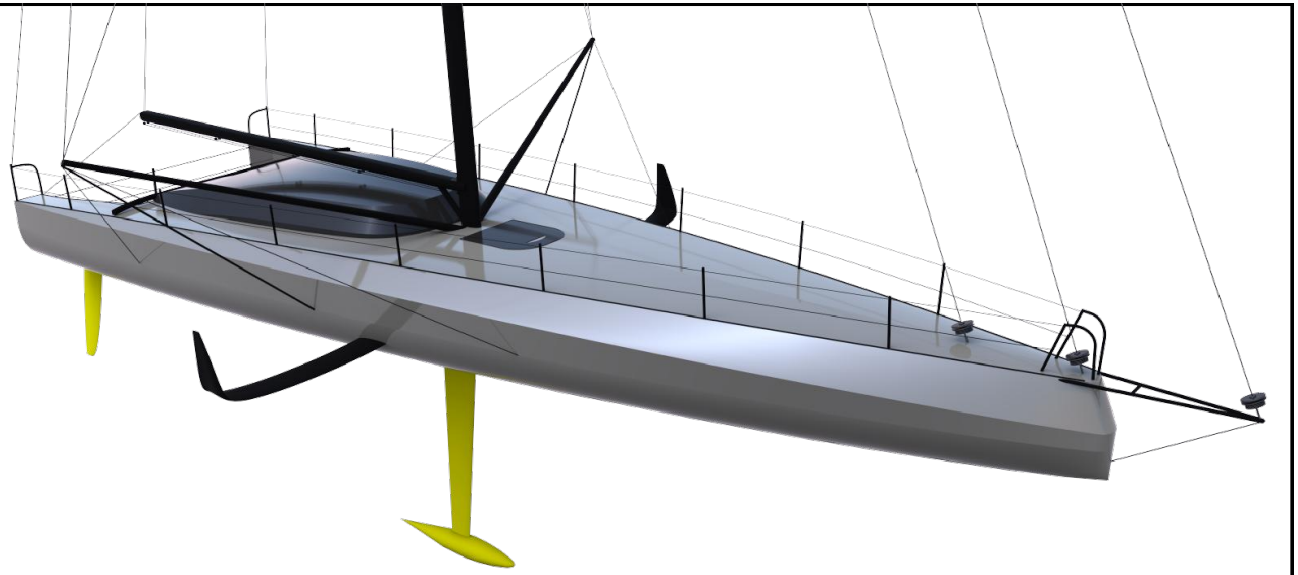

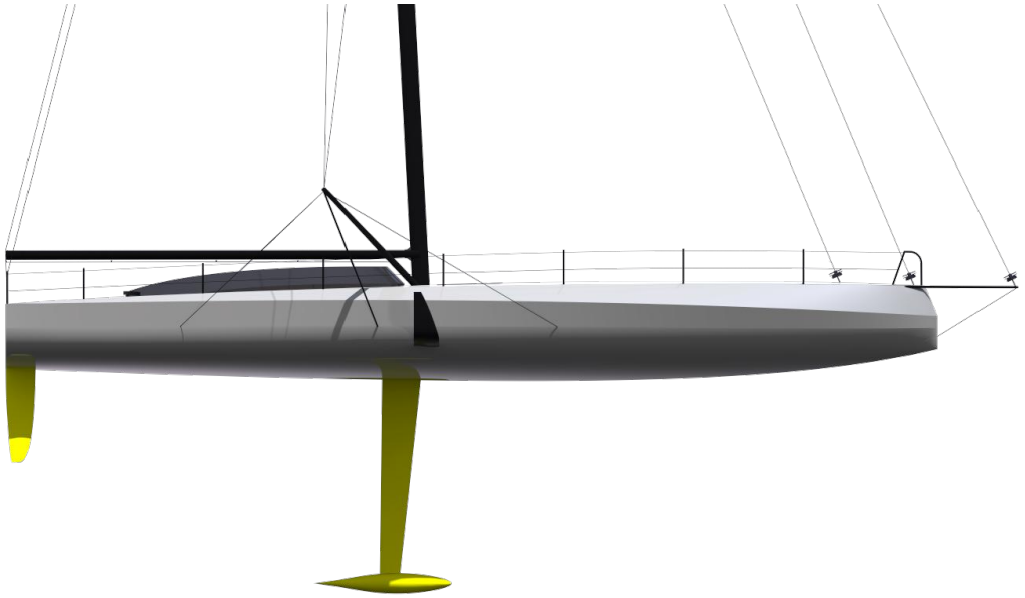

Main particulars		
LOA	20.117	m
Hull length	18.288	m
LWL	16.58	m
BOA	5.6	m
BWL	4.11	m
Displacement	7.864	t
Water draft	4.5	m
Air draft	29	m
Prismatic coeff.	0.44	-
Max. UPW SA	320	m^2
Max. DW SA	580	m^2
Mast type	Wing	-

SOLENT UNIVERSITY

Issue date: 01/06/2022	Format: A4	File name: IMOCA_grey.dwg
Drawn by: Lazare GOURNAY		Projection method: Multiple
Drawing number: 12		**Drawing title: IMOCA not painted Perspective view 1**
	Sheet: 1 of 2	

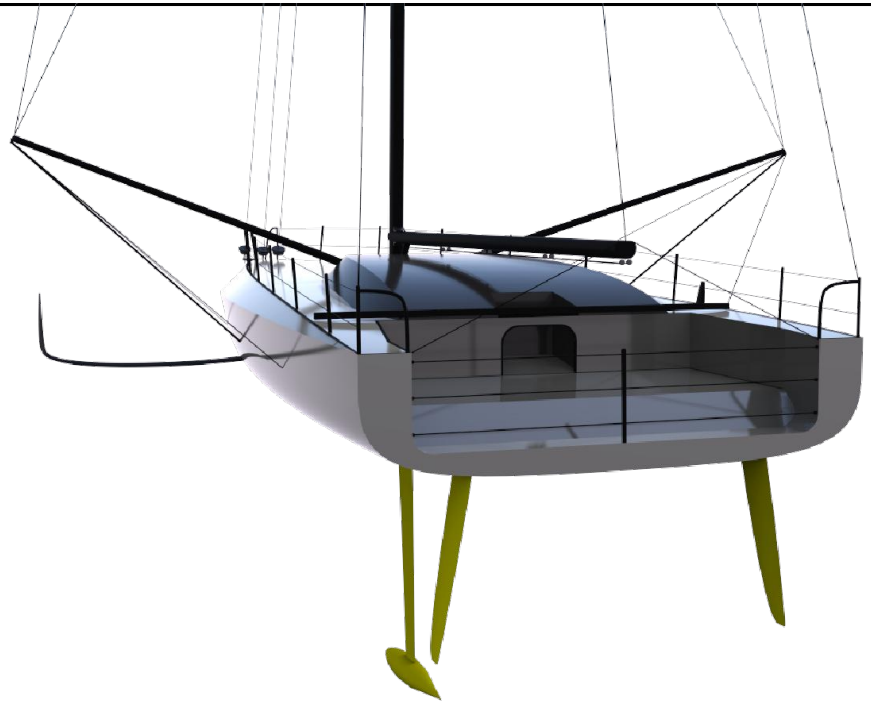

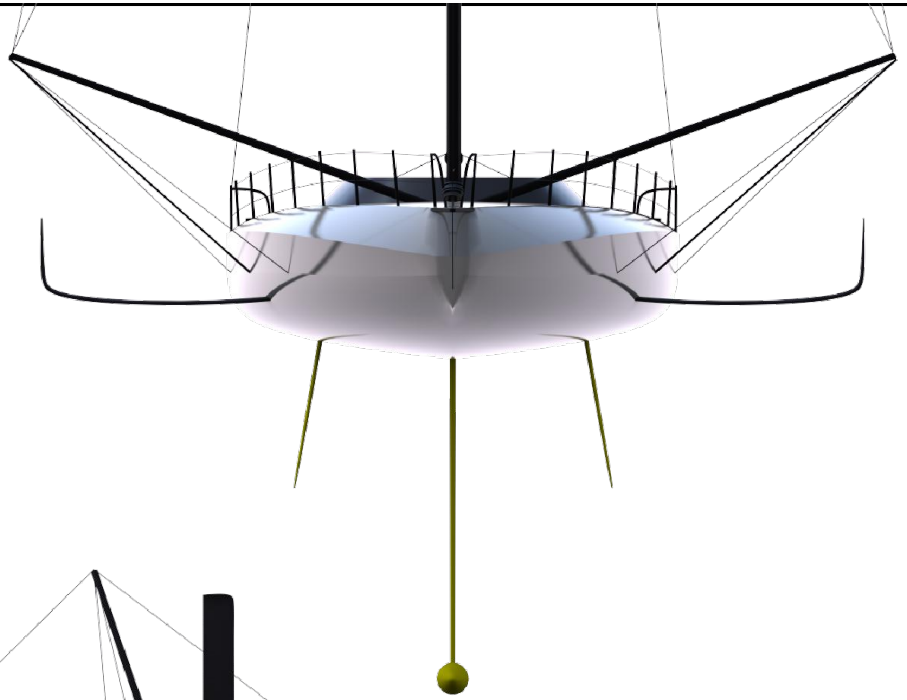

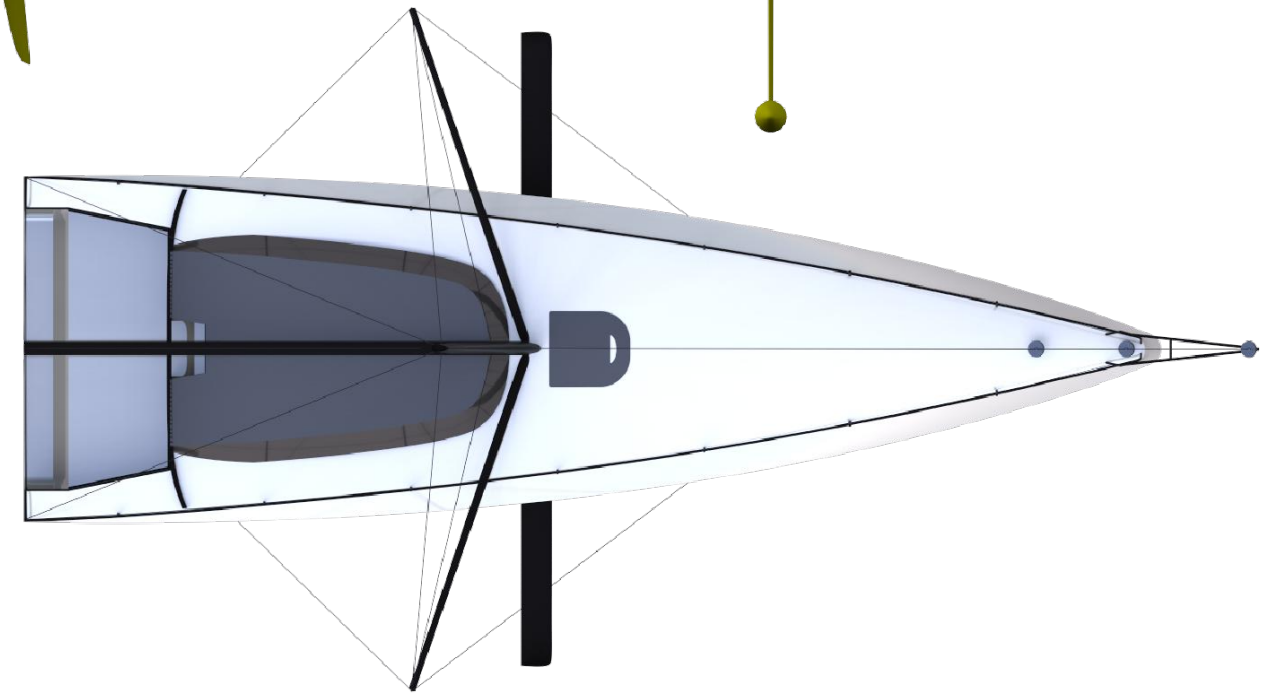

Main particulars		
LOA	20.117	m
Hull length	18.288	m
LWL	16.58	m
BOA	5.6	m
BWL	4.11	m
Displacement	7.864	t
Water draft	4.5	m
Air draft	29	m
Prismatic coeff.	0.44	-
Max. UPW SA	320	m^2
Max. DW SA	580	m^2
Mast type	Wing	-

SOLENT UNIVERSITY

Issue date: 01/06/2022	Format: A4	File name: IMOCA_grey.dwg
Drawn by: Lazare GOURNAY		Projection method: Multiple
Drawing number: 13		**Drawing title: IMOCA not painted Perspective view 2**
	Sheet: 2 of 2	

Main particulars

Name	Union Solidaire	-
LOA	20.117	m
Hull length	18.288	m
LWL	16.58	m
BOA	5.6	m
BWL	4.11	m
Displacement	7.864	t
Water draft	4.5	m
Air draft	29	m
Prismatic coeff.	0.44	-
Max. UPW SA	320	m^2
Max. DW SA	580	m^2
Mast type	Wing	-

SOLENT UNIVERSITY

Issue date: 01/06/2022	Format: A4	File name: Union_Solidaire.dwg
Drawn by: Lazare GOURNAY		Projection method: Multiple
Drawing number: 14		**Drawing title: IMOCA Union Solidaire Perspective view 1**
	Sheet: 1 of 2	

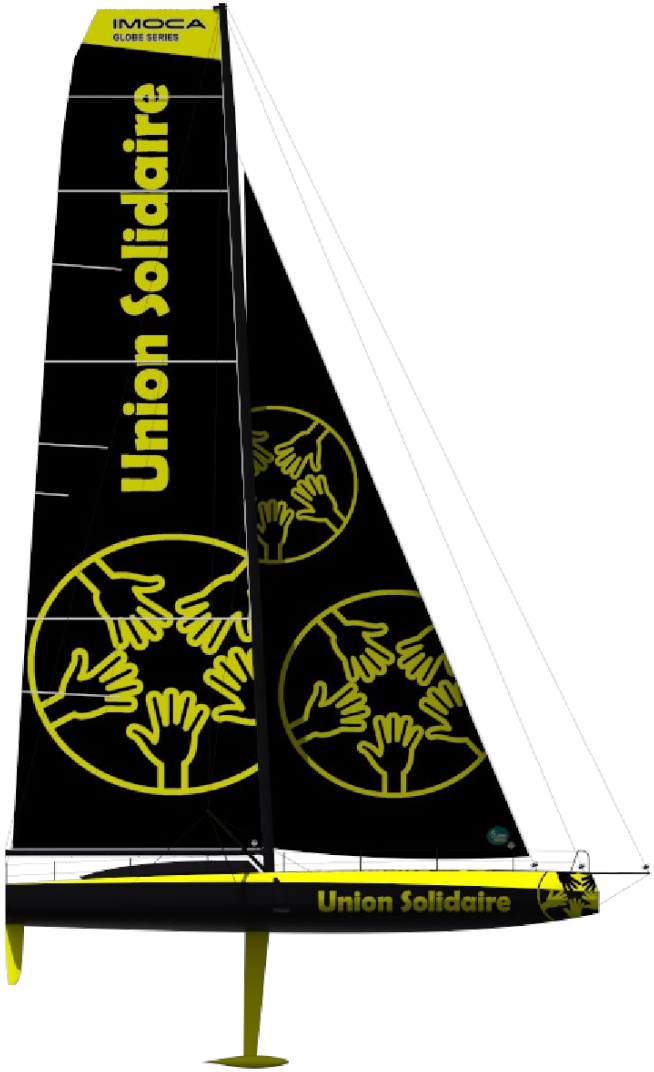

Main particulars

Name	Union Solidaire	-
LOA	20.117	m
Hull length	18.288	m
LWL	16.58	m
BOA	5.6	m
BWL	4.11	m
Displacement	7.864	t
Water draft	4.5	m
Air draft	29	m
Prismatic coeff.	0.44	-
Max. UPW SA	320	m^2
Max. DW SA	580	m^2
Mast type	Wing	-

SOLENT UNIVERSITY

Issue date: 01/06/2022	Format: A4	File name: Union_Solidaire.dwg
Drawn by: Lazare GOURNAY		Projection method: Multiple
Drawing number: 15		**Drawing title: IMOCA Union Solidaire Perspective view 2**
	Sheet: 2 of 2	